

Innovation of Chemistry & Materials for Sustainability

<https://insuf.org/journal/icms>

Open Access, Peer-Reviewed



Photo Credit: Dr. Vishal A. Mahajan

Editor-in-Chief

Prof. Dr. Susanta Banerjee



Published by

INSUF PUBLICATIONS (OPC) PVT. LTD.

CIN No: U90005WB2024OPC272576

About the Journal

The Journal *Innovation of Chemistry & Materials for Sustainability* is a comprehensive publication that focuses on the latest research and developments in the field of sustainable chemistry and materials science. This journal provides a platform for scientists, researchers, and industry professionals to share their findings and innovations that contribute to a more sustainable future. Covering a wide range of topics such as green chemistry, renewable materials, and eco-friendly processes, this journal is a valuable resource for those working towards a more sustainable world.

Aims & Scope

Introducing the scope of the new journal, Innovation of Chemistry & Materials for Sustainability (ICMS) will cover all topics related to chemistry and materials in the widest possible sense, but there should be a sustainable chemistry aspect for successful submissions. ICMS publishes original papers, short communications and perspectives, and review articles in all areas of chemistry and materials for a safer and cleaner future. Interdisciplinary contributions are encouraged, encompassing a wide range of topics including, but not limited to, the following:

- Catalysis (homogeneous, heterogeneous and bio-catalysis)
- Green chemistry for sustainable processing routes (microwaves, ultrasounds, photochemistry, electrochemistry, flow chemistry, etc.)
- Lipid valorization – Biorefining
- Polymers: Synthetic polymers and elastomers, polymer membranes/ composites/ fibres, responsive/ functional polymers, nano structured polymers, biocompatible and biodegradable polymers
- Innovation of chemistry and materials for sustainable agriculture & pharmaceutical practices
- Bio-based chemicals, fuels, materials
- Renewable energy sources (wind, solar) and storage,
- CO₂ capture, utilization and carbon neutrality
- Chemistry and materials for circular economy
- Nano-materials for energy generation, water treatment, and environmental remediation.

Journal Particulars

Title:	Innovation of Chemistry & Materials for Sustainability
Journal Title Abbreviations:	<i>Innov. Chem. Mater. Sustain.</i>
Frequency:	Biannually
ISSN:	3049-0146 (Online); 3049-2548 (Print)
Publisher:	Insuf Publications (OPC) Pvt. Ltd.
Refereed:	Peer Review
Editor-in-Chief:	Prof. Dr. Susanta Banerjee
Copyright:	Insuf Publications (OPC) Pvt. Ltd.
Starting Year:	2024
Subject:	Chemistry/Crystallography/Mineralogy
Language:	English
Publication Format:	Online & Print
Distribution:	Open Access
Contact Nos.:	+91-9933060646; +918902278875
Email Ids:	me-icms@insuf.org ; eic-icms@insuf.org
Website:	https://insuf.org/journal/icms/index
Address:	BD51, Gitanjali Apartment, FL 5B, Rabindra Pally, Prafulla Kanan, North 24 Pgs, Kolkata, West Bengal, INDIA, PIN-700101.

Innovation of Chemistry & Materials for Sustainability, an open access journal under the CC BY-NC-ND license.

Website: <https://insuf.org/journal/icms>

Published by Insuf Publications (OPC) Pvt. Ltd.; Website: <https://insuf.org/>

Address: BD51, Gitanjali Apartment, FL 5B, Rabindra Pally, Prafulla Kanan, North 24 Pgs, Kolkata, West Bengal, INDIA, PIN-700101.

Email: gargiagarwala@gmail.com; me-icms@insuf.org Contact Nos.: +919933060646; +918902278875.

Editors & Editorial Board

Editor-in-Chief

Susanta Banerjee

Professor (HAG) & Institute Chair Professor
Chairperson, Central Research Facility
Former Head, Materials Science Centre
Indian Institute of Technology Kharagpur
Kharagpur - 721302, India.
E-mails: susanta@matsc.iitkgp.ac.in; eic-icms@insuf.org
Website: <https://www.iitkgp.ac.in/department/MS/faculty/ms-susanta>

Managing Editor

Gargi Agarwala Mahato

Director, Insuf Publications (OPC) Pvt. Ltd.
(CIN No: U90005WB2024OPC272576)
BD51, Gitanjali Apartment, FL 5B, Rabindra Pally
Prafulla Kanan, North 24 Pgs, West Bengal
Kolkata-700101, India.
E-mails: gargiagarwala@gmail.com; me-icms@insuf.org
Website: <https://www.insuf.org>

Advisory Board

Sourav Pal, FNA, FASc, FNASc, FRSC

Professor and Head, Department of Chemistry,
Ashoka University, Sonapat, Haryana, INDIA
Honorary Professor, Indian Institute of Science Education and
Research (IISER) Kolkata, Former- Director, IISER Kolkata
Former- Director, CSIR-NCL, Pune & Former Professor IIT
Bombay
E-mail: sourav.pal@ashoka.edu.in
Website: <https://www.ashoka.edu.in/profile/sourav-pal/>

Suprakas Sinha Ray

Director, DSI-CSIR Nanotechnology Innovation Centre
Manager, Centre for Nanostructures & Adv. Materials
University of Johannesburg (Distinguished Professor),
University of Pretoria (Extraordinary Professor), S. Africa
E-mails: rsuprakas@csir.co.za; ssinharay@uj.ac.za
Website: <https://www.csir.co.za/>

Shoubhik Das

Chair of the Organic Chemistry I
University of Bayreuth
Universitätsstr. 30
Bayreuth, 95447, Germany
Email: Shoubhik.Das@uni-bayreuth.de
Website: <https://www.shoubhikdas.uni-bayreuth.de/de/index.html>

Surya K. De CChem, FRSC, FRSM, FICS, FSASS

Councilor, American Chemical Society, Washington DC, USA
Director of Chemistry
Conju-Probe, PO Box 927685,
San Diego, CA, USA
Email: suryakde@sandiegoacs.org
Website: <https://conju-probe.com/>

Rui Shang

Professor, Department of Chemistry,
Graduate School of Science, The University of Tokyo,
Molecular Innovation Building 7F, Nakamura Lab 7- 3-1
Hongo, Bunkyo-ku, 113-0033 Tokyo, Japan
E-mail: rui@chem.s.u-tokyo.ac.jp
Website: <https://moltech.jp/ja/rui-shang>

Eufrânio N. da Silva Júnior FRSC

Professor of Organic Chemistry
Institute of Exact Sciences, Department of Chemistry
Federal University of Minas Gerais, Brazil
Email: eufranio@qui.ufmg.br
Website: <https://www.eufranolab.com/>

Tarun Kumar Mandal

Senior Professor, Polymer Science Unit,
Indian Association for the Cultivation of Science, Jadavpur,
Kolkata- 700032, INDIA
Email: psutkm@iacs.res.in
Website: <https://iacs.res.in/athusers/index.php?navid=0&userid=IACS0083#561903>

Amit Das

Head of Research Group Smart & Functional Elastomers
Leibniz Institute of Polymer Research Dresden
Hohe Strasse 6, D-01069 Dresden, Germany
Adjunct Professor (Functional Elastomers)
Fellow Finland Distinguished Professor Program
Department of Materials Science, Tampere University, Finland
Emails: amit.das@tuni.fi das@ipfdd.de
Website: <https://www.ipfdd.de/de/organisation/organigramm/personal-homepages/dr-amit-das/>

Debabrata Maiti, FRSC, FASc

Editor-in Chief, Synlett
Institute Chair Professor, Department of Chemistry
Indian Institute of Technology Bombay
Powai, Mumbai-400076, INDIA
E-mail: dmaiti@iitb.ac.in
Website: <https://www.dmaiti.com/>

Rakeshwar Bandichhor FRSC, CChem, SSWB, BB, MB

Vice President & Head, Chemistry - API - Process R&D,
Vice-Chair, ACS-India Chapter (South India), Organic Process R
& D (OPRD), ACS-Editorial Advisory Board Member
Dr. Reddy's Laboratories, Hyderabad, INDIA
Email: rakeshwarb@drreddys.com
Website: <https://www.drreddys.com/>

Seema Agarwal

Professor, Lehrstuhl für Makromolekulare Chemie II
Gebäude NWII, Universität Bayreuth
Universitätsstrasse 30
95440, Germany
Email: Seema.Agarwal@uni-bayreuth.de
Website: <https://www.mci.uni-bayreuth.de/en/team/team-agarwal/agarwal-seema/index.php>

Pedro Aguirre

Pedro Aguirre A.
Departamento de Química Inorgánica y Analítica
Facultad de Ciencias Químicas y Farmacéuticas
Universidad de Chile, Sergio Livingstone 1007,
Independencia, Santiago, Chile
Email: paguirre@ciq.uchile.cl
Website: <https://portafolio-academico.uchile.cl/perfil/26715-Pedro-Abel-Aguirre-%c3%81lvarez>

Sarim Dastgir, DPhil (oxon), MRSC

Green Global Group, USA
E-mail: sarim.dastgir@lmh.oxon.org
Website: <https://ggt-usa.com/>

Gerda Fouche

Department of Chemistry, University of Pretoria, Private Bag
X20, Pretoria 0001, S. Africa
Former- Head, Bioscience, CSIR-Pretoria
Email: GFouche@csir.co.za; fouche51@gmail.com
Website: https://scholar.google.co.za/citations?hl=en&user=H_vgBhwAAA&view_op=list_works

Associate Editors

Naresh Kumar

Assistant Professor, Department of Chemistry,
SRM University, Delhi-NCR, Sonapat, Haryana 131029, INDIA
Email: editor-icms@insuf.org
Website: <https://www.srmuniversity.ac.in/faculty/dr-naresh-kumar>

Tanvir Arfin

Senior Scientist, Air Resource (Assistant Professor-AcSIR)
Environmental Resource Planning & Management
CSIR-National Environmental Engineering Research Institute
(NEERI)
Nehru Marg, Nagpur-440020, INDIA
Email: environchem-icms@insuf.org
Website: <https://neeri.irins.org/profile/222662>

Surajit Rakshit

Assistant Professor, Department of Chemistry
Institute of Science, Banaras Hindu University
Banaras Hindu University, Varanasi, INDIA
Email: physchem-icms@insuf.org
Website: <https://srakshitchem.wixsite.com/surajit>

Jaya Lakkakula

Assistant Professor
Amity University Maharashtra, Mumbai, INDIA
Email: mat-icms@insuf.org
Website: https://www.amity.edu/mumbai/aib/faculty_details.aspx?mpgid=1162&pgidtrail=1162&facultyid=2272

Bikram Keshari Agrawalla

Scientist,
Roche Diagnostics GmbH, Penzberg, GERMANY
Email: chembio-icms@insuf.org
Website: https://scholar.google.com.sg/citations?hl=en&user=LSMr1yoAAA&AJ&view_op=list_works&sortby=pubdate

Milan Bera

Ramanujan Faculty Fellow
Photocatalysis & Synthetic Methodology Lab (PSML)
Office: J1-101, First Floor, J1 Block
Amity Institute of Click Chemistry Research & Studies (AICCRS)
Amity University, Sector-125, Noida-201303, U.P., INDIA
Email: orgchem-icms@insuf.org
Website: <https://miluom.wixsite.com/mblab>

Kapileswar Seth

Assistant Professor
Department of Medicinal Chemistry
National Institute of Pharmaceutical Education and Research
(NIPER)-Guwahati, INDIA
Email: nano-icms@insuf.org
Website: <https://sites.google.com/niperguwahati.in/drkapileswarseth>

Rama Layek

Assistant Professor (Tenure Track), School of Engineering
Science, Department of Separation Science,
LUT University, FINLAND
Email: polymer-icms@insuf.org
Website: <https://research.lut.fi/converis/portal/detail/Person/13706711>

Aymen Skhiri

Postdoctoral Fellow, Institut de chimie de Nice
Cote d'Azur University, Avenue Valrose 06300 Nice, FRANCE
Email: inorgchem-icms@insuf.org
Website: <https://scholar.google.fr/citations?user=pPfhFv4AAAAJ&hl=fr>

Longzhi Zhu

Lecturer, School of Chemistry & Chemical Engineering,
Hunan Institute of Science and Technology, Yueyang, PR
CHINA
Email: catalysis-icms@insuf.org
Website: <https://orcid.org/0000-0001-5161-9944>

Research Ethics & Integrity Team (Email: integrity-icms@insuf.org)

Suparna Chatterjee

STEM Education Teacher Preparation,
Administration and Leadership
College of Health, Education and Social Transformation
New Mexico State University, New Mexico, USA
Email: suparna@nmsu.edu; integrity-icms@insuf.org (Shared)
Website: https://tpal.nmsu.edu/faculty-directory/dr-suparna_chatterjee.html

Myungwon Choi

Technische Universität München, München, GERMANY
Email: go29mas@mytum.de; integrity-icms@insuf.org (Shared)
Website:

Sawsan Salameh

Al-Quds University, PALESTINE
Email: ssalameh@staff.alquds.edu; integrity-icms@insuf.org (Shared)
Website: <https://www.alquds.edu/en/faculty-team/sawsan-salama/>

Debashis Majee

Yale-NUS College, SINGAPORE
Email: debashis@yale-nus.edu.sg; integrity-icms@insuf.org (Shared)
Website: <https://www.yale-nus.edu.sg/>

Yogesh Kumar Walia

Career Point University Hamirpur, INDIA
Email: yogesh.che@cuh.in; support-icms@insuf.org
Website: <https://cuh.in/leadership/>

Zeynab Fakhar

Aburaihan Pharmaceutical Co. Tehran, IRAN
Email: zb.fakhar@gmail.com; integrity-icms@insuf.org (Shared)
Website: <https://en.aburaihan.com/>

Tulika Chakrabarti

Sir Padampat Singhania University, Udaipur, INDIA
Email: tulika.chakrabarti@spsu.ac.in; integrity-icms@insuf.org (Shared)
Website: <https://www.spsu.ac.in/faculty-of-applied-sciences/faculty-members/>

Publication Ethics

The **Innovation of Chemistry & Materials for Sustainability (ICMS)** is dedicated to maintaining the utmost integrity in publication ethics. Submissions to the journal must consist of original contributions. The submitting author bears the responsibility of securing agreement from all co-authors and obtaining necessary consent from sponsors before submitting an article. Authors are accountable for the content of their articles, with ultimate responsibility resting on them rather than on the Editors or the Publisher.

Similarly, the **ICMS** pledges to conduct thorough and unbiased double-blind peer reviews of submitted works for publication, ensuring fairness and objectivity. Our intention is to avoid any conflicts of interest between our editorial and review staff and the materials under review.

Responsibilities of Editors

Publication decision: The responsibility of determining which articles submitted to the journal should be published lies with the editor. These decisions should always be influenced by the validation and importance of the work to researchers and readers. The editor may take direction from the journal's advisory board policies and must adhere to legal obligations concerning issues like defamation, copyright violation, and plagiarism.

Fair play: An editor ought to assess manuscripts based on their intellectual merit, free from consideration of the authors' race, gender, sexual orientation, religious beliefs, ethnic circumstantial, citizenship, or political convictions.

Confidentiality: Confidentiality must be maintained by the editor and all editorial/reviewer personnel, refraining from exposing any details regarding a submitted manuscript to individuals other than the corresponding author, reviewers, advisory board members, and the publisher, as deemed necessary.

Disclosure and Conflict of Interest: Information or insights gained through peer review are measured advantaged and must be preserved confidentially, without manipulation for personal gain. Editors are assigned to guarantee that all contributors disclose any appropriate challenging interests, and corrections should be issued if such conflicts come to light post-publication. If necessary, further measures such as retractions or expressions of concern may be implemented.

Participation and Collaboration in Investigations: An editor is anticipated to promptly address ethical complaints related to a submitted manuscript or published paper, in collaboration with the publisher. These actions typically comprise reaching out to the author to measure the complaint, considering the claims made, and potentially extending communication to relevant institutions and research entities. If the complaint is validated, corrective actions such as issuing a correction, retraction, expression of concern, or other appropriate measures may be taken. It's indispensable to thoroughly examine all reported instances of unethical publishing behavior, regardless of when they come to light, even if it's years after publication.

Responsibilities of Reviewers

Participation in Editorial Decision: Reviewers should decline invitations to review manuscripts if they have an evident conflict of interest and disclose the nature of the conflict. Conflict of interest refers to circumstances that could potentially lead to an unfair evaluation of the manuscript. Editors may intentionally select reviewers with particular perspectives to ensure a balanced assessment. Reviewers with suspicions regarding conflicts of interest are encouraged to seek clarification from the Editor.

Confidentiality: Confidentiality must be endorsed by reviewers regarding the manuscripts they assess. It is improper to utilize data from these manuscripts prior to their publication. Equally improper is the sharing of this data with colleagues or reproducing the manuscript for any reason. If reviewers desire to utilize information from a manuscript accepted for publication, they should request the Editor to communicate with the author(s) for permission.

Objectivity Criteria: Reviewers who accept the task of evaluating a manuscript are expected to obey to the designated timeframe for completing their reviews. In the event that meeting this deadline becomes unfeasible, reviewers are encouraged to promptly notify the editorial office. They should request guidance regarding whether to decline the review or appeal an extension for a specified duration.

Acknowledgement of Source: Reviewers who are unable to complete a manuscript review within the designated timeframe should respectfully decline the request. It is mandatory upon reviewers to approach both the author and the manuscript with professionalism and courtesy. In cases where reviewers protect any bias towards the researchers or the research, they should withdraw from participating in the review process. Similarly, if there exists a conflict of interest with the research or its sponsors, reviewers are responsible for disclosing this information to the editors.

Responsibilities of Authors

Reporting guidelines: Authors reporting original research must provide a precise description of their methodology and impartially discuss its implications. Accurate representation of essential data is imperative, with papers containing ample detail and references for replication. Deliberate misrepresentation is unethical and intolerable.

Data availability and retention: Authors may be requested to submit raw data for editorial review and should be willing to grant public access where possible. Additionally, authors should commit to retaining such data for a reasonable period post-publication.

Ensuring Originality and Avoiding Plagiarism: Authors must assure the creation of entirely unique content. Any utilization of others' work or words should be properly recognized through citation or quotation. Plagiarism displays in various ways, such as bestowing someone else's paper as one's own, reproducing significant portions of another's work without acknowledgment, or appropriating research findings from others. Engaging in any form of plagiarism is unethical in publishing and is not accepted.

Authors may be mandatory to confirm that their manuscript has not been concurrently submitted to another journal for review. Such practices waste the time of editors and peer reviewers and can potentially harm the integrity of the research by appearing in multiple publications simultaneously. The submitting author embraces the responsibility of ensuring that all co-authors and sponsors have agreed to the submission before sending the paper.

Acknowledgement of Sources: It is crucial to appropriately acknowledge the contributions of others. Authors are grateful to reference influential publications that have influenced their work. Confidential information obtained through private exchanges, whether through conversation, correspondence, or discussions with third parties, should not be utilized or disclosed without categorical written consent from the source. Similarly, information acquired during the provision of confidential services, such as manuscript reviewing or grant evaluation, should not be hired without obtaining explicit written permission from the relevant author involved in these services.

Authorship of the Paper: Authorship ought to be reserved for individuals who have substantially contributed to the conception, design, implementation, or interpretation of the study being described. Those who have made striking contributions should be credited as co-authors. In cases where others have been involved in significant aspects of the research project, they should be acknowledged or listed as contributors. The corresponding author is responsible for ensuring that all relevant co-authors are included in the article and that no irrelevant/guest co-authors are included. Additionally, the corresponding author must ensure that all co-authors have reviewed and approved the final version of the paper and have consented to its submission for publication.

Hazards and Human or Animal Integrity: If the work involves the use of chemicals, procedures, or equipment with inherent unusual hazards, the author must explicitly describe these in the manuscript. Authors conducting research involving experimental animals and human subjects should obtain approval from the relevant Ethical committee in agreement with the "Principles of Laboratory Animal Care." The Method section of the manuscript should include a statement confirming approval for the investigation and the acquisition of informed consent.

Disclosure and Conflicts of Interest: Authors must divulge any financial or significant conflicts of interest in their manuscript that could potentially disturb the findings or understanding of their work. Additionally, they should provide transparency regarding all sources of financial assistance for the project.

Fundamental errors in published works: If an author identifies a remarkable error or inaccuracy in their published work, they are forced to promptly notify the journal editor or publisher and collaborate with them to retract or rectify the paper. In the event that the editor or publisher becomes aware through a third party that a published work contains a significant error, it is the author's responsibility to swiftly retract or amend the paper, or present evidence to the editor affirming the accuracy of the original paper.

Responsibilities of the Publisher

We are dedicated to confirming that editorial decisions remain uninfluenced by advertising or any other commercial revenue.

Innovation of Chemistry & Materials for Sustainability, an open access journal under the CC BY-NC-ND license.

Website: <https://insuf.org/journal/icms>

Published by Insuf Publications (OPC) Pvt. Ltd.; Website: <https://insuf.org/>

Address: BD51, Gitanjali Apartment, FL 5B, Rabindra Pally, Prafulla Kanan, North 24 Pgs, Kolkata, West Bengal, INDIA, PIN-700101.

Email: gargiagarwala@gmail.com; me-icms@insuf.org Contact Nos.: +919933060646; +918902278875.

Plagiarism Policy

The Innovation of Chemistry & Materials for Sustainability (ICMS) serves as a platform for both national and international researchers operating within similar fields. In the current digital landscape, plagiarism has transitioned into an online phenomenon. It has been observed that numerous individuals and researchers are illicitly appropriating the work of others and presenting it as their own in various journals. As a response, the ICMS is dedicated to publishing only original, high-quality research and vehemently discourages all forms of plagiarism.

Any individual or researcher found engaging in plagiarism risks being blacklisted and permanently barred from publishing their work in our journals. Additionally, the respective head of departments and the affiliated university of the plagiarist will be promptly notified, emphasizing the necessity for serious action to be taken against such misconduct.

Instructions for Authors

Manuscript submission

Authors are requested to review the submission instructions before sending their articles. It ensures a smooth review process. The journal template is readily accessible on our website. Authors should adhere to the formatting guidelines specified in the template. For convenience, we encourage authors to submit their articles through our online platform. This facilitates faster processing and tracking of submissions. Should you encounter any difficulties or have inquiries, please don't hesitate to reach out to us via email support-icms@insuf.org; me-icms@insuf.org

We are committed to assisting you throughout the submission process. The approval of a manuscript is subject to meeting the requirements of the *Innovation of Chemistry and Materials for Sustainability* (ICMS).

Authors are requested to follow the instructions before submitting the article. The template of the journal is available in the website. Authors are advised to submit the article online. Please contact us (support-icms@insuf.org; me-icms@insuf.org) if you find any complication.

The author details instruction is mentioned bellow.

Manuscript Preparation

Length and Word Count

- For a full-length article should be within 4000 words (10-12 pages, including Figures, References, Footnotes, Caption, Tables etc.)
- Short communication should be within 2500 words (4-6 pages), excluding references, footnotes, caption, tables, etc.
- The review article should be within 12000 words, including references, footnotes, caption, tables.
- Conference proceedings should be within 3000 words (6-8 pages)
- Book reviews should be within 2500 words (4-6 pages)
- Guest Editorials (by invitation only) should be within 1200 words (maximum)

Please contact us (support-icms@insuf.org) if you need further clarification/ guidance/ support.

Language and Style

All manuscripts must adhere to high standards of English proficiency. Papers with substandard language will be returned automatically for revision prior to review. Authors are encouraged to use either British or U.S. English consistently throughout their work. ICMS endeavors to adhere to the scientific terminology outlined by IUPAC guidelines and utilizes SI units wherever applicable. Before submitting, it falls on the author to guarantee that the scientific content is both accurate and comprehensible to the referees. Please contact us (support-icms@insuf.org) if any doubt.

The format should be following manner:

Title of article: Open Sans (align to left), 16 font size and bold;

Author's name: Open Sans (Center text), 11 font size and normal;

Affiliation/s: Open Sans (Center text), 8 font size and normal;

Abstract title (Open Sans; align to left; 11 font size bold): **Abstract text** in Open Sans (Justify text), 8 font size and normal; Single paragraph within 200 words

Keywords title (Open Sans; align to left; 11 font size bold): **Keywords text** in Open Sans (align to left), 8 font size and italic; 3-5 keywords.

Introduction title (Open Sans; align to left; 11 font size bold; 1st order heading): Main text in Open Sans (Justify text), 8.5 font size and normal;

Results and Discussion title section (Open Sans; align to left; 11 font size bold; 1st order heading): Main text in Open Sans (Justify text), 8.5 font size and normal;

Results and Discussion title sub section (Open Sans; align to left; 8.5 font size bold; 2nd order heading): Main text in Open Sans (Justify text), 8.5 font size and normal;

Conclusions title section (Open Sans; align to left; 11 font size bold; 1st order heading): Main text in Open Sans (Justify text), 8.5 font size and normal;

Experimental title section (Open Sans; align to left; 11 font size bold; 1st order heading): Main text in Open Sans (Justify text), 8.5 font size and normal;

Experimental title sub section (Open Sans; align to left; 8.5 font size bold; 2nd order heading): Main text in Open Sans (Justify text), 8.5 font size and normal;

Supporting Information title section (Open Sans; align to left; 11 font size bold; 1st order heading): Main text in Open Sans (Justify text), 8.5 font size and normal;

Author Contribution Declaration title section (Open Sans; align to left; 11 font size bold; 1st order heading): Main text in Open Sans (Justify text), 8.5 font size and normal;

Data Availability Declaration title section (Open Sans; align to left; 11 font size bold; 1st order heading): Main text in Open Sans (Justify text), 8.5 font size and normal;

Acknowledgements title section (Open Sans; align to left; 11 font size bold; 1st order heading): Main text in Open Sans (Justify text), 8.5 font size and normal;

References title section (Open Sans; align to left; 11 font size bold; 1st order heading): Main text in Open Sans (Justify text), 7 font size and normal;

Cover Letter

ICMS suggests that authors provide a cover letter along with their submitted manuscripts, as it aids editors or referees in comprehending the significance of the work. Please suggest **four potential referees** who are familiar with your work.

Please adhere to the following order of presentation:

Author name and affiliation: The author(s) should comprise the full first and last names. In cases where there are multiple authors, it should be clearly stated who will handle correspondence regarding the paper, designated as the corresponding author, and denoted with a single asterisk (*) in superscript. Additional authors and their corresponding addresses should be indicated with superscripts a, b, c, etc. The corresponding author's contact information, including email address, full postal address, telephone number, and fax number, should be provided.

Author's Name:

Open Sans (Centered text), 11 font size, normal

Affiliation/s:

Open Sans (Centered text), 8 font size, normal

Abstract: The abstract must succinctly encapsulate the article by outlining the addressed questions and highlighting the study's key findings. It should not function as an introduction or include references. This section should comprise a single paragraph, approximately 200 words in length, providing a pertinent overview of the work.

Abstract title:

Open Sans; align to left; 11 font size bold

Abstract text:

Open Sans (Justify text), 8 font size and normal; Single paragraph within 200 words.

Keywords: Immediately following the abstract, include 3-5 concise keywords. It should be included 80 characters including spaces. These keywords aid in indexing the article for readers. Keywords like "keyword1, keyword2, keyword3," etc., are recommended.

Keywords title (Open Sans; align to left; 11 font size bold): Keywords text in Open Sans (align to left), 8 font size and italic.

Introduction: The article encompasses its scientific significance, historical context, relevance to other fields, and its objectives.

Introduction title (Open Sans; align to left; 11 font size bold; 1st order heading): Main text in Open Sans (Justify text), 8.5 font size and normal;

Material and Methods: The writing should contain enough detail for others to replicate the author(s)'s work.

Material and Methods title section (Open Sans; align to left; 11 font size bold; 1st order heading): Main text in Open Sans (Justify text), 8.5 font size and normal;

Material and Methods title sub section (Open Sans; align to left; 8.5 font size bold; 2nd order heading): Main text in Open Sans (Justify text), 8.5 font size and normal.

Results and Discussion: This section can either be integrated or maintained as distinct, and can also be subdivided further if necessary. Technical details should be avoided in this section.

Results and Discussion title section (Open Sans; align to left; 11 font size bold; 1st order heading): Main text in Open Sans (Justify text), 8.5 font size and normal;

Results and Discussion title sub section (Open Sans; align to left; 8.5 font size bold; 2nd order heading): Main text in Open Sans (Justify text), 8.5 font size and normal.

Conclusion: Compose the final statement for the article, encapsulating the paper's key conclusions succinctly.

Conclusions title section (Open Sans; align to left; 11 font size bold; 1st order heading): Main text in Open Sans (Justify text), 8.5 font size and normal

Acknowledgments: Recognize the individuals, grants, funds, and other contributors who significantly influence the content of this article. Funding organizations should be identified by their full names.

It's essential to adhere to research integrity by acknowledging your funding agencies and any infrastructural or personal assistance received during manuscript preparation.

References: References ought to be sequentially numbered, such as 1, 2, 3, 4, and so forth. In the text, references must be indicated by consecutive superscript numbers, like (e.g., ¹ or ^{1,2,3}). References title section (Open Sans; align to left; 11 font size bold; 1st order heading): Main text in Open Sans (Justify text), 7 font size and normal. The reference list should be arranged in the order of their initial mention in the text and formatted accordingly.

(1) For article: (a) F. (Firstname initial) M. (Middlename initial) Surname (Lastname), F. (Firstname initial) M. (Middlename initial) Surname (Lastname), F. (Firstname initial) M. (Middlename initial) Surname (Lastname). Title of the article. *Journal Name (Abbreviated)*. Year, Volume, first page. [Mention DOI link here](#) (b) F. (Firstname initial) M. (Middlename initial) Surname (Lastname), F. (Firstname initial) M. (Middlename initial) Surname (Lastname), F. (Firstname initial) M. (Middlename initial) Surname (Lastname). Title of the article. *Journal Name (Abbreviated)*. Year, Volume, first page. [Mention DOI link here](#).

(2) For book: (a) Editors name in *Title of book*, Vol. X (Eds.: S. K. Sinha, A. B. Madan, S. K. Ghosh, S. Shukla), Cambridge, Year, Ch.X, page range. [Mention DOI link here](#). (b) A. Engel, *Title of book*, Publishers, Oxford, Year, Ch.X, pp. 215-310. [Mention DOI link here](#)

(3) (a) F. (Firstname initial) M. (Middlename initial) Surname (Lastname), F. (Firstname initial) M. (Middlename initial) Surname (Lastname), F. (Firstname initial) M. (Middlename initial) Surname (Lastname). Title of the article. *arXiv preprint (Abbreviated)* Year, [Mention DOI link here](#)

(4) For Crystal Information: Deposition numbers (CCDC numbers) xxxxxx (for X), yyyyyy (for Y), and zzzzzz (for Z) contain the supplementary crystallographic data for this paper.

Tables and Figures

Tables and figures need to be integrated within the text. Each table should have a concise descriptive title positioned above it, accompanied by a clear legend, and any footnotes should be appropriately marked below. Refrain from using vertical lines. Tables and figures should be sequentially numbered as they appear in the text, labeled as Table 1, Table 2, etc., for tables, and Fig. 1, Fig. 2, etc., for figures. Figures must be fully labeled, considering potential size adjustments. Captions should be double-spaced.

If there are images, tables, photographs, diagrams, graphs, etc., in the article that have been published elsewhere (such as in books, journals, conference presentations, etc.), the author is accountable for acquiring permission from the original author, publisher, or copyright holder to reproduce the material.

Equations

Each equation should be displayed on a separate line, with appropriate punctuation placed before and after it. All equations must be sequentially numbered, with the number of the equation placed near the right-hand margin. Avoid using bars above or below letters, and refrain from using subscripts on subscripts. Sufficient space must be allocated for marking superior and inferior letters or numbers. Overcrowded equations can result in compositional errors. When referencing equations in the text, use the following format: "Equation (5) follows from substituting Eqs. (2) and (3) into Eq. (4)."

Nomenclature

The nomenclature ought to adhere to present American standards. Whenever feasible, writers should employ systematic designations that align with those utilized by the Chemical Abstracts Service or IUPAC.

External Review

The process of external review commences when the editor dispatches the manuscript for evaluation. Upon receiving the reports, the editor deliberates based on the recommendations and the manuscript's revision history, then notifies the author of the decision via a decision letter.

Decisions for initial submissions are as follows:

- Manuscripts with negative or inadequately supportive reviews will be declined.
- In all other cases, including mixed reviews, the manuscript will be returned for revision with guidance for resubmission.
- Authors are required to accompany resubmissions with a cover letter summarizing revisions and addressing the editor's and/or reviewers' concerns. Resubmitted manuscripts typically undergo re-evaluation by previous reviewers and occasionally new ones.

Revised Manuscript

Authors are expected to submit a revised manuscript within 10 days for minor changes and within 3 weeks for major revisions. Failure to meet these deadlines will result in the manuscript being considered withdrawn, and any subsequent submissions will be treated as new contributions. Authors may request additional time from the editor if necessary.

After acceptance:

Copyright Policy

Innovation of Chemistry & Materials for Sustainability (ICMS) typically does not accept articles that have previously appeared in a similar form, regardless of language. Please confirm that your submission is not under consideration for publication elsewhere. Authors must be willing to transfer copyright to **ICMS** and **Insuf Publications (OPC) Pvt. Ltd**, and all authors must agree to submit the paper to ICMS. If the article includes previously published images, tables, photographs, diagrams, or graphs, authors are responsible for obtaining permission from the original copyright holders.

To share your article after it has been published in ICMS, please refer to our Open Access policy.

Copyright transfer: Authors will be requested to assign copyright of the article to the publisher, guaranteeing the broadest protection and dissemination of information in accordance with copyright laws.

Proof reading: The corresponding author will be provided with a proof and is expected to return it to the publisher within three days of receipt. Only typos errors should be corrected; any other alterations will be reviewed and amended, as late corrections cannot be accommodated. The final proof must be approved by the corresponding author(s). Failure to obtain approval may result in the withdrawal of the article from publication.

Correction and Retraction Policy:

Corrections

Corrections are issued when the accuracy of published information significantly impacts the publication record. These corrections are included in the following release under the section titled "Corrections and Addendum".

Retractions

Retractions occur when the primary conclusion of a paper is significantly compromised. Readers are advised to initially reach out to the original paper's authors and subsequently inform the journal, attaching any correspondence exchanged with the authors. The editor will seek feedback from reviewers. Retraction of the article may be warranted in instances of multiple submissions, plagiarism, or fraudulent data usage.

Impact Factor

This journal, launched in June 2024, will undergo annual evaluation of its impact factor by various indexing agencies in 2025, with routine updates provided here.

Year	Impact Factor
2024	XXXX (Available in 2026)

Innovation of Chemistry & Materials for Sustainability, an open access journal under the CC BY-NC-ND license.

Website: <https://insuf.org/journal/icms>

Published by Insuf Publications (OPC) Pvt. Ltd.; Website: <https://insuf.org/>

Address: BD51, Gitanjali Apartment, FL 5B, Rabindra Pally, Prafulla Kanan, North 24 Pgs, Kolkata, West Bengal, INDIA, PIN-700101.

Email: gargiagarwala@gmail.com; me-icms@insuf.org Contact Nos.: +919933060646; +918902278875.

Policy on Ethics and Governance

The Innovation of Chemistry & Materials for Sustainability (ICMS) adheres to globally acknowledged ethical standards for scientific publishing.

Authorship

This journal invites submissions from academics and industry researchers across all fields outlined in our "Aims & Scope". The corresponding author is required to list all co-authors and contributors, with the agreement of each author to be named and to submit the article to this journal.

To receive authorship credit, one must satisfy three fundamental criteria:

- Significant involvement in formulating the study's conception and design, gathering and analyzing data, and interpreting findings
- Drafting or refining the article to ensure intellectual coherence
- Providing scientific endorsement for the final iteration

People engaged in a research project who don't meet the journal's authorship requirements can be acknowledged in the Acknowledgements section. This may include those who offered advice, provided research facilities, oversaw the department, or secured financial support.

The author's affiliation must accurately reflect their status at the time of completing the work. For instance, if an author was affiliated with a different company, university, or institution when the work was done, that should be indicated as their affiliation. If an author's affiliation has since changed, their current affiliation can be noted as "Current address...".

All eligible authors must be included on the list, with no restriction on the number of authors per paper. The order of authors is not specified by us.

Authors seeking publication in this journal must possess appropriate qualifications and be prepared to furnish evidence upon request. This may include one or more of the following:

- Proof of present or previous association with an institution (such as a university, research institute, or company).
- Membership in an acknowledged national or international scientific organization.
- Confirmation of a documented publication history in respected scientific journals.
- The corresponding author must possess an ORCID identifier

The author(s) designated as corresponding should furnish at least one institutional email address that has been authenticated for our documentation.

Acknowledgements

Please reflect mentioning any individuals, organizations, or departments that have contributed to the project through data provision, equipment support, services (such as analytical services), image sharing, funding, or inspiring discussions. However, they may not qualify as co-authors for the paper. All individuals named in the Acknowledgements must provide consent to be mentioned.

Copyright holders should be acknowledged beside the corresponding image or data they provided.

Peer review policy

All articles will undergo assessment by referees, also referred to as peer reviewers, to evaluate the scientific merit and suitability for publication. Referees are chosen from a global pool of proficient scientists with recent contributions in the pertinent field(s). The *Innovation of Chemistry & Materials for Sustainability* (ICMS) typically engages single-blind peer review. This entails that referees are responsive of the authors' identities, while the referees' reports remain anonymous.

At the Editor's discretion, double-blind peer review may be applied instead of single-blind review. In this approach, the referees are uninformed of the authors' identities. Every effort will be made to secrete authors' identities, although thorough privacy cannot be guaranteed.

Referees suggested by the author

Authors are welcome to suggest potential referees upon submission within cover letter. Additionally, if there are any referees the authors feel should not be approached due to potential conflicts of interest, they should inform the Editor. However, the final choice of referees will be at the decision of the Editor.

It's important to note that providing inaccurate information, such as suggesting referees with false identities or contact details, will lead to rejection of the manuscript.

***For any inquiry/complain regarding policy on ICMS research ethics, please contact research ethics and integrity team (Email: integrity-icms@insuf.org)**

Article Processing Charges

What is the rationale behind ICMS requiring authors to pay publication fees?

All original research papers published by *Innovation of Chemistry & Materials for Sustainability* (ICMS) are immediately and permanently accessible online at no cost upon publication. We ensure that neither university libraries nor individual readers will ever need to purchase a subscription or pay any pay-per-view fees to access articles in the electronic format of any journal. Consequently, ICMS does not generate revenue from electronic subscriptions or pay-per-view fees.

However, the online publication process does incur expenses, including the setup and maintenance of publication infrastructure, ongoing journal operations, manuscript processing through peer review, editing, publishing, maintaining scholarly records, and archiving. To offset these costs, ICMS levies publication fees, also known as Article Processing Charges (APCs), from authors. Subscription charges are applicable only for the printed version of the journal. APCs are payable upon acceptance of a manuscript for publication.

Journal Title	Regular APC*
<i>Innovation of Chemistry & Materials for Sustainability</i> (ICMS)	\$150 (Rs. 12000/-)

*Authors from Low-Income Countries receive APC reductions. There is no APC for invited article.

***For any inquiry, please feel free to contact us,**

Email: gargiagarwala@gmail.com; me-icms@insuf.org

Contact Nos.: +919933060646; +918902278875

Note: ICMS does not require Article Submission Charges, also referred to as Submission Fees, which are typically payable upon manuscript submission. Additionally, ICMS does not impose charges based on the number of pages, inclusion of colour figures, or any other items that other publishers often levy fees for.

It's worth noting that ICMS's standard Article Processing Charges (APC) are notably below average. Despite this, ICMS remains committed to enhancing the quality of both authorship and readership experiences through various means, such as:

- **Providing detailed article-level metrics** to track the reach and impact of individual publications.
- **Covering production expenses**, including copyediting, typesetting, formatting, and assigning **Digital Object Identifiers (DOIs)**.
- **Maintaining and hosting the journal's website** to ensure continuous online access to articles.
- **Calculating journal performance indicators**, such as the two-year Google-based Journal Impact Factor (2-GJIF).
- **Archiving articles on Porch** to guarantee long-term digital preservation and accessibility.
- **Facilitating indexing and discoverability** by submitting articles to multiple databases and search engines.
- **Supporting administrative functions**, including staff compensation, IT infrastructure, and author services.
- **Managing the editorial and peer review process**, which includes coordinating reviewers, handling revisions, and ensuring editorial quality and decision-making integrity.

Authors should also consider the cost-effectiveness or value for money of publishing Open Access with ICMS, which the organization believes it excels at. However, further research is necessary to fully understand this aspect.

SUBSCRIPTION INFORMATION

Subscription type: Library/ Institution/ Industry/ Personal

Name: Mr./Ms./Dr/Prof: Designation:

Organization: Address for Communication:

City: State: PIN:

Tel. (off.): (Mobile): (Resi.):

Email:

Date:

Signature of Subscriber:

Innovation of Chemistry & Materials for Sustainability, an open access journal under the CC BY-NC-ND license.

Website: <https://insuf.org/journal/icms>

Published by Insuf Publications (OPC) Pvt. Ltd.; Website: <https://insuf.org/>

Address: BD51, Gitanjali Apartment, FL 5B, Rabindra Pally, Prafulla Kanan, North 24 Pgs, Kolkata, West Bengal, INDIA, PIN-700101.

Email: gargiagarwala@gmail.com; me-icms@insuf.org Contact Nos.: +919933060646; +918902278875.

SUBSCRIPTION FORM

(Innovation of Chemistry & Materials for Sustainability)

No. of Years	Subscription Charges*
1 st Year	\$500 (Rs.30000/-)
2 nd Year	\$800 (Rs.50000/-)
3 rd Year	\$1000 (Rs.70000/-)
4 th Year	\$1200 (Rs.90000/-)
5 th Year	\$1500 (Rs.110000/-)

Mode of Payment

Subscriptions must be paid in advance, with all rates covering postage and taxes. We kindly ask subscribers to include payment with their order when possible. Issues will be sent only upon receipt of payment. Payments can be made via online transfer, and the details should be sent to the director of INSUF PUBLICATIONS (OPC) PVT. LTD. (Email: gargiagarwala@gmail.com) or Managing Editor, ICMS (Email: me-icms@insuf.org) or Editor, ICMS (Email: editor-icms@insuf.org).

Payment Details:

Beneficiary Name: **Insuf Publications (OPC) Private Limited**

Bank Name: **HDFC Bank**; Branch Name: **Kestopur**; Bank Account No.: **50200097905680** (Current Account)

RTGS/NEFT IFSC Code: **HDFC0002492**; Branch Address: **HDFC Bank LTD, Akashdeep Apartments, 3AC-232,1 Prafulla Kanan, Kolkata – 700101, West Bengal, INDIA.**

You can also place your journal orders using the following methods:

1. Email your order to me-icms@insuf.org, editor-icms@insuf.org, or gargiagarwala@gmail.com.
2. To order by phone, call us at +91-9933060646 or +91-8902278875.
3. For orders via regular mail, please send your complete subscription information and payment details to:

Director,

Insuf Publications (OPC) Pvt. Ltd.

Address: BD51, Gitanjali Apartment, FL 5B, Rabindra Pally, Prafulla Kanan, Kolkata-700101, West Bengal, INDIA.

Contact: +919933060646; +918902278875. Email: gargiagarwala@gmail.com; me-icms@insuf.org Website: <https://insuf.org/>

Table of Content

S. No.	Title	Author's Name (s)	Page Nos.
1.	Fostering Sustainable Innovation: Blueprints for Tomorrow (Editorial)	Susanta Banerjee	001-001
2.	Democratize the Dissemination of Knowledge and Hurry on a Greener, Sustainable Planet (Notes)	Gargi Agarwala Mahato	002-002
3.	Insights on Metal-Free Type I Photosensitizers for Photodynamic Therapy	Roopa and Naresh Kumar	003-010
4.	Mastering Chirality: Unlocking Bioactive Natural Products with Oxazaborolidines and Oxazaborolidinones	Yogesh Kumar Walia, Souvik Sarkar, Soma Das Pradhan, and Prasun Kanti Pradhan	011-029
5.	Recent Development and Challenges in Metal Chalcogenide Quantum Dots: From Material Design Strategies to Applications	Pratibha Chahal, Aayushi Goel, and Avinash Singh	030-046
6.	Advances in Green and Sustainable Photo Redox Catalysis for Organic Transformation	Yafia Kousin Mirza, Partha Sarathi Bera, Ajeet Kumar Pandey, and Milan Bera	047-057
7.	Polypharmacological Constituents and Potential Activities of <i>Bergenia ciliata</i> : A Concise Review	Nirza Moktana and Anindita Banerjee	058-065
8.	The Significance of Air Pollution in the Process of Stone Deterioration	Abhishek Singh, Tanvir Arfin, Nikhila Mathew, and Abha Tirpude	066-075
9.	Composites of Chitosan for Biomedical Applications	Ayanjeet Chowdhury, Samyak Dhale, RBK Dinesh Kumar, Andrew Biju John, Jaya Lakkakula, and Nilesh S. Wagh	076-092
10.	Preparation and Characterization of Aloe Maculata/Chitosan Composite Gel for Wound Healing Application	Hilda Ngomane, Lungiselwa Ndzabandzaba, and Vuyiswa Jane Mkhabela	093-097

Note: You can visit our website <https://insuf.org/journal/icms> to access these articles.

We invite you to submit your valuable article for the January-June 2025 issue of our open access journal.

Note: Please be aware that there are no Article Processing Charges (APC) for this issue. Additionally, we will never take APC for invited review articles.

Fostering Sustainable Innovation: Blueprints for Tomorrow

Dear Esteemed Colleagues and Readers,

It is with great pleasure and anticipation that I extend my warmest welcome to you all as the Founding Editor-in-Chief of *Innovation of Chemistry & Materials for Sustainability* (ICMS), an open-access journal dedicated to advancing research at the intersection of chemistry and materials science for sustainable future as traditional subscription-based models often limit the accessibility of research findings to a privileged few, hindering the potential for widespread knowledge dissemination. Thus, this open access holds immense significance in today's rapidly evolving academic landscape to break down these barriers and provide researchers, scholars, scientists, and the public at large with unlimited access to valuable scientific knowledge.

As we stand at the beginning of a new era, characterized by exceptional global challenges and opportunities, the imperative for innovation in chemistry and materials science has never been more pressing. Climate change, resource depletion, environmental pollution, and societal inequality are among the complex issues that demand our unwavering attention and concerted action. However, in the face of these challenges, we also find ourselves at the dawn of a remarkable era of scientific discovery and technological advancement, where the synergistic application of chemistry and materials science holds immense promise for driving positive change. ICMS emerges as an inspiration of hope and a catalyst for progress in this transformative passage towards a more sustainable future. Our journal is devoted to publishing cutting-edge research that not only expands the frontiers of knowledge but also translates scientific insights into concrete explanations with real-world impact. By raising interdisciplinary collaboration and promoting the principles of open access and transparency, we aim to accelerate the pace of innovation and facilitate the dissemination of ground-breaking discoveries to a global audience.

Innovation is the foundation of growth, and it is our steady commitment to foster ground-breaking research that pushes the boundaries of what is possible. From novel materials design to sustainable synthesis methods, from renewable energy technologies to waste valorization strategies, our journal will showcase the latest advancements that hold the promise of a brighter future for generations to come. Our journal is poised to be a beacon of light in this transformative era, where innovation converges with sustainability to forge a path toward a greener and more equitable world.

At the heart of our mission lies a deep-seated belief in the power of science to address the most pressing challenges facing humanity. Through rigorous peer review and editorial excellence, we strive to uphold the highest standards of scholarship and integrity, ensuring that the research published in our journal is of the utmost quality and significance. Furthermore, we are firmly committed to promoting diversity, equity, and inclusion within our editorial team, authorship, and readership, recognizing that innovation thrives in environments that embrace diverse perspectives and experiences.

As we embark on this journey together, I extend my heartfelt gratitude to our esteemed editorial board, and dedicated reviewers, invited researchers, practitioners, policymakers, and visionary authors who have entrusted us with their invaluable contributions from around the world to join us in our quest for sustainable solutions.



Whether you are a seasoned expert or a budding scholar, your contributions are invaluable in shaping the discourse and driving meaningful change. Together, let us harness the power of innovation in chemistry and materials science to build a more resilient, equitable, and sustainable future for a brighter tomorrow.

Thank you for your support, and I look forward to embarking on this exciting adventure with you.

Warm regards,



Susanta Banerjee 

Professor (HAG) & Institute Chair Professor
Chairperson, Central Research Facility
Former Head, Materials Science Centre
Indian Institute of Technology Kharagpur
Kharagpur - 721302, India.

Author Information

Email: susanta@matsc.iitkgp.ac.in

Biography

Prof. Dr. Susanta Banerjee has been associated with the Indian Institute of Technology Kharagpur, India, for over 18 years. He previously served as the head of the Materials Science Centre (May 2014 to May 2017) and is currently the Institute Chair Professor and Chairperson of Central Research Facility. Before joining IIT Kharagpur he served 14 years as Scientist at DRDO and GE India Technology Centre, Bangalore. He is the recipient of the prestigious AvH fellowship from Germany and a fellow of the WAST. Prof. Banerjee has supervised over 30 doctoral and 45 master's theses in polymer and materials science and engineering. He has completed many exciting projects at DRDO, GEITC, and IIT-Kharagpur, driven by his passion for advocating future sustainability.

Notes

The views expressed in this editorial agreed by the Insuf Publications.

Democratize the Dissemination of Knowledge and Hurry on a Greener, Sustainable Planet

Dear Scientists, and Policymakers,

I am thrilled to announce the launch of our open access journal, *Innovation of Chemistry & Materials for Sustainability* (ICMS). As the Managing Editor, it is my honor to initiate this platform dedicated to develop the frontiers of sustainable chemistry and materials science.

In today's world, sustainability is not simply a catchphrase, but a necessity; it is a crucial and essential guiding scientific research and technological innovation. Thus, our collective responsibility to nurture sustainable solutions are more urgent. Our journal is committed to publish cutting-edge research that addresses the pressing challenges facing our planet, from developing eco-friendly materials to designing renewable energy solutions.

What sets our journal apart is its emphasis on open access, ensuring that groundbreaking research is freely accessible to scientists, policymakers, and the general public worldwide. By fostering collaboration and knowledge sharing, we aim to accelerate progress towards a more sustainable future.

I invite researchers, scholars, and practitioners from across the globe to join us on this exciting journey. Whether you are working on novel materials synthesis, green chemistry methodologies, or sustainable manufacturing processes, we welcome your contributions to our journal.

Together, let us push the boundaries of scientific breakthrough to create a world where chemistry and materials science pave the way for a more sustainable tomorrow. I believe you will

support our open access journal ICMS to democratize the dissemination of information and to consider as a catalyst for changing in the pursuit of a sustainable future. By sharing knowledge freely and transparently, we unlock the potential to transform challenges into opportunities, paving the way for a greener, more resilient world.



Best regards,

Ms. Gargi Agarwala Mahato,
Managing Editor, *Innov. Chem. Mater. Sustain.* (ICMS)
Director, Insuf Publications (OPC) Pvt. Ltd.

Author Information

Emails. me-icms@insuf.org; gargiagarwala@gmail.com

Biography

Ms. Gargi Agarwala Mahato is associated with journalism profession last seventeen years. She is also serving as Editor-in-Chief in Uttarapath. Her area of interest is women empowerment, changing pattern of tribal life, and create awareness sustainability.

Cover Page: The Indian Scops Owl



Photo Credit: Dr. Vishal A. Mahajan

Cover Page Image

A well-camouflaged sub-adult Indian scops owl in Aravalli mountain range takes refuge in old tree trunks, allowing it to evade predators and it can produce a distinctive high-pitched "whuk" call, which serves for social interaction and attracting mates.

REVIEW ARTICLE

Insights on Metal-Free Type I Photosensitizers for Photodynamic Therapy

Roopa^a and Naresh Kumar^{b*}

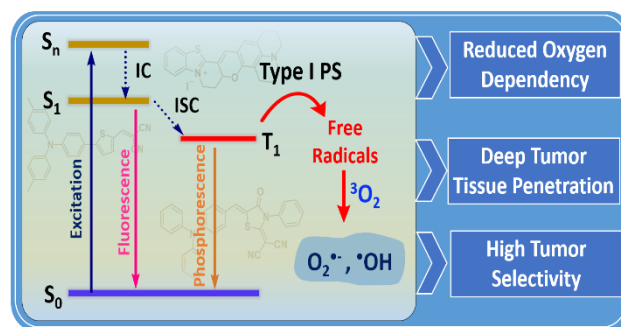
^aDepartment of Chemistry, I. K. Gujral Punjab Technical University, Kapurthala 144603 Punjab, India

^bDepartment of Chemistry, SRM University, Delhi-NCR, Sonapat-131029, Haryana, India

*Correspondence: naresh.chem.ia@gmail.com

Abstract: Non-invasive treatment techniques have drawn a lot of interest due to the rising need for precise and secure cancer treatment.

One such treatment method is photodynamic therapy (PDT), which uses the light irradiation of photosensitizers (PSs) to produce reactive oxygen species (ROS), which kill cancer cells. Most of the conventional photosensitizers used in the PDT process rely on molecular oxygen to produce cytotoxic ROS, known by the name of type II PSs. Because type II PSs requires oxygen to produce ROS, their full potential is not realized in hypoxic tumor tissues. On the other hand, type I PSs can increase the effectiveness of PDT in hypoxic tumor tissues since they rely less on oxygen to produce ROS. Consequently, it has become increasingly crucial to develop type I PSs to treat hypoxic malignancies. Numerous type I PSs of inorganic origin have been developed so far. Nonetheless, certain issues like poor biodegradability and persistent toxicity exist. Type I PSs based on organic compounds were developed in response to these concerns since they are comparatively more biocompatible and biodegradable. Therefore, in this article, we describe recent developments in the development of organic type I PSs for the PDT.



Keywords: photosensitizer, photodynamic therapy, superoxide anion, hypoxia.

Contents

Biographical Information	3
1. Introduction	3
2. PDT Mechanisms	4
3. Need for type 1 organic PSs	4
4. Type 1 organic PSs	4
5. Conclusion	8
Author Contribution Declaration	8
Data Availability Declaration	8
Acknowledgements	8
References	8

1. Introduction

Photodynamic therapy (PDT) is a light-promoted approach that uses functional molecules, known as photosensitizer (PS), to induce cell death via the generation of reactive chemical species.¹ The idea that light and a chemical agent can be combined has a long history. The benefits of sunlight as a therapy were employed in ancient Egypt, China, and India to treat skin cancer, vitiligo, psoriasis, and rickets.² The current form of PDT can be traced back to the discoveries made by Oscar Raab in 1900, who found that light and acridine orange together are fatal to paramecia.³ Researchers have used light and small functional molecules to cure a variety of ailments, particularly cancer, throughout the past century.⁴ A major cause of death on a global scale is cancer.⁵ Nowadays, cancer patients are usually treated with a combination of multiple approaches including chemotherapy, surgery, and radiation therapy. However, some disadvantages of these traditional treatments include their high invasiveness, lack of selectivity, and serious adverse health effects.⁶ In contrast to these traditional treatments, photodynamic therapy (PDT), a recently established therapeutic procedure, has demonstrated excellent

prospects for the treatment of cancer with superior safety and therapeutic success.⁷ The PDT process is characterized by the conversion of molecular oxygen into reactive oxygen species (ROS) to kill the cancer cells. The photosensitizers (PSs), light, and tissue oxygen are the main components of the photodynamic therapy. Photosensitizers are a key component in the PDT process's effectiveness.

Roopa received her PhD under the supervision of Dr. Vandana Bhalla in 2012 at Guru Nanak Dev University, Amritsar, India. She worked as a specially appointed researcher at PPSM, ENS Paris Saclay, Université Paris Saclay. Presently, she is working as an Assistant Professor at the Department of Chemistry, IKG-PTU. Her research focuses on fluorescent probes for species of environmental and biological importance.



Naresh Kumar received his PhD from Guru Nanak Dev University, India. He then joined PPSM, ENS Paris Saclay, Université Paris Saclay as a postdoctoral fellow. From 2016–18, he worked as a JSPS researcher at Osaka University in the laboratory of Professor Kazuya Kikuchi. Presently, he is working as an Assistant Professor at SRM University, Delhi-NCR, India. His research interests include synthetic probe-based molecular recognition and imaging.



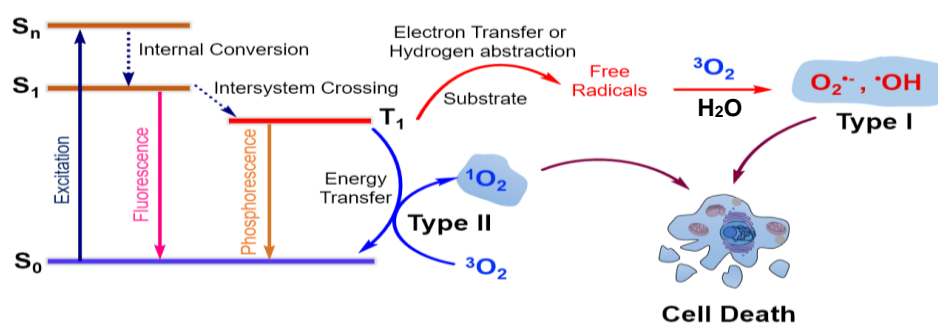


Figure 1. A schematic representation of PDT mechanisms, type I and II.

This is due to the fact that PS, when activated by light, releases its excited-state energy or electron into the surrounding tissue oxygen or substrate, resulting in the production of reactive oxygen species (ROS), which kill cancer cells. PDT has the advantage of selectively targeting cancer cells or tissue while preserving normal cells, as PSs introduce cytotoxicity when exposed to specific light types.

2. PDT Mechanisms

There are primarily two kinds of PDT processes, which are based on the mechanisms that generate ROS.⁸ Photoreactions where PSs based on electron transfer generate superoxide anion ($O_2^{\bullet -}$) species are involved in the type I PDT process (Figure 1). On the other hand, if PSs produce singlet oxygen (1O_2) by an energy transfer mechanism, then a PDT process is type II (Figure 1). Though PDT has advanced quickly, its use as a first-choice therapeutic method is limited by the absence of an optimal photosensitizer that can satisfy the cancer treatment requirements. The development of photosensitizers with the necessary characteristics, such as deep tissue penetration, high ROS production ability, near-infrared (NIR) absorption, and tumor selectivity, has been the focus of efforts to improve PDT efficiency.

Most of the PSs developed to date are based on a type II mechanism (Figure 1) in which generated 1O_2 is used to kill malignant cells.⁹ For the type II PDT approach, a number of PSs of both organic and inorganic origins have been produced; some of these have even been given approval to treat cancer.^{1b,9} Low oxygen levels, which result in hypoxia, are a characteristic of tumors. Since type II PS requires oxygen for the generation of singlet oxygen, the type II PDT process exhibits reduced therapeutic efficacy in hypoxic tumor tissues.¹⁰ The oxygen requirement of type II PDT process limits its efficacy, even though it is combined with other reagents to overcome the oxygen deficiency.¹¹ On the other side, because of its lower oxygen requirement than type II PDT, type I PDT has demonstrated tremendous potential in combating against hypoxic malignancies. When exposed to radiation, type I PS generated excited PS in its singlet state by absorbing light energy. Radiative or non-radiative pathways can return the excited PS to its ground state. Alternatively, to produce PS in its triplet excited state (Figure 1), the singlet excited PS can go through intersystem crossing. This triplet state of PS is converted into an anion radical or a cationic species through electron or proton transfer to biological substrates such as cell membranes or electron-rich molecules. After further interaction with water or molecular oxygen, the anionic radical or cationic species form cytotoxic superoxide anion ($O_2^{\bullet -}$) or hydroxyl radicals ($\bullet OH$).¹² With type I PDT, as opposed to type II PDT, it is possible to improve the therapeutic efficacy against oxygen-depleted (hypoxic) tumors. Consequently, the development of

type I photosensitizers, which have a reduced oxygen dependence, is getting attention.

3. Need for type I organic PSs

Type I PS have been developed using different molecular platforms. For instance, TiO_2 , because of its charge-separate state formation, have been reported to generate superoxide radical.¹³ Metal-complexes of transition metals and inorganic nanocomposites have been developed as a type I PSs.¹⁴ However, the high level of immunotoxicity, low tissue penetration depth, and poor repeatability of these complex materials limit their clinical application. Given these factors, molecules of organic origin are suitable because of their easy preparation, remarkable repeatability, diverse structures, and customizable properties. Thus, there has been a focus on developing type I PSs based on organic compounds in recent years. In this article, we are discussing the type I PSs of organic origin developed for PDT in the last few years.

4. Type I organic PSs

Numerous metal-based compounds have been used as type I photosensitizers in PDT, as was previously mentioned. Unfortunately, most inorganic PSs have a poor rate of biodegradation and may persist in body tissues for extended periods of time, which raises the possibility of long-term toxicity. In contrast, organic molecules are relatively biocompatible in nature, easy to metabolize, and characterized by low toxicity.¹⁵ Nile blue is an organic dye molecule that, with some modifications, has been shown to exhibit ROS generation ability and is employed in photodynamic therapy.¹⁶ In 2018, Peng and colleagues developed a type I photosensitizer molecule **1** (ENBS-B) based on the Nile blue fluorophore (Figure 2).¹⁷ According to the described investigations, **1** has a great capacity to produce $O_2^{\bullet -}$ in a hypoxic environment when exposed to light. Molecule **1** showed strong absorption at ~660 nm and an emission band at ~660 nm. The absorbance of the **1** in the longer wavelength region is useful to get deeper probe penetration as well as to reduce the chances of phototoxicity. According to the authors, light irradiation of **1** produces $O_2^{\bullet -}$, which causes cellular lysosomes and nuclei to break down and causes cancer cells to undergo apoptosis. Though, **1** showed selectivity towards cancer cells due to its biotin unit, its low retention in malignant cells results in an inadequate therapeutic approach. Furthermore, one of the prerequisites for the activation of PSs and the successful completion of the PDT process is the absorption of light by PSs located deep within malignant tissues. This is an important fact because, deep within malignant tissues, most PSs have poor light absorption, which limits their applicability.

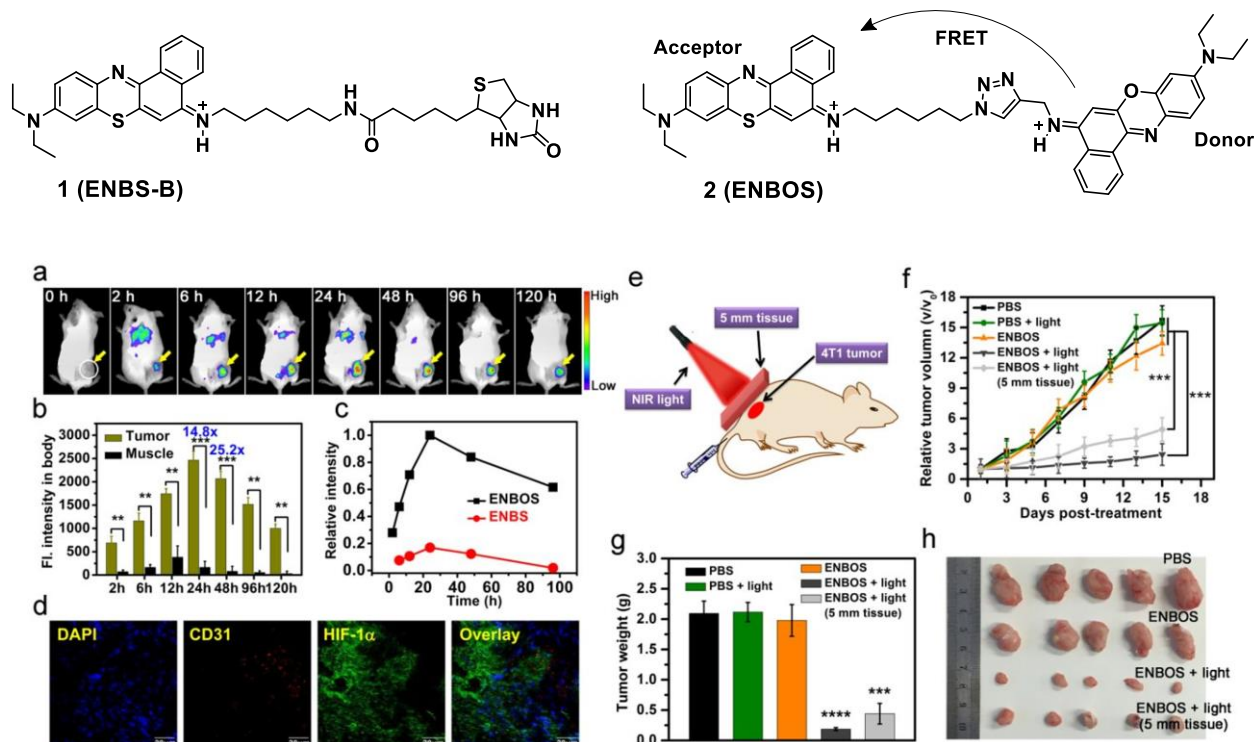


Figure 2. Structures of 1 (ENBS-B) and 2 (ENBOS). (a) 14T1 tumor-bearing mice's in vivo fluorescence imaging upon an intravenous injection of 1 (ENBS-B). (b) Change in ENBOS fluorescence in the tumor and surrounding muscle tissues. (c) Time dependent relative fluorescence of ENBOS and ENBS (without acceptor unit) in 4T1 tumors. (d) Tumor slice immunofluorescence imaging. (e) Diagram showing ENBOS-mediated PDT in deep hypoxic tumor. (f) Relative tumor volume. (g and h) Average tumor weights and associated tumor images. Figures a-e, adapted with permission from ref. 18. Copyright 2019 American Chemical Society.

In this context, Peng and coworkers have developed a FRET (Förster resonance energy transfer)-derived PS, 2 (ENBOS), to achieve enhanced light absorption ability and thus high $O_2^{\cdot -}$ production deep inside the hypoxic tumor tissues (Figure 2).¹⁸ The reported PS was the combination of Nile blue dye (energy donor) and a benzophenothiazine unit (energy acceptor). 2 showed a strong absorption in the region between 600 and 750 nm with a molar absorptivity of $71000 \text{ M}^{-1}\text{cm}^{-1}$ suggesting its high light absorption ability. First, the authors have demonstrated that the cells loaded with 2 upon NIR light irradiation at a 21% oxygen level result in the significant generation of $O_2^{\cdot -}$. The studies further confirmed the $O_2^{\cdot -}$ generation under hypoxic cellular conditions (2% oxygen level). Furthermore, the reported PS was effectively utilized to initiate ROS ($O_2^{\cdot -}$) production in deep tumorous tissue, supporting this design as a helpful tactic to improve the PDT mechanism's effectiveness. This is confirmed by the data shown in Fig. 2g and 2h, which revealed that this strategy produces prominent inhibition (84%) of tumor growth.

Using the Nile blue molecule, Peng and Kim et al. have reported a PS, 3 (SORgenTAM), as a binary $O_2^{\cdot -}$ photo-generator in the malignant tissue (Figure 3).¹⁹ The reported PS localized in the mitochondria and restrict the intracellular oxygen consumption, making enough O_2 available for the PDT in the cancer cells. The study provides new insights on how to overcome the limitations of the conventional PDT method. Utilizing Nile blue dye, Yi et al. have also recently developed a mitochondrion specific type I PS, 4, which, when photo activated, changes the activity of the caspase-3 protein, causing apoptotic and pyroptotic cell death (Figure 3).²⁰ In addition to Nile blue, hemicyanine derivative have also been employed to generate type-I PS.²¹

For a molecule to act as a photosensitizer, it is important that the molecule exhibit a significant intersystem crossing (ISC) process. Because spin orbital coupling can promote the ISC process, heavy atoms are usually incorporated into the molecular structure to achieve efficient ISC crossing and thus the reactive oxygen species generation. However, heavy atoms, due to their toxicity, are not favorable. The alternative to

introducing the ISC process is to use an electron donor and electron acceptor architecture.²² The donor-acceptor molecular system can reduce the energy gap between the singlet excited state (S_1) and triplet excited state (T_1), thus promoting the ISC mechanism. Using this strategy, a variety of type II photosensitizers have been developed. Tang and coworkers reported a type I photosensitizer by employing a donor-acceptor system, 5, derived from the combination of the phosphindole oxide core and triphenylamine (Figure 4).²³ In 5, the phosphindole oxide unit is the acceptor part, while triphenylamine is the donor part. Because of the strong electron-accepting ability of the phosphindole oxide core, 5, upon irradiation, accepts external electrons, causing radical anion formation. This radical anion then transfers the electron to the nearby substrate and leads to the formation of $O_2^{\cdot -}$ species. The in vitro studies suggested that the reported probe localized mainly in the endoplasmic reticulum. As a result, the phototoxicity observed is because of the damage to the endoplasmic reticulum. Further, the in vivo studies validate the working of the reported photosensitizer in the photodynamic therapy. This example clearly demonstrates how the donor-acceptor architecture can be modulated to achieve the generation of type I reactive oxygen species. The AIE (aggregation-induced emission) mechanism in conjunction with donor-acceptor architecture has been extensively utilized in recent years to produce type I ROS species. Radiative decay in the aggregate state of AIE-based PSs is useful to enhance ROS formation, which is one of their advantages.²⁴ The research group of B. Z. Tang employed this strategy to develop type I PSs. In one of their studies, they have demonstrated the role of AIE in combination with donor-acceptor to obtain type I PS (6) with enhanced ROS generation (Figure 4).²⁵

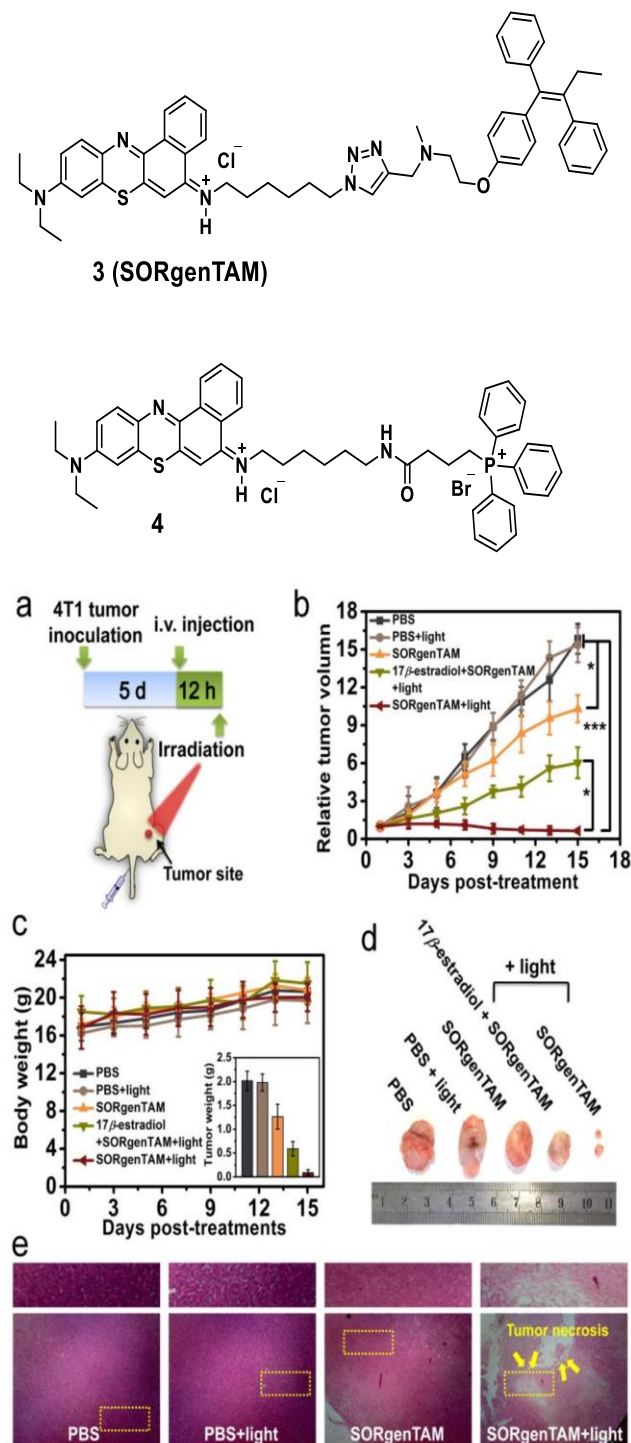


Figure 3. (a) A schematic representation of the 3 (SORgenTAM) in vivo hypoxic tumor phototherapy experiment. (b) Tumor development in vivo after intravenous injection. (c) Mice's average body weight alterations during the course of the therapy. (d) Mice tumor images with various treatments. (e) Pathological study of tumor tissues obtained 24 hours after different treatments using H&E staining. Figures a-e, adapted with permission from ref. 19. Copyright 2020 American Chemical Society.

In this particular study, the design of PS (**6**) is derived from the TPA (triphenylamine) donor and styrylpyridine cation acceptor. By using the type I mechanism to target the organelles including mitochondrial and lysosomes, the reported PS was demonstrated to cause cell apoptosis. A number of type I PSs for PDT have been developed by employing this approach.²⁶ Some of the recently published type 1 PS based on the donor-acceptor framework are given in the table 1.

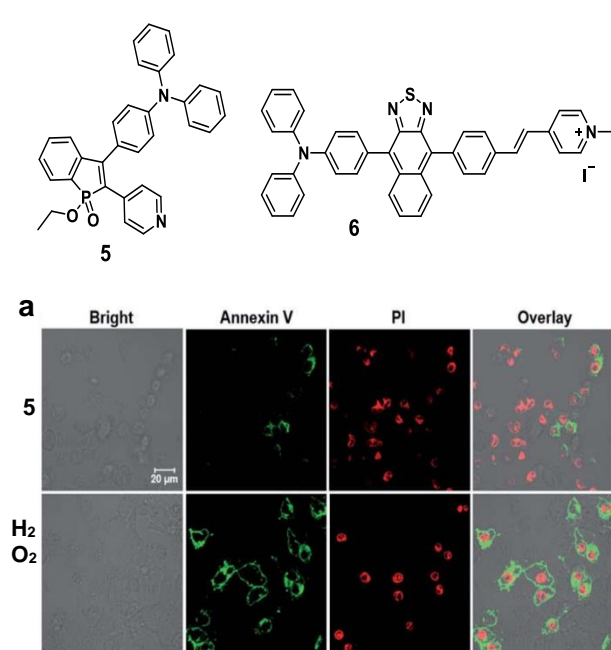
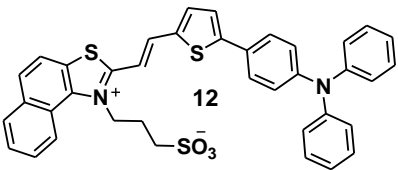
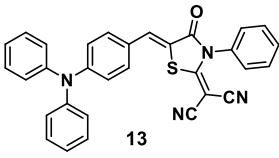
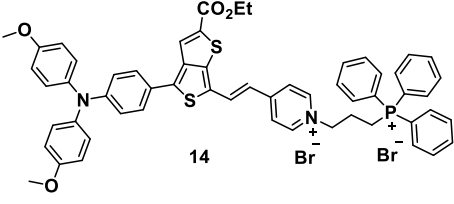
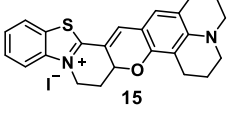
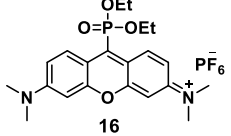


Figure 4. Structure of 5 and 6. (a) Cell apoptosis analysis after treatment by PDT using 5 as the PS (white light irradiation with 20 mW cm⁻² for 30 min) and further culturing for 12 h or H₂O₂ for 6 h. Figure 4a, reproduced from Ref. 23 with permission from the Royal Society of Chemistry.

Table 1. Recently reported type I organic PSs for the PDT process.

Molecular structure	References
<p>7</p>	28
<p>8</p>	29
<p>9</p>	30
<p>10</p>	31
<p>11 n = 3, 6, 10</p>	32

	33
	34
	35
	36
	37

Supramolecular interactions have attracted a lot of attention in nanomaterials and therapeutics over the past several years because they offer a simple way to control the functional molecules.²⁷ Supramolecular self-assembled structures have therefore also been investigated as a method of producing reactive oxygen species in photodynamic treatment.³⁸ In 2018, Yoon and coworkers reported a zinc complex of phthalocyanine-based self-assembled nanostructures as PS for efficient ROS generation via the type I mechanism.^{14a} A promising photodynamic action against bacteria was demonstrated by the produced nanostructured PS. Likewise, Yang and coworkers have developed a nano-dimensions based drug delivery system based on the combination of ergosterol and chlorin e6 (PS).³⁹ The authors have confirmed that the resulting supramolecular system has increased ROS generation ability and, thus, phototoxicity towards cancer cells through the type I PDT process. In another example, pillar[5]arene linked with L-arginine as a host and a Nile blue derivative as a guest employed to generate nano-micelles, which selectively target and release the Nile blue PS in cancer cells.⁴⁰ According to the studies, the PS effectively produces type I ROS in a hypoxic environment following release, which results in the death of cancer cells. Moreover, the pillar[5]arene derivative damages the cancer cells' cellmembrane and aids in the apoptotic process. Similar host-guest interactions were employed by Yang et al. to develop type I ROS production to kill cancer cells under hypoxic conditions.⁴¹ Kida and coworkers demonstrated that amphiphilic rhodamine/fluorescein derivatives in the aqueous medium form supramolecular assemblies that can generate reactive oxygen species (ROS) through the electron transfer mechanism when exposed to visible light (Figure 5).⁴² The fundamental idea is that

in its self-assembled state, the amphiphilic rhodamine or fluorescein produces a charge-separated (CS) state that can continue into the type I pathway to produce reactive oxygen species (ROS). At the same time, this also suggests an approach to convert type II PS into a type I PS. This is validated by converting fluorescein (FI-C2) which acts as a type II PS (Figure 5.) into type I PS by using amphiphilic fluorescein derivative (FI-C18).⁴²

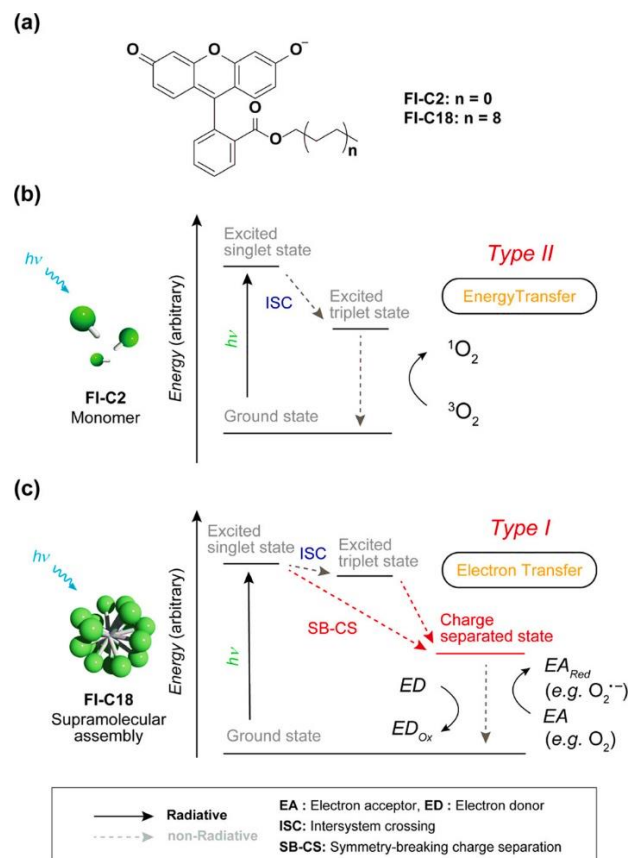


Figure 5. (a) Molecular structures of fluorescein derivatives. (b) Type II mechanism exhibited by FI-C2 (monomer state). Type I mechanism displayed by FI-C18 (assembly state). Adapted with permission from ref. 42b. Copyright 2022 American Chemical Society.

Kida and colleagues have further utilized the C-S state produced self-assembled organic molecule to develop a type I PS for the PDT process. For this, they have synthesized an amphiphilic rhodamine derivative **17** (Rh19-MA-C18) that, when self-assembled, functioned as type I PS and had a notable PDT effect on malignant cells (Figure 6).⁴³ The reported PS was developed on rhodamine fluorophore linked to a long alkyl chain to achieve the amphiphilic nature of the molecule. The fluorescence spectrum of **17** in DMSO displayed an emission at 567 nm, while in an aqueous buffer a quenched emission was observed. The behavior in the aqueous buffer was ascribed to the aggregate state of the **17**. This was further suggested by the broad absorption band of **17** in the aqueous buffer. The authors have validated that the self-assembled state of **17** in water with light irradiation ($\lambda_{ex} = 520$ nm) can produce $O_2^{\cdot -}$ via type I mechanism. Further, **17** exhibited a good photodynamic effect against cancer cells and on tumor tissue (Figure 7).

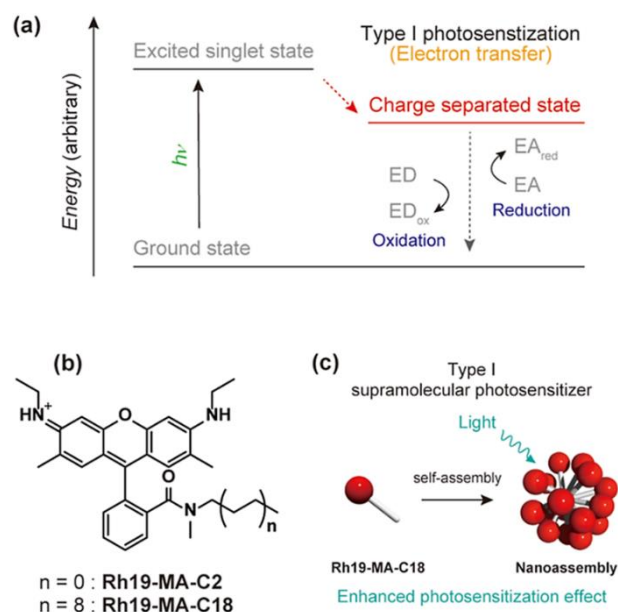


Figure 6. (a) Mechanism of type I photosensitization based on 17. EA (electron acceptor), EA_{red} (reductant of electron acceptor, ED (electron donor), ED_{ox} (oxidant of electron donor). (b) Structures of 17 (Rh19-MA-C18) and 18 (Rh19-MA-C2). (c) Schematic illustration of supramolecular type I PS based on 17. Adapted with permission from ref. 43. Copyright 2022 American Chemical Society.

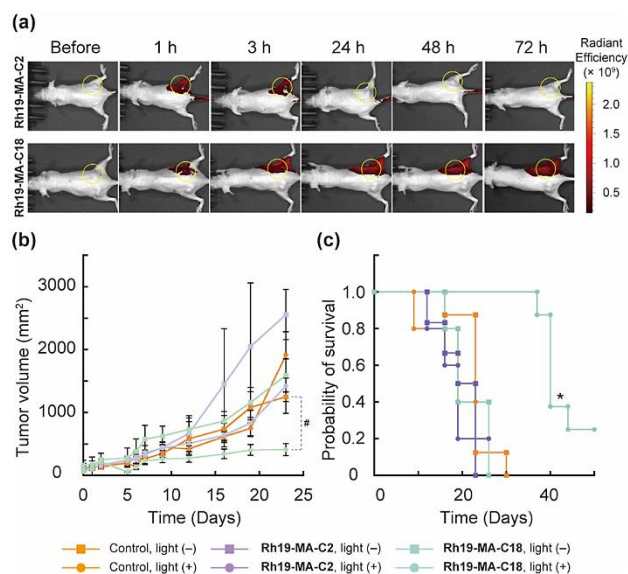


Figure 7. (a) In vivo fluorescent images of the dye distribution after injection of Rh19-MA-C18 (17) and Rh19-MA-C2 (18). (b) Tumor volume analysis (each group $n \geq 5$). (c) Survival probability after injection of Rh19-MA-C18 (17) and Rh19-MA-C2 (18). Adapted with permission from ref. 43. Copyright 2022 American Chemical Society.

Using PC9 tumor-bearing mice in in vivo tests, it was demonstrated that Rh19-MA-C18 (17) worked well for PDT. Following injection, fluorescence signals were recorded (Figure 7a), demonstrating Rh19-MA-C18's excellent bioretention and supporting its usefulness for PDT in deep tissue. The study split the mice into six groups and looked at the PDT effect of Rh19-MA-C18 on tumor cells. The findings demonstrated that while tumor size expanded under various circumstances, Rh19-MA-C18 (17) and light were able to decrease it (Figure 7b and c). Mice survival rates were also markedly increased by Rh19-MA-C18 (17)-based PDT, with some mice surviving for as long as 50 days. This study highlights the possibility of supramolecular nano-assembly as a practical method for the development of type I PS for the photodynamic therapy. This finding additionally presents the possibility that type II PS can be easily converted into type I PS through simple chemical changes.

5. Conclusion

Photodynamic therapy is a potential method for treating cancer that has seen substantial development and application in clinical practice due to its noninvasiveness and excellent therapeutic selectivity. A wide range of inorganic based compounds have been extensively explored as PSs for PDT. Nevertheless, inorganic photosensitizers are associated with many disadvantages including toxic nature of heavy metal ions and low biodegradation. In contrast, organic PSs have the potential to address such issues with promising clinical applications. As described earlier, PSs developed on type I mechanisms are less oxygen-dependent because of the disproportionation reaction, are the preferable choices in the PDT process as tumor tissues are characterized by oxygen deficiency. Because of these reasons, in recent times, attention has been given to developing organic molecules-based type I PSs for the PDT process. To date, several approaches have been developed to generate organic molecules derived type I PSs for the PDT process. For instance, introducing the donor-acceptor groups in the PS design to enhance the intersystem crossing (ISC) is one of the useful strategies to develop type I PSs. A number of organic type I PSs have been developed using this approach. Moreover, mechanisms such as AIE have combined with the donor-acceptor architecture to obtain type I PSs. Nonetheless, visible light activates the majority of type I PSs, irrespective of their organic or inorganic origin. This limits their therapeutic efficacy as well as their broader use. Additionally, working of the PSs for the tumor region deep inside the tissues is another concern as the visible light has limited tissue permeability. Therefore, developing organic type I PSs for PDT activated by NIR light is of great significance as it can offer deep tissue penetration. Likewise, low energy nature of NIR light is beneficial to minimize the harmful effect on the normal tissues. Further, tumor selectivity is another concern as it can lead to the accumulation of the PSs in normal tissues. Overcoming these challenges is crucial to maximizing the benefits of PDT and requires the integration of additional cancer treatment strategies.

Author Contribution Declaration

Roopa: article design, reviewplan and manuscript draft manuscript; **Kumar:** supervision, review and editing.

Data Availability Declaration

There are no new data were created hence data sharing is not applicable.

Acknowledgements

We are thankful to the I.K. Gujral Punjab Technical University Kapurthala and SRM University, Delhi-NCR, Sonapat for research facilities

References

- (a) C. M. Moore, D. Pendse, M. Emberton. Photodynamic therapy for prostate cancer—a review of current status and future promise. *Nat. Rev. Urol.* **2009**, *6*, 18–30. DOI: <https://doi.org/10.1038/nrcuro1274>
- (b) W. Fan, P. Huang, X. Chen. Overcoming the Achilles' heel of photodynamic therapy. *Chem. Soc. Rev.* **2016**, *45*, 6488. <https://doi.org/10.1039/C6CS00616G>
- (a) R. Ackroyd, C. Kelly, N. Brown, M. Reed. The history of photodetection and photodynamic therapy. *Photochem. Photobiol.* **2001**, *74*, 656. [https://doi.org/10.1562/0031-8655\(2001\)0740656THOPAP2.0.CO;2](https://doi.org/10.1562/0031-8655(2001)0740656THOPAP2.0.CO;2)
- J. D. Spikes. The origin and meaning of the term "photodynamic" (as used in "photodynamic therapy", for example). *J. Photochem. Photobiol. B Biol.* **1991**, *9*, 369. [https://doi.org/10.1016/1011-1344\(91\)80172-E](https://doi.org/10.1016/1011-1344(91)80172-E)
- J. P. Celli, B. Q. Spring, I. Rizvi, C. L. Evans, K. S. Samkoe, S. Verma, B. W. Pogue, T. Hasan. Imaging and Photodynamic Therapy: Mechanisms, Monitoring, and Optimization. *Chem. Rev.* **2010**, *110*, 2795. <https://doi.org/10.1021/cr900300p>

5. V. P. Chauhan, R. K. Jain. Strategies for advancing cancer nanomedicine. *Nat. Mater.* **2013**, *12*, 958. <https://doi.org/10.1038/nmat3792>
6. (a) W. Fan, B. Yung, P. Huang, X. Chen. Nanotechnology for Multimodal Synergistic Cancer Therapy. *Chem. Rev.* **2017**, *117*, 13566. <https://doi.org/10.1021/acs.chemrev.7b00258> (b) P. Yang, S. Gai, J. Lin. Functionalized mesoporous silica materials for controlled drug delivery. *Chem. Soc. Rev.* **2012**, *41*, 3679. <https://doi.org/10.1039/C2CS15308D>
7. (a) L. B. Josefsen, R. W. Boyle. Unique Diagnostic and Therapeutic Roles of Porphyrins and Phthalocyanines in Photodynamic Therapy, Imaging and Theranostics. *Theranostics* **2012**, *2*, 916. <https://doi.org/10.1039/c2tn00457f> (b) K. Han, S. -B. Wang, Q. Lei, J. -Y. Zhu, X. -Z. Zhang. Ratiometric Biosensor for Aggregation-Induced Emission-Guided Precise Photodynamic Therapy. *ACS Nano* **2015**, *9*, 10268. <https://doi.org/10.1021/acs.nano.5b04243> (c) T. C. Pham, V. -N. Nguyen, Y. Choi, S. Lee, J. Yoon. Recent Strategies to Develop Innovative Photosensitizers for Enhanced Photodynamic Therapy. *Chem. Rev.* **2021**, *121*, 13454. <https://doi.org/10.1021/acs.chemrev.1c00381>
8. C. S. Foote. Definition of Type I and Type II Photosensitized Oxidation. *Photochem. Photobiol.* **1991**, *54*, 659. <https://doi.org/10.1111/j.1751-1097.1991.tb02071.x>
9. H. Shi, P. J. Sadler. How promising is phototherapy for cancer? *Br. J. Cancer* **2020**, *123*, 871. <https://doi.org/10.1038/s41416-020-0926-3>
10. J. Moan, S. Sommer. Oxygen Dependence of the Photosensitizing Effect of Hematoporphyrin Derivative in NHIK 3025 Cells. *Cancer Res.* **1985**, *45*, 1608.
11. (a) Y. Cheng, H. Cheng, C. Jiang, X. Qiu, K. Wang, W. Huan, A. Yuan, J. Wu, Y. Hu. Perfluorocarbon nanoparticles enhance reactive oxygen levels and tumour growth inhibition in photodynamic therapy. *Nat. Commun.* **2015**, *6*, 8785. <https://doi.org/10.1038/ncomms9785> (b) J. Kim, H. R. Cho, H. Jeon, D. Kim, C. Song, N. Lee, S. H. Choi, T. Hyeon. Continuous O₂-Evolving MnFe₂O₄ Nanoparticle-Anchored Mesoporous Silica Nanoparticles for Efficient Photodynamic Therapy in Hypoxic Cancer. *J. Am. Chem. Soc.* **2017**, *139*, 10992. <https://doi.org/10.1021/jacs.7b05559>
12. (a) K. Plaetzer, B. Krammer, J. Berlanda, F. Berr, T. Kiesslich. Photophysics and photochemistry of photodynamic therapy: fundamental aspects. *Laser. Med. Sci.* **2008**, *24*, 259. <https://doi.org/10.1007/s10103-008-0539-1> (b) A. Kamkaew, S. H. Lim, H. B. Lee, L. V. Kiew, L. Y. Chung and K. Burgess. BODIPY dyes in photodynamic therapy. *Chem. Soc. Rev.* **2013**, *42*, 77. <https://doi.org/10.1039/C2CS2516H>
13. Y. Li, W. Zhang, J. Niu, Y. Chen. Mechanism of Photogenerated Reactive Oxygen Species and Correlation with the Antibacterial Properties of Engineered Metal-Oxide Nanoparticles. *ACS Nano* **2012**, *6*, 6164. <https://doi.org/10.1021/nn300934k>
14. (a) X. Li, D. Lee, J. -D. Huang, J. Yoon. Phthalocyanine-Assembled Nanodots as Photosensitizers for Highly Efficient Type I Photoreactions in Photodynamic Therapy. *Angew. Chem. Int. Ed.* **2018**, *57*, 9885. <https://doi.org/10.1002/anie.201806551> (b) Z. Lv, H. Wei, Q. Li, X. Su, S. Liu, K. Y. Zhang, W. Lv, Q. Zhao, X. Li, W. Huang. Achieving efficient photodynamic therapy under both normoxia and hypoxia using cyclometalated Ru(II) photosensitizer through type I photochemical process. *Chem. Sci.* **2018**, *9*, 502. <https://doi.org/10.1039/C7SC03765A> (c) J. S. Nam, M.-G. Kang, J. Kang, S.-Y. Park, S. J. C. Lee, H.-T. Kim, J. K. Seo, O.-H. Kwon, M. H. Lim, H.-W. Rhee, T.-H. Kwon. Endoplasmic Reticulum-Localized Iridium(III) Complexes as Efficient Photodynamic Therapy Agents via Protein Modifications. *J. Am. Chem. Soc.* **2016**, *138*, 10968. <https://doi.org/10.1021/jacs.6b05302> (d) S. S. Lucky, N. M. Idris, Z. Li, K. Huang, K. C. Soo, Y. Zhang. Titania Coated Upconversion Nanoparticles for Near-Infrared Light Triggered Photodynamic Therapy. *ACS Nano* **2015**, *9*, 191. <https://doi.org/10.1021/nn503450t>
15. Y. Cai, W. Si, W. Huang, P. Chen, J. Shao, X. Dong. Organic Dye Based Nanoparticles for Cancer Phototheranostics. *Small* **2018**, *14*, 1704247. <https://doi.org/10.1002/sml.201704247>
16. (a) H. Abrahamse, M. R. Hamblin. New photosensitizers for photodynamic therapy. *Biochem. J.* **2016**, *473*, 347. <https://doi.org/10.1042/BJ20150942> (b) X. Zheng, U. W. Sallum, S. Verma, H. Athar, C. L. Evans, T. Hasan. Exploiting a Bacterial Drug-Resistance Mechanism: A Light-Activated Construct for the Destruction of MRSA. *Angew. Chem. Int. Ed.* **2009**, *48*, 2148. <https://doi.org/10.1002/anie.200804804> (c) O. J. Klein, H. Yuan, N. H. Nowell, C. Kaittanis, L. Josephson, C. L. Evans. An Integrin-Therapy. *Chem. Mater.* **2018**, *30*, 25. <https://doi.org/10.1021/acs.chemmater.7b03924>
17. S. Liu, B. Wang, Y. Yu, Y. Liu, Z. Zhuang, Z. Zhao, G. Feng, A. Qin, B. Z. Tang. Cationization-Enhanced Type I and Type II ROS Generation for Photodynamic Treatment of Drug-Resistant Bacteria. *ACS Nano* **2022**, *16*, 9130. <https://doi.org/10.1021/acsnano.2c01206>
18. L. Feng, C. Li, L. Liu, Z. Wang, Z. Chen, J. Yu, W. Ji, G. Jiang, P. Zhang, J. Wang, B. Z. Tang. Acceptor Planarization and Donor Rotation: A Facile Strategy for Realizing Synergistic Cancer Phototherapy via Type I PDT and PTT. *ACS Nano* **2022**, *16*, 4162. <https://doi.org/10.1021/acsnano.1c10019>
19. J. Zhao, R. Huang, Y. Gao, J. Xu, Y. Sun, J. Bao, L. Fang, S. Gou. Realizing Near-Infrared (NIR)-Triggered Type I PDT and PTT by Maximizing the Electronic Exchange Energy of Perylene Dimide-Based Photosensitizers. *ACS Materials Lett.* **2023**, *5*, 1752. <https://doi.org/10.1021/acsmaterialslett.3c00436>
20. M. M. S. Lee, D. M. Lin, J. H. C. Chau, E. Y. Yu, D. Ding, R. T. K. Kwok, D. Wang, B. Z. Tang. Adipocyte-Targeting Type I AIE Photosensitizer for Obesity Treatment via Photodynamic Lipid Peroxidation. *ACS Nano* **2023**, *17*, 11039. <https://doi.org/10.1021/acsnano.3c03654>
21. Z. Li, F. Ni, S. Jia, L.-H. Gao, H. Yuan, K.-Z. Wang. Bipolar Hemicyanine-Based Photodynamic Modulation of Type I Pathway for Efficient Sterilization and Real-Time Monitoring. *ACS Appl. Bio Mater.* **2022**, *5*, 2549. <https://doi.org/10.1021/acsbm.2c00394>
22. Y. Wang, Y. Sun, J. Ran, H. Yang, S. Xiao, J. Yang, C. Yang, H. Wang, Y. Liu. Utilization of Nonradiative Excited-State Dissipation for Promoted Phototheranostics Based on an AIE-Active Type I ROS Targeted, Highly Diffusive Construct for Photodynamic Therapy. *Sci. Rep.* **2017**, *7*, 13375. <https://doi.org/10.1038/s41598-017-13803-4>
23. M. Li, J. Xia, R. Tian, J. Wang, J. Fan, J. Du, S. Long, X. Song, J. W. Foley, X. Peng. Near-Infrared Light-Initiated Molecular Superoxide Radical Generator: Rejuvenating Photodynamic Therapy against Hypoxic Tumors. *J. Am. Chem. Soc.* **2018**, *140*, 14851. <https://doi.org/10.1021/jacs.8b08658>
24. M. Li, T. Xiong, J. Du, R. Tian, M. Xiao, L. Guo, S. Long, J. Fan, W. Sun, K. Shao, X. Song, J. W. Foley, X. Peng. Superoxide Radical Photogenerator with Amplification Effect: Surmounting the Achilles' Heels of Photodynamic Oncotherapy. *J. Am. Chem. Soc.* **2019**, *141*, 2695. <https://doi.org/10.1021/jacs.8b13141>
25. M. Li, Y. Shao, J. H. Kim, Z. Pu, X. Zhao, H. Huang, T. Xiong, Y. Kang, G. Li, K. Shao, J. Fan, J. W. Foley, J. S. Kim, X. Peng. Unimolecular Photodynamic O₂-Economizer to Overcome Hypoxia Resistance in Phototherapeutics. *J. Am. Chem. Soc.* **2020**, *142*, 5380. <https://doi.org/10.1021/jacs.0c00734>
26. Z. Yi, X. Qin, L. Zhang, H. Chen, T. Song, Z. Luo, T. Wang, J. Lau, Y. Wu, T. B. Toh, C.-S. Lee, W. Bu, X. Liu. Mitochondria-Targeting Type-I Photodrug: Harnessing Caspase-3 Activity for Pyroptotic Oncotherapy. *J. Am. Chem. Soc.* **2024**, *146*, 9413. <https://doi.org/10.1021/jacs.4c01929>
27. Y. Zhang, M. Zhao, J. Miao, W. Gu, J. Zhu, B. Cheng, Q. Li, Q. Miao. Hemicyanine-Based Type I Photosensitizers for Antihypoxic Activatable Photodynamic Therapy. *ACS Materials Lett.* **2023**, *5*, 3058. <https://doi.org/10.1021/acsmaterialslett.3c00933>
28. (a) S. Liu, H. Zhang, Y. Li, J. Liu, L. Du, M. Chen, R. T. K. Kwok, J. W. Y. Lam, D. L. Phillips, B. Z. Tang. Strategies to Enhance the Photosensitization: Polymerization and the Donor-Acceptor Even-Odd Effect. *Angew. Chem., Int. Ed.* **2018**, *57*, 15189. <https://doi.org/10.1002/anie.201810326> (b) W. Wu, D. Mao, F. Hu, S. Xu, C. Chen, C.-J. Zhang, X. Cheng, Y. Yuan, D. Ding, D. Kong, B. Liu. A Highly Efficient and Photostable Photosensitizer with Near-Infrared Aggregation-Induced Emission for Image-Guided Photodynamic Anticancer Therapy. *Adv. Mater.* **2017**, *29*, 1700548. <https://doi.org/10.1002/adma.201700548> (c) M. Kang, C. Zhou, S. Wu, B. Yu, Z. Zhang, N. Song, M. S. Lee, W. Xu, F. J. Xu, D. Wang, L. Wang, B. Z. Tang. Evaluation of Structure-Function Relationships of Aggregation-Induced Emission Luminescence for Simultaneous Dual Applications of Specific Discrimination and Efficient Photodynamic Killing of Gram-Positive Bacteria. *J. Am. Chem. Soc.* **2019**, *141*, 16781. <https://doi.org/10.1021/jacs.9b07162>
29. Z. Zhuang, J. Dai, M. Yu, J. Li, P. Shen, R. Hu, X. Lou, Z. Zhao, B. Z. Tang. Type I photosensitizers based on phosphindole oxide for photodynamic therapy: apoptosis and autophagy induced by endoplasmic reticulum stress. *Chem. Sci.* **2020**, *11*, 3405. <https://doi.org/10.1039/D0SC00785D>
30. F. Hu, S. Xu, B. Liu. Photosensitizers with Aggregation-Induced Emission: Materials and Biomedical Applications. *Adv. Mater.* **2018**, *30*, 1801350. <https://doi.org/10.1002/adma.201801350>
31. Q. Wan, R. Zhang, Z. Zhuang, Y. Li, Y. Huang, Z. Wang, W. Zhang, J. Hou, B. Z. Tang. Molecular Engineering to Boost AIE-Active Free Radical Photogenerators and Enable High-Performance Photodynamic Therapy under Hypoxia. *Adv. Funct. Mater.* **2020**, *30*, 2002057. <https://doi.org/10.1002/adfm.202002057>
32. (a) P. Xiao, Z. Shen, D. Wang, Y. Pan, Y. Li, J. Gao, L. Wang, D. Wang, B. Z. Tang. Precise Molecular Engineering of Type I Photosensitizers with Near-Infrared Aggregation-Induced Emission for Image-Guided Photodynamic Killing of Multidrug-Resistant Bacteria. *Adv. Sci.* **2022**, *9*, 104079. <https://doi.org/10.1002/advs.202104079> (b) X. Zhao, Y. Dai, F. Ma, S. Misal, K. Hasrat, H. Zhu and Z. Qi. Molecular engineering to accelerate cancer cell discrimination and boost AIE-active type I photosensitizer for photodynamic therapy under hypoxia. *Chem. Eng. J.* **2021**, *410*, 128133. <https://doi.org/10.1016/j.cej.2020.128133> (c) Z. Liu, Q. Wang, W. Qiu, Y. Lyu, Z. Zhu, X. Zhao, W. H. Zhu. AIE-active luminogens as highly efficient free-radical ROS photogenerator for image-guided photodynamic therapy. *Chem. Sci.* **2022**, *13*, 3599. <https://doi.org/10.1039/D2SC00067A> (d) K. Chen, P. He, Z. Wang, B. Z. Tang. A Feasible Strategy of Fabricating Type I Photosensitizer for Photodynamic Therapy in Cancer Cells and Pathogens. *ACS Nano* **2021**, *15*, 7735. <https://doi.org/10.1021/acsnano.1c01577>
33. (a) X. Ma, Y. Zhao. Biomedical Applications of Supramolecular Systems Based on Host-Guest Interactions. *Chem. Rev.* **2015**, *115*, 7794. <https://doi.org/10.1021/cr500392w> (b) M. Li, Z. Luo, Y. Zhao. Self-Assembled Hybrid Nanostructures: Versatile Multifunctional Nanoplatforams for Cancer Diagnosis and Generator. *ACS Appl. Mater. Interfaces* **2022**, *14*, 225. <https://doi.org/10.1021/acsaami.1c19008>
34. G. Yang, S.-B. Lu, C. Li, F. Chen, J.-S. Ni, M. Zha, Y. Li, J. Gao, T. Kang, C. Liu, K. Li. Type I macrophage activator photosensitizer against hypoxic tumors. *Chem. Sci.* **2021**, *12*, 14773. <https://doi.org/10.1039/D1SC04124J>
35. S. Zhou, R. Li, Y. Li, Y. Wang, L. Feng. A tailored and red-emissive type I photosensitizer to potentiate photodynamic immunotherapy. *J. Mater. Chem. B* **2022**, *10*, 8003. <https://doi.org/10.1039/D2TB01578A>
36. H. Huang, S. Long, D. Huang, J. Du, J. Fan and X. Peng. A photosensitizer with conformational restriction for enhanced photodynamic therapy. *Chem. Commun.* **2021**, *57*, 9100. <https://doi.org/10.1039/D1CC03591F>
37. Y. Wang, J. Li, Y. Zhang, Y. Nan, X. Zhou. Rational design of a meso phosphate-substituted pyronin as a type I photosensitizer for photodynamic therapy. *Chem. Commun.* **2022**, *58*, 7797. <https://doi.org/10.1039/D2CC02124B>
38. L. Zhao, Y. Xing, R. Wang, F. Yu, F. Yu. Self-Assembled Nanomaterials for Enhanced Phototherapy of Cancer. *ACS Appl. Bio Mater.* **2020**, *3*, 86. <https://doi.org/10.1021/acsbm.9b00843>
39. J. Cheng, H. Zhao, L. Yao, Y. Li, B. Qi, J. Wang, X. Yang. Simple and Multifunctional Natural Self-Assembled Sterols with Anticancer Activity-Mediated Supramolecular Photosensitizers for Enhanced Antitumor Photodynamic Therapy. *ACS Appl. Mater. Interfaces* **2019**, *11*, 29498. <https://doi.org/10.1021/acsaami.9b07404>
40. S. Chao, Z. Shen, B. Li, Y. Pei, Z. Pei. An L-arginine-functionalized pillar[5]arene-based supramolecular photosensitizer for synergistically enhanced cancer therapeutic effectiveness.

- Chem. Commun.* **2023**, 59, 3455. <https://doi.org/10.1039/D3CC00123G>
41. (a) K. X. Teng, L. Y. Niu and Q. Z. Yang. A host–guest strategy for converting the photodynamic agents from a singlet oxygen generator to a superoxide radical generator. *Chem. Sci.* **2022**, 13, 5951. <https://doi.org/10.1039/D2SC01469F> (b) K. X. Teng, L. Y. Niu, N. Xie and Q. Z. Yang. Supramolecular photodynamic agents for simultaneous oxidation of NADH and generation of superoxide radical. *Nat. Commun.* **2022**, 13, 6179. <https://doi.org/10.1038/s41467-022-33924-3>
42. (a) H. Shigemitsu, Y. Tani, T. Tamemoto, T. Mori, X. Li, Y. Osakada, M. Fujitsuka, T. Kida. Aggregation-induced photocatalytic activity and efficient photocatalytic hydrogen evolution of amphiphilic rhodamines in water. *Chem. Sci.* **2020**, 11, 11843. <https://doi.org/10.1039/D0SC04285D> (b) H. Shigemitsu, K. Ohkubo, K. Sato, A. Bunno, T. Mori, Y. Osakada, M. Fujitsuka, T. Kida. Fluorescein-Based Type I Supramolecular Photosensitizer via Induction of Charge Separation by Self-Assembly. *JACS Au* **2022**, 2, 1472. <https://doi.org/10.1021/jacsau.2c00243>
43. H. Shigemitsu, K. Sato, S. Hagio, Y. Tani, T. Mori, K. Ohkubo, Y. Osakada, M. Fujitsuka, T. Kida. Amphiphilic Rhodamine Nano-assembly as a Type I Supramolecular Photosensitizer for Photodynamic Therapy. *ACS Appl. Nano Mater.* **2022**, 5, 14954. <https://doi.org/10.1021/acsanm.2c03192>

REVIEW ARTICLE

Mastering Chirality: Unlocking Bioactive Natural Products with Oxazaborolidines and Oxazaborolidinones

Yogesh Kumar Walia^{a*}, Souvik Sarkar^b, Soma Das Pradhan^c, and Prasun Kanti Pradhan^{b*}

^aDepartment of chemistry, School of Basic and Applied Sciences, Career Point University Hamirpur, Himachal Pradesh, 176041 India.

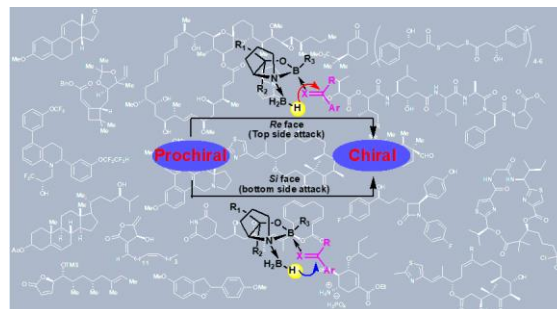
^bTCG Lifesciences Limited, Block BN, Plot 7, Sector-V, Salt Lake, Kolkata, West Bengal, 700091 India.

^cCentre for Distance and Online Education, Vidyasagar University, Midnapore, West Bengal, 721102 India.

*Correspondence: yogesh.che@cpuhi.in; drpkp@yahoo.com

Abstract: Catalytic asymmetric synthesis has appeared as the preferred method for producing enantiomerically pure compounds, marking significant advancements in recent years. In biological processes, asymmetric catalysis governs the synthesis of chiral compounds, facilitated through the chirality transfer following reactant binding at enzyme active sites. A revolutionary milestone in this area was the discovery of oxazaborolidine chiral catalysts by Corey, Bakshi, and Shibata (CBS catalysts), empowering the enantioselective reduction of various functional groups. This discovery has had profound implications across industry and academia, establishing oxazaborolidines as pivotal tools for achieving chirality in chemical systems. The application of oxazaborolidines and their derivatives have been extensively explored for enantioselective reductions of various functional groups. While previous review articles focused on specialized functional groups, this review provides an overview (last fifteen years) of practical advancements in the use of borane-oxazaborolidine catalysts for the enantioselective reduction of challenging functional groups such as ketones, ketimines, and oximes. These advancements have facilitated the synthesis of various building blocks for natural products. We also highlighted the potential of oxazaborolidinones as it remains largely underutilized, presenting an exciting opportunity for future investigations.

Keywords: *enantioselective, oxazaborolidine, oxazaborolidinone, hydride transfer, reduction.*



Contents

Biographical Information	11
1. Introduction	11
2. Oxazaborolidine synthesis and its use in asymmetric borane reduction	12
3. Synthesis of natural products congeners	14
4. Synthesis of Chiral Intermediates, Ligands and Building Blocks	17
5. Oxazaborolidinone	21
6. Conclusion	24
Author Contribution Declaration	24
Data Availability Declaration	24
Acknowledgements	24
References	24

1. Introduction

Chirality is crucial in biological, chemical, pharmaceuticals and material science. In recent years, remarkable advancement has been attained in catalytic asymmetric processes. Catalytic asymmetric synthesis has emerged the most desired technique to make enantiomerically pure compounds. Asymmetric catalysis enables the production of asymmetric compounds in biological processes. Natural processes drive reactants bind enzyme active sites by chirality transfer. Most commonly in chemical systems, one of the reactants binds to the chiral catalyst which then influences the other reactant by transferring the chirality.¹

In the mid-20th century, the discovery of NaBH₄ (1942)² and LiAlH₄ (1945)³, known for their typical reducing properties, transformed synthetic organic chemistry. Chemist began exploring complex metal hydrides, including LiAlH₄ and LiBH₄, for use in synthetic organic chemistry. Over the next thirty years, numerous studies investigated "mixture reagents," like LiAlH₄ combined with chiral 1,2-diols, 1,2-aminoalcohols, 1,2-diamines, hydroxymethyl oxazolines, BF₃, and chiral amino acid esters.⁴ These systems demonstrated good enantioselectivity but were rarely used in organic synthesis due to issues like catalyst solubility, unknown reactive species, and a lack of mechanistic understanding of enantioselectivity. While Mosher and Yamaguchi achieved promising results with Darvon alcohol and LiAlH₄, these problems persisted.⁵

Prof. Yogesh K. Walia completed his Ph.D. from Barkatullah University (formerly Bhopal University) in 2010. His research focuses on interdisciplinary areas like natural product and synthetic chemistry, environmental protection. Currently, he serves as a Professor of Organic Chemistry and also holds the position of Controller of Examinations at Career Point University in Hamirpur, India. He supervised several master's and Ph.D. scholars.



Souvik Sarkar has completed his undergraduate and postgraduate studies from Kalyani University, West Bengal, India. Presently, he is working as a Team Lead in TCG Life Sciences Pvt. Ltd. (TCGLS), Kolkata, West Bengal, India. With over 18 years of experience in synthetic organic chemistry within an industrial setting, he is particularly fascinated in troubleshooting complex synthetic chemistry challenges.



Dr. Soma Das Pradhan completed her undergraduate and postgraduate studies at Vidyasagar University, West Bengal, India. Then She joined the group of Prof. D. K. Bhattacharyya, Calcutta University for her Ph. D. studies. Her interests focus on synthesis and characterization of surfactants produced biotechnologically and biosurfactants produced from living organisms. She is working as Assistant Professor of Chemistry at Vidyasagar University, West Bengal, India.



Dr. Prasun Kanti Pradhan earned his Ph.D. in 2006 from the CSIR-IICB (Jadavpur University), Kolkata, West Bengal, India focused on synthetic studies of β -aryl ethyl amine derivatives. He did postdoctoral research in asymmetric catalysis in the laboratory of Professors Masato Kitamura and Ryoji Noyori in Noyori's Organic Synthesis Group, under RCMS fellowship at Nagoya University, Japan. In 2010, he joined TCG Life Sciences Pvt. Ltd. in Kolkata, where he currently serves as a Senior Lead Scientist.



Although applicable to certain substrates, the high costs limited the practicality of this reducing system. After thirty years of attempting to combine these reducing agents with different chiral ligands for efficient asymmetric synthesis, results persisted disappointing. Finally, in the 1980s, Itsuno and his coworkers achieved encouraging outcomes with mixtures of chiral 1,2-amino alcohols and borane (Figure 1).⁶ They used borane and chiral amino alcohols (1-4) (obtained from α -amino acids) to reduce aromatic ketones into the corresponding secondary alcohols with up to 60% stereoselectivity. The amino alcohols (1-4) formed complexes with borane (alkoxy-amine-borane complexes), releasing one

equivalent of hydrogen gas at -70 to 0°C . However, they could not afford a mechanistic clarification for the detected enantioselectivity.⁷ It was Noyori who first provided a clear mechanistic explanation for high enantioselectivity using a mixture of (S)- or (R)-BINOL, LiAlH_4 , and ethanol, known as the Noyori reagent.⁸

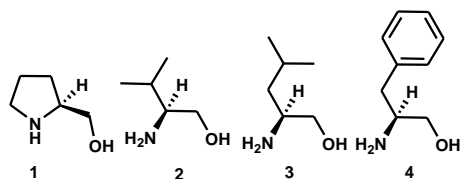
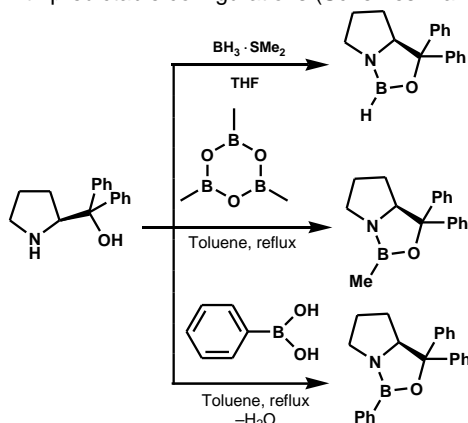


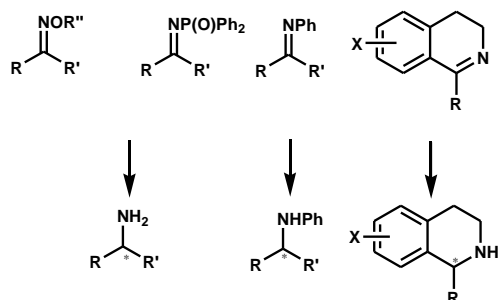
Figure 1. Amino alcohols used by Itsuno and co-workers.

2. Oxazaborolidine synthesis and its use in asymmetric borane reduction

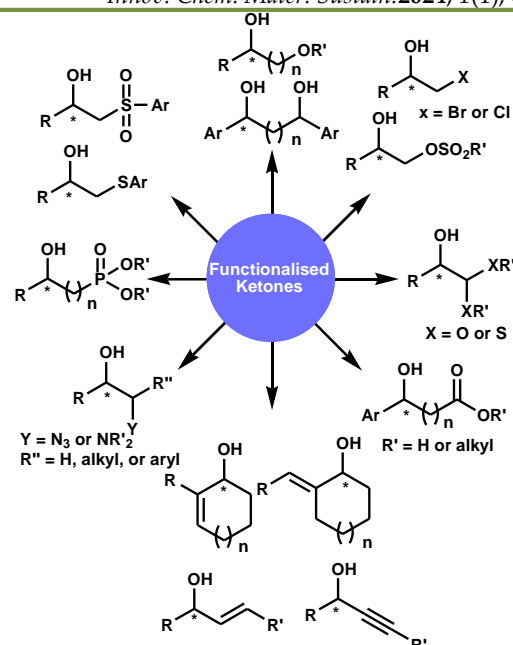
These critical annotations resulted in the discovery of chiral oxazaborolidine catalysts by Corey, Bakshi, and Shibata (CBS catalysts)⁹ for the enantioselective reduction of various achiral ketones, known as CBS reduction. The CBS catalysts were prepared by reacting amino alcohol with two equivalents of BH_3 in THF or BMS at 30°C for 6 hours. Different borane sources and reaction conditions were also explored for making oxazaborolidine catalysts (Scheme 1).¹⁰ There are more reports on the enantioselective reduction of prochiral ketones than on the reduction of oximes or ketimines.¹¹ For prochiral ketones, these reductions are highly effective for most aryl alkyl ketones including various functionalized ketones such as heterocyclic ketones, α -hydroxy ketones, diketones, α -halo- and sulfonyloxy ketones, α -keto acetals or thioacetals, α , β -enones and ynones, keto esters, keto phosphates, α -azido ketones, meso-imides, β -keto sulfides and sulfones, and biaryl ketones and lactones. The use of even 2 mol% of oxazaborolidine catalyst achieves high enantioselectivity with predictable configurations (Schemes 2 and 3).



Scheme 1. Synthesis of oxazaborolidine (Corey-Bakshi-Shibata Reagent).

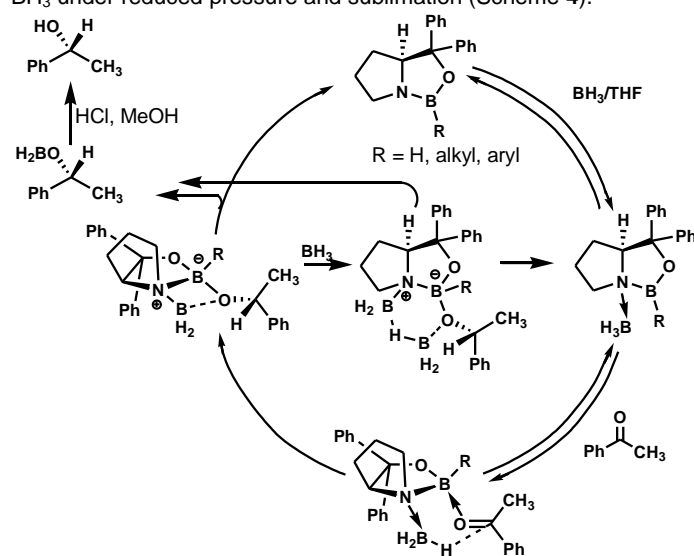


Scheme 2. Asymmetric reduction of ketimines by borane-oxazaborolidine.



Scheme 3. Asymmetric reduction of functionalized ketones by borane-oxazaborolidine.

They established the reaction of amino alcohols with two equivalents of BH_3 in THF at 35°C formed two equivalents of H_2 gas and the oxazaborolidine, which was achieved in pure form upon subsequent elimination of the solvent and excess BH_3 under reduced pressure and sublimation (Scheme 4).



Scheme 4. Enantioselective reduction of ketones by oxazaborolidine proposed by Corey.

The pioneering discovery of oxazaborolidine marked a milestone, leading to the rapid expansion of CBS reduction, which is now considered a major synthetic method for the asymmetric reduction of prochiral ketones. This reduction technique has broad applications, including the synthesis of (1) chiral ligands, (2) intermediates, (3) bioactive compounds, and (4) natural products.

The use of the above-mentioned stoichiometric reagents achieved remarkable success, but it required at least one equivalent of the reagents. This drawback, due to the low availability and high cost of the reagents, accentuated the need to develop catalytic methods for these sorts of reductions. Later, Itsuno and Corey observed high enantioselectivity with predictable configurations in the reduction of prochiral ketones, even with just 2 mol% of oxazaborolidine (Figure 2).¹²

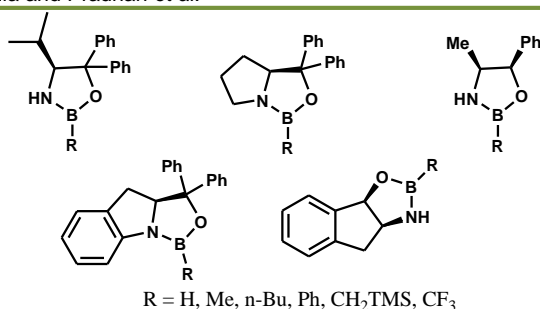


Figure 2. Selected oxazaborolidines.

However, these borane exporters have certain limitations for large-scale implementations, including high sensitivity to air and moisture, low concentration and stability of $\text{BH}_3\text{-THF}$, and the high volatility, flammability, and nasty scent of BMS.

The oxazaborolidine-catalyzed borane reductions have been extensively studied by Itsuno¹³ and Corey¹⁴. Given the numerous reviews till date, this review attention on the fresh applications of chiral borane-oxazaborolidines in synthetic organic chemistry.¹⁵ Baranowska-Łaczowska and colleagues theoretically investigated B-substituted oxazaborolidine-borane complexes using MP2 and DFT/B3LYP methods. They observed that in closed structure complexes, the oxazaborolidine ring with a B-H-B bond is more planar compared to open complexes, due to a rigid hydrogen bridge between the boron atoms.^{16a} The interaction energies in the closed complexes are 1.5 to 2.5 times greater than those in the open complexes, with the highest values found in B-trifluoromethyl substituted complexes. This increase is likely due to the strong electron-withdrawing trifluoromethyl (CF_3) group, which reduces electron density on the B1 atom and leads to the formation of a B-H-B bond (Figure 3). The enhanced interactions in B-trifluoromethyl complexes suggest they may be more stable and easier to isolate, despite the computational model not considering factors like solvent effects.

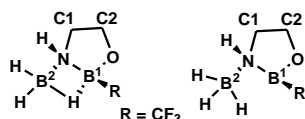
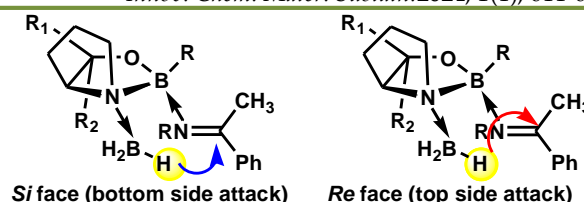


Figure 3. Close vs open ring in B-H-B bond.

Kettouche *et al.* explored the origin of selectivity in the [2+2] cycloaddition step of the enantioselective reduction of ketone mechanism by a *B*-methoxy oxazaborolidine catalyst resulted from (–)- β -pinene.^{16b} They provided a clear clarification of the construction of O-B and N-B bonds through a two-stage, one-step mechanism using electron localization function topological analysis. They proposed that the stability difference between these bonds primarily arises from the methanediyl group alignment within the pinene skeleton.

In connection with the enantioselective reduction of ketamine, Nacereddine *et al.* studied theoretically to understand the origin of enantioselectivity by using transition state theory and DFT methods at the B3LYP/6-31G(d,p) level by oxazaborolidine catalyst.^{19c} Their findings show that hydride transfer to the *Si* face is more favorable than to the *Re* face. Analysis of non-covalent interactions and molecular electrostatic potential reveals that several favorable interactions during the *Si* face hydride transfer contribute to the observed enantioselectivity (Figure 4). Additionally, Electron Localization Function topological analysis directs that the hydride transfer mechanism occurs through a non-concerted three-stage.

Figure 4. Interactions during the hydride transfer (*Re* & *Si* face).

Bach and Daniel provided an outstanding overview on the diversity and intricacy of chiral 1,3,2-oxazaborolidine catalysts used in asymmetric photochemical reactions. They emphasized the significance of the B-H-B bridging interaction in B-substituted oxazaborolidine- BH_3 complexes. In these reductions, oxazaborolidines serve both as catalysts and stoichiometric reagents for asymmetric induction. Among these, the well-known, commercially available CBS reagents and their analogues are widely recognized as some of the utmost effective asymmetric catalysts for such reductions.^{14,17} Typically, oxazaborolidine-mediated borane reductions are conducted by adding prochiral ketones, imines, or oximes to a mixture of oxazaborolidine and borane transporters in a suitable solvent at ambient temperature. Although, Corey and his team introduced fluorine substituents into the chiral ligand, resulting in a new, second-generation of chiral oxazaborolidinium cationic class which is effective even at loadings of 1–2 mol %.¹⁸ These species, when combined with various Lewis acids, are highly effective for Diels-Alder reactions, achieving good yields and high enantioselectivities (>95% ee) and these new catalysts particularly appealing for large-scale production. They found that using the strong acid triflimide (TiF_2NH) in a CH_2Cl_2 solution enhances the catalytic activity of these oxazaborolidines. The combination of TiF_2NH with biscoordinating Lewis acids TiCl_4 or SnCl_4 as coactivators significantly boosts catalytic efficiency. This increase in acidity with TiF_2NH is notably greater when paired with biscoordinating agents like TiCl_4 and SnCl_4 compared to monocoordinating salts, even strong Lewis acids including AlBr_3 and BBr_3 in CH_2Cl_2 or $\text{CH}_2\text{Cl}_2/\text{toluene}$. The enhanced acidity of TiF_2NH is attributed to the formation of a stabilized cyclic anionic complex with TiCl_4 , suggesting broader applicability. The activation of fluorinated oxazaborolidines using $\text{TiF}_2\text{NH-TiCl}_4$ has been demonstrated its effectiveness while use in the enantioselective (4 + 2) cycloaddition reaction to afford α,β -unsaturated acid chlorides (Figure 5).

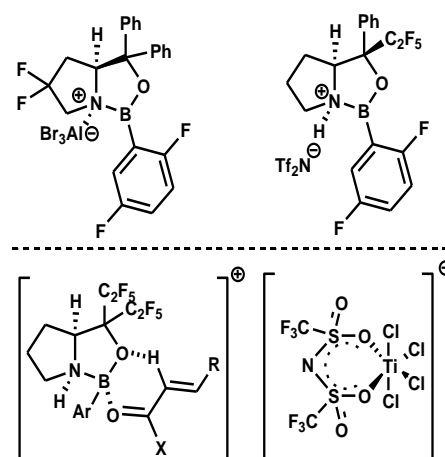
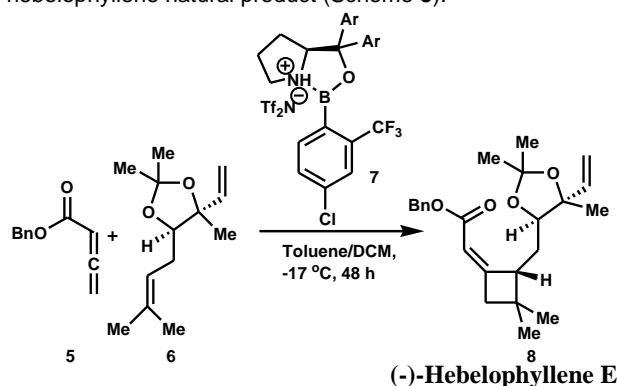


Figure 5. Corey's Second Generation Catalysts (Top); reactive complex for [4+2]-cycloaddition reactions (Bottom)

First, Brown *et al.* achieved the synthesis of hebelophyllene E (**8**) and established its previously strange relative configuration by synthesizing *epi*-ent-hebelophyllene E. The key of the methodology was the catalytic enantioselective [2+2]

cycloaddition step using a novel oxazaborolidine catalyst **7**, which facilitated the reaction of alkenes **6** and allenates **5** to produce chiral geminal dimethylcyclobutanes adduct with high functional-group tolerance. This tactic permitted a late-stage cycloaddition with a completely functionalized alkene, trailed by a diastereoselective reduction, leading to the hebelophyllene natural product (Scheme 5).¹⁹



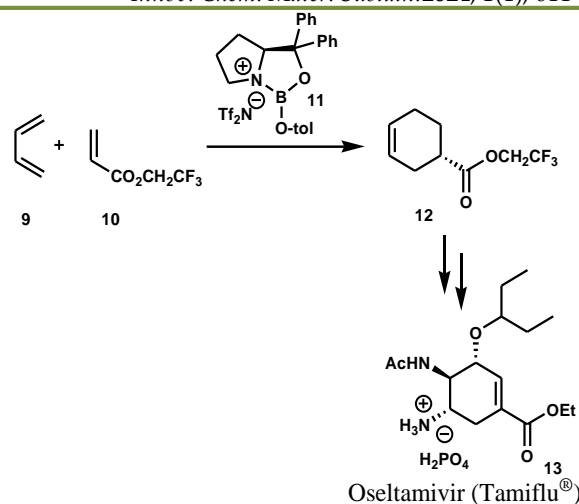
Scheme 5. Enantioselective [2+2] cycloaddition by oxazaborolidine catalyst.

3. Synthesis of natural products congeners

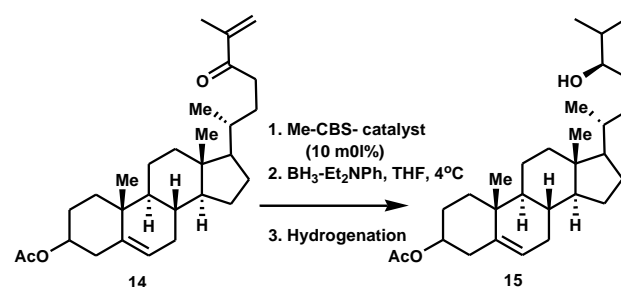
Oxazaborolidines have demonstrated to be extremely beneficial and versatile catalysts in the synthesis of various biologically significant complex molecules, such as estrone, desogestrel, laurenditerpenol, and dolabellane-type marine natural products, including the oral antifu drug oseltamivir (Tamiflu®). The development of the avian virus N1H5 raises the opportunity of a pandemic wave of deadly flu, demanding prompt action.²⁰ Therefore, the total synthesis of oseltamivir offers several advantages over existing procedures and has the potential to rise the production rate.

A short, scalable, and straightforward enantioselective Diels–Alder reaction route was reported by Corey *et al.*²¹ for synthesizing the anti-influenza neuraminidase inhibitor oseltamivir (Tamiflu® **13**) from 1,3-butadiene (**9**) and acrylate **10**. The reaction of butadiene **9** with trifluoroethyl acrylate (**10**), in the presence of *S*-prolinol-derived oxazaborolidine cation catalyst **11**, formed the adduct **12**. This adduct was then further elaborated through multiple steps to synthesize oseltamivir (**13**) (Scheme 6).

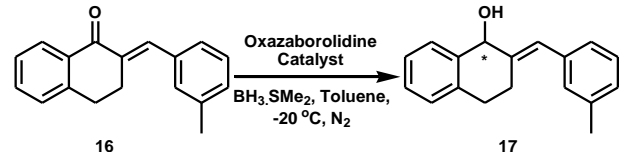
Enantioselective reduction of α -methylene ketones using oxazaborolidine-catalyst have reported Ishibashi *et al.*^{22a} efficiently and conducted the reaction using borane–diethylaniline ($\text{BH}_3\text{-Et}_2\text{NPh}$) as a stoichiometric reducing agent. Combining this method with the successive hydrogenation of the allylic alcohol produced enhanced stereoselectivity during the reduction of 24-oxocholesteryl ester to 24-(*R*)-hydroxycholesteryl ester. Under optimized conditions, the oxazaborolidine (Me-CBS)-catalyzed reduction of **14** afforded the allylic alcohol intermediate with 87% yield and high enantioselectivity (*R/S* 97.5:2.5). The hydrogenation of *exo*-methylene group regioselectively was achieved the intermediate using H_2 and Wilkinson's catalyst, resulting in (*R*)-hydroxycholesteryl acetate **15** with 84% yield (Scheme 7). Tülay Yıldız developed a synthetic approach to produce new chiral allylic alcohols **17** through the enantioselective reduction of (*E*)- α,β -unsaturated ketones **16**. This method employs oxazaborolidine catalysts, which are derived from amino alcohol and trimethylboroxine, and achieves high enantioselectivity and chemoselectivity. The reduction is carried out in toluene at -20 °C and typically completes within 0.5–2 hours (Scheme 8).^{22b}



Scheme 6. Enantioselective Diels–Alder reaction using chiral oxazaborolidine catalyst.



Scheme 7. Enantioselective reduction of α -methylene ketone.



Scheme 8. Enantioselective reduction of α -methylene ketone.

Epothilones represent an encouraging new class of anticancer drugs (Figure 6). Preclinical studies have exposed that epothilones effectively bind to and alleviate microtubules, similar to paclitaxel but with some differences, and they are effective in tumor representations resistant to paclitaxel. Clinical data from phase I and phase II trials are accessible for BMS-247550, BMS-310705, EPO906, and KOS-862. Like taxanes, epothilones prevent cancer cell division by intrusive with tubulin. However, early trials suggest that epothilones deal better effectiveness and milder adversarial effects compared to taxanes.²³

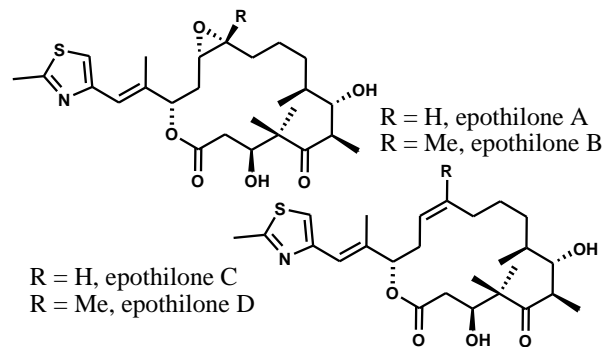
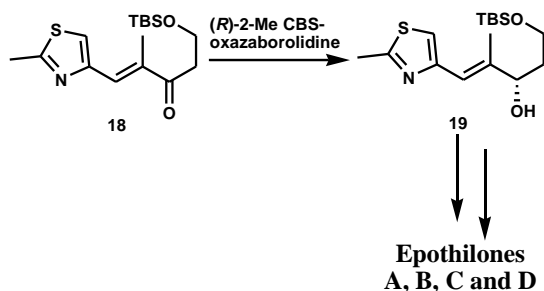


Figure 6. Structure of Epothilones A, B, C and D.

Reiff *et al.*²⁴ successfully accomplished the total synthesis of epothilones A, B, C, and D using novel and efficient asymmetric synthetic methods to prepare two key building

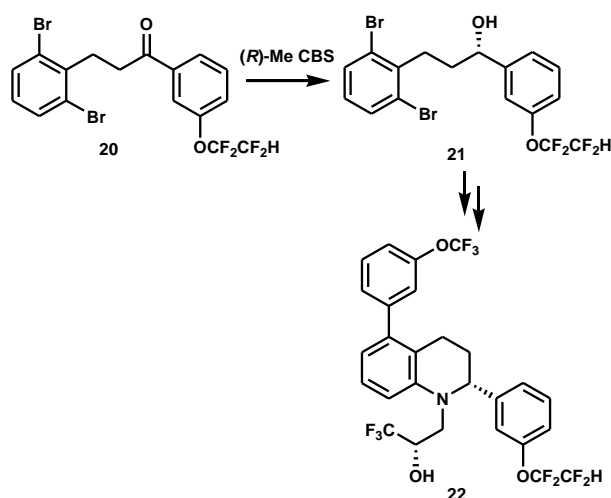
blocks (Scheme 9). A decisive step in this synthesis was the asymmetric reduction of (*E*)-5-(tert-butyldimethylsilyloxy)-2-methyl-1-(2-methylthiazol-4-yl)pent-1-en-3-one **18**, achieved using (*R*)-Me-CBS-oxazaborolidine to yield (*S*)-alcohol **19**. The final epothilone products were achieved through a well-established total synthetic strategy.²⁵



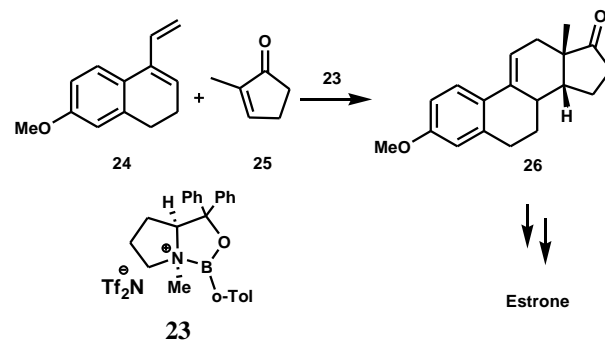
Scheme 9. Total synthesis of Epothilones A, B, C and D.

Rano *et al.*²⁶ reported the asymmetric synthesis of 3,4-dihydro-2-[3-(1,1,2,2-tetrafluoroethoxy)phenyl]-5-[3(trifluoromethoxy)phenyl]- α -(trifluoromethyl)-1-(2*H*)-quinoline ethanol **22**, a cholesteryl ester transfer protein (CEPT) inhibitor. The asymmetric alcohol intermediate **21** was achieved through the chiral reduction of a ketone using Corey's (*R*)-Me CBS oxazaborolidine reagent and a tetrahydroquinoline core was formed *via* a Cu-mediated intramolecular amination reaction. Additionally, the synthesis of the prochiral ketone **20** was enhanced by eradicating the use of a harmful aryltin reagent (Scheme 10).

First, Canales *et al.*²⁷ reported the synthesis of hitherto mysterious N-methyl oxazaborolidine cations **23**, specifically a cationic proline derivative that functions as a stronger chiral Lewis acid than the typical oxazaborolidine catalyst. They presented a new method for synthesizing oxazaborolidines by reacting lithium aryl borohydrides with amino alcohol salts. This cationic oxazaborolidine reagent is highly effective in [4+2] cycloaddition reactions. For instance, the diene 7-methoxy-4-vinyl-1,2-dihydro-naphthalene **24** reacted with the 2-methyl-cyclopent-2-enone dienophile **25** to produce the adduct **26** in noble yield and with extraordinary enantioselectivity (Scheme 11). Several diverse examples, including estrone, demonstrate the broad applicability of this catalytic methodology.



Scheme 10. Total synthesis of 3, 4-dihydro-2-[3-(1,1,2,2-tetrafluoroethoxy)phenyl]-5-[3-(trifluoromethoxy)phenyl]- α -(trifluoromethyl)-1-(2*H*)-quinoline ethanol.

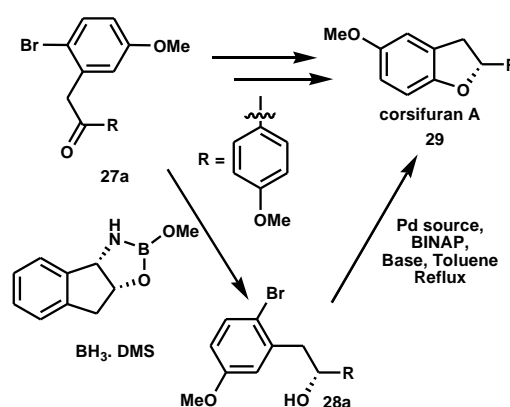


Scheme 11. Asymmetric [4+2] cycloaddition reaction by N-methyl oxazaborolidine cations.

Corsifuran A (**29**) is one of three corsifurans, featuring a 4',5-dioxygenated-2-arylbenzofuran skeleton. This compound was isolated from the Mediterranean liverwort *Corsinia coriandrina*.²⁸ The skeleton of corsifuran is believed to be biogenetically derived from a stilbenoid precursor, and the biogenic material has been validated to possess high enantiomeric purity.²⁹

The asymmetric reduction of ketones using borane-oxazaborolidine could potentially enable the synthesis of various natural products.^{30a} Adams *et al.* successfully synthesized enantiomerically pure corsifuran A for first time through an enantioselective reduction procedure, enabling the validation of the absolute stereochemistry of the natural product. The asymmetric reduction of ketone **27a** with the B-OMe oxazaborolidine derived from either (1*R*,2*S*)- or (1*S*,2*R*)-*cis*-1-amino-indan-2-ol afforded the *S* and *R* enantiomers of the alcohol **28a** with 76% and 78% enantiomeric excess, respectively. Further, recrystallization of the alcohol lead to in >99% enantiomeric purity. Corsifuran A (**29**) was then obtained *via* cycloetherification using numerous palladium catalysts along with widespread ligands and bases (Scheme 12).^{30b}

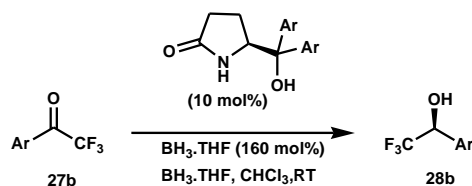
Kawanami *et al.*^{30c} reported the enantioselective reduction of the highly reactive prochiral trifluoromethyl ketone **27b** to its corresponding alcohol **28b** using an oxazaborolidine catalyst produced *in situ* from BH₃-THF with chiral lactam alcohol. This catalyst assisted the enantioselective reduction of trifluoromethyl ketones **27b** in CHCl₃ at room temperature, achieving up to 86% enantiomeric excess (ee) (Scheme 13).



Scheme 12. Asymmetric synthesis of corsifuran A through an enantioselective oxazaborolidine reduction.

They also found that CHCl₃, a polar halogenated organic solvent, was optimal for attaining high enantioselectivities with reactive trifluoromethyl ketones, as CH₂Cl₂ generally provides

lower ee compared to THF and toluene in the asymmetric reduction of typical ketones. This practical method offers several advantages, including stability towards air and moisture and milder reaction conditions compared to previously reported methods.³¹ They also investigated the influence of BF_3 on the enantioselective reduction of trifluoromethyl ketones **27b** with a chiral lactam alcohol and borane. They found that $\text{BF}_3 \cdot \text{THF}$ improved the enantioselectivity of the reduction of reactive trifluoromethyl ketones at room temperature. The $\text{BF}_3 \cdot \text{THF}$ addition to an in situ generated oxazaborolidine catalyst, derived from the chiral lactam alcohol and borane, boosted both the enantioselectivity (up to 90% ee) and yield (up to 91%).^{30d}

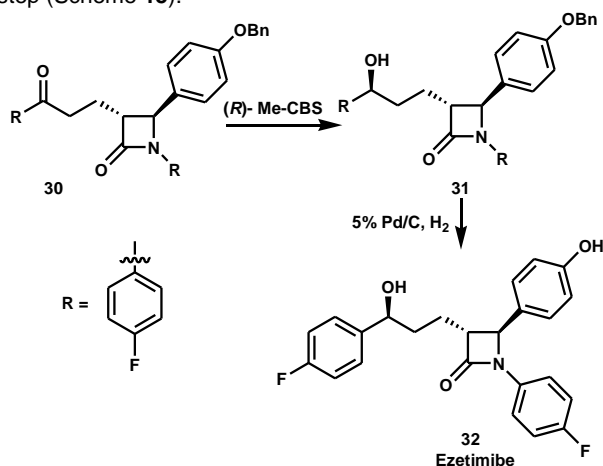


Scheme 13. Enantioselective reduction of trifluoromethyl ketones by borane-oxazaborolidine derived from a chiral lactam alcohol.

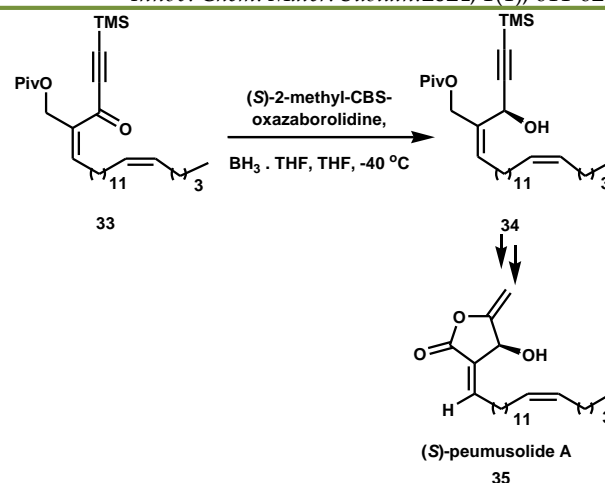
Sasikala *et al.*³² developed an efficient, cost-effective, and scalable synthesis of ezetimibe (**32**), an antihypercholesterolemia drug. Chiral oxazolidinone chemistry was engaged to establish the necessary stereochemistry of the β -lactam ring **30**, while chiral oxazaborolidine was used to determine the stereochemistry of the hydroxyl group. This synthesis significantly reduces costs and facilitates large-scale production of ezetimibe (Scheme 14).

Tamura *et al.*³³ reported the total synthesis of peumusolide A (**35**), an inhibitor of MAPK/ERK kinase (MEK) with a non-antagonistic nuclear export signal (NES)³⁴ mode, derived from the South American medicinal plant *Peumus boldus* Molina. Peumusolide A has been established to be an encouraging anti-tumor skeleton, showing selective growth inhibition in MEK-activated tumor cells.³⁵ In addition to peumusolide A, numerous related polyketides with extraordinary biological activities have also been identified.³⁶

Peumusolide A had been synthesised *via* an enantioselective reduction of 4-en-1-yn-3-one **33** to form corresponding alcohol **34** with the use of chiral oxazaborolidine as the vital reaction step (Scheme 15).

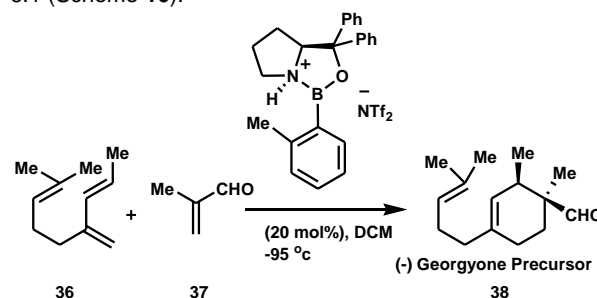


Scheme 14. Synthesis of ezetimibe.



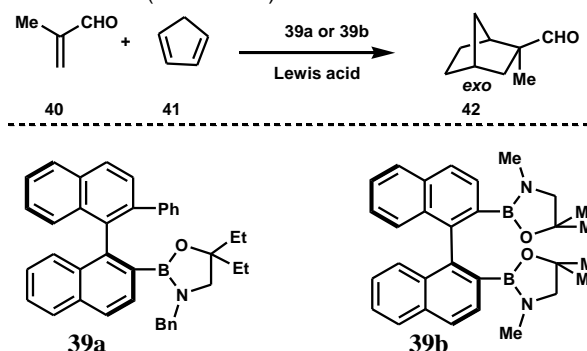
Scheme 15. Total synthesis of (S)-peumusolide A.

The total syntheses of the odorants georgyone, arborone, and associated structural congeners was reported by Corey and Hong³⁷. A decisive step in each synthesis was the intermolecular Diels–Alder reaction between diene **36** and 2-methylacrolein **37**, catalyzed by (S)-oxazaborolidinium salt. This reaction was extremely enantioselective, producing the adduct **38** through an *exo* [2+4] pathway with 96% enantiomeric excess and a 76% yield. For instance, in the synthesis of (–)-georgyone, the intermediate was achieved with 96% enantiomeric excess and a diastereomeric ratio of 6:1 (Scheme 16).



Scheme 16. Oxazaborolidinium salt catalysed intermolecular Diels–Alder reaction.

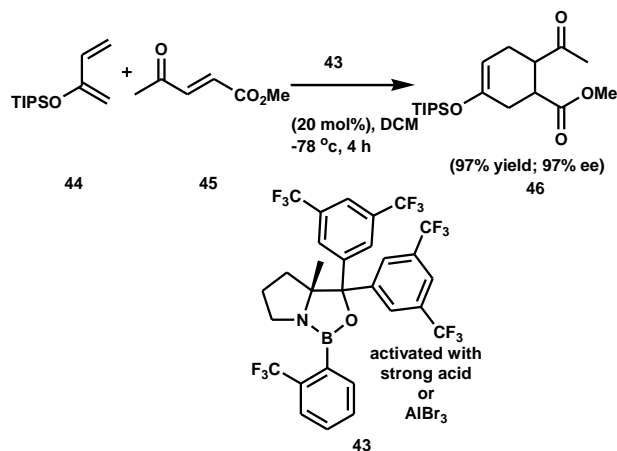
Shimoda and Yamamoto developed a novel axially chiral oxazaborolidine catalyst (**39a**), which combines a chiral boronic acid with a readily modifiable achiral amino alcohol.^{38a} This catalyst demonstrated effective in a Diels–Alder reaction between diene **41** and dienophile **40**, yielding the desired adduct with notable enantioselectivity. Furthermore, the bis(oxazaborolidine) catalyst (**39b**), featuring two Lewis acidic centers, achieved even greater enantioselectivity in the Diels–Alder reaction (Scheme 17).



Scheme 17. Axially chiral oxazaborolidine catalysts for effective Diels–Alder [4+2] reaction.

Chen *et al.*^{38b} described a catalytic, highly regio- and enantioselective Diels–Alder reaction involving (*E*)-4-oxopent-

2-enoates (**45**) as dienophiles and diene **44** to afford the adduct **46**. This reaction was facilitated by oxazaborolidines **43**, which were activated into cationic chiral catalysts using either the strong acid triflimide or AlBr_3 (Scheme 18).



Scheme 18. Catalytic regio- and enantioselective [4+2] Diels-Alder reaction.

4. Synthesis of Chiral Intermediates, Ligands and Building Blocks

The synthesis of several therapeutic agents and complex natural products depends on the accessibility of chiral intermediates, which serve as essential building blocks for further structural and stereochemical variations. Asymmetric catalysis has turned into one of the most resourceful methods for preparing a diverse range of small molecules in highly enantiomerically-enriched forms.

Cho³⁹ reviewed the use of chiral oxazaborolidine-mediated borane reductions for prochiral ketones and ketimines. This approach has been extensively engaged for the greatly effective asymmetric synthesis of a wide array of chiral natural products, building blocks, bioactive compounds, intermediates, and ligands, all of which feature chiral alcohol or amine functionalities in their structures.

Xiao *et al.*⁴⁰ employed natural product skeletons as novel chiral synthons for asymmetric catalytic transformations and presented a new class of structurally stiff tricyclic chiral ligands for asymmetric catalysis. They described the design and synthesis of these fresh chiral ligands and their effectiveness in the asymmetric reduction of ketones, achieving good yields and enantioselectivities. They exploited a tryptophan-based hexahydropyrrolo [2,3-*b*]indole skeleton as a rigid chiral backbone to achieve enantiocontrol, benefiting from its tricyclic and structurally rigid nature (Figure 7). This chiral oxazaborolidine ligand was synthesized *in situ* for the reduction of functionalized ketones.

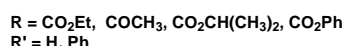
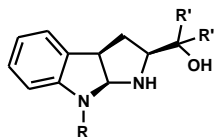


Figure 7. Natural product skeletons used for oxazaborolidine catalyst.

Yune *et al.*⁴¹ reported the enantioselective reduction of prochiral ketones using mesoporous silica-supported oxazaborolidines in a heterogeneous phase (Figure 8). They estimated how immobilization of oxazaborolidines on silica, with different substituents on the boron and nitrogen atoms, affected the enantioselective reduction of acetophenone. The performance of the silica-supported oxazaborolidines was

compared to their homogeneous analogs by changing several parameters.

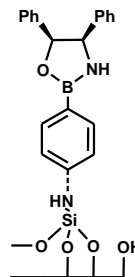
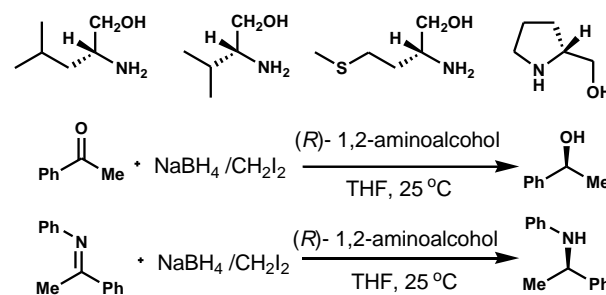


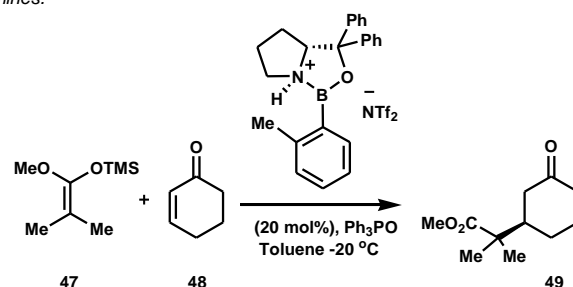
Figure 8. Silica supported oxazaborolidine catalyst.

Kettouche *et al.*⁴² introduced a fresh method for preparing oxazaborolidine catalysts *in situ*, employing 1,2-aminoalcohol, NaBH_4 , and CH_2I_2 for the asymmetric reduction of prochiral ketones and imines (Scheme 19). The oxazaborolidine catalyst is handily synthesized at room temperature in THF using 1,2-aminoalcohols and BH_3 generated from the sodium borohydride/ CH_2I_2 reagent system. This *in situ* prepared oxazaborolidine/ BH_3 reagent system is effective for reducing prochiral ketones and N-substituted imines to their corresponding alcohols and amines with reasonable to good enantiomeric excesses. This method delivers a relatively humble and inexpensive methodology for this broadly used transformation in synthesis.

Corey and his colleagues⁴³ accompanied a catalytic, enantioselective Michael addition reaction using 20 mol% of catalyst. The reaction among a silyl ketene acetal **47** and cyclohexenone **48** formed the 1,4-addition product **49** with a yield of 91% and an enantiomeric excess of 90% (Scheme 20).



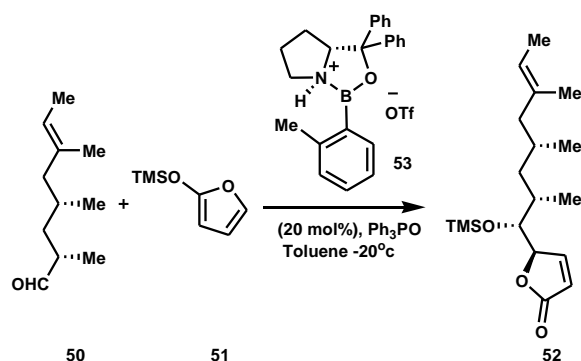
Scheme 19. Asymmetric reduction of prochiral ketones and N-substituted imines.



Scheme 20. Enantioselective Michael addition reaction by oxazaborolidinium salt.

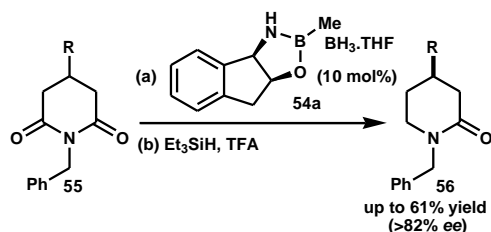
Application of chiral oxazaborolidinium salts in asymmetric vinylogous Mukaiyama Aldol reaction, was reported first by Boeckman *et al.*⁴⁴ The synthesis of butenolide **52** was achieved with good diastereoselectivity by adding trimethylsiloxyfuran **51** to aldehyde **50** in the presence of oxazaborolidine catalyst **53**. Incorporating additional methyl substituents on the diphenyl group of the oxazaborolidinium

salt enhanced the diastereoselectivity to over 90% with an 80% yield (Scheme 21).



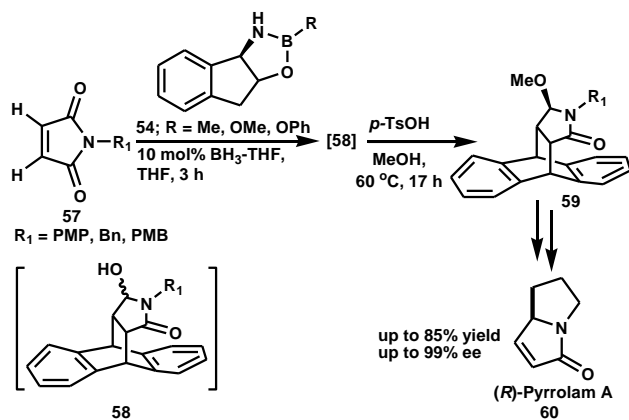
Scheme 21. Asymmetric vinylogous Mukaiyama Aldol reaction by Oxazaborolidinium salts.

Jones *et al.*^{45a} described an enantioselective reductive desymmetrization of glutarimides **55** using an oxazaborolidine catalyst **54a** derived from *cis*-1-amino-indan-2-ol. The reaction was shown to proceed *via* a stereoablative mechanism, which boosted the enantioselectivity of the intermediate hydroxy-lactam. The process accommodated various substituents at the 4-position **56**, achieving with 61% enantiomeric excesses exceeding 82% (Scheme 22).



Scheme 22. Enantioselective reductive desymmetrization of glutarimides by borane-oxazaborolidine.

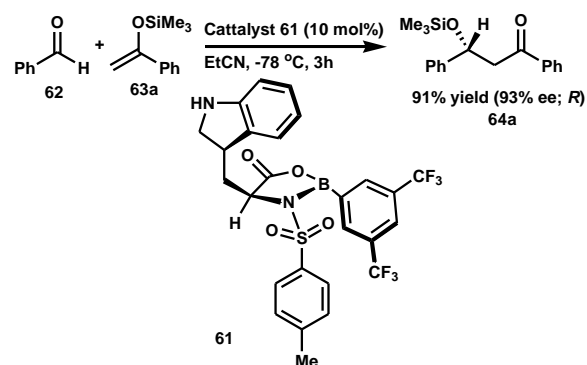
The same group also accomplished enantioselective catalytic desymmetrization of maleimides by temporarily removing an internal mirror plane and using stereoablative over-reduction. This approach led to the synthesis of (*R*)-pyrrolam A (**60**).^{45b} In this over reduction course is critical for attaining product with yield 85% and up to 99% ee (Scheme 23)



Scheme 23. Asymmetric desymmetrization of maleimides leading to synthesis of (*R*)-pyrrolam A.

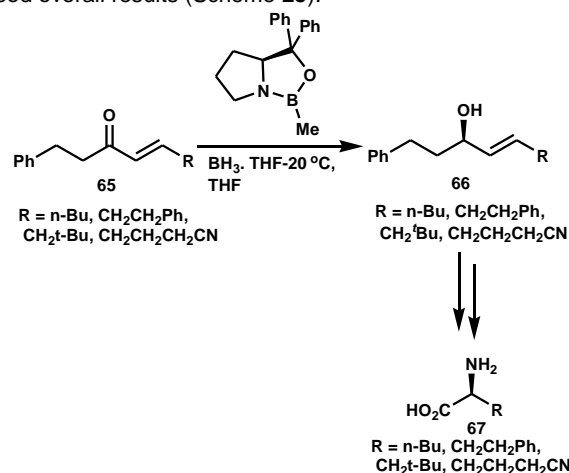
Grayson and Farrar reported that their computational analyses have introduced a new reaction model with benzaldehyde **62** and alkene **63a** for the noncovalent interactions in the

oxazaborolidine **61** catalyzed Mukaiyama aldol reaction, which aligns with experimental selectivity and has been validated for systems with less polarized and nonaromatic boron substituents.⁴⁶ The observed selectivity is explained by π - π interactions present in the major transition states, which are geometrically infeasible in the minor transition states due to the orientation of nucleophilic binding (Scheme 24).



Scheme 24. Model reaction for computational analysis.

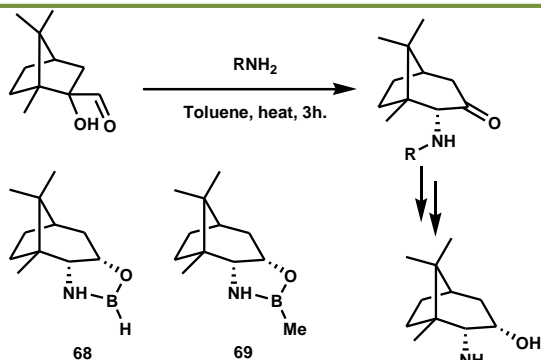
Drummond *et al.*⁴⁷ developed a new general method for preparing optically active α -amino acids. The process comprises a key ruthenium-catalyzed cross-coupling reaction to produce a range of α,β -unsaturated ketones **65**, which are then reduced to allylic secondary alcohols **66** using a chiral Me-CBS oxazaborolidine. The resulting alcohol endures a thermal Overman rearrangement to form a series of allylic trichloroacetimidates, which are subsequently transformed to the target α -amino acids **67** under standard conditions, yielding good overall results (Scheme 25).



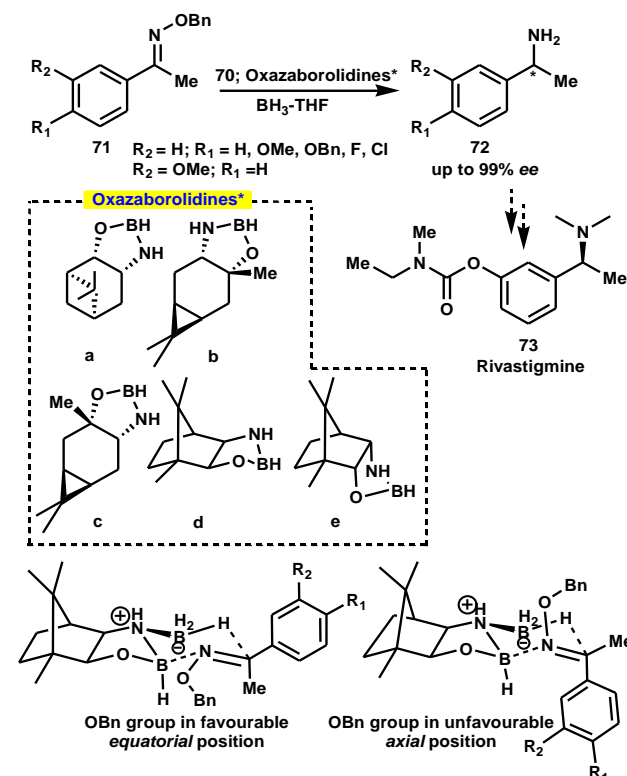
Scheme 25. Synthesis of optically active α -amino acid.

Yang *et al.*⁴⁸ established a novel camphor-based chiral amino alcohol and described its use in the asymmetric reduction of prochiral aryl ketones by borane at room temperature, utilizing oxazaborolidines derived from chiral amino alcohols. The oxazaborolidine **69** demonstrated greater selectivity compared to **68** (Scheme 26).

Zaidlewicz *et al.* were introduced of some new class of oxazaborolidine derived from terpene and used for enantioselective reduction of prochiral ketones and oximeethers.⁴⁹ They found that the reduction of (*E*)-ketoxime O-benzyl ethers **71** using borane catalyzed by terpene-derived oxazaborolidines **70** specifically those derived from (1*R*)-nopinone and (1*R*)-camphor produced the corresponding amines up to 99% enantiomeric excess. In contrast, oxazaborolidines derived from (1*S*)-2-carene and (1*S*)-3-carene exhibited lower selectivity. Additionally, (*S*)-1-(3-methoxyphenyl)ethanamine (**72**), a key intermediate for synthesizing (*S*)-rivastigmine (**73**), was obtained with 94% ee by reducing (*E*)-1-(3-methoxyphenyl)ethanone O-benzyl oxime using borane and oxazaborolidine generated from (*S*)-valinol (Scheme 27).^{49e}



Scheme 26. Synthesis of a novel camphor based chiral amino alcohol for preparing oxazaborolidine catalyst.

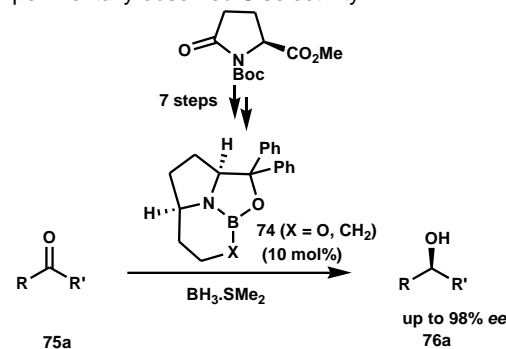


Scheme 27. Enantioselective reduction of ketoxime ethers by terpene-derived oxazaborolidines.

Breuning's group presented two novel tricyclic 1,3,2-oxazaborolidines **74**, synthesized in seven steps from methyl Boc-L-pyrroglutamate. These compounds feature an ortho- and peri-fused 5/5/6-ring system with a B–N bond forming one of the ring junctions.⁵⁰ Asymmetric borane reduction of ketones **75a**, the B-alkoxy bridged derivative succeeds superb enantioselectivities (up to 98% ee), with activity akin to that of the standard CBS catalyst. In contrast, the closely related B-alkyl bridged derivative shows lower enantioselectivities and reduced activity, as confirmed by competition experiments (Scheme 28).

Kettouche conducted an in-depth DFT study using wB97XD/6-31G(d,p) to explore the mechanism of enantioselective ketone reduction catalyzed by a B-methoxy-oxazaborolidine derived from (–)-β-pinene.⁵¹ The study revealed that the reaction occurs in six steps: (a) formation of the active catalyst-borane adduct (Figure 9a), (b) coordination of the aromatic ketone to the catalyst-borane adduct (Figure 9b), (c) transfer of a hydrogen atom from the boron atom to the prochiral carbon center (Figure 9c), (d) creation of a four-membered ring (B–O–B–N) through a [2 + 2] cycloaddition (Figure 9d), (e) opening of the four-membered ring (B1–O2–B3–N4) (Figure 9e), and (f) regeneration of the catalyst (Figure 9f).

Kettouche concluded that the stereoselectivity of the reaction is determined by the intramolecular hydride transfer from the BH₃ moiety to the Si or Re face of the carbonyl substrate. The S-type chirality of the reduced products aligns with experimental results (Figure-9). Additionally, non-covalent interaction analysis of the most favorable transition state advocates a dispersive interaction between the hydrogen atom of the methanediyl group within the pinene skeleton. The stabilization provided by the two-atom [O–B] unit helps explain the experimentally observed S selectivity.



Scheme 28. Enantioselective reduction of reactive ketones by oxazaborolidine catalyst.

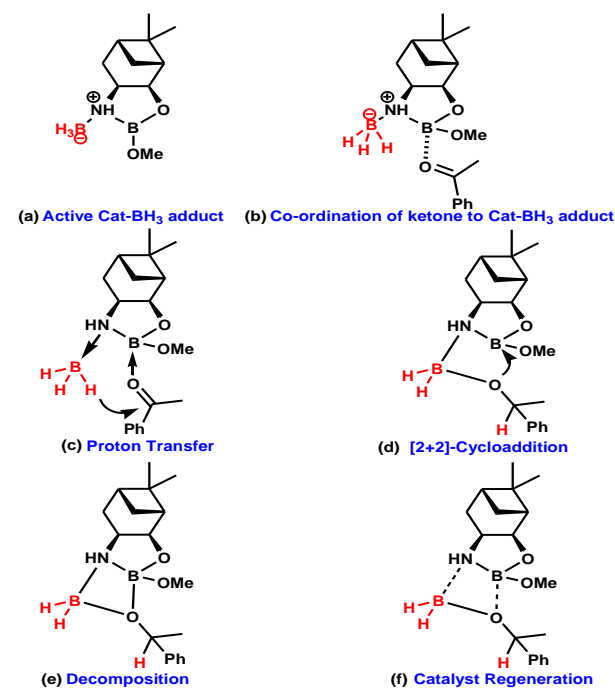
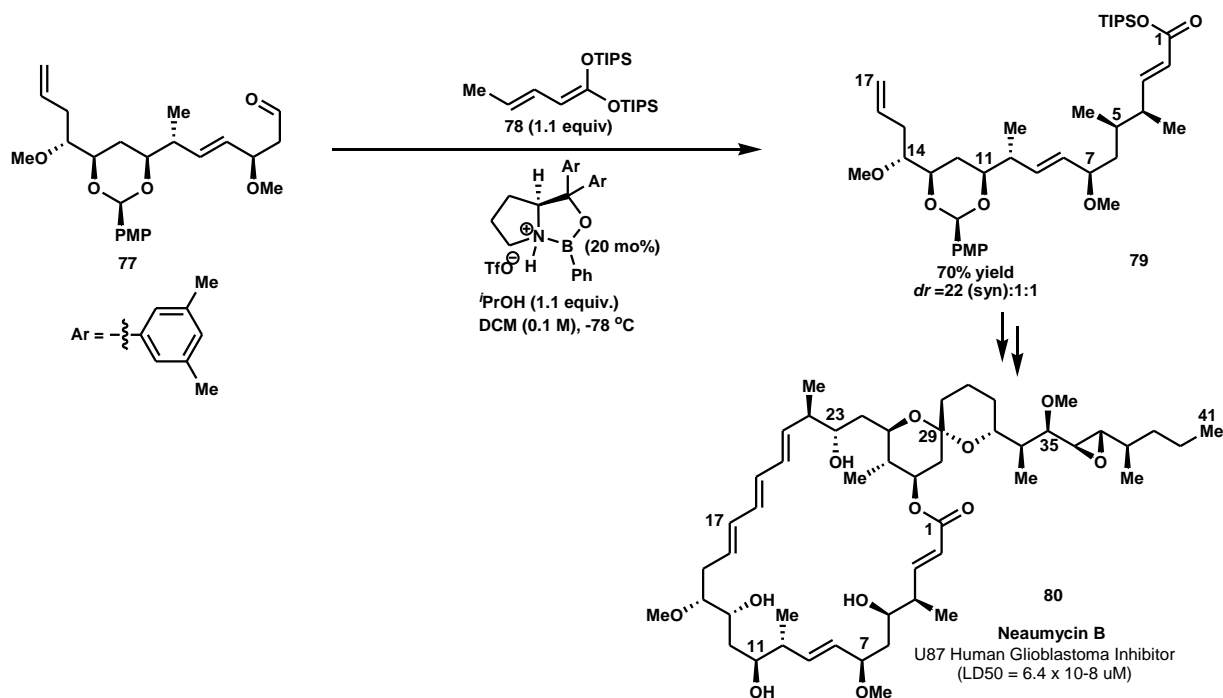


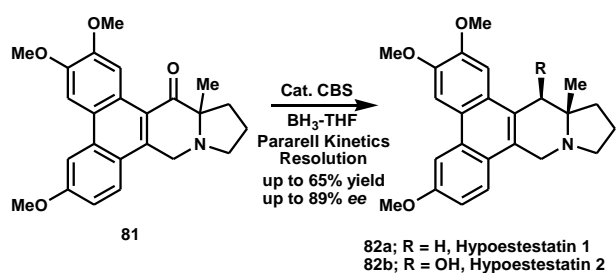
Figure 9. Proposed catalytic steps based on DFT analyses

Krische *et al.*⁵² fruitfully synthesized neaumycin B (**80**), a femtomolar inhibitor of U87 human glioblastoma, utilizing Ru-JOSIPHOS-catalyzed C–C bond-forming reactions. The key intermediate **79** to accessing neaumycin B (**80**) was the development of an asymmetric vinylogous Mukaiyama aldol (VMA) reaction specifically designed for linear aliphatic aldehydes **77**, a novel route for terminally methylated dienyl ketene acetals (Scheme 29).

Disadee and Ruchirawat described an enantioselective synthesis of both natural and unnatural hypoestestatin **82a** and **82b** analogues with high yields (~91%) and significant enantioselectivity (up to 89% ee).⁵³ This was achieved through the parallel kinetic resolution of racemic ketones **81** using CBS-oxazaborolidine-catalyzed reduction, which produced two separable diastereomeric alcohols. Notably, this was the first

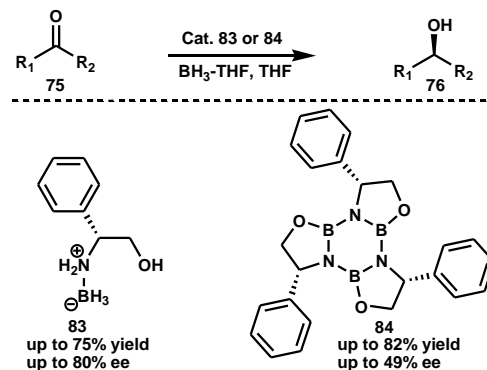
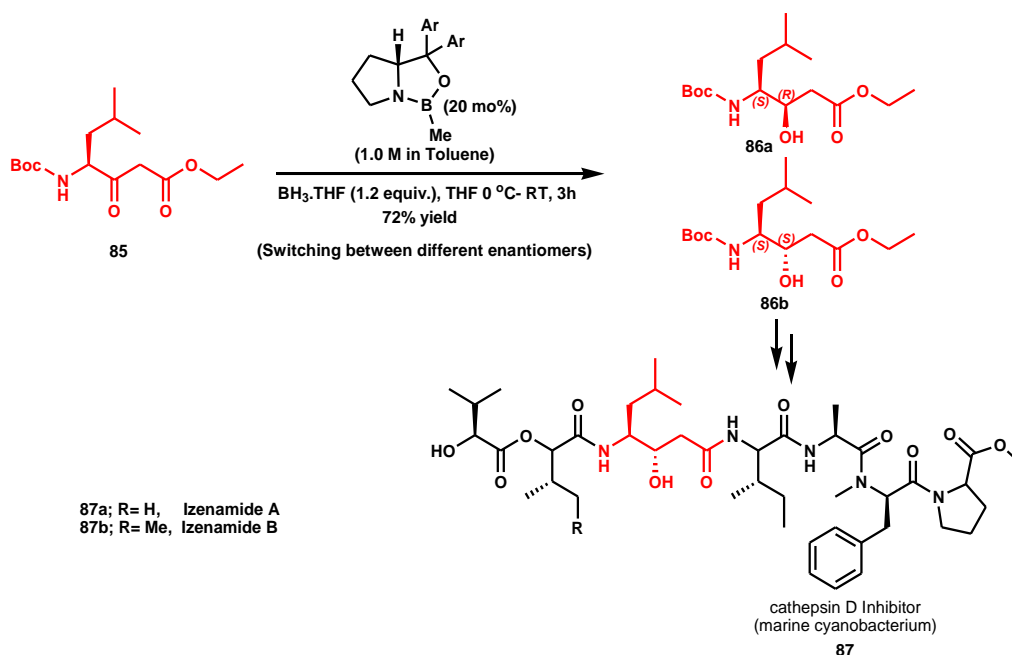


Scheme 29: Oxazaborolidine-catalyzed Vinylogous Mukaiyama Aldol reaction leading to Neaumycin B (80)



Scheme 30. Oxazaborolidine-catalyzed asymmetric reduction for seco-hypoestestatin 1 and 2.

time demonstrated the catalytic asymmetric reduction for seco-hypoestestatin 1 and 2.

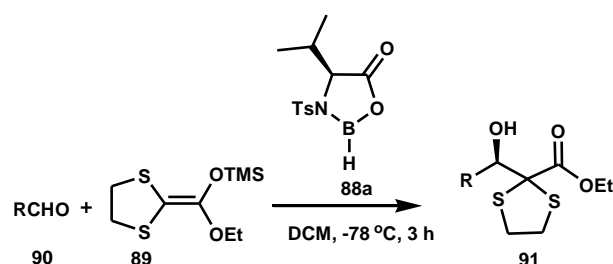
Scheme 31. Enantioselective ketone reduction by *N*-boranes (noncyclic) and tris(oxazaborolidine)borazines (cyclic) derived from chiral β -amino alcohol.

Scheme 32: Enantioselective synthesis of Izenamide A and B by oxazaborolidine catalysts.

This approach embraces potential for adapting racemic mixtures into enantioenriched forms, which could be useful for numerous biological assays in the future (Scheme 30). Vougioukalakis *et al.*⁵⁴ thoroughly examined the influence of chiral β -amino alcohol *N*-boranes (noncyclic, **83**) and their corresponding tris(oxazaborolidine)borazines (cyclic; **84**) on the catalytic asymmetric reduction of prochiral ketones **75**. Both cyclic and noncyclic catalysts commendably twisted secondary alcohols **76** with an ~82% yield. Interestingly, polycyclic borazine catalyst proved stability merely in nonprotic dry organic solvents, whereas the noncyclic catalyst persisted stable in both aqueous and organic solvents (Scheme 31). Sharma and colleagues described an efficient, concise, and scalable alternative method for synthesizing Izenamide A (**87a**) and B (**87b**) with high stereoselectivity.⁵⁵ Their tactic involves the enantioselective reduction of *N*-Boc γ -amino β -keto esters **85** to the corresponding alcohols **86** using 2-methyl-CBS-oxazaborolidine catalysts. They also demonstrated that by switching between different enantiomers of the 2-methyl-CBS-oxazaborolidine catalyst, they could synthesize both diastereomers of the alcohol. This methodology could be of excessive significance, as γ -amino β -ketoesters exemplify a key motif in drug discovery (Scheme 32).

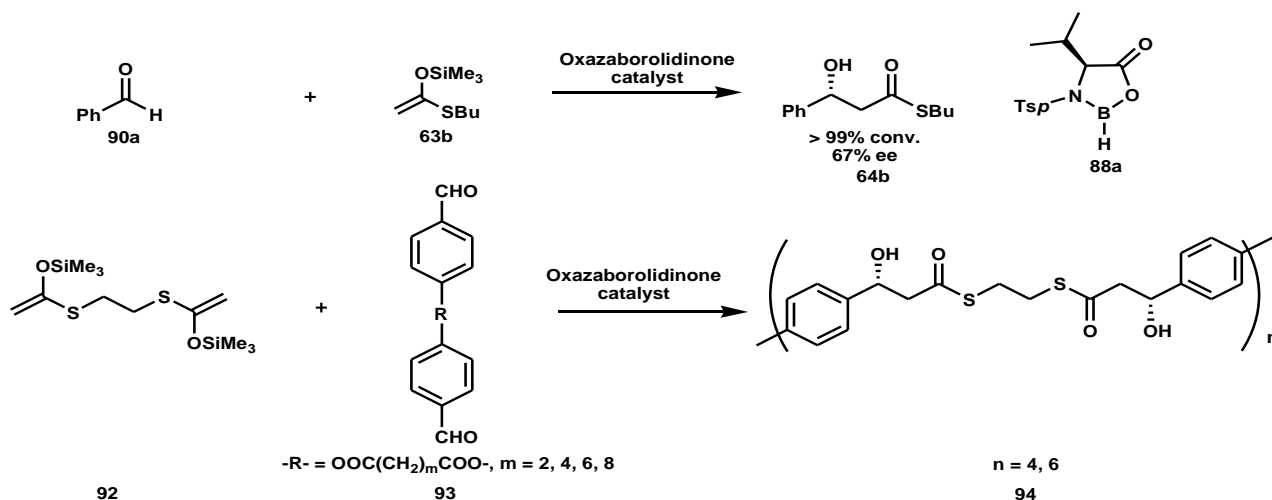
5. Oxazaborolidinone

The enantioselective reduction of prochiral carbonyls and ketimines has been widely studied with oxazaborolidine catalysts compared to oxazaborolidinones. Kiyooka *et al.*⁵⁶ were the first to report an aldol reaction encouraged by a chiral oxazaborolidinone **88a**. This reaction involved a silyl ketene acetal **89** derived from ethyl 1,3-dithiolane-2-carboxylate and aldehyde **90**, resulting in the synthesis of acetate aldols **91** with high enantiomeric purity (Scheme 33).



Scheme 33. Chiral oxazaborolidinone catalyzed aldol reaction.

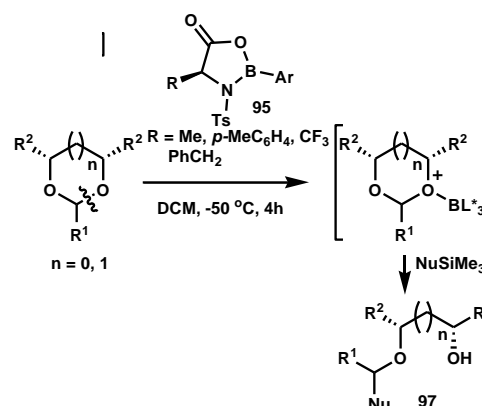
Komura *et al.*⁵⁷ discovered that the asymmetric repetitive Mukaiyama Aldol reaction among bis(trimethylsilyl)ketene



Scheme 34: Asymmetric Mukaiyama aldol reaction by oxazaborolidinone catalyst.

thioacetal) **92** and dialdehydes **93**, when executed in the presence of chiral oxazaborolidinone **88a**, yielded optically active poly(β -hydroxy thioester) **94**. The extent of asymmetric induction during polymerization was measured through a model reaction and by chiral HPLC analysis of the degradation products of the chiral polymers (Scheme 34). Simple Mukaiyama Aldol reaction also responded under this conditions.

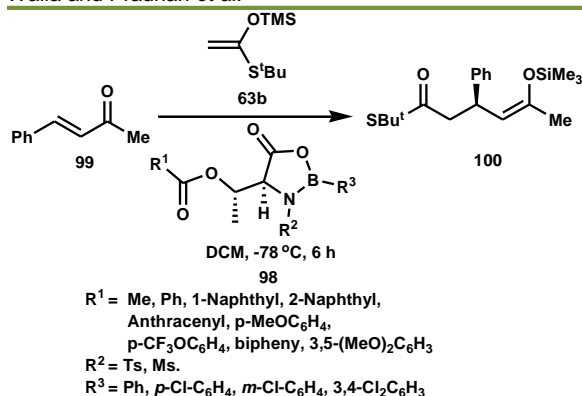
Harada *et al.*⁵⁸ reported the inter- and intra-molecular differentiation of enantiotopic dioxane acetals **96** using an oxazaborolidinone **95** mediated enantioselective ring-cleavage reaction. They also perceived the kinetic resolution of racemic 1,3-alkanediols and the asymmetric desymmetrization of *meso*-1,3-polyols (Scheme 35).



Scheme 35. Oxazaborolidinone catalyzed enantioselective ring-cleavage reaction.

Wang *et al.*⁵⁹ reported enantioselective Lewis acid-catalyzed Mukaiyama-Michael reactions of acyclic enones **99** with trimethylsilyl ketene *S,O*-acetal **63b**, using allo-threonine-derived *O*-aroyl-*B*-phenyl-*N*-tosyl-1,3,2-oxazaborolidin-5-ones **98** as catalysts to produce **100** (Scheme 36). This model for asymmetric induction was recommended based on the correlation among catalyst structures and their enantioselectivities.

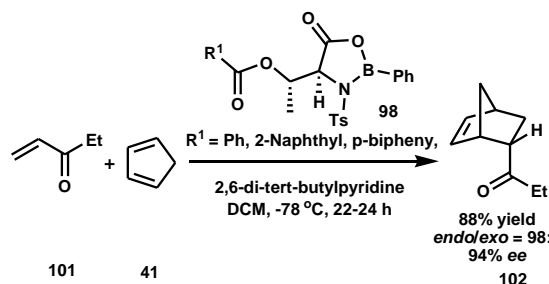
This new class of oxazaborolidinone catalysts **98** compromises a convenient method for producing enantioenriched γ -ketoacid thiol esters. Various alkenyl methyl ketones were effectively used as Michael acceptors, accomplishing enantiomeric excess values of 85-90% with the use of 10 mol% of the catalyst.



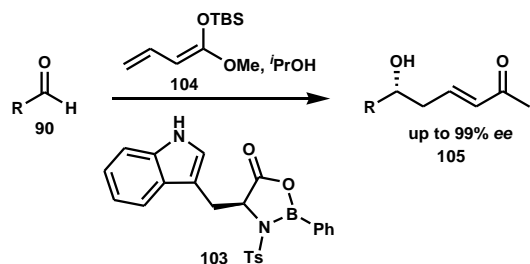
Scheme 36. Oxazaborolidinone catalysed enantioselective Mukaiyama-Michael reactions.

Harada and Singh⁶⁰ reported an enantioselective Diels-Alder reaction between acyclic enone dienophile **101** and diene **41**, catalyzed by allo-threonine-derived chiral oxazaborolidinone (10-20 mol%). This reaction produced the Diels-Alder adduct **102** with high yield, excellent endo selectivity, and 94% enantiomeric excess (Scheme 37).

Simsek *et al.*⁶¹ developed oxazaborolidinone-promoted vinylogous Mukaiyama aldol reactions. They used tryptophan-derived B-phenyl oxazaborolidinone **103** for the enantioselective vinylogous Mukaiyama aldol reaction between O,O-silyl ketene acetal **104** and aldehyde **90**, facilitating efficient entrees to chiral building blocks **105** for polyketide synthesis (Scheme 38). Their studies also emphasized that isopropyl alcohol is compulsory as an additive to overturn the racemic TBS-catalyzed pathway and enhance enantioselectivity. For α -chiral aldehydes, they demonstrated that selecting proper protecting groups is crucial for achieving high selectivities. In the context of total syntheses, *R*-chiral aldehydes were utilized as substrates, revealing that TBS ethers afforded useful selectivities compared to PMB-protected substrates when the right protecting groups were chosen.



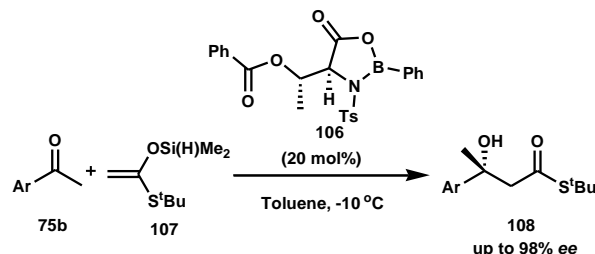
Scheme 37. Allo-threonine-derived chiral oxazaborolidinone catalysed Diels-Alder reaction.



Scheme 38. B-phenyloxazaborolidinone derived from tryptophane catalysed Mukaiyama aldol reaction.

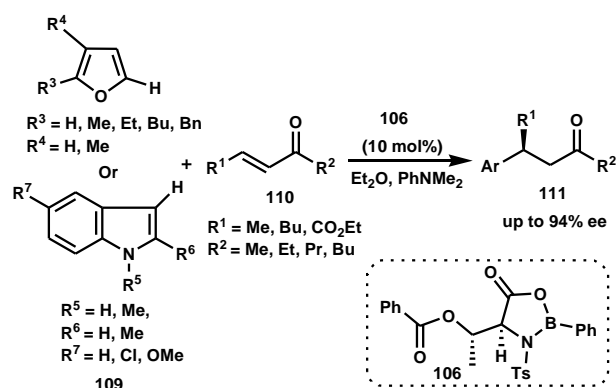
Adachi *et al.*^{62a} established an asymmetric aldol reaction catalyzed by allo-threonine-derived oxazaborolidinone **106**.

This reaction comprises nonactivated aromatic ketones **75b** and silyl ketene S,O-acetals **107**, yielding tertiary hydroxy carbonyl compounds **108** with high enantioselectivity (Scheme 39). They found that using dimethylsilyl ketene S,O-acetals instead of the conventional trimethylsilyl derivatives are crucial for achieving both effective catalytic activity and high selectivity.



Scheme 39. Asymmetric Aldol reaction of nonactivated aromatic ketones by oxazaborolidinone.

They also confirmed the enantioselective Friedel-Crafts alkylation of electron-rich heteroaromatics **109**, such as furans and indoles, with α,β -unsaturated ketones **110** using same oxazaborolidinone catalyst **106**. This work marked the first successful enantioselective Friedel-Crafts alkylation of furans with a monodentate α,β -unsaturated ketone using oxazaborolidinone catalysis (Scheme 40). Additionally, the catalyst system was effectively applied to the alkylation of indoles, widening the range of substrates. The presence of *N,N*-dimethylaniline as an additive was found to be essential for achieving high enantioselectivity.^{62b}



Scheme 40. Enantioselective Friedel-Crafts alkylation reaction by oxazaborolidinone.

Micoine *et al.*⁶³ have reported an efficient total synthesis of the antiproliferative macrolide and cell migration inhibitor lactimidomycin **113** (Scheme 41). The synthesis involved the key intermediate, the strained 12-membered 1,3-enyne **112**, which was elaborated to the final target through a highly diastereoselective Mukaiyama aldol reaction. This reaction was controlled using tryptophan-derived B-phenyloxazaborolidinone **103** as a strategic component.

Costantino *et al.*⁶⁴ introduced the first example of chiral oxazaborolidinones attached to α -layered zirconium phosphonates, demonstrating the versatility of these zirconium-based materials. They established heterogeneous catalysts that executed effectively in Mukaiyama aldol reactions, yielding good enantiomeric excess. The catalysts were derived from a mixed zirconium sulfophenylphosphonate methanphosphonate chiral borane **114** (Figure 10).

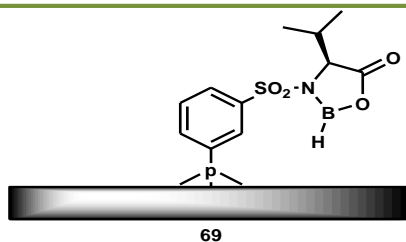


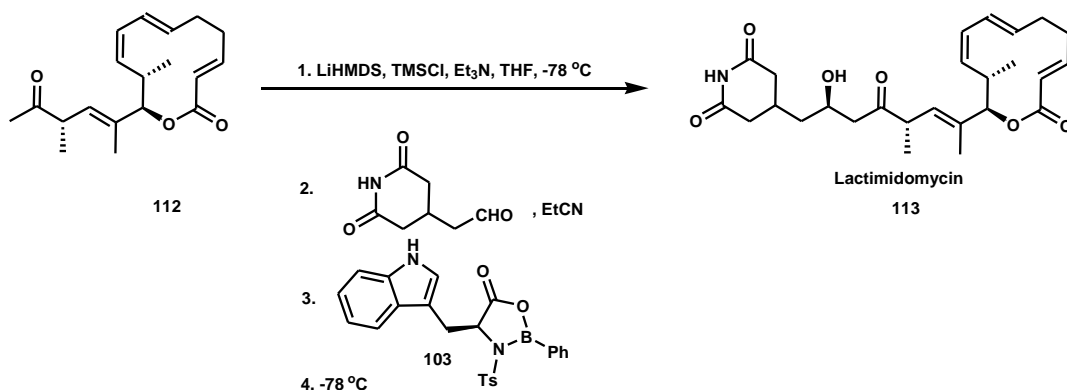
Figure 10. Oxazaborolidinone on the surface of lamella of α - $\text{Zr}[\text{O}_3\text{PC}_6\text{H}_4\text{SO}_2\text{NHCH}(\text{CH}(\text{CH}_3)_2\text{COOH})](\text{O}_3\text{PCH}_3).n\text{H}_2\text{O}$.

While these heterogeneous catalysts exhibited somewhat lower performance compared to their homogeneous counterparts, the results are encouraging. This suggests substantial potential for similar systems utilizing insoluble zirconium phosphonates. The layered compounds were characterized using various techniques and subsequently reacted with BH_3 -THF to obtain the heterogeneous chiral oxazaborolidinone.

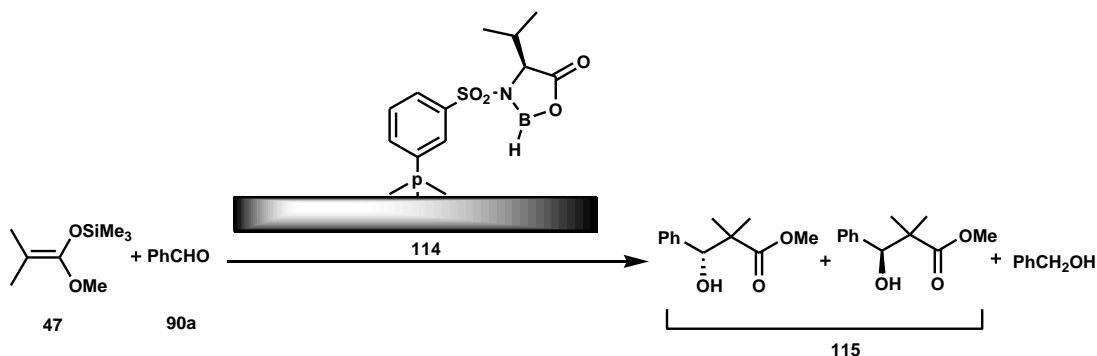
In this process, aldehyde **90a** and silyl ketene acetal **47** were reacted with the oxazaborolidinone immobilized on the surface of lamellar α - $\text{ZrO}_3\text{PC}_6\text{H}_4\text{SO}_2\text{NHCH}(\text{CH}(\text{CH}_3)_2\text{COOH}).n\text{H}_2\text{O}$ **114**, resulting in the formation of the corresponding secondary alcohol **115** with up to 50% enantiomeric excess and traces of benzyl alcohol (Scheme 42).

Gieseler *et al.*⁶⁵ have recently presented an asymmetric vinylogous Mukaiyama aldol reaction using aldehyde-derived silyl dienol ethers with an oxazaborolidinone catalyst. Unsaturated aldehydes assist as valuable building blocks for further conversions in polyketide synthesis. This approach, which comprises standard transformations and the conjugate addition of hydrides followed by internal protonation, enables the synthesis of α -chiral aldehydes. The methodology affords an efficient route to *R*-substituted δ -hydroxy- α,β -unsaturated aldehydes **119** by reacting alkyl or aryl aldehydes **117** with silyl dienol ethers **118** using catalyst **116** (Scheme 43). These δ -hydroxy- α,β -unsaturated aldehydes **119** are precursors for asymmetric protonation in the total synthesis of angiolam.⁶⁶ Kalesse *et al.*⁶⁷ described an oxazaborolidinone-mediated asymmetric bisvinylogous Mukaiyama Aldol reaction with alkene **120** and aldehyde **90** that supports the rapid formation of conjugated dienols **121**. This approach extends the vinylogy principle by adding two additional carbons and could be performed with a readily available Lewis acid within reasonable reaction times. It accommodates a wide variety of aromatic and aliphatic aldehydes, facilitating the synthesis of complex building blocks for polyketide construction (Scheme 44).

Du *et al.*⁶⁸ reported the total synthesis of 27-Deoxylyngbyabellin A (**124**), a secondary metabolite from marine cyanobacteria, achieved in 10 linear steps with an overall yield of approximately 10%. A crucial intermediate, (*S*)- β -hydroxy ester **123**, was obtained through a chiral oxazaborolidinone-mediated asymmetric aldol reaction between silyl ketene acetal **47** and aldehyde **122** to afford 56% yield. This (*S*)- β -hydroxy ester **123**, together with two essential

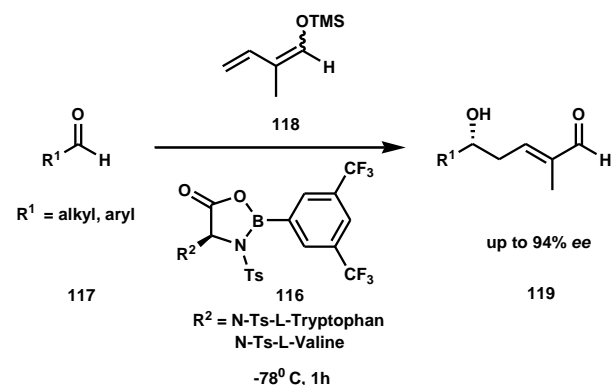


Scheme 41. Total synthesis of lactimidomycin.

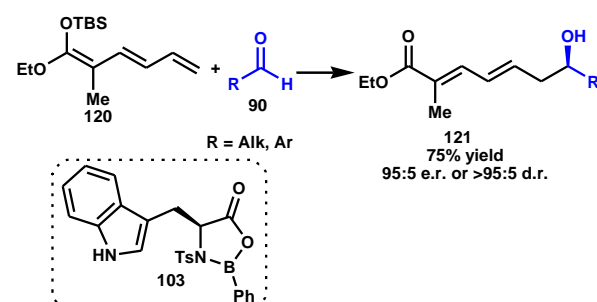


Scheme 42. Chiral oxazaborolidinone anchored γ -layered Zr-phosphonate catalyst for Mukaiyama aldol reaction.

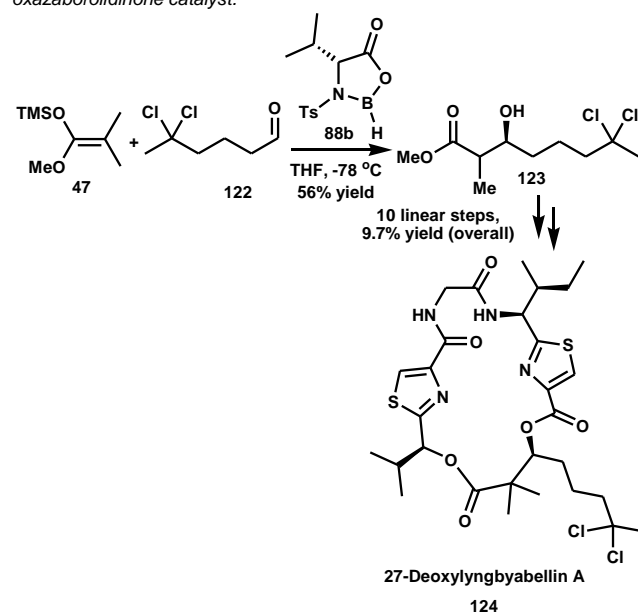
thiazole units, was subsequently assembled to produce the 27-Deoxylyngbyabellin A natural product (Scheme 45).



Scheme 43. Asymmetric vinylogous Mukaiyama aldol reaction by oxazaborolidinone catalyst.



Scheme 44. Asymmetric vinylogous Mukaiyama aldol reaction by oxazaborolidinone catalyst.



Scheme 45. Total synthesis of 27-Deoxylyngbyabellin A.

6. Conclusion

Over the years, the use of oxazaborolidine and borolidinone catalysts (or stoichiometric reagent) for reducing various functionalities has been broadly validated by researchers, particularly for their key applications in synthesizing bioactive natural products and building blocks. It is clear from this comprehensive review that the oxazaborolidine catalysed enantioselective reductions play significant roles both industrial and academic settings. In contrast, the use of oxazaborolidinone catalysts remains relatively unexplored, so there is a substantial opportunity to take up further

investigation in this. Although, its numerous application in various chemical reactions, especially asymmetric catalysis but there are few drawbacks such as limited stability as its highly air and moisture sensitive nature; sometime difficult to control reactivity for its stoichiometric uses leads to undesired side product; highly expensive fluorinated oxazaborolidine catalyst. The study of reactions catalyzed by oxazaborolidines and oxazaborolidinones holds huge potential, innovative developments, and more fascinating aspects are expected to originate from this area by enhancing stability using more robust functional groups or protective groups, adjusting reactivity to minimize side products, and lowering catalyst costs through more economical synthetic routes.

Author Contribution Declaration

YKW: designing, drafting manuscript, literature collections, and editing; **SS:** literature collections and updating recent work; **SDP:** drafting manuscript, and editing; **PKP:** drafting, editing and finalizing the manuscript.

Data Availability Declaration

There are no new data were created hence data sharing is not applicable.

Acknowledgements

We thankful to Dr. Sanjit Kumar Mahato, Specially Appointed Assistant Professor, Osaka university, Japan (Currently at PI Industries Ltd., Udaipur, Rajasthan, India) for providing critical feedback on mechanistic insight. Prof. Walia thanks to Career Point University Hamirpur for providing the infrastructure.

References

- Noyori, R. In *Asymmetric Catalysis in Organic Synthesis*; John Wiley & Sons: New York, **1994**.
- H. I. Schlesinger, H. C. Brown, H. R. Hoekstra, L. R. Rapp. Reactions of Diborane with Alkali Metal Hydrides and Their Addition Compounds. New Syntheses of Borohydrides. Sodium and Potassium Borohydrides. *J. Am. Chem. Soc.* **1953**, *75*, 199. <https://doi.org/10.1021/ja01097a053>
- A. F. Finholt, A. C. Jr. Bond, H. I. Schlesinger. Acylations of Esters with Esters to Form β-Keto Esters Using Sodium Amide. *J. Am. Chem. Soc.* **1947**, *69*, 119. <https://doi.org/10.1021/ja01193a033>
- (a) E. R. Grandbois, S. I. Howard, J. D. Morrison. *Asymmetric Synthesis* **1983**, *2*, Academic Press, New York, pp. 71–90. (b) J. W. ApSimon, T. L. Collier, Recent advances in asymmetric synthesis-II. *Tetrahedron* **1986**, *42*, 5157. [https://doi.org/10.1016/S0040-4020\(01\)82073-1](https://doi.org/10.1016/S0040-4020(01)82073-1) (c) H. Haubenstock. *Topics in Stereochemistry* **1983**, *14*, Wiley, New York, pp. 231–300. (d) T. Mukaiyama, M. Asami. In *Topics in Current Chemistry, Organic Chemistry*, **1985**, *127*, Springer, Berlin, pp. 133-167. (e) A. I. Meyers, P. M. Kendall. Synthesis via oxazolines. VII. Asymmetric reduction of ketones with chiral hydride reagents. *Tetrahedron Lett.* **1974**, *15*, 1337. [https://doi.org/10.1016/S0040-4039\(01\)82482-5](https://doi.org/10.1016/S0040-4039(01)82482-5) (f) M. F. Grundon, D. G. McCleery, J. W. Wilson. *ibid.* **1976**, *17*, 295.
- (a) S. Yamaguchi, H. S. Mosher. Asymmetric reductions with chiral reagents from lithium aluminum hydride and (+)-(2S,3R)-4-dimethylamino-3-methyl-1,2-diphenyl-2-butanol. *J. Org. Chem.* **1973**, *38*, 1870.

- <https://doi.org/10.1021/jo00950a020> (b) R. S. Brinkmeyer, V. M. Kapoor. Asymmetric reduction. Reduction of acetylenic ketones with chiral hydride agent. *J. Am. Chem. Soc.* **1977**, 99, 8339. <https://doi.org/10.1021/ja00467a047> (c) N. Cohen, R. J. Lopresti, C. Neukom, G. Saucy. Asymmetric reductions of α , β -acetylenic ketones and acetophenone using lithium aluminum hydride complexed with optically active 1,3-amino alcohols. *J. Org. Chem.* **1980**, 45, 582. <https://doi.org/10.1021/jo01292a006>
6. (a) A. Hirao, S. Itsuno, S. Nakahama, N. Yamazaki. Asymmetric reduction of aromatic ketones with chiral alkoxy-amineborane complexes. *J. Chem. Soc. Chem. Commun.* **1981**, 315. <https://doi.org/10.1039/C39810000315> (b) S. Itsuno, A. Hirao, S. Nakahama, N. Yamazaki. Asymmetric synthesis using chirally modified borohydrides. Part 1. Enantioselective reduction of aromatic ketones with the reagent prepared from borane and (S)-valinol. *J. Chem. Soc. Perkin Trans. 1* **1983**, 1673. <https://doi.org/10.1039/P19830001673>
7. S. Itsuno, M. Nakano, K. Miyazaki, V. Masuda, K. Ito, A. Hirao, S. Nakahama. Asymmetric synthesis using chirally modified borohydrides. Part 3. Enantioselective reduction of ketones and oxime ethers with reagents prepared from borane and chiral amino alcohols. *J. Chem. Soc. Perkin Trans.* **1985**, 2039. <https://doi.org/10.1039/P19850002039>
8. (a) R. Noyori, I. Tomino, Y. Tanimoto, M. Nishizawa. Asymmetric synthesis via axially dissymmetric molecules. 6. Rational designing of efficient chiral reducing agents. Highly enantioselective reduction of aromatic ketones by binaphthol-modified lithium aluminum hydride reagents. *J. Am. Chem. Soc.* **1984**, 106, 6709. <https://doi.org/10.1021/ja00334a041> (b) R. Noyori, I. Tomino, M. Yamada, M. Nishizawa. Asymmetric synthesis via axially dissymmetric molecules. 7. Synthetic applications of the enantioselective reduction by binaphthol-modified lithium aluminum hydride reagents. *J. Am. Chem. Soc.* **1984**, 106, 6717. <https://doi.org/10.1021/ja00334a042>
9. (a) E. J. Corey, R. K. Bakshi, S. Shibata. Highly enantioselective borane reduction of ketones catalyzed by chiral oxazaborolidines. Mechanism and synthetic implications. *J. Am. Chem. Soc.* **1987**, 109, 5551. <https://doi.org/10.1021/ja00252a056> (b) E. J. Corey, T. Shibata, T. W. Lee. Asymmetric Diels-Alder Reactions Catalyzed by a Triflic Acid Activated Chiral Oxazaborolidine. *J. Am. Chem. Soc.* **2002**, 124, 3808. <https://doi.org/10.1021/ja025848x>
10. E. J. Corey, C. J. Helal. Reduction of Carbonyl Compounds with Chiral Oxazaborolidine Catalysts: A New Paradigm for Enantioselective Catalysis and a Powerful New Synthetic Method. *Angew. Chem. Int. Ed.* **1998**, 37, 1986. [https://doi.org/10.1002/\(SICI\)1521-3773\(19980817\)37:15<1986::AID-ANIE1986>3.0.CO;2-Z](https://doi.org/10.1002/(SICI)1521-3773(19980817)37:15<1986::AID-ANIE1986>3.0.CO;2-Z)
11. C. Puigjaner, A. V. Ferran, A. Moyano, M. A. Pericàs, A. Riera. A New Family of Modular Chiral Ligands for the Catalytic Enantioselective Reduction of Prochiral Ketones. *J. Org. Chem.* **1999**, 64, 7902. <https://doi.org/10.1021/jo990942q>
12. (a) S. Itsuno, M. Nakano, K. Miyazaki, H. Masuda, K. Ito, A. Hirao, S. Nakahama. Asymmetric synthesis using chirally modified borohydrides. Part 3. Enantioselective reduction of ketones and oxime ethers with reagents prepared from borane and chiral amino alcohols. *J. Chem. Soc., Perkin Trans. 1* **1985**, 2039. <https://doi.org/10.1039/P19850002039> (b) S. Itsuno, Y. Sakurai, K. Ito, A. Hirao, S. Nakahama. Catalytic Behavior of Optically Active Amino Alcohol-Borane Complex in the Enantioselective Reduction of Acetophenone Oxime O-Alkyl Ethers. *Bull. Chem. Soc. Jpn.* **1987**, 60, 395. <https://doi.org/10.1246/bcsj.60.395> (c) S. Itsuno, Y. Sakurai, K. Shimizu, K. Ito. Asymmetric reduction of ketoxime O-alkyl ethers with chirally modified $\text{NaBH}_4\text{-ZrCl}_4$. *J. Chem. Soc., Perkin Trans. 1* **1990**, 1859. <https://doi.org/10.1039/P19900001859> (d) E. J. Corey, R. K. Bakshi, S. Shibata. Highly enantioselective borane reduction of ketones catalyzed by chiral oxazaborolidines. Mechanism and synthetic implications. *J. Am. Chem. Soc.* **1987**, 109, 5551. <https://doi.org/10.1021/ja00252a056> (e) E. J. Corey, R. K. Bakshi, S. Shibata, C.-P. Chen, V. K. Singh. A stable and easily prepared catalyst for the enantioselective reduction of ketones. Applications to multistep syntheses. *J. Am. Chem. Soc.* **1987**, 109, 7925. <https://doi.org/10.1021/ja00259a075> (f) R. Berenguer, J. Garcia, J. Vilarrasa. Enantioselective reduction of ketones catalysed by 1,3,2-oxazaborolidines prepared from phenylglycine. *Tetrahedron: Asymmetry* **1994**, 5, 165. [https://doi.org/10.1016/S0957-4166\(00\)86163-7](https://doi.org/10.1016/S0957-4166(00)86163-7) (g) G. J. Quallich, J. F. Blake, T. M. Woodall. A combined synthetic and ab initio study of chiral oxazaborolidines structure and enantioselectivity relationships. *J. Am. Chem. Soc.* **1994**, 116, 8516. <https://doi.org/10.1021/ja00098a012> (h) N. N. Joshi, M. Srebnik, H. C. Brown. Chiral Oxazaborolidines as Catalysts for the Enantioselective Addition of Diethylzinc to Aldehydes. *Tetrahedron Lett.* **1989**, 30, 5551. [https://doi.org/10.1016/S0040-4039\(01\)93797-9](https://doi.org/10.1016/S0040-4039(01)93797-9) (h) Y. Hong, Y. Gao, X. Nie, C. M. Zepp. *cis*-1-amino-2-indanol in asymmetric synthesis. Part I. A practical catalyst system for the enantioselective borane reduction of aromatic ketones. *Tetrahedron Lett.* **1994**, 35, 6631. [https://doi.org/10.1016/S0040-4039\(00\)73453-8](https://doi.org/10.1016/S0040-4039(00)73453-8)
13. (a) A. Hirao, S. Itsuno, S. Nakahama, N. Yamazaki. Asymmetric reduction of aromatic ketones with chiral alkoxy-amineborane complexes. *J. Chem. Soc., Chem. Commun.* **1981**, 315. <https://doi.org/10.1039/C39810000315> (b) S. Itsuno, M. Nakano, K. Miyazaki, H. Masuda, K. Ito, A. Hirao, S. Nakahama. Asymmetric synthesis using chirally modified borohydrides. Part 3. Enantioselective reduction of ketones and oxime ethers with reagents prepared from borane and chiral amino alcohols. *J. Chem. Soc., Perkin Trans.* **1985**, 2039. <https://doi.org/10.1039/P19850002039>
14. (a) E. J. Corey, R. K. Bakshi, S. Shibata. Highly enantioselective borane reduction of ketones catalyzed by chiral oxazaborolidines. Mechanism and synthetic implications. *J. Am. Chem. Soc.* **1987**, 109, 5551. <https://doi.org/10.1021/ja00252a056> (b) E. J. Corey, R. K. Bakshi, S. Shibata, C.-P. Chen, V. K. Singh. A stable and easily prepared catalyst for the enantioselective reduction of ketones. Applications to multistep syntheses. *J. Am. Chem. Soc.* **1987**, 109, 7925. <https://doi.org/10.1021/ja00259a075> (c) E. J. Corey, M.

- Azimioara, S. Sarshar. X-Ray crystal structure of a chiral oxazaborolidine catalyst for enantioselective carbonyl reduction. *Tetrahedron Lett.* **1992**, 33, 3429. [https://doi.org/10.1016/S0040-4039\(00\)92654-6](https://doi.org/10.1016/S0040-4039(00)92654-6)
15. For review, see: (a) D. P. Schwinger, T. Bach. Chiral 1,3,2-oxazaborolidine catalysts for enantioselective photochemical reactions. *Acc. Chem. Res.* **2020**, 53, 1933. <https://doi.org/10.1021/acs.accounts.0c00379> (b) Y. Kawanami, R. C. Yanagita. Practical Enantioselective Reduction of Ketones Using Oxazaborolidine Catalysts Generated *In Situ* from Chiral Lactam Alcohols. *Molecules* **2018**, 23, 1. <https://doi.org/10.3390/molecules23102408> (c) S. Y. Shim, D. H. Ryu. Enantioselective Carbonyl 1,2- or 1,4-Addition Reactions of Nucleophilic Silyl and Diazo Compounds Catalyzed by the Chiral Oxazaborolidinium Ion. *Acc. Chem. Res.* **2019**, 52, 2349. <https://doi.org/10.1021/acs.accounts.9b00279> (d) B. T. Cho. Recent advances in the synthetic applications of the oxazaborolidine-mediated asymmetric reduction. *Tetrahedron*, **2006**, 62, 7621. <https://doi.org/10.1016/j.tet.2006.05.036> (e) B. T. Cho. *Boronic Acids: Preparation and Applications in Organic Synthesis*; D. G. Hall, Ed.; Wiley-VCH: Weinheim, **2005**; Chapter 11, p 411. (f) S. Itsuno. *Comprehensive Asymmetric Catalysts*; E. N. Jacobsen, A. Pfaltz, H. Yamamoto, Eds.; Springer: New York, NY, **1999**; Vol. 1, p 289. (g) E. J. Corey, C. J. Helal. Reduction of Carbonyl Compounds with Chiral Oxazaborolidine Catalysts: A New Paradigm for Enantioselective Catalysis and a Powerful New Synthetic Method. *Angew. Chem., Int. Ed.* **1998**, 37, 1986. [https://doi.org/10.1002/\(SICI\)1521-3773\(19980817\)37:15<1986::AID-ANIE1986>3.0.CO;2-Z](https://doi.org/10.1002/(SICI)1521-3773(19980817)37:15<1986::AID-ANIE1986>3.0.CO;2-Z) (g) L. Deloux, M. Srebnik. Asymmetric boron-catalyzed reactions. *Chem. Rev.* **1993**, 93, 763. <https://doi.org/10.1021/cr00018a007> (h) V. K. Singh. Practical and Useful Methods for the Enantioselective Reduction of Unsymmetrical Ketones. *Synthesis* **1992**, 605. <https://doi.org/10.1055/s-1992-26174> (i) S. Wallbaum, J. Martens. Asymmetric syntheses with chiral oxazaborolidines. *Tetrahedron: Asymmetry* **1992**, 3, 1475. [https://doi.org/10.1016/S0957-4166\(00\)86044-9](https://doi.org/10.1016/S0957-4166(00)86044-9)
16. (a) K. Z. Łączkowski, Z. Czyżnikowska, R. Zales'ny, A. Baranowska-Łączkowska. The B–H–B bridging interaction in B-substituted oxazaborolidine–borane complexes: a theoretical study. *Struct. Chem.*, **2013**, 24, 1485. <https://doi.org/10.1007/s11224-012-0178-9> (b) H. S. Kettouche, A. Djerourou. Insights into the origin of selectivity for [2+2] cycloaddition step reaction involved in the mechanism of enantioselective reduction of ketones with borane catalyzed by a B-methoxy oxazaborolidine catalyst derived from (–)-β-pinene: an HMDFT and combined topological ELF, NCI and QTAIM study. *Theor. Chem. Acc.* **2021**, 140, 150. <https://doi.org/10.1007/s00214-021-02848-4> (c) Z. Lachtar, A. K. Nacereddine, A. Djerourou. Understanding the origin of the enantioselectivity and the mechanism of the asymmetric reduction of ketimine generated from acetophenone with oxazaborolidine catalyst. *Struct. Chem.* **2020**, 31, 253. <https://doi.org/10.1007/s11224-019-01400-2>
17. M. Masui, T. Shioiri. A Practical Method for Asymmetric Borane Reduction of Prochiral Ketones Using Chiral Amino Alcohols and Trimethyl Borate. *Synlett* **1997**, 3, 273. <https://doi.org/10.1055/s-1997-779>
18. (a) K. M. Reddy, E. Bhimireddy, B. Thirupathi, S. Breitler, S. Yu, E. J. Corey. Cationic chiral fluorinated oxazaborolidines. More potent second-generation catalyst for highly enantioselective cycloaddition reactions. *J. Am. Chem. Soc.* **2016**, 138, 2443. <https://doi.org/10.1021/jacs.6b00100> (b) B. Thirupathi, S. Breitler, K. M. Reddy, E. J. Corey. Acceleration of Enantioselective Cycloadditions Catalyzed by Second-Generation Chiral Oxazaborolidinium Triflimidates by Biscoordinating Lewis Acids. *J. Am. Chem. Soc.* **2016**, 138, 10842. <https://doi.org/10.1021/jacs.6b08018>
19. J. M. Wahl, M. L. Conner, M. K. Brown. Synthesis of (–)-Hebelophyllene E: An Entry to Geminal Dimethyl-Cyclobutanes by [2+2] Cycloaddition of Alkenes and Allenates. *Angew. Chem. Int. Ed.* **2018**, 57, 4647. <https://doi.org/10.1002/anie.201801110>
20. A. Moscona. Neuraminidase Inhibitors for Influenza. *New Engl. J. Med.* **2005**, 353, 1363. <https://doi.org/10.1056/NEJMra050740>
21. Y. Y. Yeung, S. Hong, E. J. Corey. A Short Enantioselective Pathway for the Synthesis of the Anti-Influenza Neuramidase Inhibitor Oseltamivir from 1,3-Butadiene and Acrylic Acid. *J. Am. Chem. Soc.* **2006**, 128, 6310. <https://doi.org/10.1021/ja0616433>
22. (a) J. Matsuo, T. Kozai, O. Nishikawa, Y. Hattori, H. Ishibashi. Oxazaborolidine-Catalyzed Enantioselective Reduction of α-Methylene Ketones to Allylic Alcohols. *J. Org. Chem.* **2008**, 73, 6902. <https://doi.org/10.1021/jo8011013> (b) T. Yıldız. An oxazaborolidine-based catalytic method for the asymmetric synthesis of chiral allylic alcohols. *Tetrahedron: Asymmetry*, **2015**, 26, 497. <https://doi.org/10.1016/j.tetasy.2015.03.008>
23. (a) S. Goodin, M. P. Kane, E. H. Rubin. Epothilones: Mechanism of Action and Biologic Activity. *J. Clin. Oncol.* **2004**, 22, p. 2015. <https://doi.org/10.1200/JCO.2004.12.0> (b) D. M. Bollag, P. A. McQueney, J. Zhu, O. Hensens, L. Koupal, J. Liesch, M. Goetz, E. Lazarides, C. M. Woods. Epothilones, a New Class of Microtubule-stabilizing Agents with a Taxol-like Mechanism of Action, *Cancer Res.* **1995**, 55, 2325. (c) K. C. Nicolaou, F. Roschangar, D. Vourloumis. Chemical Biology of Epothilones. *Angew. Chem., Int. Ed.* **1998**, 37, 2014. [https://doi.org/10.1002/\(SICI\)1521-3773\(19980817\)37:15<2014::AID-ANIE2014>3.0.CO;2-2](https://doi.org/10.1002/(SICI)1521-3773(19980817)37:15<2014::AID-ANIE2014>3.0.CO;2-2) (d) C. R. Harris, S. J. Danishefsky. Complex Target-Oriented Synthesis in the Drug Discovery Process: A Case History in the dEpoB Series. *J. Org. Chem.* **1999**, 64, 8434. <https://doi.org/10.1021/jo991006d> (e) K. H. Altmann, M. Wartmann, T. O'Reilly. Epothilones and related structures- a new class of microtubule inhibitors with potent in vivo antitumor activity. *Biochim. Biophys. Acta*, **2000**, 1470, M79. [https://doi.org/10.1016/s0304-419x\(00\)00009-3](https://doi.org/10.1016/s0304-419x(00)00009-3) (f) K. C. Nicolaou, A. Ritzen, K. Namoto. Recent developments in the chemistry, biology and medicine of the epothilones Dedicated to Drs Margaret Harris and Muriel Hall of Bedford College, London, for their dedicated and inspiring teachings and research contributions in celebration of their retirement. *Chem. Commun.* **2001**, 1523. <https://doi.org/10.1039/B104949F> (g) M. Wartmann, K. H. Altmann. The biology and medicinal chemistry of epothilones. *Curr. Med. Chem.: Anti-Cancer Agents* **2002**, 2, 123. <https://doi.org/10.2174/1568011023354489> (h) E. B.

- Watkins, A. G. Chittiboyina, M. A. Avery. Recent Developments in the Syntheses of the Epothilones and Related Analogues. *Eur. J. Org. Chem.* **2006**, 4071. <https://doi.org/10.1002/ejoc.200600149> (i) E. B. Watkins, A. G. Chittiboyina, J.-C. Jung, M. A. Avery. The Epothilones and Related Analogues-A Review of Their Syntheses and Anti-Cancer Activities. *Curr. Pharm. Des.* **2005**, *11*, 1615. <https://doi.org/10.2174/1381612053764742> (j) F. Feyen, F. Cachoux, J. Gertsch, M. Wartmann, K.-H. Altmann. Epothilones as Lead Structures for the Synthesis-Based Discovery of New Chemotypes for Microtubule Stabilization. *Acc. Chem. Res.* **2008**, *41*, 21. <https://doi.org/10.1021/ar700157x> (k) R. J. Kowalski, P. Giannakakou, E. Hamel. Activities of the Microtubule-stabilizing Agents Epothilones A and B with Purified Tubulin and in Cells Resistant to Paclitaxel (Taxol®). *J. Biol. Chem.* **1997**, *272*, 2534. <https://doi.org/10.1074/jbc.272.4.2534> (l) W. M. Smit, J. Sufliarsky, S. Spanik, M. Wagnerov, S. Kaye, A. M. Oza, M. Gore, K. J. Williams, A. Johri, W. W. T. B. Huinink. *J. Clin. Oncol.* **2005**, *23*, 16S. (m) S. McMeekin, R. Patel, C. Verschraegan, P. Celano, J. Burke, S. Plaxe, P. Ghatage, M. Giurescu, C. Stredder, Y. Wang. In *33rd Congress of the European Society for Medical Oncology*, **2008**. (n) C. Sessa, A. Perotti, A. Llado, S. Cresta, G. Capri, M. Voi, S. Marsoni, I. Corradino, L. Gianni. *Ann. Oncol.* **2007**, *18*, 1548. (o) A. Stopeck, S. Moulder, S. Jones, J. Cohen, M. McDowell, G. Cropp, Z. Zhong, S. Wells, A. Hannah, H. Burris. *J. Clin. Oncol.* **2007**, *25*, 2571. (p) S. Bhushan, C. M. Walko, *Ann. Pharmacother.* **2008**, *42*, 1252.
24. E. A. Reiff, S. K. Nair, J. T. Henri, J. F. Greiner, B. S. Reddy, R. Chakrasali, S. A. David, T. L. Chiu, E. A. Amin, R. H. Himes, D. G. V. Velde, G. I. Georg. Total Synthesis and Evaluation of C26-Hydroxyepothilone D Derivatives for Photoaffinity Labeling of β -Tubulin. *J. Org. Chem.* **2010**, *75*, 86. <https://doi.org/10.1021/jo901752v>
25. (a) A. S. Pilcher, P. DeShong. Improved protocols for the selective deprotection of trialkylsilyl ethers using fluorosilicic acid. *J. Org. Chem.* **1993**, *58*, 5130. <https://doi.org/10.1021/jo00071a023> (b) D. Schinzer, A. Bauer, O. M. Bohm, A. Limberg, M. Cordes, Total Synthesis of (-)-Epothilone A. *Chem. Eur. J.* **1999**, *5*, 2483. [https://doi.org/10.1002/\(SICI\)1521-3765\(19990903\)5:9<2483::AID-CHEM2483>3.0.CO;2-N](https://doi.org/10.1002/(SICI)1521-3765(19990903)5:9<2483::AID-CHEM2483>3.0.CO;2-N) (c) K. C. Nicolaou, S. Ninkovic, F. Sarabia, D. Vourloumis, Y. He, H. Vallberg, M. R. V. Finlay, Z. Yang. Total Syntheses of Epothilones A and B via a Macrolactonization-Based Strategy. *J. Am. Chem. Soc.* **1997**, *119*, 7974. <https://doi.org/10.1021/ja971110h> (d) K. C. Nicolaou, D. Hepworth, N. P. King, M. R. V. Finlay, R. Scarpelli, M. M. A. Pereira, B. Bollbuck, A. Bigot, B. Werschkun, N. Winssinger. Total Synthesis of 16-Desmethylepothilone B, Epothilone B10, Epothilone F, and Related Side Chain Modified Epothilone B Analogues. *Chem. Eur. J.* **2000**, *6*, 2783. [https://doi.org/10.1002/1521-3765\(20000804\)6:15<2783::AID-CHEM2783>3.0.CO;2-B](https://doi.org/10.1002/1521-3765(20000804)6:15<2783::AID-CHEM2783>3.0.CO;2-B) (e) K. C. Nicolaou, D. Hepworth, M. R. V. Finlay, N. Paul King, B. Werschkun, A. Bigot. Synthesis of 16-desmethylepothilone B: improved methodology for the rapid, highly selective and convergent construction of epothilone B and analogues. *Chem. Commun.* **1999**, 519. <https://doi.org/10.1039/A809954E> (f) J. P. Genet, V. Ratovelomanana-Vidal, M. C. Cano de Andrade, X. Pfister, P. Guerreiro, J. Y. Lenoir. Practical asymmetric hydrogenation of β -keto esters at atmospheric pressure using chiral Ru (II) catalysts. *Tetrahedron Lett.* **1995**, *36*, 4801. [https://doi.org/10.1016/0040-4039\(95\)00873-B](https://doi.org/10.1016/0040-4039(95)00873-B) (g) D. F. Taber, L. J. Silverberg. Enantioselective reduction of β -keto esters. *Tetrahedron Lett.* **1991**, *32*, 4227. [https://doi.org/10.1016/S0040-4039\(00\)92134-8](https://doi.org/10.1016/S0040-4039(00)92134-8) (h) L. A. Paquette, R. A. Jr. Galemno, J. C. Caille, R. S. Valpey. Synthetic studies relating to the structure of senoxydene. A sequential annulation approach to angular triquinane construction capable of varied tetramethyl substitution patterns. *J. Org. Chem.* **1986**, *51*, 686. <https://doi.org/10.1021/jo00355a019> (i) J. Mulzer, A. Mantoulidis, E. Oehler. Total Syntheses of Epothilones B and D. *J. Org. Chem.* **2000**, *65*, 7456. <https://doi.org/10.1021/jo0007480> (j) K. C. Nicolaou, M. R. V. Finlay, S. Ninkovic, F. Sarabia. Total synthesis of 26-hydroxy-epothilone B and related analogs via a macrolactonization based strategy. *Tetrahedron* **1998**, *54*, 7127. [https://doi.org/10.1016/S0040-4020\(98\)00352-4](https://doi.org/10.1016/S0040-4020(98)00352-4)
26. T. A. Rano, G. H. Kuo. Improved Asymmetric Synthesis of 3,4-Dihydro-2-[3-(1,1,2,2-tetrafluoroethoxy)phenyl]-5-[3-(trifluoromethoxy)phenyl]- α -(trifluoromethyl)-1(2H)-quinolineethanol, a Potent Cholesteryl Ester Transfer Protein Inhibitor. *Org. Lett.* **2009**, *11*, 2812 <https://doi.org/10.1021/ol900639j> and the references cited therein.
27. (a) E. Canales, E. J. Corey. Highly Enantioselective [4 + 2] Cycloaddition Reactions Catalyzed by a Chiral N-Methyl-oxazaborolidinium Cation. *Org. Lett.* **2008**, *10*, 3271. <https://doi.org/10.1021/ol8011502> (b) Q.-Y. Hu, G. Zhou, E. J. Corey, Application of Chiral Cationic Catalysts to Several Classical Syntheses of Racemic Natural Products Transforms Them into Highly Enantioselective Pathways. *J. Am. Chem. Soc.* **2004**, *126*, 13708 <https://doi.org/10.1021/ja046154m> and the references cited therein.
28. S. H. von Reuss, W. A. König. Corsifurans A-C, 2-arylbenzofurans of presumed stilbenoid origin from Corsinia coriandrina (Hepaticae). *Phytochemistry* **2004**, *65*, 3113. <https://doi.org/10.1016/j.phytochem.2004.10.002>
29. B. D. Gates, P. Dalidowicz, A. Tebben, S. Wang, J. S. Sweton. Mechanistic aspects and synthetic applications of the electrochemical and iodobenzene bistrifluoroacetate oxidative 1,3-cycloadditions of phenols and electron-rich styrene derivatives. *J. Org. Chem.* **1992**, *57*, 2135. <https://doi.org/10.1021/jo00033a040>
30. (a) M. P. Krzemiński. 13.7. Asymmetric Reduction of Acetophenone with Borane Catalyzed by B-Methoxy-oxazaborolidine. **2016**, 803. <https://doi.org/10.1039/9781849739634-00803> (b) H. Adams, N. J. Gilmore, S. Jones, M. P. Muldowney, S. H. von Reuss, R. Vemula. Asymmetric Synthesis of Corsifuran A by an Enantioselective Oxazaborolidine Reduction. *Org. Lett.* **2008**, *10*, 1457. <https://doi.org/10.1021/ol800239q> (c) Y. Kawanami, K. Hoshino, W. Tsunoi. Enantioselective reduction of trifluoromethyl ketones using an oxazaborolidine catalyst generated in situ from a chiral lactam alcohol. *Tetrahedron: Asymmetry* **2011**, *22*, 1464.

- <https://doi.org/10.1016/j.tetasy.2011.08.006> (d) Y. Harauchi, C. Takakura, T. Furumoto, R.C. Yanagita, Y. Kawanami. Effect of BF₃ on the enantioselective reduction of trifluoromethyl ketones using a chiral lactam alcohol with borane. *Tetrahedron: Asymmetry*, **2015**, 26, 333. <https://doi.org/10.1016/j.tetasy.2015.02.011>
31. (a) E. J. Corey, X. Cheng, K. A. Cimprich, S. Sarshar. Remarkably effective and simple syntheses of enantiomerically pure secondary carbinols from achiral ketones. *Tetrahedron Lett.* **1991**, 32, 6835. [https://doi.org/10.1016/0040-4039\(91\)80419-7](https://doi.org/10.1016/0040-4039(91)80419-7) (b) E. J.; Corey, J. O. Link, R. K. Bakshi. A mechanistic and structural analysis of the basis for high enantioselectivity in the oxazaborolidine-catalyzed reduction of trihalomethyl ketones by catecholborane. *Tetrahedron Lett.* **1992**, 33, 7107. [https://doi.org/10.1016/S0040-4039\(00\)60848-1](https://doi.org/10.1016/S0040-4039(00)60848-1) (c) V. Stepanenko, M. D. Jesus, W. Correa, I. Guzman, C. Vazquez, W. Cruz, M. Ortiz-Marciales, C. L. Barnes. Enantioselective reduction of prochiral ketones using spiroborate esters as catalysts. *Tetrahedron Lett.* **2007**, 48, 5799. <https://doi.org/10.1016/j.tetlet.2007.06.086> (d) T. Korenaga, K. Nomura, K. Onoue, T. Sakai. Rational electronic tuning of CBS catalyst for highly enantioselective boranereduction of trifluoroacetophenone. *Chem. Commun.* **2010**, 46, 8624. <https://doi.org/10.1039/C0CC03706K>
32. C. H. V. A. Sasikala, P. R. Padi, V. Sunkara, P. Ramayya, P. K. Dubey, V. B. R. Uppala, C. Praveen. An Improved and Scalable Process for the Synthesis of Ezetimibe: An Antihypercholesterolemia Drug. *Org. Process Res. Dev.* **2009**, 13, 907. <https://doi.org/10.1021/op900039z>
33. S. Tamura, S. Doke, N. Murakami. Total synthesis of peumusolide A, NES non-antagonistic inhibitor for nuclear export of MEK. *Tetrahedron* **2010**, 66, 8476. <https://doi.org/10.1016/j.tet.2010.08.025>
34. S. Asano, T. Nakamura, M. Adachi, M. Yoshida, M. Yanagida, E. Nishida. CRM1 is responsible for intracellular transport mediated by the nuclear export signal. *Nature* **1997**, 390, 308. <https://doi.org/10.1038/36894>
35. S. Tamura, Y. Hattori, M. Kaneko, N. Shimizu, S. Tanimura, M. Khono, N. Murakami. Peumusolide A, unprecedented NES non-antagonistic inhibitor for nuclear export of MEK. *Tetrahedron Lett.* **2010**, 51, 1678. <https://doi.org/10.1016/j.tetlet.2010.01.068>
36. (a) C.-Y. Chen, C.-H. Chen, Y.-C. Lo, B.-N. Wu, H.-M. Wang, W.-L. Lo, C.-M. Yen, R.-J. Lin. Anticancer Activity of Isoobtusilactone A from *Cinnamomum kotoense*: Involvement of Apoptosis, Cell-Cycle Dysregulation, Mitochondria Regulation, and Reactive Oxygen Species. *J. Nat. Prod.* **2008**, 71, 933. <https://doi.org/10.1021/np070620e> (b) P.-L. Kuo, C.-Y. Chen, T.-F. Tzeng, C.-C. Lin, Y.-L. Hsu. Involvement of reactive oxygen species/c-Jun NH2-terminal kinase pathway in kotomolide A induces apoptosis in human breast cancer cells. *Toxicol. Appl. Pharmacol.* **2008**, 229, 215. <https://doi.org/10.1016/j.taap.2008.01.034>
37. S. Hong, E. J. Corey. Enantioselective Syntheses of Georgyone, Arborone, and Structural Relatives. Relevance to the Molecular-Level Understanding of Olfaction. *J. Am. Chem. Soc.* **2006**, 128, 1346. <https://doi.org/10.1021/ja057483x>
38. (a) Y. Shimoda, H. Yamamoto. New oxazaborolidine catalyst for the Diels-Alder Reaction, *Synthesis* **2017**, 49, 175. <https://doi.org/10.1055/s-0036-1588082> (b) S. -L. Zhang, Y. Lu, Y.-H. Li, K.-Y. Wang, J. -H. Chen, Z. Yang. Catalytic and Enantioselective Diels-Alder Reactions of (E)-4-Oxopent-2-enoates. *Org. Lett.* **2017**, 19, 3986. <https://doi.org/10.1021/acs.orglett.7b01692>
39. B. T. Cho. *Aldrichimica Acta* **2002**, 35, 3.
40. J. Xiao, Z. Z. Wong, Y. P. Lu, T. P. Loha. Hexahydropyrrolo[2,3-b]indoles: A New Class of Structurally Rigid Tricyclic Skeleton for Oxazaborolidine-Catalyzed Asymmetric Borane Reduction. *Adv. Synth. Catal.* **2010**, 352, 1107. <https://doi.org/10.1002/adsc.200900908>
41. J. H. Yune, F. Quignard, K. Molvinger. Enantioselectivity Induced by Oxazaborolidine Supported on Mesoporous Silica or by Its Analog in Homogeneous Phase. *Molecules* **2010**, 15, 3643. <https://doi.org/10.3390/molecules15053643> and cited therein.
42. H. S. Kettouche, A. H. Djerourou. A New Method for the Preparation of Oxazaborolidine Catalyst In Situ Using 1,2-Aminoalcohol, Sodium Borohydride, and Diiodomethane for the Asymmetric Reduction of Prochiral Ketones and N-Substituted Imines. *The Open Catalysis Journal*, **2009**, 2, 96. <https://doi.org/10.2174/1876214X00902010096>
43. D. Liu, S. Hong, E. J. Corey. Enantioselective synthesis of bridged-or fused-ring bicyclic ketones by a catalytic asymmetric Michael addition pathway. *J. Am. Chem. Soc.* **2006**, 128, 8160. <https://doi.org/10.1021/ja063332y>
44. R. K. Jr. Boeckman, J. E. Pero, D. J. Boehmler. Toward the Development of a General Chiral Auxiliary. Enantioselective Alkylation and a New Catalytic Asymmetric Addition of Silyloxyfurans: Application to a Total Synthesis of (-)-Rasfonin. *J. Am. Chem. Soc.* **2006**, 128, 11032. <https://doi.org/10.1021/ja063532%2B>
45. (a) I. U. Kutama, S. Jones. Enantioselective Desymmetrization of Glutarimides Catalyzed by Oxazaborolidines Derived from *cis*-1-Amino-indan-2-ol. *J. Org. Chem.* **2015**, 80, 1468. <https://doi.org/10.1021/acs.joc.5b02177> (b) B. J. Marsh, H. Adams, M. D. Barker, I. U. Kutama, S. Jones. Enantioselective catalytic desymmetrization of maleimides by temporary removal of an internal mirror plane and stereoablative over-reduction: synthesis of (*R*)-pyrrolam A. *Org. Lett.* **2014**, 16, 3780. <https://doi.org/10.1021/ol5016702>
46. E. H. E. Farrar, M. N. Grayson. Noncovalent Interactions in the Oxazaborolidine-Catalyzed Enantioselective Mukaiyama Aldol. *J. Org. Chem.* **2022**, 87, 15, 10054. <https://doi.org/10.1021/acs.joc.2c01039>
47. L. J. Drummond, A. Sutherland. Asymmetric synthesis of allylic secondary alcohols: a new general approach for the preparation of α -amino acids. *Tetrahedron* **2010**, 66, 5349. <https://doi.org/10.1016/j.tet.2010.05.066>
48. T. F. Yang, C. H. Shen, C. T. Hsu, L. H. Chen, C. H. Chuang. Selective reaction of camphor-derived exo-formyl [2.2.1]bicyclic carbinol with alkyl primary amines: application to the preparation of new chiral catalysts for asymmetric reduction of aryl ketones. *Tetrahedron* **2010**, 66, 8734. <https://doi.org/10.1016/j.tet.2010.09.008>
49. (a) M. P. Krzeminski, M. Zaidlewicz. Asymmetric reduction of ketoxime derivatives and N-alkylketimines

- with borane–oxazaborolidine adducts. *Tetrahedron: Asymmetry* **2003**, *14*, 1463. [https://doi.org/10.1016/S0957-4166\(03\)00314-8](https://doi.org/10.1016/S0957-4166(03)00314-8) (b) M. Zaidlewicz, A. Tafelska-Kaczmarek, A. Prewysz-Kwinto. Enantioselective reduction of benzofuryl halomethyl ketones: asymmetric synthesis of (*R*)-bufuralol. *Tetrahedron: Asymmetry* **2005**, *16*, 3205. <https://doi.org/10.1016/j.tetasy.2005.08.012> (c) M. J. Bosiak, M. P. Krzeminski, P. Jaisankar, M. Zaidlewicz. Asymmetric synthesis of *N*-1-(heteroaryl)ethyl-*N*-hydroxyureas. *Tetrahedron: Asymmetry* **2008**, *19*, 956. <https://doi.org/10.1016/j.tetasy.2008.03.026> (d) K. Z. Łączkowski, M. M. Pakulski, M. P. Krzemiński, P. Jaisankar, M. Zaidlewicz. Asymmetric synthesis of *N*-substituted *N*-hydroxyureas. *Tetrahedron: Asymmetry* **2008**, *19*, 788. <https://doi.org/10.1016/j.tetasy.2008.03.008> (e) M. M. Pakulski, S. K. Mahato, M. J. Bosiak, M. P. Krzeminski, M. Zaidlewicz. Enantioselective reduction of ketoxime ethers with borane–oxazaborolidines and synthesis of the key intermediate leading to (*S*)-rivastigmine. *Tetrahedron: Asymmetry* **2012**, *23*, 716. <https://doi.org/10.1016/j.tetasy.2012.05.008>
50. J. Kaldun, A. Krimalski, M. Breuning. Enantioselective borane reduction of ketones catalysed by triclinal 1,3,2-oxazaborolidines. *Tetrahedron Lett.* **2016**, *57*, 2492. <https://doi.org/10.1016/j.tetlet.2016.04.091>
51. H. S. Kettouche. A DFT study on the reaction mechanism of enantioselective reduction of ketones with borane catalyzed by a *B*-methoxy-oxazaborolidine catalyst derived from (–)- β -pinene. *J. Mol. Model.* **2020**, *26*:27. <https://doi.org/10.1007/s00894-019-4276-0>
52. X. Liang, M. Yoo, T. Schempp, S. Maejima, M. J. Krische. Ruthenium-Catalyzed Butadiene-Mediated Crotylation and Oxazaborolidine-Catalyzed Vinylogous Mukaiyama Aldol Reaction for The Synthesis of C1–C19 and C23–C35 of Neomycin B. *Angew. Chem. Int. Ed.* **2022**, *61*, e20221478. <https://doi.org/10.1002/anie.202214786>
53. W. Disadee, S. Ruchirawat. Oxazaborolidine-catalyzed reductive parallel kinetic resolution of ketones from β -nitro-azabicycles for the synthesis of chiral hypostestastins 1, 2. *Org. Biomol. Chem.*, **2021**, *19*, 8794. <https://doi.org/10.1039/D1OB01608C>
54. A. Pinaka, D. Dimotikali, B. Chankvetadze, K. Papadopoulos, G. C. Vougioukalakis. Catalytic Asymmetric Reduction of Prochiral Ketones with Chiral β -Amino Alcohol *N*-Boranes and the Corresponding Tris(oxazaborolidine)borazines. *Synlett* **2013**, *24*, 2401. <https://doi.org/10.1055/s-0033-1339943>
55. M. V. Reddy, P. Shyamala, A. K. Sharma. An efficient, concise, and scalable synthesis of Izenamide A and B via asymmetric reduction of γ -amino β -keto ester using 2-methyl-CBS-oxazaborolidine catalysts. *Results in Chemistry*, **2023**, *5*, 100756. <https://doi.org/10.1016/j.rechem.2022.100756>
56. S. Kiyooka, M. A. Hema. A chiral oxazaborolidinone-promoted aldol reaction with a silyl ketene acetal from ethyl 1,3-dithiolane-2-carboxylate. Synthesis of acetate aldols in high enantiomeric purity. *Tetrahedron: Asymmetry*, **1996**, *7*, 2181. [https://doi.org/10.1016/0957-4166\(96\)00265-0](https://doi.org/10.1016/0957-4166(96)00265-0)
57. K. Komura, S. Itsuno. Asymmetric Aldol Polymerization of Bis(trimethylsilyl)ketene thioacetal and Dialdehyde. *Chem. Lett.* **2001**, 730. <https://doi.org/10.1246/cl.2001.730>
58. T. Harada, T. Egusa, Y. Igarashi, M. Kinugasa, A. Oku. Inter- and Intramolecular Differentiation of Enantiotopic Dioxane Acetals through Oxazaborolidinone-Mediated Enantioselective Ring-Cleavage Reaction: Kinetic Resolution of Racemic 1,3-Alkanediols and Asymmetric Desymmetrization of Meso-1,3-polyols. *J. Org. Chem.* **2002**, *67*, 7080. <https://doi.org/10.1021/jo025944g>
59. X. Wang, S. Adachi, H. Iwai, H. Takatsuki, K. Fujita, M. Kubo, A. Oku, T. Harada. Enantioselective Lewis Acid-Catalyzed Mukaiyama–Michael Reactions of Acyclic Enones. Catalysis by allo-Threonine-Derived Oxazaborolidinones. *J. Org. Chem.* **2003**, *68*, 10046. <https://doi.org/10.1021/jo035379x>
60. R. S. Singh, T. Harada. Enantioselective Diels–Alder Reaction of Acyclic Enones Catalyzed by allo-Threonine-Derived Chiral Oxazaborolidinone. *Eur. J. Org. Chem.* **2005**, 3433. <https://doi.org/10.1002/ejoc.200500356>
61. S. Simsek, M. Horzella, M. Kalesse. Oxazaborolidinone-Promoted Vinylogous Mukaiyama Aldol Reactions. *Org. Lett.* **2007**, *9*, 5637. <https://doi.org/10.1021/ol702640w>
62. (a) S. Adachi, T. Harada. Asymmetric Mukaiyama Aldol Reaction of Nonactivated Ketones Catalyzed by allo-Threonine-Derived Oxazaborolidinone. *Org. Lett.* **2008**, *10*, 4999. <https://doi.org/10.1021/ol802087u> (b) S. Adachi, F. Tanaka, K. Watanabe, T. Harada. Oxazaborolidinone-Catalyzed Enantioselective Friedel–Crafts Alkylation of Furans and Indoles with α,β -Unsaturated Ketones. *Org. Lett.* **2009**, *11*, 5206. <https://doi.org/10.1021/ol9021436>
63. K. Micoine, A. Fürstner. Concise Total Synthesis of the Potent Translation and Cell Migration Inhibitor Lactimidomycin. *J. Am. Chem. Soc.* **2010**, *132*, 14064. <https://doi.org/10.1021/ja107141p>
64. U. Costantino, F. Fringuelli, M. Nocchetti, O. Piermatti. Chiral borane of layered α -Zirconium-*N*-(*m*-sulfophenyl)-*l*-Valine-Phosphonate Methanophosphonate promoters for the asymmetric Mukaiyama Aldol reaction. *Appl. Catal., A*, **2007**, *326*, 100. <https://doi.org/10.1016/j.apcata.2007.04.007>
65. M. T. Gieseler, M. Kalesse. Asymmetric Vinylogous Mukaiyama Aldol Reaction of Aldehyde-Derived Dienolates. *Org. Lett.* **2011**, *13*, 2430. <https://doi.org/10.1021/ol2006727>
66. (a) A. Kena Diba, C. Noll, M. Richter, M. T. Gieseler, M. Kalesse. Intramolecular Stereoselective Protonation of Aldehyde-Derived Enolates. *Angew. Chem., Int. Ed.* **2010**, *49*, 8367. <https://doi.org/10.1002/anie.201004619> (b) W. Kohl, B. Witte, B. Kunze, V. Wray, D. Schomburg, H. Reichenbach, G. Höfle. Antibiotika aus Gleitenden Bakterien, XXVII. Angiolam A –ein neues Antibiotikum aus *Angiococcus disciformis* (Myxobacterales). *Liebigs Ann. Chem.* **1985**, 2088. <https://doi.org/10.1002/jlac.198519851016>
67. A. Eggert, C. Etling, L. Millbrodt, G. Schulz, M. Kalesse. Oxazaborolidinone-Mediated Asymmetric Bisvinylogous Mukaiyama Aldol Reaction. *Org. Lett.* **2021**, *23*, 22, 8722. <https://doi.org/10.1021/acs.orglett.1c03165>
68. Y. Zhang, Y. Liu, Y. Du. First Total Synthesis of 27-Deoxylyngbyabellin A. *Synthesis* **2021**, *53*, 2874. <https://doi.org/10.1055/a-1478-9088>

REVIEW ARTICLE

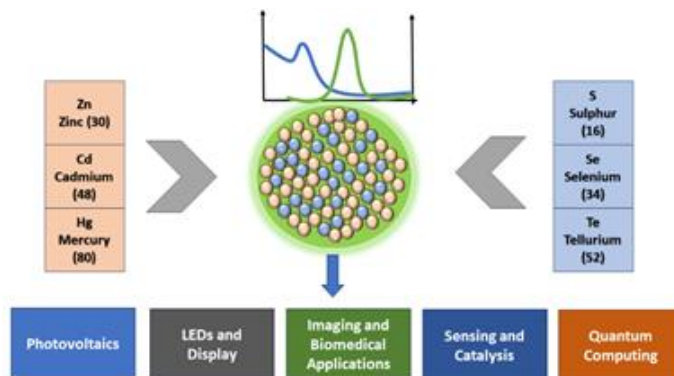
Recent Development and Challenges in Metal Chalcogenide Quantum Dots: From Material Design Strategies to Applications

Pratibha Chahal, Aayushi Goel and Avinash Singh* 

Department of Chemistry, SRM University Delhi-NCR, Sonapat-131029, Haryana, India

*Correspondence: avinash.s@srmuniversity.ac.in

Abstract: Nanotechnology advancements in recent times have led to the development of various metal chalcogenide quantum dots (QDs), including binary QDs (metal sulfide, selenide, and telluride) and alloyed QDs (cadmium selenium telluride). These QDs are valued for their distinctive optoelectronic and functional properties, including intrinsic (quantum confinement) and extrinsic (high surface area) effects influenced by size, shape, and surface characteristics. This review article mainly focuses on the most recent advancements in the synthesis, properties, and applications of metal chalcogenide QDs. We cover different synthesis approaches, including solvothermal, wet chemical, aqueous, photochemical, mechanochemical, and green synthesis, and explain how these techniques impact their properties. We then examine the diverse applications of QDs, including LEDs, biomedical, photovoltaics, neuromorphic, photodetector, photocatalysis, and sensing. Lastly, we explore the challenges and future opportunities for metal chalcogenide quantum dots. This article will provide a deeper understanding of the metal chalcogenide QDs. Moreover, it is beneficial for the researchers to make efficient QDs with various applications.



Keywords: chalcogenide, QDs, quantum confinement, synthesis, properties, applications.

Contents

Biographical Information	30
1. Introduction	31
1.1 Properties	34
2. Synthesis of Chalcogenide QDs	32
3. Applications	35
3.1 Photovoltaics	36
3.2 Photodetectors	36
3.3 Photocatalysis	36
3.4 LED & Display	37
3.5 Biomedical	38
3.6 Environmental Applications	39
3.7 Quantum Computing	39
3.8 Neuromorphic/Memory	39
4. Challenges & Future's Perspective	40
5. Conclusion	40
Author Contribution Declaration	40
Data Availability Declaration	40
Acknowledgements	40
References	41

1. Introduction

Modern, multidisciplinary nanotechnology has arisen from the development and research with inorganic nanomaterials which include metal, metal oxide, and semiconductor nanoparticles.¹

Quantum Dots (QDs) were first discovered by the Russian scientist Alexey Ekimov in 1981 in a glass matrix while he was employed at the Vavilov State Optical Institute in St. Petersburg.² However, it was Louis Brus, a semiconductor researcher at AT&T Bell Laboratories in New Jersey, who found the first colloidal solutions of QDs.² Brus referred to QDs as "small semiconductor crystallites". Later Mounji Bawendi and coworkers worked extensively to synthesize CdS, CdSe, and other chalcogenide QDs in the upcoming years.³ For their contribution to the discovery and synthesis of QDs, Alexey Ekimov, Louis Brus and Mounji Bawendi were awarded the Nobel Prize in chemistry in 2023.

Pratibha Chahal received her master's degree in chemistry with a specialization in physical chemistry from Maharshi Dayanand University, Rohtak in 2020. She qualified Net JRF (2022), HTET (2022), and CTET (2023). At present, she is pursuing PhD from SRM University, Delhi-NCR, Sonapat under the guidance of Dr. Avinash Singh. Her research interest lies in semiconductor QDs and nanotechnology.



Aayushi Goel is from Samalkha, Haryana, India. She completed her BSc in Chemistry from Kurukshetra University, Kurukshetra, Haryana and is pursuing MSc Chemistry (2024) from SRM University, Delhi-NCR, Sonapat. Her research interest is in nanotechnology and material science.



Dr. Avinash Singh studied BSc (Hons), Chemistry and MSc, Chemistry from Banaras Hindu University, and obtained his PhD from Radiation & Photochemistry Division, Bhabha Atomic Research Centre (BARC), Mumbai, India in 2018. Currently, he is serving as Assistant Professor in the Department of Chemistry, SRM University Delhi-NCR, Sonapat. His research interest lies in semiconductor nanomaterials, radiation chemistry and photochemistry.



In the past few years, semiconductor metal chalcogen based QDs have attracted wide interest in bioimaging and biomedical industries due to their good optoelectronic properties.⁴ QDs are semiconductor nanocrystals that are small enough to display size-dependent characteristics and come in the range of 1-10 nm.⁴ These are zero-dimensional nanomaterials, the terms "quantum" and "dot" imply that the particles—electrons, which transfer electricity—are restricted and have well-defined energy levels.⁵ They are restricted in all three spatial directions⁶ due to which these nanocrystals are also referred to as "low-dimensional" quantum structures.^{7,8}

Most of the QDs are made from the combination of metal (group I and II) and chalcogens (group VI).⁹ Chalcogens are the elements in the periodic table that belong to group VI elements including oxygen, sulfur (S), selenium (Se),

tellurium (Te), and polonium (Po).¹⁰ Out of these, the metal oxide is not considered chalcogenide as these oxides have different chemical properties in comparison to sulphide, selenide, and telluride¹¹. The common chalcogens which are used in the preparation of QDs are sulphur, selenium, and tellurium¹². Po is highly radioactive hence it is not used in the synthesis of QDs. The synthesis of semiconductor NCs in an aqueous medium primarily relies on Lewis's acid/base reactions, which invariably involve H^+ , OH^- , and H_2O . A chemical species that gives away an electron pair is called a Lewis base, and the one that accepts a base's electron pair is termed a Lewis acid.¹³ These are further divided based on their polarizability by the HSAB concept (Hard and soft acids and bases). "Soft" species are large in size, low-charge and weakly polarizable are "Hard" species. However, they are relatively small, and high-charge.¹³ This is the one of important concepts for the understanding of solubility of various kinds of compounds. Chalcogen ions like S^{2-} , Se^{2-} , and Te^{2-} are considered soft bases, whereas transition metal ions, based on their oxidation state, can be "soft" acids¹³ like Cd^{2+} , or "borderline" acids, such as Pb^{2+} and Zn^{2+} . According to the HSAB principle, chalcogens easily make insoluble compounds with the most of transition metal ions in water because of the poor solubility of their products. When compared with solids created by hard-hard interactions, the bonds in soft-soft interactions are stronger, which provides transition metal chalcogenides with their semiconducting properties.¹³ We can modify the size and composition, to obtain luminescence across the entire spectrum i.e. from UV to IR.¹³ The colloidal technique, which precipitates semiconductor crystals from a solution, yields the smallest structures.¹⁴

QDs are classified into different categories: binary, ternary or quaternary¹⁵ based on their composition. A binary QD has two elements (most commonly one metal from group II (Zn, Cd, Hg) and one chalcogen). Similarly, ternary, and quaternary QDs consist of three and four elements respectively. Examples of some most widely used binary QDs are ZnS, CdS, CdSe, etc. ZnCdS, ZnCdSe, are CuInS are examples of ternary QDs. Copper Zinc Tin Selenide (CZTS) is an example of quaternary QDs. Chemically and structurally, ternary I-III-VI and binary II-VI semiconductors differ from one another. PbS, CdS, or InAs are examples of binary semiconductor compounds that can be used to create binary QDs, which are semiconductor crystals at the nanoscale size.¹⁶ Ternary QDs composed of group I-III-VI elements exhibit lower toxicity and radiation stability elements which sparked increased interest in their application to cancer treatment.¹⁷ The term "artificial atoms"¹⁸ is frequently used to describe them since they can be made to resemble actual atoms in terms of their discrete electronic energy levels and electronic wave functions.¹⁹

One of the most extensive studies of chalcogenide based QDs is of II-VI semiconductors. Cadmium selenide (CdSe) is among the most significant semiconductors that have a size less than the Bohr radius of exciton (5.7 nm)²⁰ with a moderate band gap (E_g) of 1.75 eV at 300 K.²¹ CdSe QDs are highly luminescent, fluorescent and have better quantum yield with flexible processability.²² It was possible to create and analyze a CdSe QDs sensitized solar cell (QDSSC). It is possible to create QDs that have the potential to both absorb and emit light across the whole solar spectrum.²²

Saad *et al.*²³ reported the formation of CdSe QDs attached with chosen metal phthalocyanine (MPc) (like ZnPc and CuPc), employing the hot-injection organometallic approach. The resulting QDs exhibit same particle size and spherical morphology. They found CdSe QDs show clear photoluminescence (PL) peak of shorter wavelength.²³ QDs have the capacity for sensing as have proven beneficial in different specific applications, such as medicine and optoelectronics. Their intrinsic photostability, long fluorescence lifetime, and excitation wavelength far from the emission are the key justifications for their application in medicine.²⁴

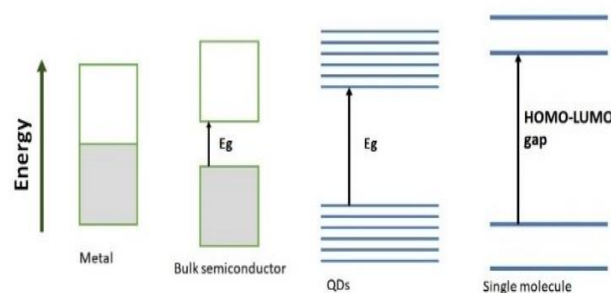


Figure 1: The band structure from metal to bulk semiconductor to QDs and molecules.

1.1 Properties

QDs and bulk materials differ in certain ways.^{24,25} Bulk materials are bigger whereas QDs are so small, they have a large surface-to-volume ratio, results in QDs exhibit a high degree of reactivity. In contrast, bulk materials are significantly large. Unlike, bulk materials, which present a continuous range of energy levels, QDs feature quantized energy levels shown as delta-like function in the density of states^{23,24} demonstrated in figure 2. The smallest QDs can be achieved using the colloidal technique, where semiconductor crystals are precipitated out of a solution²⁶. Temperature is an essential component in the synthesis process, and using high boiling point solvents helps to maintain controlled reactions.²⁶ Nanocrystallites, can exhibit optical, electronic, and structural characteristics that are frequently absent from both isolated molecules and macroscopic solids.²⁷ Nanocrystallites of semiconductors have specific electronic transitions that are tunable with size²⁸. They can be highly polarizable when they are excited, making them useful for optoelectronic applications.²⁸ Lia *et al.*²⁹ reported suitable applications of ZnS QDs that optical properties can be changed based on their size due to quantum size effect. As discussed QDs have size in nanometer scale, and are made up of element from groups II to VI or III to V, which have dimensions smaller than the Bohr exciton radius.^{30,31}

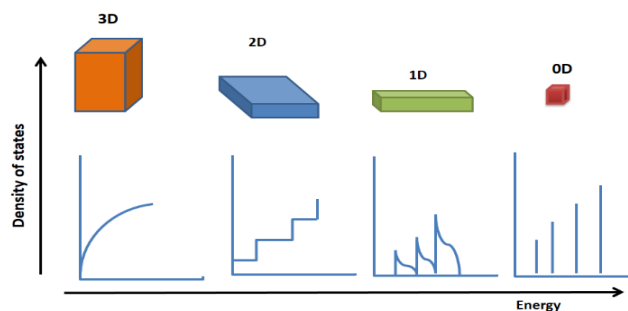


Figure 2: Variation of density of states for 3D, 2D, 1D and 0D materials

Quantum Confinement Effect: Another important effect which describes the particle size i.e. Quantum confinement effect. Quantum confinement effects elucidate the behavior of electrons through the use of energy levels, potential holes, electron energy bands, valence bands, and conduction bands. This phenomenon is observed when the particle size is significantly smaller than electron's wavelength consequently, the band gap energy increases as the QDs diameter decreases. As a result, both the absorption and emission spectral band edges of the QDs shift to shorter wavelengths as the particle size decreases, showing significant size dependence.³² Andersen *et al.*³³ reported that quantum confinement effect creates the energy levels further a part as the particles size reduced. They study various

features due to the varying size limits on each energy level. One significant effect of quantum confinement in CdSe semiconductor QDs is that rises in the band gap with decreasing QD size. Since this is observed as a rise in the lowest exciton peak's energy as the QD's radius decreased.³³

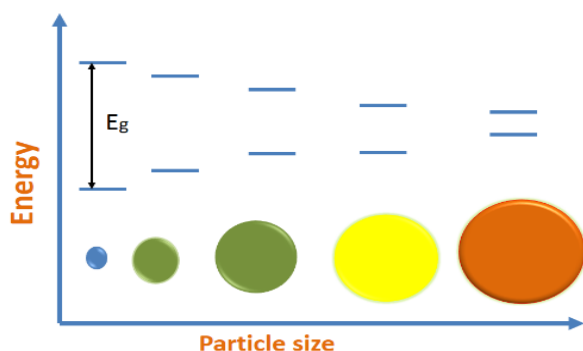


Figure 3: Variation in band gap with the size of the QDs as a consequence of quantum confinement effect.

Size-dependent: The optical properties of metal chalcogenide QDs depends upon shape and size of the QDs. Smaller particle size leads to a larger band gap hence the excitonic peak position is towards the smaller wavelength which keep on increasing upon increasing in particle size.³⁴ A small and uniform sized QD have a clear excitonic peak and a sharp emission profile. A color change from pale green to pale orange and finally to red with increasing particle size, showing a rise in particle size from Oswald ripening³⁴ (fig. 3). Because of their small size, QD electrons are trapped in a small space, even when their sizes are smaller than the exciton Bohr radius.³⁵ This implies that a significant energy level splitting occurs after an electron and a hole separate in an electron-hole pair.³⁵

The Bohr exciton radius refers to the distance in the model of the exciton pair (electron-hole pair). In bulk, the size exceeds the Bohr radius (figure 4). hence the quantum confinement effect is not observed. However, upon reduction in size below the Bohr radius (in the nano region) the energy level of the semiconductor becomes discrete due to confinement of exciton pair which is described as the quantum confinement effect.

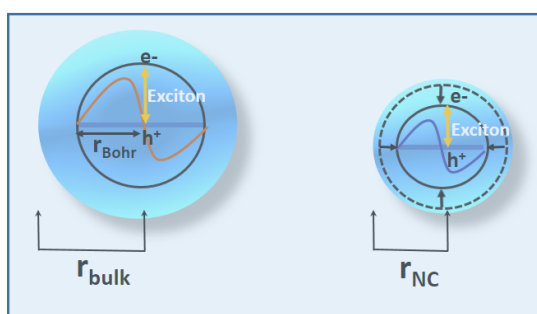


Figure 4: The Bohr radius in the bulk and nanocrystals

The band gap calculated by the Tauc equation (equation 1) and the particle size calculated by the Brus equation (equation 2) provides an estimate of the particle size.³⁶

The band gap calculated by the Tauc equation (equation 1) is given below:

Tauc equation:

$$(\alpha h\nu) = B(h\nu - E_g)^r \quad (1)$$

B = constant, r is the index which depends on nature of the electronic transition ($r = \frac{1}{2}$ for direct band gap semiconductor and $r = 2$ for indirect band gap semiconductor).

α = absorption coefficient

$h\nu$ is the photon energy

E_g = optical band gap

Tauc equation is used to calculate optical transition energy.

Using CdS and CdSe as examples, Brus (1984) provided the first theoretical calculation for a spherical semiconductor colloidal nanocrystal based on effective mass approximation.³⁷ The band gap energy in Brus's calculation is

$$\Delta E(r) = E_g + \left[\frac{h^2}{8r^2} \left(\frac{1}{m_e^*} + \frac{1}{m_h^*} \right) \right] \quad (2)$$

E_g = bulk band gap

h = Planck's constant, r = radius of QD

m_e is the mass of electron, m_h is the mass of electron hole

Apart from these two equations Scherrer equation can also be employed for the determination of mean size of particle using the XRD pattern. The Scherrer equation (equation 3)

$$D = K\lambda / \beta \cos \theta \quad (3)$$

K is the Scherrer constant, λ is wavelength of the X-ray beam, β is the Full width at half maximum (FWHM) of the peak, θ is the Bragg angle.

The Scherrer constant, whose value is typically taken to be 0.9, indicates the particle's form³⁸. To determine the crystal grain size, the Scherrer equation utilizes the width of the largest XRD peak for a specific sample.³⁸

Composition of the QDs: The optical properties of the QDs is also governed with the composition of the QDs. A bulk semiconductor having smaller size metal ions and chalcogenide ions have large band gap and a semiconductor having bigger size metal ions and chalcogenide ions have small band gap. For example- the band gap of ZnS, ZnSe and ZnTe are 3.97, 3.10 and 2.26 eV respectively. Similarly, bulk CdS, CdSe and CdTe have band gaps of 2.4, 1.74, and 1.49 eV respectively.

Surface to volume ratio: It is well established that the melting temperature of nanoparticles decreases as the surface-to-volume ratio increases. The shape also has a prominent role in determining the surface-to-volume ratio of the particles.³⁹ The shape factor compares the contact regions of spherical nanoparticles with non-spherical particles that have the same volume.⁴⁰ It is serves for account the shape difference, especially in polyhedral nanoparticles.⁴⁰

The simplest QDs are binary which are synthesized using one metal precursor and a chalcogenide. Zinc sulfide (ZnS), identified as II-VI binary compound, particular corresponding to a band gap of 4.49 eV.⁴¹ In addition, ZnS QDs are non-toxic and have good chemical stability than various semiconductor QDs. As a result, ZnS QDs are well-suited for use in electroluminescent devices, light emitting diodes (LEDs), flat-panel displays, sensors, optoelectronic devices and photocatalysis in water purification.⁴¹

The another binary QD i.e. Cadmium selenide NCs display a range of colors and luminescence, with smaller crystal sizes corresponding to higher energy transitions.^{30,42}

2. Synthesis of Chalcogenide QDs

Binary QDs are synthesized using one metal precursor and a chalcogenide. Li et al.⁴¹ adeptly formulated using a controlled solvothermal synthesis approach with a size of not more than 3 nm. The method is much easier for controlling size than the other traditional methods. Also, the absorption and luminescence showed new characteristics which may be caused by the quantum

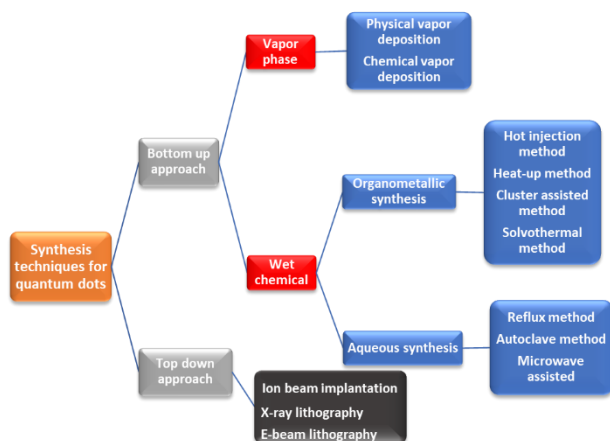


Figure 5: Various Techniques for Synthesis of Nanomaterials.

confinement effect including a considerable concentration of point defects in the lattice. Selecting a solvent is also an essential consideration for the wet chemical synthesis of QDs.⁴³ CdSe nanostructures using hot-injection method in aqueous solvent were synthesized successfully. CdSe particle sizes from 2.27 nm to 3.75 nm have controllable optical properties. The stabilizing agents such as TOP-TOPO, MPA, starch etc. used to synthesize high-quality CdSe QDs.⁴² Generally, high-quality CdSe QDs occur in organic solvent through a hot injection method that employs long-chain hydrocarbon as ligands.⁴⁴

Earlier, we recognized the efficient, one pot approach and easily scalable aqueous formation of starch capped CdSe QDs by photoirradiation and further explored its applications in detecting heavy metal ions.⁸ CdSe QDs are among the most extensively studied and important II-VI semiconductors. It has optoelectronic properties due to very small size (in nm range) that is smaller than Bohr radius of exciton which is known as quantum confinement effect. QD are prepared using different methods as discussed above. The stable and highly luminescent QDs can be prepared using reactivity variation among Cd and Zn as well as Se and S precursors which have a wider range of emission wavelength (500-600nm)⁴⁵. It focuses on the synthesis of CdSe QDs without requiring any extra additional reducing agent, no inert atmosphere or high temperature.⁸ The TEM studies revealed that the size of QDs is very small which confirms the presence of strong confinement effect. QDs once extracted are used in the detection of Cu^{2+} , Hg^{2+} , and Cr^{6+} ions.⁸

Figure 5 summarizes the various methods for QD production, showing that top-down methods reduce bulk material sizes, while bottom-up methods use chemical precursors from group II-VI elements for QDs synthesis.

Top-down approach: It includes breaking down large pieces of particles into nanostructures. This approach is good for making structures with long-range order and macroscopic connections. Strategies utilized for top-down approaches are X-ray lithography and E-beam lithography.⁴⁷

Bottom-up approach: It includes collecting single atoms into bigger nanostructures. This approach is best for gathering and building up short-range order at nanoscale measurements. Strategies utilized for bottom-up approaches incorporate pyrolysis, solvothermal forms, and sol-gel strategies.⁴⁷

The synthesis method used can affect the size of the QDs, which in turn affects their characteristics and applications. This category can be divided into vapor phase and wet chemical methods.

Hydrothermal technique: A productive technique that creates QDs in an aqueous medium using an autoclave. Using this technique, inorganic salt is crystallized in an aqueous medium at a temperature and pressure that are regulated.⁴⁸

The electrochemical method: An affordable technique that creates QDs with distinctive chemical and physical properties through electrochemical etching.⁴⁹

Hot-injection: A novel method that produces homogeneous nucleation by supersaturating monomers through fast precursor injection. It is common practice to create monodisperse colloidal QDs using this technique.⁵⁰

Microwave synthesis: A quick and affordable way to create QDs through microwave heating.

Ligand exchange: A well-studied method that uses bifunctional ligands to substitute the original ligands on the QD surface, making them water-soluble. This method is frequently employed for transferring QDs to an aqueous phase.

This category includes phase and wet chemical methods. Colloidal synthesis, a wet chemical method, has gained considerable interest in preparing QDs. Wet chemical methods are among the most widely used techniques for the synthesis of QDs. It includes the synthesis of QDs using aqueous and non-aqueous (organic) solvent. Various methods such as organometallic route, soft-chemical method, sonochemical method, hydrothermal method, electrochemical method are widely used methods for the formation of QDs. Another approach to preparing QDs is the photochemical process. Our group²¹ had synthesized Cadmium selenide (CdSe) QDs in an aqueous solution, utilizing UV photo-irradiation with L-Cysteine as stabilizing agent.

As photochemical method does not require the use of hazardous chemicals and stringent laboratory conditions. The QDs prepared from this method were found to have tunable fluorescence.²³ CdSe QDs synthesized by wet chemical method is the most common route which involves organometallic precursor in a coordinating solvent.²⁴ A decrease in the diameter of the particles below approximately 10 nm leads to band gap enlargement and shifts toward the blue region and achieving the particle size about 3 nm in diameter.²⁴ Bansal *et al.*²⁹ have synthesized highly luminescent organic molecule capped Cadmium Sulphide (CdS) QDs with 69% PLQY in solutions.²⁹

Ternary QDs have gained considerable interest in recent years. Mohanta *et al.*³⁰ reported bioconjugation of composite $\text{Cd}_{1-x}\text{Zn}_x\text{S}$ -NCs (with $x = \frac{1}{4}, 0, 0.5$ and 0.75). According to proponents of bioconjugate nanocrystals (NCs), the decay component resulting from free exciton recombination occurs nine times more quickly than the component resulting from surface recombination emission. By understanding the photoluminescence decay of bio-conjugated NCs contributes in the applications like biomolecular labelling, sensing and electrophysiology.²⁶

Yakoubi *et al.*³¹ reported low-cost aqueous synthesis of ternary QDs. They produced high quality CdZnS QDs, including those doped with Cu. They observed that the fluorescence and absorption spectra of CdZnS nanocrystals could be tuned by changing the stoichiometric ratio of Cd/Zn precursors in the host CdZnS QDs capped with different capping agents like 3-mercaptopropionic acid (MPA), L-cysteine, N-acetyl-L-cysteine (NAC), mercaptosuccinic acid (MSA), and glutathione (GSH). They successfully synthesized highly stable QDs and due to their favorable water dispersibility they can be used for biolabeling applications.³¹ As the capping used was NAC, the photoluminescence quantum yield (PL QY) obtained was the highest (27%), MPA (9%) and GSH (3%).³¹ The dots formed with NAC as a capping agent display the highest PL QY.³¹

One more work is reported where the synthesized QDs have impressive oxidation stability, acid stability, and photostability in both aqueous solutions and within the intracellular environment³². Zhan *et al.*³² described a double-shell structure through one-pot aqueous synthesis via microwave assisted technique. The size obtained was very small (~3.2nm) which implies that the CdSe/CdS/CdZnS core-shell

QDs can serve as a favorable candidate for fluorescent QDs based biological applications due to its lower cytotoxicity.³³ Colloidal QDs may be applied in bulk solution or as a solid film.³⁹ The technique where the reactants typically interact in the gaseous phase at elevated temperatures and deposit on the surface of sample comes in the category of bottom-up approach method which is known as chemical vapor deposition.⁴⁶

Table 1: Synthesis of various QDs their particle size, band gap, and applications with references

S.No.	QDs	Synthesis Route	Particle Size (nm)	Band Gap (eV)	Applications	References
1	ZnO	Green synthesis	5-10	3.37	Drug delivery	53
2	ZnS	Green synthesis	2-6	3.58	Used for fabrication	54
3	ZnSe	Wet chemical method	2-10	2.7	Vivo imaging and solar cells	55,56,57
4	CdO	Aqueous synthesis	2-3	1.36-2.3	In optoelectronic devices	58
5	CdS	Mechanochemical method	4-8	2.42	Economic approach for single-target-imaging application.	59
6	CdSe	Photochemical synthesis, electrochemical	2-7	1.91-2.84	Sensing heavy metal ions	7,20,21
7	CdTe	Aqueous synthesis	3.4	1.44	Making LEDs and sensors	4
8	CdZnS	Wet chemical method	<5	2.4-3.7	In optoelectronics devices (used as photoconductive and heterojunction solar cells)	60,61
9	CdZnSe	Wet chemical method	2-4	1.5-3	Fabrication of QLEDs	62
10	CuInS ₂	Solvothermal approach	2-4	1.5	Fabrication of affordable solar cells and enhanced efficiency	63

Aboulaich *et al.*³¹ reported synthesis of CdS via one-pot non-injection hydrothermal approach that involved cadmium chloride, mercaptopropionic acid (MPA), and thiourea as initial substances. The average size of QDs obtained is 3.5nm which has the highest photoluminescence i.e. 20%. The characterization of CdS@MPA QDs involved photoluminescence spectroscopy and UV-Vis, TEM, X-ray

diffraction. As shown in figure 6(a) the UV-vis spectra of CdS@MPA QDs, synthesized with a Cd²⁺/thiourea/MPA molar ratio of 1/1.7/2.3 and Cd²⁺ concentration of 5 mM, after different heating times (45 min, 1 h, 1.5 h, 2 and 3 h). The wavelength at which bulk CdS exhibits absorption edge is 515 nm. All samples, with the exception of CdS QDs that were heated for three hours, had distinct initial excitonic peaks at 363, 369, 382, 387, and 409 nm for 45 minutes, 1h, 1.5h, 2h, and 3 hours of heating, respectively. These peaks were linked to 1sh-1se excitonic transitions. The CdS sample's absorption spectra (t = 3 h) are wider, yet the variance of the absorption peaks shows that the particles expand quickly as the reaction time extends. The size dispersion gradually becomes less focused as a result of Ostwald ripening.³¹ With time, PL intensity shifted towards red region. Fig 6 (c) shows digitally prepared QDs after 3h. It is shows PL emission between 375 and 460nm. The colloidal solution of the as prepared QDs after 3 hours is shown in fig. 6 (b).

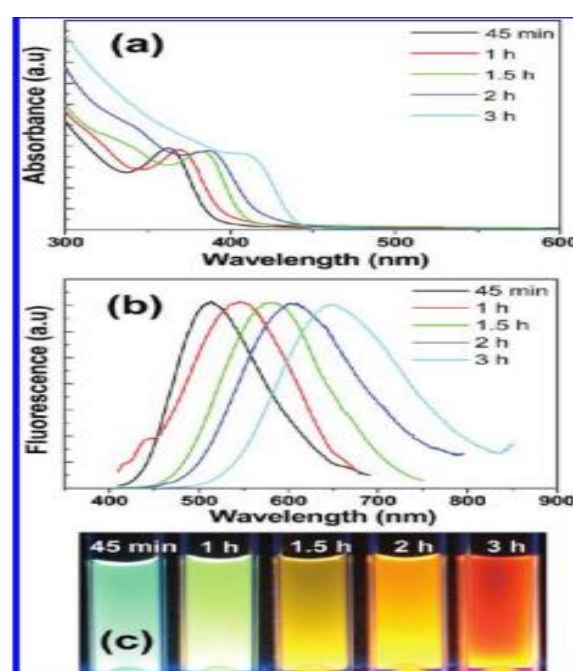


Figure 6 (a) UV-Visible (b) PL Spectra of CdS@MPA QDs after different reaction times at 100° C (c) Digital picture of CdS under UV excitation (reproduced with permission from ref 19. copyright 2012).

Other important characterization methods include transmission electron microscopy (TEM) and X-ray powder diffraction (XRD). Both provide the information about the crystal structure of the QDs. Furthermore, TEM also provides the exact shape and size of primary QDs. Broad peaks in the XRD pattern of CdS@MPA QDs indicate the sample's nano-

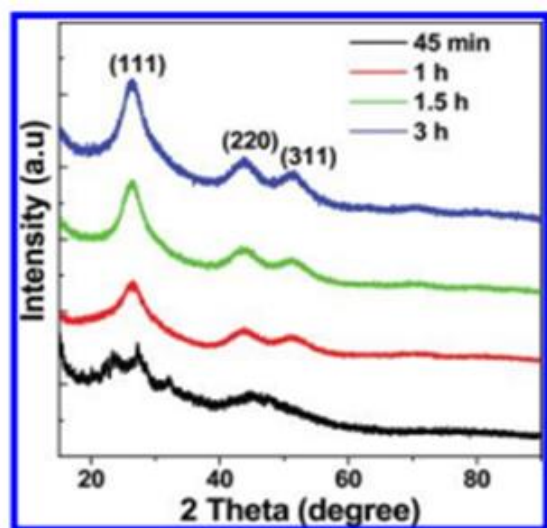


Figure 7: XRD patterns of the as-prepared CdS@MPA QDs as a function of heating time (reproduced with the permission from ref 19. copyright 2012).

scale size (Figure 7) The peaks are found at $2\theta = 26.5^\circ$, 43.9° , and 51.6° , aligned with the (111), (220), and (311) directions, indicating that the nanoparticles have a cubic zinc blende form.³¹

Meng *et al.*³⁴ reported aqueous synthesis of ternary QDs i.e. CdZnS using solvothermal method.

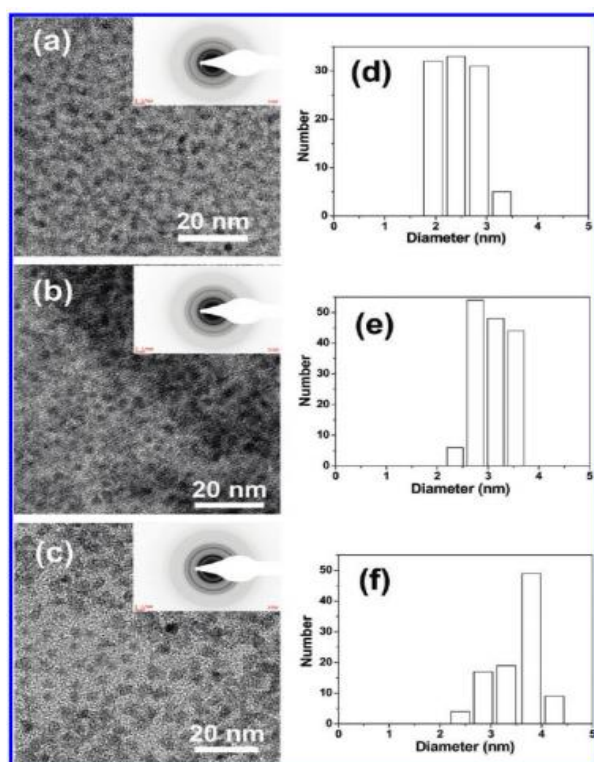


Figure 8: TEM images of CdS nano crystallites prepared under hydrothermal conditions for (a) 45 min, (b) 1.5 h, and (c) 3 h. Insets show the SAED patterns. (d-f) Corresponding size distributions (reproduced with the permission from ref 19. Copyright 2012).

Figure 8(a-c) display the TEM images of the CdS nanocrystallites that were prepared during 45 minutes, 1.5 hours, and 3 hours of heating, respectively. The corresponding selected area electron diffraction (SAED) patterns for CdS@MPA QDs are displayed in the insets of fig. 8 (a–c). The dependence of CdS QD particle size on heating duration is confirmed by figure 8 (d–f).

ZnCdS is a solid solution semi-conductor that combines the advantages of both ZnS and CdS materials by introducing ZnS into the lattice of CdS, resulting in a regulable crystal structure. The morphological and dimensional characteristics of the photocatalysts were investigated with scanning electron microscopy (SEM). As shown in figure 9 (a, b), the CdZnS QDs exhibit a uniform and regular surface morphology and the average size recorded was about 300 nm.

The XRD patterns of ZnCdS are illustrated in figure 10. The precursor pure ZnCdS exhibits prominent peaks at $2\theta = 24.8^\circ$, 26.5° , 28.1° , 43.6° , 47.8° , and 51.8° aligning to (100), (002), (101), (110), (103), and (112) crystal planes of the hexagonal phase of CdS respectively.

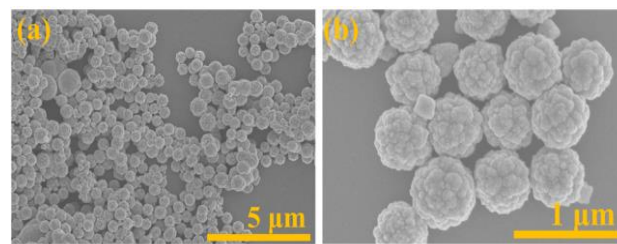


Figure 9: SEM images of CdZnS QDs showing globular morphology (reproduced with the permission from ref 43. copyright 2024)

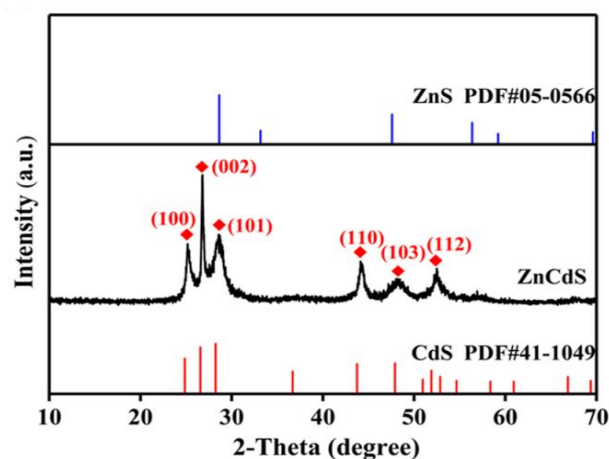


Figure 10: XRD patterns of ZnCdS. and corresponding peaks of ZnS and CdS (reproduced with the permission from ref. 43. copyright 2024)

3. Applications

Chalcogenide-based QDs have drawn prodigious research interest within optical-related devices, including photovoltaic cells, photodetectors, photosensors, photoelectrochemical devices, phototransistors, solar cells, catalysis, and drug delivery. When designing QDs for specific applications, several key factors should be considered, such as surface chemistry, size and shape, stability, toxicity, composition, and scalability. A variety of these applications are commercially accessible and have become integrated into our everyday lives (figure 11).

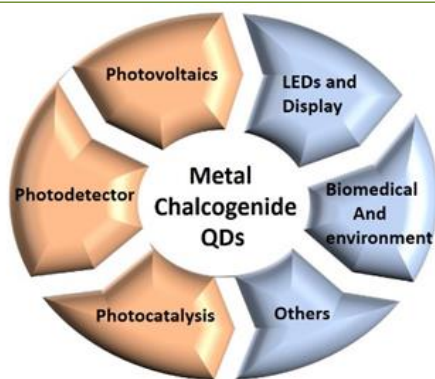


Fig. 11: Applications of Chalcogenide-Based QDs

Below we detail notable works based on these applications.

3.1 PHOTOVOLTAICS

Metal chalcogenide QDs have promising uses in photovoltaics, particularly in solar cell technology. Firstly, their tunable bandgaps enable the optimization of light absorption across various wavelengths, increasing the efficiency of solar energy conversion. This tunability also allows for the production of multi-junction solar cells, in which layers of QDs can be tailored to absorb different sections of the solar spectrum. Absorber material, multiple sensitizations, intermediate-band solar cells, multiple exciton generation, and tandem solar cells are a few ways metal chalcogenide QDs can be utilized in photovoltaics.⁶⁵ Chen *et al.*⁶⁶ introduced devices used in photovoltaics that are equipped with nanomaterials to raise the energy conversion regulation and its efficiency. Devices made using chalcogenide QDs like CdS, CdSe, and CdTe in a liquid-type electrolyte have shown cell efficiencies lying from 3 to 6%.⁶⁷ This is significant because it demonstrates the potential of these materials help to design better-performing solar energy systems. Furthermore, various strategies are being explored to improve the photocatalytic water-splitting capability of metal chalcogenide QDs. These include cocatalyst, element doping, creating heterojunction, and plasmonic material photosensitization.⁶⁷ Alam *et al.*⁶⁹ reported the combination of CdSe QDs with ZnO nanowires to create hybrid solar cells with up to 50-60% internal quantum efficiencies and sensitized-type solar cells with an efficiency of power conversion of roughly 2.7%, which are based on TiO₂ inverse opal with CdSe QDs as sensitizers. Singh *et al.*⁷⁰ reported avenues for improvement used to modify the bandgap of QDs (CdSe and CdTe), such as post-synthesis chemical remedies, co-sensitization, deposition techniques, and doping of sensitizers.

Zhu *et al.*⁷¹ introduced tandem solar cells that utilize lead chalcogenide (PbS, PbSe) QDs, which exhibit excellent quantum confinement effects and can include the full infrared range of solar radiation by changing their size. This makes them highly potential cost-effective infrared photovoltaic devices. The primary component influencing the CdS QDSSC performance, according to observations of Padmaperuma *et al.*⁷², appears to be the ICR process at the CdS QD/TiO₂ interface. According to Mumin *et al.*⁷³ supercritical carbon dioxide synthesis was used to spread core-shell CdS/ZnS QDs into copolymers. Additionally, the layout of CdSe QD materials for converting energy purposes was helped by theoretical research using DFT calculations.⁷⁴ By simulating various surface modifications or doping scenarios using DFT calculations, researchers can explore strategies to enhance specific properties of metal chalcogenides QDs for applications such as solar cells, optoelectronic devices, sensors, and catalysis. A table summarizing the photovoltaic properties of various metal chalcogenide QDs is mentioned here.

Table 2: Various Metal Chalcogenide-based QDs and Their Photovoltaic Efficiency

QDs	J _{sc} (mA cm ⁻²)	V _{oc} (V)	PCE (%)	Reference
CdS/CdSe	15.77	0.579	0.521	74
Zn-Cu-In-S	4.34	0.51	2.01	75
CdSe _x Te _{1-x}	20.78	0.653	8.21	76
CdTe/CdSe _x T _{1-x}	16.20	0.621	7.24	77
CdTe	2.10	0.68	0.87	78
Zn-Cu-In-Se	11.11	0.59	4.13	79
Zn-Cu-In-Se	26.49	0.77	13.85	80
CuInS ₂	11.33	0.68	3.13	81
CdS/CdSe	32.247	0.629	8.28	82
Zn-Cu-In-Se	26.98	0.772	13.84	83
Zn-Cu-In-S-Se	25.51	0.78	14.4	84
CdSeTe	10.048	0.664	3.379	85

3.2 PHOTODETECTORS

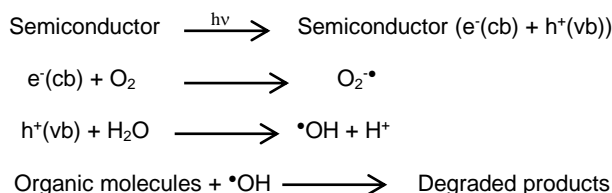
QD photodetectors have applications in visible and IR-light cameras, machine vision, spectroscopy, and fluorescent biomedical imaging. Photodetection can be observed by different kinds of devices, like light-dependent resistors or photodiodes. The traditional photodetectors are bulk semiconductor based hence they are not very stable and flexible. In addition, they have expensive substrates, and the movement of charge carriers is restricted. QDs have been playing an important role in integrating these pre-existing technological platforms to enhance their performance⁸⁷. Tang *et al.*⁸⁸ demonstrated a two-step ligand-exchange technique, by using this method an improved responsivity in PbS QDs photodetectors can be observed in the IR spectral region. Printing methods were also implemented to PbS QDs devices, including photodetector arrays⁹⁰, and broadband photoconductors.⁸⁹ IR photoconductive photodetectors are fabricated from Ag₂Se QDs.⁹¹ By using a fast microwave-polyol approach, photoconductors were developed from highly packed PbS QDs films.⁹²

Infrared photodetectors are broadly used in security monitoring, the vision of machines, autonomous automobiles, as well as other fields.^{93,94} Traditional IR photodetectors are often based on materials like InGaAs and HgCdTe which offer commendable reliability, wide-band detection capabilities, high sensitivity, and long-time stability.⁹⁵ While effective, these materials suffer from limitations such as complex production processes, substantial fabrication costs, and poor compatibility with silicon-based readout integrated circuits.^{96,97} Zhao *et al.*⁹⁸ have explored lead chalcogenide colloidal QDs (CQDs) (PbTe, PbSe, and PbS, etc.) to develop efficient and affordable IR photodetectors. Another exciting avenue is mercury chalcogenide CQDs, having similar advantages: solution processability, better compatibility with silicon substrates, and scant manufacturing costs. They hold great potential for use in IR imaging and detection.^{99,100} CQDs show potential for dual-band photodetectors due to their changeable bandgaps. These photodetectors are garnering significant interest due to their promising applications in biological detection, environmental surveillance, and optical communication. They can process signals from both visible (VIS) and short-wave infrared (SWIR) wavebands, providing greater precision and detailed images of detected materials compared to single band detectors. Zhao *et al.*¹⁰¹ have been exploring the detector utilizing HgTe along with CdTe CQDs as sensing layers. Between the layers of CdTe and HgTe, n-type ZnO is introduced. This layer achieves a responsivity of 0.5 AW⁻¹ for the visible band (peaking at 700 nm) and 1.1 A W⁻¹ for the SWIR band (peaking at 2100nm). The detectivity reaches 1.1 × 10¹¹ Jones at +3V (for VIS) and 4.5 × 10¹¹ Jones at -2V (for SWIR).

3.3 Photocatalysis

Metal chalcogenide QDs are useful in photocatalysis arising from their proficiency in absorbing light over an extensive range from UV to visible regions, hence increasing sunlight harvesting. Their nanoscale dimension allows for an extensive surface area and many active reaction sites. They

also allow to separate electron-hole pairs efficiently, lowering recombination and boosting charge carrier lifespan, which is critical for photocatalysis. Functionalization and hybridization with other materials can enhance their performance. Photocatalysts can be applied in a variety of processes, such as treatment of wastewater, conservation energy, self-cleaning applications, antifouling, sterilization, and air purification.^{102,103} Some semiconductors can mineralize organic contaminants, such as halo hydrocarbons, aromatics, insecticides, pesticides, surfactants, and dyes. Mainly binary chalcogenides such as TiO₂, ZnO, CdS, ZnS, and Fe₂O₃ are utilized for photocatalytic properties. In addition to binary chalcogenides, some examples of ternary chalcogenides such as SrZrO₃, PbCrO₄, CuInS₂, Cu₂SnS₃, XGaS₂¹⁰⁴ (X= Ag or Cu), SnSb₂S₅ etc. and quaternary chalcogenides such as GeSbSeEr,¹⁰⁴ Cu₂ZnSnS₄ etc. have also been used. Exposure of photocatalysts to light of an appropriate wavelength causes an electron within the valence band to absorb photon energy and become excited in the conduction band, leading to the creation of a hole in the valence band simultaneously. These holes and electrons participate in redox reactions on the semiconductor's surface. A general reaction mechanism for the photocatalysis process can be represented as follows:



The excited electron is capable of reducing substrates or combining with electron acceptors like O₂, whether present on the semiconductor surface or dissolved in water, thereby converting it to a superoxide radical anion O₂^{•−}. The hole, in contrast, can oxidize organic molecules to produce R[•] or engage with [−]OH or H₂O to form [•]OH radicals. Other highly oxidizing like peroxide radicals also contribute to the photodegradation of organic substrates. The [•]OH radical is a very potent oxidizer and effectively decomposes azo dyes and pollutants. The photocatalysis process is explained in the figure given below (Figure 12):

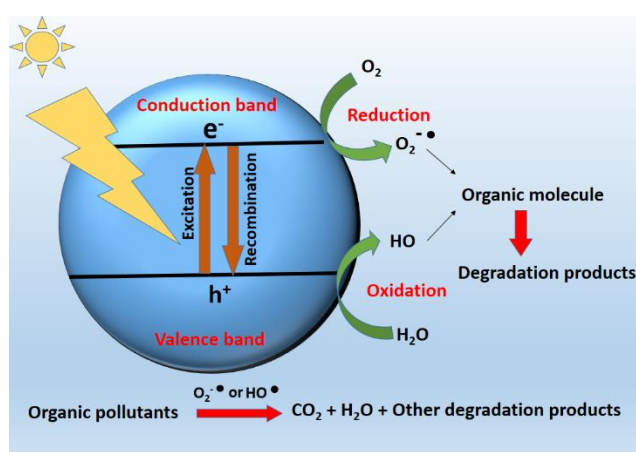


Figure 12: Schematic of generation of exciton pair and their reaction in the photocatalysis process.

Photocatalysts play a significant role in various applications, including pollutant degradation, hydrogen formation via water splitting, and carbon dioxide reduction. Metal chalcogenides contribute to accelerating photoreactions, driving advancements in these fields. Weiss and Weix *et al.*^{106,107}

demonstrated the Cd chalcogenide QDs were able to operate carbon-carbon coupling reactions. With the help of carbon QD-sensitized TiO₂/Pt nanocomposites, light-driven H₂ production was achieved.¹⁰⁸

Enzymatic activation has been demonstrated separately by assembling DNA cells and CdSe/CdZnS/ZnS core shell and CdSe/ZnS core-shell QDs.¹⁰⁹ Metal chalcogenide QDs have been explored for photocatalytic air cleansing, including volatile organic compounds decomposition and the removal of air pollutants. Luminescent nanotags also be the application of metal chalcogenide QDs. Durmusoglu *et al.*¹¹⁰ proposed using luminescent nanotags (hybrid coated PbS and PbS/CdS QDs) for authenticating fossil fuel products. Combining the luminescent properties of CdTe QDs with superparamagnetic maghemite (Fe₂O₃) cores, these QDs are hybrid nanoprobe. By incorporating these nanoprobe, one can efficiently detect and visualize defects or anomalies in materials submerged in water baths.¹¹¹ Meng *et al.*¹¹² created a catalyst for an effective photocatalytic nitrogen reduction process (PNMM) by loading bismuth metal on ZnCdS nanospheres. The photocatalyst's ammonia generation efficiency was greatly enhanced by Bi nanoparticle under light. The 3% Bi@ZnCdS produced 58.93 μmolg^{−1}h^{−1} ammonia using lactic acid under air, nearly 7.7 times more efficient than pure ZnCdS.

3.4 LED and Display

One of the main applications of metal chalcogenide QDs is LEDs for the production of highly efficient and stable red, green, and blue light emissions. Metal chalcogenide QDs improve LEDs and display technologies by allowing for tunable emission qualities, which results in more brilliant colors and greater color purity. They enable more efficient light-emitting layers, which reduces energy usage and increases gadget lifespan. There are stability and lifetime concerns of organic LEDs and other LEDs. However, the QDs-based LEDs are inherently stable and have a longer lifetime. The lifetime of LEDs is affected by various factors like- oxidation, heat, exposure to UV light, etc. Various strategies like- core-shell engineering, surface passivation, and architecture optimization are adopted to improve the lifetime of QDs. These QDs can often be carefully designed to emit light at specific wavelengths, which makes them useful for developing a variety of colors for LED displays and lighting applications. Furthermore, metal chalcogenide QDs have also been used to enhance the color rendering index (CRI) of LEDs, leading to more accurate and natural color reproduction. Additionally, metal chalcogenide QDs can be used to enhance the stability and lifetime of LEDs by improving their resistance to environmental influences including humidity and temperature. The PbX QDs can effectively be utilized in NIR-QLEDs with the ability to tune their emission wavelength by altering the size of QDs. The first PbX-based NIR-QLEDs achieved an external quantum efficiency (EQE) of 0.5%. Notably, EQE of NIR-QLEDs has enhanced from 2% in 2012 to 7.9% in 2018.¹¹³⁻¹¹⁷ The equation¹¹⁵ below can be utilized to calculate the efficiency of EQE of NIR-QLEDs:

$$\text{EQE} = \eta_{\text{diff}} * \eta_{\text{inj}} * \eta_{\text{PLQY}} * \chi * \eta_{\text{out}}$$

Where, η_{diff} - efficiency of injected carriers that successfully diffuse to QDs.

η_{inj} - efficiency of these carriers that transfer into QDs and form excitons.

χ - efficiency of these excitons whose states have spin-allowed optical transitions (for colloidal QDs, $\chi = 1$).

η_{PLQY} - internal QD PL QY, & η_{out} = light out-coupling efficiency.

η_{diff} and η_{inj} are two key parameters for the efficiency of NIR-QLED devices. In visible-QLEDs, it is important to choose suitable carrier transport layer materials^{118,119} to enhance η_{inj} .

The use of Cd-based QDs aims to augment material properties in conjugation with the developed shell and surface ligand.^{120,121} According to Pal *et al.*¹²², the performance of the device is affected by the thickness of the CdSe shell that encases the CdSe core of the QDs. Consequently, they achieved a maximum EQE with a 13-layer of the CdS shell, resulting in a brightness of about 1000 cdm⁻² at a low starting voltage of approximately 3V.

Chen *et al.*¹²³ introduced a technique to develop a shell layer that reduces blinking in QDs by disregarding the lattice discrepancy within the core and shell. Cadmium (II) oleate and octanethiol are employed as precursors to create high-quality CdSe/CdS core/shell QDs, effectively minimizing lattice mismatch. The PL peak width dropped from 96.2 meV for uncoated CdSe QDs to 67.1 meV for final results CdSe/CdS QDs (20nm), the highest PL QYs of 97% was observed, and 94% average on-time fractions, indicating significant suppression of blinking.

Pu *et al.*¹²⁴ presented the concept of an electrochemically stable surface-binding ligand. $T_{50} > 3800$ hours at 1000 cdm⁻² for red-emitting LEDs and $T_{50} > 10,000$ hours at 100 cdm⁻² for blue-emitting LEDs were achieved using the electrochemical inert ligand. Kim *et al.*¹²⁵ reported blue QDs created from layers of ZnS, ZnTeSe, and ZnS QDs for the advancement of InP-based QDs. They attained a full width at half maximum (FWHM) of 23 nm, with PL QYs of 85%. The EQE was 6.8% at 3.6 V and exhibited a peak luminance of 14146 cdm⁻² was achieved. Jiang *et al.*¹²⁵ proposed a In³⁺-doped strategy in Zn-Cu-Ga-S@ZnS QDs. Resulting PLQY value 95.3% was achieved. In ZnCuGaS:In@ZnS, maximum luminance 1402 cdm⁻² and EQE 2.4 % was also achieved which gave a high CRI value of 94.9. Based on this red, green, and blue photoluminescence/electroluminescence (PL/EL) spectrum of a single-component QD that is stable and balanced, meeting the requirement of lighting and display.

Hexagonal boron nitride sheets are incorporated in order to strengthen the thermal stability of devices constructed from CdSe/CdS QDs¹²⁷. Additionally, CuInS₂/ZnS QDs with dependable thiol-based ligands and amino-based ligands are recommended for the efficient development of film-type display devices¹²⁸.

Table 3: A summary of metal chalcogenide-based LED and display materials.

QD Materials	Method	Performance Summary	Reference
CdSe	Maximization of shell thickness efficiency	Achieving 1000 cdm ⁻² luminance with a 3 V turn-on voltage.	88
CdSe	Shell layering kinetics control for suppression of lattice mismatch	PL QYs 97%, FWHM 67.1 meV (20 nm).	89
CdSe	Electrochemically stable ligands	$T_{95} > 3800$ h at 1000 cd m ⁻² luminance for red emission T_{50} surpasses 10,000 h at 100 cd m ⁻² for blue.	90
ZnTeSe	ZnS/ZnTeSe/ZnS quantum well structure	EQE 6.8% at 3.6V, luminance 14146 cd m ⁻² , FWHM 23 nm.	91
ZnCuGaS:In @ZnS	Ln ³⁺ -doping	PLQYs 95.3%, EQE 2.4%, luminance 1402 cdm ⁻²	92

3.5 Biomedical

Metal chalcogenide QDs help to promote biomedical imaging by providing improved luminescence, which improves picture quality and sensitivity. Their size-dependent optical features enable tunable emission wavelengths, allowing for multi-color imaging and tracking of many targets at the same time. Researchers are involved in the reduction of the toxicity of chalcogenide QDs for their use in biological applications by

their surface functionalizing with biocompatible coatings, investigating less toxic core compositions, controlling QD size and dosage, and utilizing bioconjugation for targeted delivery. Their surface alterations allow for focused imaging of certain cells or tissues, which improves diagnostic accuracy. Furthermore, metal chalcogenide QDs have extended photoluminescence lifetimes and are resistant to photobleaching, increasing the reliability and duration of imaging experiments. Overall, these characteristics make them useful instruments for cancer diagnosis and immediate tracking of biological processes. In the biomedical field, the numerous uses of metal chalcogenide QDs such as bioimaging, single-QD tracking of extracellular and intracellular targets, therapeutics, fluorescence resonance energy transfer (FRET), gene technology, detection, etc.¹²⁹ Their small size, high quantum yield, and tunable emission wavelengths make them ideal for labeling and tracking biological molecules and cells in living systems. They can be constructed to focus on certain tissues or cells, making them useful for therapeutic delivery and intervention. QDs have been employed for different applications both in vivo and in vitro imaging. In 1998, the research teams of Alivisatos and Nie separately presented the first examples of a QD system in bioimaging. Su *et al.*¹³⁰ developed a sensor to measure pH inside the cells utilizing AgInS₂/ZnS QDs to differentiate between cancerous and healthy cells. This pH sensor can be used to image living cells with in various pH solutions and cell lines by combining QDs with fluorescent lifetime imaging microscopy. Interestingly, this sensor examined the cervical cells that were ejected from 20 patients. According to findings, this sensor can provide a higher sensitivity to traditional cytology in the clinic, opening the door for effective noninvasive cervical cancer screening. In the context of COVID-19, metal chalcogenide QDs have been explored for their potential in bioimaging, biosensing, and even in therapies targeting virus.¹³¹ They can be engineered for prompt theranostic applications of severe acute respiratory syndrome coronavirus 2 (SARS-CoV-2). Several II-IV QDs are known as fluorescent markers for bioimaging applications. For example, the CdSe/ZnS QDs linked with streptavidin and immunoglobulin G (IgG) are used to image the breast cancer cells through the recognition of HER2 biomarker¹³² while CuInS₂/ZnS QDs, which have low nonspecific binding and easily conjugated to other molecules, making them useful cell imaging markers.¹³³ Additionally, Nguyen *et al.*¹³⁴ demonstrated CuInS₂/ZnS (CIS/ZnS) QDs that were linked to neutravidin served to trace biotinylated actin. Bioconjugated QDs are highly useful in targeted drug delivery, gene delivery, bioimaging, pathogen detection, etc. Li *et al.*¹³⁵ synthesized biocompatible Mn-doped CuInSe₂ QDs functionalized with folic acid that had a fluorescence performance of 31.2% in NIR-II. These QDs are found to gather mostly in 4T1 breast cancer tumors and can be utilized for NIR fluorescence imaging. Clinical diagnostics CA125, a very sensitive test for an ovarian tumor marker, was introduced with the help of CdTe QDs and SiO₂@polydopamine core-shell nanoparticles.¹³⁶ Freitas *et al.*¹³⁷ demonstrated that CdSe/ZnS QDs were used to identify HER-2-ECD breast cancer cells' biomarkers (CA15-3) while CdSe/ZnS QDs associated with antibodies to trace the presence of breast cancer cells.¹³⁸ Protein measurements, protein interaction monitoring, and enzyme activity assays have all taken advantage of the conformational shift resulting from FRET. Forester resonance energy-transfer method was used to modify CdSe/CdS/ZnS QDs and antibodies marked with terbium to create a sensor that can detect adenosine diphosphate.¹³⁹ In bacterial cells and model membranes, CdSe and ZnSe together with a ZnS Shell appeared membrane disturbance activity.¹⁴⁰ CuInS/ZnS QDs with infrared emission were developed by Lv *et al.*¹⁴¹ for tumor phototherapy. These QDs effectively obtained bimodal tumor treatment using PDT and PTT. Under 660 nm laser irradiation, the tumor cells were successfully eradicated from

selectivity and rapid response/recovery times of 50/115 s. To detect NH_3 gas, Sharma *et al.*¹⁵¹ developed two-dimensional (2D) tungsten disulphide (WS_2) nanosheets coated by tin oxide (SnO_2) QDs. Low NH_3 concentrations resulted in a low LOD (~ 10 ppb) and high sensitivity ($\sim 175\% \text{ ppm}^{-1}$) due to the improved response. When analyzed to WS_2 QD as CO_2 gas sensor, the Ru@WS_2 QD exhibits fewer impacts under various humid circumstances.¹⁵²

3.7 Quantum Computing

Quantum computing has a wide area of uses and has numerous future benefits including drug design & development, computational chemistry, cleaner fertilization, electronic materials discovery, solar capture, better batteries, cybersecurity & cryptography, financial modeling, artificial intelligence& machine learning. QDs are a possible method for quantum computing that has gained traction as potential building blocks for solid-state quantum devices in recent years. QDs provide a platform for investigating several ways of approaching quantum computation, such as information storage, quantum gate operations, and qubit implementation. QD technology is demonstrating potential in solid-state quantum computation and offers avenues for implementation in quantum information processing (figure 13).¹⁵³

Toxic gases can be harmful to ecosystems and human health, making their presence in the environment a major global problem. Anthropogenic sources such as power plants, manufactures, or smoke are the major source for hazardous gases (such as NH_3 , CO_x , H_2S , SO_x , and NO_x that have been released into the atmosphere. Human senses are unable to identify several of the hazardous gases at low amounts, and some of the gases have no smell at all.¹⁴⁶ Geng *et al.*¹⁴⁷ developed a feasible approach for detecting NO_2 gas at room temperature employing a PbSe QD gel substrate. Firstly, CdSe QD gels were created and then converted into PbSe QD gels via a cation exchange method. The gas sensing was conducted under various LED light irradiation conditions, with the greatest findings achieved under violet light illumination. The sensor responded linearly to NO_2 concentrations ranging from 0.003 to 1.32 ppm, with a low LOD of 3 ppb and excellent response/recovery times (27 and 102 s). The scientists employed heavy metal QDs to create a NO_2 sensor with a lower LOD at room temperature. Under UV irradiation at 40 °C, the ZnO/SnO₂ composite (SZQ1%) with a molar ratio of 1:100 demonstrates outstanding NO_2 gas detecting characteristics with a LOD of 100 ppb.¹⁴⁸ Lin *et al.*¹⁴⁹ created a flexible and portable NO_2 sensor by modifying nylon fibres with ZnO QDs and reducing graphene oxide (rGO). The sensor has a linear response from 20 to 100 ppm and a LOD of 20 ppm at 25°C. The sensor performed well with response and recovery times of about 216 seconds and 668 seconds, respectively. The scientists incorporated the portable fibre sensor with an electrical module to create an over-limit monitoring system for NO_2 values above 20 ppm. Liu *et al.*¹⁵⁰ created CuSbS_2 QDs/rGO composites via hot injection to make gas sensors. The composites showed high NH_3 detection ability at room temperature (23 °C) and a low LOD of 500 ppb. Furthermore, the sensor demonstrated excellent

To further the capabilities of quantum computing, researchers are currently actively investigating and creating QD-based technologies. Nonetheless, there are a few obstacles to be addressed, like qubit interactions and manufacturing flaws, which restrict the use of QDs in the realm of quantum computing. The key to overcoming qubit interactions is regulated interactions between adjacent qubits. Even with these great advancements, there is still much work to be done to produce reliable and strong qubit interactions. Errors and noise can enter the system as a result of fabrication flaws, which can result in misleading calculations. Therefore, to simplify the scaling-up of QDs in the realm of quantum technologies, a precise controlled synthesis methodology is essential. Systems encoded within QDs have fewer internal degrees of freedom and are more effectively isolated from the outside world than systems with higher dimensions. There is growing interest in the possible uses of QDs for solid-state quantum computing because of these two properties, which are help extend the coherence periods of the qubit states contained within the dot.¹⁵⁴

QDs have a wide band gap and high electron mobility. This enables them beneficial for advanced electronic devices like floating gate memory systems and neuromorphic hardware devices. Semiconductor QDs are a popular choice for photonic applications due to their compatibility with (Complementary Metal-Oxide-Semiconductor) CMOS-based processing methods. These devices offer great optical absorption, structural stability, and cost-effective production for vast area coverage. The density of states, band gap, material properties also surface effects (nature of the capping agent) govern the electronic properties of QDs that are very

significant for photonic applications and affect their performance in electronic devices. A rapid way to recover the performance was achieved by Jeong *et al.*¹⁵⁵ of CdSe QD floating gates utilizing low-intensity light. The concept of using QDs as the active element in memristors has become more and more favored in recent times due to its advantages, which include high quality, the ability to integrate with electronic devices, and low power consumption. Wu *et al.*¹⁵⁶ determined a ZnO/CsPbBr₃ QDs-based memristor with a low operating voltage (1V) and a high ON/OFF ratio (>105). Spintronics also has garnered a great deal of interest recently as a potential field for next-generation electronics due to its ability to reduce energy consumption and increase performance in classic electronics. It is utilizing the electron's spin state in QDs to create new electrical devices. Researchers are investigating metal chalcogenides due to their potential for energy-efficient neuromorphic computing. Neuromorphic computing aims to mimic the brain's computational abilities, emphasizing low power consumption and parallel processing. In terms of energy consumption, the human brain is about 10⁶ times more efficient than typical CMOS logic. Low-range stimuli can trigger short-range mechanisms like structural phase shifts and coupled electron systems. These materials have the potential to create effective synaptic devices and memristors in neuromorphic systems.¹⁵⁷ Neuromorphic memristors derived from 2D TMCs hold great potential in brain-inspired computing and high-performance AI.¹⁵⁸ Using 2D materials in vertical memristors allows for scaling to thicknesses of 10 nm or even less, resulting in reduced operating voltage and great integration density. This is advantageous for less power applications.¹⁵⁹ Xu *et al.*¹⁶⁰ discussed advancements in neuromorphic optical and electronic devices, aiming to imitate the human brain to improve efficient energy use and data processing performance. Brain-like chips and in-memory computing systems benefit from PCM-based devices. The all-around benefits of QDs for memory applications include regulated sizes with flexible changes, emission properties, high optical stability, and tunable absorption. These benefits allow the memory architecture to have desirable features like uniformity, scalability, photoswitching, and flexibility.¹⁶¹

4. Challenges & Future's Perspective

Metal chalcogenides have various applications due to their interesting properties. However, they also face several challenges in different fields. Many metal chalcogenides, particularly those containing selenium and tellurium, can become unstable when exposed to light, heat, and moisture over a sustained period, resulting in decreased performance. QD surface imperfections can trap charge carriers, resulting in non-emissive recombination. These defects can affect the efficiency of QDs in photovoltaics and LEDs. Some chalcogenides, including those containing cadmium (e.g., CdTe), are hazardous, raising environmental and health problems. Cadmium-based QDs can induce apoptosis, altered gene expression, neurotoxicity, and mitochondrial damage. This hinders their applicability in biological and clinical imaging. To overcome this problem, scientists are investigating alternate materials and formation processes to create non-toxic QDs with preferred qualities. Inefficient Na⁺ diffusion in chalcogenides can affect battery performance and Low electrical conductivity reduces rate capabilities. Ensuring the biocompatibility of QDs in biomedical applications is a significant challenge. QDs can release harmful ions in a biological environment, which is a major problem. Metal chalcogenide QDs are difficult to synthesize and require specialized equipment, limiting their applicability in many applications. Large-scale production of QDs involves issues such as maintaining consistent size and shape, efficiently scaling up synthesis methods, assuring purity and stability, and controlling environmental and safety concerns related to toxicity.

The major ongoing research on the chalcogenide QDs is in the biomedical application which aims to explore a greener and more scalable technique for the formation of these QDs. The future perspective of research and development also aims to replace the heavy and toxic metal ions with biocompatible metals like Zn, and Cu. The other challenge is to have precise control over shape, sizes and sizes, hence enhanced quantum yield and the other properties of these QDs. Overall, the future of research and development of chalcogenide QDs looks very promising and bright. The prospect of the use of QDs lies in the extensive work in the field of quantum computing, single photon emitters, and in spintronics, artificial intelligence. Integration of chalcogenide QDs with the perovskite QDs is also very interesting and challenging for improved photovoltaic performance.

5. Conclusion

Recent advances in chalcogenide QDs for practical applications consist of the creation of cadmium-free QDs, non-toxic, like those based on indium phosphide, which improve their environmental and health safety. Improved synthesis processes have allowed for greater control over size and shape, resulting in more consistent and efficient performance. Surface passivation processes have also been developed to improve stability and reduce deterioration. These improvements have increased the utilization of QDs in applications such as display technology, solar cells, and bioimaging, making them more commercially viable. In conclusion, Metal chalcogenide QDs offer a promising platform for various applications due to their distinctive physical and chemical features. The creation of metal chalcogenide QDs has advanced significantly over the years. Various approaches have been developed to achieve detailed control over the size, shape, and composition of these nanomaterials. Further, it is vital to improve the synthesis methods by exploring new precursors, solvents, and reaction conditions. This will allow for better control over QDs size distribution and surface passivation. These QDs have been widely studied for their potential applications in optoelectronic devices, solar cells, photocatalysis, and bioimaging due to their attractive properties that is high energy emission, and excellent photostability, and high quantum yield. The use of QDs in a variety of sectors has produced encouraging outcomes and created new opportunities for research and development. However, challenges including reproducibility, toxicity and stability require to be tackled for practical applications of metal chalcogenide QDs. Efforts are being made to develop eco-friendly synthesis techniques and surface modification ways to improve their biocompatibility and stability. Further investigation is required to explore the capability of metal chalcogenide QDs in emerging fields such as quantum computing and biomedical applications. Overall QDs are a fascinating area of research. Continued study and development in this area will certainly lead to exciting new advances in various technological fields.

Author Contribution Declaration

Pratibha and Aayushi conducted the literature survey together. Pratibha focused on writing the application section, while Aayushi worked on the introduction and synthesis sections. Both collaborated with Avinash to design the images. Avinash prepared the manuscript draft and contributed to the writing of the discussion and conclusion.

Data Availability Declaration

There are no new data were created hence data sharing is not applicable here.

Acknowledgements

The authors acknowledge the administration of SRM University Delhi-NCR, Sonapat for their support and encouragement.

References

1. J. Mal, Y. V. Nancharaiha, E. D. van Hullebusch, P. N. L. Lens. Metal Chalcogenide quantum dots: biotechnological synthesis and applications. *RSC Adv.* **2016**, 6, 41477. <https://doi.org/10.1039/c6ra08447h>
2. L. Manna. The Bright and Enlightening Science of Quantum Dots. *Nano Lett.* **2023**, 23, 9673. <https://doi.org/10.1021/acs.nanolett.3c03904>
3. C. B. Murray, D. J. Norris, M. G. Bawendi. Synthesis and characterization of nearly monodisperse CdE (E = S, Se, Te) semiconductor nanocrystallites. *J. Am. Chem. Soc.* **1993**, 115, 8706. <https://doi.org/10.1021/ja00072a025>
4. M. Gusain, R. Nagpal, Y. Zhan. Analysis and characterization of quantum dots. *Graphene, Nanotubes and Quantum Dots-Based Nanotechnology*, **2022** ch 29, pp 709-726. <https://doi.org/10.1016/B978-0-323-85457-3.00027-X>
5. K. T. Yong; W. C. Law, I. Roy, Z. Jing, H. Huang, M. T. Swihart, P. N. Prasad. Aqueous phase synthesis of CdTe quantum dots for biophotonics. *J. Biophotonics* **2011**, 4, 9. <https://doi.org/10.1002/jbio.201000080>
6. R. K. Kesrevari, A. K. Sharma. Nanoarchitected Biomaterials: Present Status and Future Prospects in Drug Delivery. *Nanoarchitectonics for Smart Delivery and Drug Targeting* **2016**, ch 2, pp 35-66. <https://doi.org/10.1016/B978-0-323-47347-7.00002-1>
7. N. Thejo Kalyani, S. J. Dhoble. Introduction to nano materials. Editor(s): N. Thejo Kalyani, Sanjay J. Dhoble, Marta Michalska-Domańska, B. Vengadaesvaran, H. Nagabhushana, Abdul Kariem Arof, *In Woodhead Publishing Series in Electronic and Optical Materials, Quantum Dots*, Woodhead Publishing **2023**, pp 3-40. DOI: <https://doi.org/10.1016/B978-0-323-85278-4.00010-6>
8. A. Singh, A. Guleria, S. Neogy, M. C. Rath. UV induced synthesis of starch capped CdSe quantum dots: Functionalization with thiourea and application in sensing heavy metals ions in aqueous solution. *Arab. J. Chem.* **2020**, 13, 3149. <https://doi.org/10.1016/j.arabj.2018.09.006>
9. T. Arfin, V. K. Alam, P. G. Moradeeya. Metal oxide photonic crystals and their application (designing, properties, and applications), (Ed.), S. Sagadevan, J. Podder, F. Mohammad, *In Metal Oxides, Metal Oxides for Optoelectronics and Optics-Based Medical Applications*, Elsevier, **2022**, pp. 191-204, <https://doi.org/10.1016/B978-0-323-85824-3.00010-5>
10. M. Bouroushian. Chalcogens and Metal Chalcogenides. *Electrochemistry of Metal Chalcogenides*, **2010**, ch 1, pp-1-56. <https://doi.org/10.1007/978-3-642-03967-6>
11. O. I. Micic, A. J. Nozik. Synthesis and characterization of binary and ternary III-V quantum dots. *J. Lumi.* **1996**, 70, 95. [https://doi.org/10.1016/0022-2313\(96\)00047-6](https://doi.org/10.1016/0022-2313(96)00047-6)
12. N. Chand, S. C. Thakur, P. B. Katyal, V. Barman, P. Sharma. Recent developments on the synthesis, structural and optical properties of chalcogenide quantum dots. *Sol. Energ. Mat. Sol. C.* **2017**, 168, 183. <http://dx.doi.org/10.1016/j.solmat.2017.04.033>
13. L. Jing, S. V. Kershaw, Y. Li, X. Huang, Y. Li, Andrey L. Rogach, M. Gao. Aqueous Based Semiconductor Nanocrystals. *Chem. Rev.* **2016**, 116, 10623. <https://doi.org/10.1021/acs.chemrev.6b00041>
14. A. Kiczor, P. Mergo. Synthesis of CdSe Quantum Dots in Two Solvents of Different Boiling Points for Polymer Optical Fiber Technology. *Materials* **2024**, 17, 227. <https://doi.org/10.3390/ma17010227>
15. T. Arfin. Emerging trends in lab-on-a-chip for biosensing applications, In: C. M. Hussain, S. K. Shukla, G.M. Joshi (Eds.), *Functionalized nanomaterials based devices for environmental applications: a volume in micro and nano technologies*, Elsevier, Netherlands, **2021**, pp. 199-218. <https://doi.org/10.1016/B978-0-12-822245-4.00008-8>
16. H. Huang, W. Feng, Y. Chen, J. Shi. Inorganic nanoparticles in clinical trials and translations. *Nanotoday* **2020**, 35, 1. <https://doi.org/10.1016/j.nantod.2020.100972>
17. O. A. Aladesuyi, O. S. Oluwafemi. Synthesis strategies and application of ternary quantum dots - in cancer therapy. *Nano-Struct. Nano-Obj.* **2020**, 24, 100568. <https://doi.org/10.1016/j.nanoso.2020.100568>
18. F. Mohammad, T. Arfin, H. A. Al-Lohedan. Development of graphene-based nanocomposites as potential materials for supercapacitors and electrochemicals cells, In: M. Jawaid, A. Ahmad, D. Lokhat (Eds.), *Graphene-based nanotechnologies for energy and environmental applications: Micro and nano technologies*, 1st Edition, Elsevier, Netherland, **2019**, 145-154. <https://doi.org/10.1016/B978-0-12-815811-1.00008-9>
19. D. Bera, L. Qian, T. K. Tseng, P. H. Holloway. Quantum Dots and Their Multimodal Applications: A Review. *Materials (Basel)* **2010**, 3, 2260. <https://doi.org/10.3390/ma3042260>
20. K. Surana, P. Singh, H. Rhee, B. Bhattacharya. Synthesis, characterization and application of CdSe quantum dots. *J. Ind. Eng. Chem.* **2014**, 20, 4188. <https://doi.org/10.1016/j.jiec.2014.01.019>
21. A. Singh, A. Kunwar, M. C. Rath. L-Cysteine Capped CdSe Quantum Dots Synthesized by Photochemical Route. *J. Nanosci. Nanotechnol.* **2017**, 17, 1. DOI: <http://dx.doi.org/10.1166/jnn.2018.14687>
22. M. Saad, S. Nadi, F. Ibraheem, Y. A. Badr, I. A. Mahdy, Z. M. A. El-Fattah, A. Sayed. Bright photoluminescence from CdSe quantum dots conjugated with metal phthalocyanines. *Optical Mater.* **2024**, 147, 114736. <https://doi.org/10.1016/j.optmat.2023.114736>
23. J. Drbohlavova, V. Adam, R. Kizek, J. Hubalek. Quantum Dots-Characterization, Preparation and Usage in Biological Systems. *Int. J. Mol. Sci.* **2009**, 10, 656. <https://doi.org/10.3390/ijms10020656>
24. K. Agarwal, H. Rai, S. Mondal. Quantum dots: an overview of synthesis, properties, and applications. *Mater. Res. Express* **2013**, 10, 062001. <https://doi.org/10.1088/2053-1591/acda17>
25. T. Arfin, P. Ranjan, S. Bansod, R. Singh, S. Ahmead, K. Neeti. Organic electrodes: An Introduction, In: R.K. Gupta (Ed.), *Organic electrodes: Fundamental to advanced emerging applications*, Springer, Switzerland, **2022**, pp. 1-26. https://doi.org/10.1007/978-3-030-98021-4_1
26. B. Gao, C. Shen, S. Yuan, Y. Yang, G. Chen. Synthesis of Highly Emissive CdSe Quantum Dots by Aqueous Precipitation Method. *J. Nanomater.* **2013**, 19, 1. <http://dx.doi.org/10.1155/2013/138526>
27. R. Lia, L. Tang, Q. Zhao, K. S. Teng, S. P. Laue. Facile synthesis of ZnS quantum dots at room temperature for ultra-violet Photodetector applications. *J. Chem. Let.* **2017**, 742, 137127. <https://doi.org/10.1016/j.cplett.2020.137127>
28. S. Bansod, T. Arfin, R. Singh, S. Ahmad, K. Neeti. Chemically modified carbon nanotubes for lab on chip devices, In: J. Aslam, CM. Hussain, R. Aslam (Eds.), *Chemically modified carbon nanotubes for commercial applications*, Wiley-VCH GmbH, Germany, **2023**, pp. 271-298. <https://doi.org/10.1002/9783527838790.ch12>
29. A. Valizadeh, H. Mikaeili, M. Samiei, S. Farkhani, N. Zarghami, M. kouhi, A. Akbarzadeh, S. Davaran. Quantum dots: synthesis, bioapplications, and toxicity. *Nanoscale Res. Lett.* **2012**, 7, 480. <https://doi.org/10.1186/1556-276X-7-480>
30. K. J. Nordell, E. M. Boatman G. C. Lisensky. A Safer, Easier, Faster Synthesis for CdSe Quantum Dot Nanocrystals. *J. Chem. Educ.* **2005**, 82, 1697. <https://doi.org/10.1021/ed082p1697>
31. A. Aboulaich, D. Billaud, M. Abyan, L. Balan, J. J Gaumet, Ghouti Medjadhi, J. Ghanbaja, R. Schneider. One-Pot Noninjection Route to CdS Quantum Dots via

- Hydrothermal Synthesis. *ACS Appl. Mater. Interfaces* **2012**, *4*, 2561. <https://doi.org/10.1021/am300232z>
32. A. K. Bansal, F. Antolini, S. Zhang, L. Stroea, L. Ortolani, M. Lanzi, E. Serra, S. Allard, U. Scherf, I. D. W. Samuel. Highly Luminescent Colloidal CdS Quantum Dots with Efficient Near-Infrared Electroluminescence in Light-Emitting Diodes. *J. Phys. Chem. C* **2016**, *120*, 1871. <https://doi.org/10.1021/acs.jpcc.5b09109>
 33. K. E. Andersen, C. Y. Fong, W. E. Pickett. Quantum confinement in CdSe nanocrystallites. *J. Non-Cryst. Solids* **2002**, *299*, 1105. [https://doi.org/10.1016/S0022-3093\(01\)01132-2](https://doi.org/10.1016/S0022-3093(01)01132-2)
 34. L. Meng, Q. Chen, X. Li, H. Zhang, Y. Hai, Y. Yang, X. Wang, M. Luo. Enhanced Photocatalytic Nitrogen Reduction via Bismuth Nanoparticle-Decorating ZnCdS Solid Solution. *Inorg. Chem.* **2024**, *63*, 5065. <https://doi.org/10.1021/acs.inorgchem.3c04566>
 35. W. A. A. Mohamed, H. A. E.-Gawad, S. Mekkey, H. Galal, H. Handal, H. Mousa, A. Labib. Quantum dots synthesis and future prospect applications. *Nanotechnol. Rev.* **2021**, *10*, 1926. <https://doi.org/10.1515/ntrev-2021-0118>
 36. H. T. Tung, D. V. Thuan, J. H. Kiat, D. H. Phuc. Ag⁺ ion doped on the CdSe quantum dots for quantum dot sensitized solar cells' application. *Appl. Phys. A* **2019**, *125*, 505. <https://doi.org/10.1007/s00339-019-2797-0>
 37. S. T. Harry, M. A. Adekanmbi. Confinement energy of Quantum dots and the Brus equation, *Int. J. Res.* **2020**, *8*, 318. <https://doi.org/10.29121/granthaalayah.v8.i11.2020.2451>
 38. R. Köhler, W. Neumann, M. Schmidbauer, M. Hanke, D. Grigoriev, P. Schäfer, H. Kirmse, I. Häusler, R. Schneider. Structural Characterisation of Quantum Dots by X-Ray Diffraction and TEM, *Semicond. Nanostructures* **2008**, p. 97. https://doi.org/10.1007/978-3-540-77899-8_5
 39. H. Li, H. J. Xiao, T. S. Zhu, H. C. Xuan, M. Li. Size Consideration on Shape Factor and Its Determination Role on the Thermodynamic Stability of Quantum Dots. *J. Phys. Chem. C* **2015**, *119*, 12002. <https://doi.org/10.1021/acs.jpcc.5b02230>
 40. W. H. Qi, M. P. Wang, M. Zhou, X. Q. Shen, X. F. Zhang. Modeling cohesive energy and melting temperature of nanocrystals. *J. Phys. Chem. Solids*, **2006**, *67*, 851. <http://dx.doi.org/10.1016/j.jpcs.2005.12.003>
 41. Y. Li, Y. Ding, Y. Zhang, Y. Qian. Photophysical properties of ZnS quantum dots. *J. Phys. Chem. Solids* **1999**, *60*, 13. [https://doi.org/10.1016/S0022-3697\(98\)00247-9](https://doi.org/10.1016/S0022-3697(98)00247-9)
 42. M. A. Hegazy, A. M. Hameed. Characterization of CdSe-nanocrystals used in semiconductors for aerospace applications: Production and optical properties. *NRIAG J. Astron. Geophys* **2014**, *3*, 82. <https://doi.org/10.1016/j.nrjag.2014.05.002>
 43. F. S. Riehle, K. Yu. Role of Alcohol in the Synthesis of CdS Quantum Dots. *Chem. Mater.* **2020**, *32*, 1780. <https://doi.org/10.1021/acs.chemmater.9b04009>
 44. S. Bandaru, M. Palanivel, M. Ravipati, W. Y. Wu, S. Zahid, S. S. Halkarni, G. K. Dalapati, K. K. Ghosh, B. Gulyás, P. Padmanabhan, S. Chakraborty. Highly Monodisperse, Size Tunable Glucosamine Conjugated CdSe Quantum Dots for Enhanced Cellular Uptake and Bioimaging. *ACS Omega* **2024**, *9*, 7452. <https://doi.org/10.1021/acsomega.3c04962>
 45. W. K. Bae, K. Char, H. Hur, S. Lee. Single-Step Synthesis of Quantum Dots with Chemical Composition Gradients. *Chem. Mater.* **2008**, *20*, 531. <https://doi.org/10.1021/cm070754d>
 46. A. R. C. Osypiw, S. Lee, S. M. Jung, S. Leoni, P. M. Smowton, B. Hou, J. M. Kim, G. A. J. Amarutunga. Solution-processed colloidal quantum dots for light emission, *Mater. Adv.* **2022**, *3*, 6773. <https://doi.org/10.1039/D2MA00375A>
 47. B. A. A. Jahdaly, M. F. Elsadek, B.M. Ahmed, M.F. Farahat, M.M. Taher, A.M. Khalil. Outstanding Graphene Quantum Dots from Carbon Source for Biomedical and Corrosion Inhibition Applications: A Review. *Sustainability* **2021**, *13*, 2127. <https://doi.org/10.3390/su13042127>
 48. S. Das, K. Sa, P. C Mahakul, J. Raiguru, I. Alam, B. V. R. S. Subramanyam, P. Mahanandia. Synthesis of quaternary chalcogenide CZTS nanoparticles by a hydrothermal route. *IOP Conf. Ser.: Mater. Sci. Eng.* **2018**, *338*, 012062. <https://doi.org/10.1088/1757-899X/338/1/012062>
 49. G. B. Passos, D. V. Freitas, J. M. M. Dias, E. T. Neto, M. Navarro. One-pot electrochemical synthesis of CdTe quantum dots in cavity cell. *Electrochimica Acta* **2016**, *190*, 689. <https://doi.org/10.1016/j.electacta.2016.01.016>
 50. I. A. Mir, K. Das, K. Rawat, H. B. Bohidar. Hot Injection versus Room Temperature Synthesis of CdSe Quantum Dots: A Differential Spectroscopic and Bioanalyte Sensing Efficacy Evaluation. *Colloids Surf. A: Physicochem. Eng. Aspects.* **2016**, *494*, 162. <https://doi.org/10.1016/j.colsurfa.2016.01.002>
 51. D. Mohanta, S. S. Narayanan, S. K. Pal, A. K. Raychaudhuri. Time-resolved photoluminescence decay characteristics of bovine serum albumin-conjugated semiconductor nanocrystallites. *J. Exp. Nanosci.* **2009**, *4*, 177. <https://doi.org/10.1080/17458080902866204>
 52. A. Yakoubi, T. B. Chaabane, A. Aboulaich, R. Mahiou, L. Balan, G. Medjahdi, R. Schneider. Aqueous synthesis of Cu-doped CdZnS quantum dots with controlled and efficient photoluminescence. *J. Lumin.* **2016**, *175*, 193. <https://doi.org/10.1016/j.jlumin.2016.02.035>
 53. H. Zhan, P. Zhou, K. Pan, T. He, X. He, C. Zhou, Y. He. One-pot aqueous-phase synthesis of ultra-small CdSe/CdS/ CdZnS core-shell-shell quantum dots with high-luminescent efficiency and good stability. *J. Nanopart. Res.* **2013**, *15*, 1680. <https://doi.org/10.1007/s11051-013-1680-8>
 54. K. Vidhya, M. Saravanan, G. Bhoopathi, V. P. Devarajan, S. Subanya. Structural and optical characterization of pure and starch-capped ZnO quantum dots and their photocatalytic activity. *Appl. Nanosci.* **2015**, *5*, 235. <https://doi.org/10.1007/s13204-014-0312-7>
 55. J. M. Baruah, S. Kalita, J. Narayan. Green chemistry synthesis of biocompatible ZnS quantum dots (QDs): their application as potential thin films and antibacterial agent. *Int. Nano Lett.* **2019**, *9*, 149. <https://doi.org/10.1007/s40089-019-0270-x>
 56. Q. Zhang, Li, Y. Ma, T. Zhai. ZnSe nanostructures: Synthesis, properties and applications. *Prog. Mater. Sci.*, **2016**, *83*, 472. <http://doi.org/10.1016/j.pmatsci.2016.07.005>
 57. S. Jagtapa, P. Chopadea, S. Tadepalli, A. Bhalerao, S. Gosavi. A review on the progress of ZnSe as inorganic scintillator. *Opto-Electronics Rev.* **2019**, *27*, 90. <https://doi.org/10.1016/j.opelre.2019.01.001>
 58. U. B. Memon, U. Chatterjee, M. N. Gandhi, S. Tiwari, S. P. Duttgupta. Synthesis of ZnSe Quantum Dots with Stoichiometric Ratio Difference and Study of its Optoelectronic Property. *Procedia Mater. Sci.* **2014**, *4*, 1027. <https://doi.org/10.1016/j.mspro.2014.07.393>
 59. P. A. Radi, A. G. Brito-Madurro, J. M. Madurro, N. O. Dantas. Characterization and properties of CdO nanocrystals incorporated in polyacrylamide. *Braz. J. Phys.* **2006**, *36*, 412. <https://doi.org/10.1590/S0103-97332006000300048>
 60. H. Li, H. J. Xiao, T. S. Zhu, H. C. Xuan, M. Li. Size Consideration on Shape Factor and Its Determination Role on the Thermodynamic Stability of Quantum Dots. *J. Phys. Chem. C* **2015**, *119*, 12002. <https://doi.org/10.1021/acs.jpcc.5b02230>
 61. M. Masab, H. Muhammad, F. Shah, M. Yasira, M. Hanif. Facile synthesis of CdZnS QDs: Effects of different capping agents on the photoluminescence properties.

- Mater. Sci. Semicond. Process.* **2018**, *81*, 113. <https://doi.org/10.1016/j.mssp.2018.03.023>
62. M. A. Husseina, K. A. Mohammedb, R. A. Talib. Energy band gaps and optical absorption properties of the CdZnS and CdZnS:PEO thin films prepared by chemical bath deposition. *Chalcogenide Lett.* **2022**, *19*, 239. <https://doi.org/10.15251/CL.2022.195.329>
 63. Q. Zhang, C. Nie, C. Chang, C. Guo, X. Jin, Y. Qin, F. Li, Q. Li. Highly luminescent red emitting CdZnSe/ZnSe quantum dots synthesis and application for quantum dot light emitting diodes, *Opt. Mater. Express.* **2017**, *7*, 3875. <https://doi.org/10.1364/OME.7.003875>
 64. W. Yue, S. Han, R. Peng, W. Shen, H. Geng, F. Wu, S. Tao, M. Wang. CuInS₂ quantum dots synthesized by a solvothermal route and their application as effective electron acceptors for hybrid solar cells. *J. Mater. Chem.* **2010**, *20*, 7570. <https://doi.org/10.1039/C0JM00611D>
 65. T. Arfin, S. Athar. Graphene for advanced organic photovoltaics, In: S. Kanchi, S. Ahmed, M.I. Sabela, C.M. Hussain (Eds.), *Nanomaterials: biomedical, environmental, and engineering applications*, Scrivener Publishing LLC, Beverly, **2018**, pp. 93-103. <https://doi.org/10.1002/9781119370383.ch3>
 66. G. Chen, J. Seo, C. Yang, P. N. Prasad. Nanochemistry and nanomaterials for photovoltaics. *Chem. Soc. Rev.* **2013**, *42*, 8304. <https://doi.org/10.1039/C3CS60054H>
 67. J. H. Rhee, C. C. Chung, E. W. G. Diau. A perspective of mesoscopic solar cells based on metal chalcogenide quantum dots and organometal-halide perovskites. *NPG Asia Mater.* **2013**, *5*, 68. <https://doi.org/10.1038/am.2013.53>
 68. S. C. Zhu, F. -X. Xiao. Transition metal chalcogenides quantum dots: emerging building blocks toward solar-to-hydrogen conversion. *ACS Catal.* **2023**, *13*, 7269. <https://doi.org/10.1021/acscatal.2c05401>
 69. A. Qurashi. *Metal Chalcogenide Nanostructures for Renewable Energy Applications*, Wiley, **2014**, 233-246. <https://doi.org/10.1002/9781119008934.ch10>
 70. S. Singh, Z. H. Khan, P. Kumar, M. B. Khan, P. Kumar. Quantum dots-sensitized solar cells: a review on strategic developments. *Bull. Mater. Sci.* **2022**, *45*, 81. <https://doi.org/10.1007/s12034-022-02662-z>
 71. J. Zhu, K. Lu, J. Li, Z. Liu, W. Ma. Tandem solar cells based on quantum dots. *Mater. Chem. Front.* **2024**, *8*, 1792. <https://doi.org/10.1039/D3QM01087B>
 72. S. R. Padmaperuma, M. Liu, R. Nakamura, Y. Tachibana. Photoinduced charge carrier dynamics of metal chalcogenide semiconductor quantum dot sensitized TiO₂ film for photovoltaic application. *J. Photopolym. Sci. Technol.* **2021**, *34*, 271. <https://doi.org/10.2494/PHOTOPOLYMER.34.271>
 73. M. A. Mumin, K. F. Akhter, O. O. Oyene, W. Z. Xu, P. A. Charpentier. Supercritical Fluid Assisted Dispersion of NanoSilica encapsulated CdS/ZnS quantum dots in poly(ethylene-co-vinyl Acetate) for solar harvesting films. *ACS Appl. Nano Mater.* **2018**, *1*, 3186. <https://doi.org/10.1021/acsanm.8b00390>
 74. P. Cui, P. K. Tamukong, S. Kilina. Effect of Binding Geometry on Charge Transfer in CdSe Nanocrystals Functionalized by N719 Dyes to Tune Energy Conversion Efficiency. *ACS Appl. Nano Mater.* **2018**, *1*, 3174. <https://doi.org/10.1021/acsanm.8b00350>
 75. M. A. Hossain, J. R. Jennings, C. Shen, J. H. Pan, Z. Y. Koh, N. Mathews, Q. Wang. CdSe sensitized mesoscopic TiO₂ solar cells exhibiting >5% efficiency: redundancy of CdS buffer layer. *J. Mater. Chem.* **2012**, *22*, 16235. <https://doi.org/10.1039/C2JM33211F>
 76. N. Guijarro, E. Guillén, T. Lana-Villarreal, R. Gómez. Quantum dot-sensitized solar cells based on directly adsorbed zinc copper indium sulfide colloids. *Phys. Chem. Chem. Phys.* **2014**, *16*, 9115. <https://doi.org/10.1039/C4CP00294F>
 77. K. Zhao, Z. Pan, I. Mora-Sero, E. Canovas, H. Wang, Y. Song, X. Gong, J. Wang, M. Bonn, J. Bisquert, X. Zhong. Boosting power conversion efficiencies of quantum-dot-sensitized solar cells beyond 8% by recombination control. *J. Am. Chem. Soc.* **2015**, *137*, 5602. <https://doi.org/10.1021/jacs.5b01946>
 78. J. Yang and X. Zhong. CdTe based quantum dot sensitized solar cells with efficiency exceeding 7% fabricated from quantum dots prepared in aqueous media. *J. Mater. Chem. A* **2016**, *4*, 16553. <https://doi.org/10.1039/C6TA07399A>
 79. A. Arivarasan, S. Bharathi, V. Vijayaraj, G. Sasikala, R. Jayavel. Evaluation of reaction parameters dependent optical properties and its photovoltaics performance of CdTe QDs. *J. Inorg. Organomet. Polym. Mater.* **2018**, *28*, 1263. <https://doi.org/10.1007/s10904-018-0803-1>
 80. G. Shen, Z. Du, Z. Pan, J. Du, X. Zhong. Solar paint from TiO₂ particles supported quantum dots for photoanodes in quantum dot-sensitized solar cells. *ACS Omega* **2018**, *3*, 1102. <https://doi.org/10.1021/acsomega.7b01761>
 81. H. Zhang, W. Fang, W. Wang, N. Qian, X. Ji. Highly efficient Zn-Cu-In-Se quantum dot-sensitized solar cells through surface capping with ascorbic acid. *ACS Appl. Mater. Interfaces* **2019**, *11*, 6927. <https://doi.org/10.1021/acsami.8b18033>
 82. B. Fu, C. Deng, L. Yang. Efficiency enhancement of solid-state CuInS₂ quantum dot-sensitized solar cells by improving the charge recombination. *Nanoscale Res. Lett.* **2019**, *14*, 198. <https://doi.org/10.1186/s11671-019-2998-7>
 83. P. Xu, X. Chang, R. Liu, L. Wang, X. Li, X. Zhang, X. Yang, D. Wang, W. Lu. Boosting power conversion efficiency of quantum dot-sensitized solar cells by integrating concentrating photovoltaic concept with double photoanodes. *Nanoscale Res. Lett.* **2020**, *15*, 188. <https://doi.org/10.1186/s11671-020-03424-8>
 84. Y. Lin, H. Song, J. Zhang, H. Rao, Z. Pan, X. Zhong. Hole transport materials mediating hole transfer for high efficiency quantum dot sensitized solar cells. *J. Mater. Chem. A* **2021**, *9*, 997. <https://doi.org/10.1039/D0TA10702F>
 85. H. Song, Y. Lin, M. Zhou, H. Rao, Z. Pan, X. Zhong. Zn-Cu-In-S-Se quinary "green" alloyed quantum-dot-sensitized solar cells with a certified efficiency of 14.4%. *Angew. Chem. Int. Ed.* **2020**, *60*, 6137. <https://doi.org/10.1002/anie.202014723>
 86. E. Elibol. Quantum dot sensitized solar cell design with surface passivated CdSeTe QDs. *Sol. Energy* **2020**, *206*, 741. <https://doi.org/10.1016/j.solener.2020.06.002>
 87. G. Konstantatos, E. H. Sargent. Nanostructured materials for photon detection. *Nat. Nanotechnol.* **2010**, *5*, 391. <https://doi.org/10.1038/nnano.2010.78>
 88. H. Tang, J. Zhong, W. Chen, K. Shi, G. Mei, Y. Zhang, Z. Wen, P. Müller-Buschbaum, D. Wu, K. Wang, X. W. Sun. Lead Sulfide Quantum Dot Photodetector with Enhanced Responsivity through a Two-Step Ligand-Exchange Method. *ACS Appl. Nano Mater.* **2019**, *2*, 6135. <https://doi.org/10.1021/acsanm.9b00889>
 89. B. Cook, M. Gong, D. Ewing, M. Casper, A. Stramel, A. Elliot, J. Wu. Inkjet Printing Multicolor Pixelated QDs on Graphene for Broadband Photodetection. *ACS Appl. Nano Mater.* **2019**, *2*, 3246. <https://doi.org/10.1021/acsanm.9b00539>
 90. N. Mahmoud, W. Walravens, J. Kuhs, C. Detavernier, Z. Hens, G. Roelkens. Micro-Transfer-Printing of Al₂O₃-Capped Short Wave-Infrared PbS Quantum Dot Photoconductors. *ACS Appl. Nano Mater.* **2019**, *2*, 299. <https://doi.org/10.1021/acsanm.8b01915>
 91. B. Hafiz, M. R. Scimeca, P. Zhao, I. J. Paredes, A. Sahu, D. K. Ko. Silver Selenide Colloidal QDs for Mid Wavelength Infrared Photodetection. *ACS Appl. Nano Mater.* **2019**, *2*, 1631. <https://doi.org/10.1021/acsanm.9b00069>


92. A. Paliwal, S. V. Singh, A. Sharma, A. Sugathan, S. W. Liu, S. Biring, B. N. Pal. Microwave-Polyol Synthesis of Sub-10-nm PbS Nanocrystals for Metal Oxide/Nanocrystal Heterojunction Photodetectors. *ACS Appl. Nano Mater.* **2018**, *1*, 6063. <https://doi.org/10.1021/acsanm.8b01194>
93. E. Lhuillier, P. Guyot-Sionnest. Recent Progresses in Mid Infrared Nanocrystal Optoelectronics. *IEEE J. Sel. Top. Quantum Electron.* **2017**, *23*, 6000208. <https://doi.org/10.1109/JSTQE.2017.2690838>
94. X. Lyu. Recent Progress on Infrared Detectors: Materials and Applications. *HSET* **2022**, *27*, 191. <https://doi.org/10.54097/hset.v27i.3747>
95. J. Chen, J. Chen, X. Li, J. He, L. Yang, J. Wang, F. Yu, Z. Zhao, C. Shen, H. Guo, L. Guanhai, X. Chen, W. Lu. High-performance HgCdTe avalanche photodetector enabled with suppression of band-to-band tunneling effect in mid-wavelength infrared. *NPJ Quantum Mater.* **2021**, *6*, 2397. <https://doi.org/10.1038/s41535-021-00409-3>
96. L. Ciura, M. Kopytko, P. Martyniuk. Low-frequency noise limitations of InAsSb_x and HgCdTe-based infrared detectors. *Sens. Actuators A Phys.* **2020**, *305*, 111908. <https://doi.org/10.1016/j.sna.2020.111908>
97. K. Batty, I. Steele, C. Copperwheat. Laboratory and On-sky Testing of an InGaAs Detector for Infrared Imaging. *Publ. Astron. Soc. Pac.* **2022**, *134*, 65001. <https://doi.org/10.1088/1538-3873/ac71cc>
98. X. Zhao, H. Ma, H. Cai, Z. Wei, Y. Bi, X. Tang, T. Qin. Lead chalcogenide colloidal QDs for infrared photodetectors. *Materials* **2023**, *16*, 5790. <https://doi.org/10.3390/ma16175790>
99. Q. Hao, H. Ma, X. Xing, X. Tang, Z. Wei, X. Zhao, M. Chen. Mercury Chalcogenide colloidal quantum dots for infrared photodetectors. *Material* **2023**, *16*, 7321. <https://doi.org/10.3390/ma16237321>
100. Y. Tian, H. Luo, M. Chen, C. Li, S. V. Kershaw, R. Zhang, A. L. Rogach. Mercury chalcogenide colloidal QDs for infrared photodetection: from synthesis to device applications. *Nanoscale* **2023**, *15*, 6476. <https://doi.org/10.1039/D2NR07309A>
101. P. Zhao, T. Qin, G. Mu, S. Zhang, Y. Luo, M. Chen, X. Tang. Band-engineered dual-band visible and short infrared photodetector with metal chalcogenide colloidal quantum dots. *J. Mater. Chem. C* **2023**, *11*, 2842. <https://doi.org/10.1039/D3TC00066D>
102. A. Maimulyanti, A. R. Prihadi, B. Mellisani, I. Nurhidayati, F. A. Rachmawati Putri, F. Puspita, R. W. Widarsih. Green Extraction Technique to Separate Tannin from Coffee Husk Waste Using Natural Deep Eutectic Solvent (NADES). *Rasayan J. Chem.* **2023**, *16*, 2239. <http://dx.doi.org/10.31788/RJC.2023.1638334>
103. R. Bushra, T. Arfin, M. Oves, W. Raza, F. Mohammad, M. A. Khan, A. Ahmed, A. Azam, M. Muneer. Development of PANI/MWCNTs decorated with cobalt oxide nanoparticles toward multiple electrochemical, photocatalytic and biomedical application sites. *New J. Chem.* **2016**, *40*, 9448. <https://doi.org/10.1039/C6NJ02054B>
104. Y. -H. Liu, C. -L. Yang, M. -S. Wang, X. -G. Ma, Y. -G. Yi. Ternary chalcogenides XGsS₂ (X = Ag or Cu) for photocatalytic hydrogen generation from water splitting under irradiation of visible light. *Int. J. Quantum Chem.* **2020**, *120*, 26166. <https://doi.org/10.1002/qua.26166>
105. C. Kumari, P. Sharma, S. Chhoker. Photocatalytic activity of quaternary chalcogenide for methylene blue degradation. *AIP Conf. Proc.* **2024**, *2995*, 020066. <https://doi.org/10.1063/5.0177995>
106. J. A. Caputo, L. C. Frenette, N. Zhao, K. L. Sowers, T. D. Krauss, D. J. Weix. General and Efficient C-C Bond Forming Photoredox Catalysis with Semiconductor Quantum Dots. *J. Am. Chem. Soc.* **2017**, *139*, 4250. <https://doi.org/10.1021/jacs.6b13379>
107. Z. Zhang, K. Edme, S. Lian, E. A. Weiss. Enhancing the Rate of Quantum-Dot-Photocatalyzed Carbon-Carbon Coupling by Tuning the Composition of the Dot's Ligand Shell. *J. Am. Chem. Soc.* **2017**, *139*, 4246. <https://doi.org/10.1021/jacs.6b13220>
108. Y. Zhou, S. Yang, D. Fan, J. Reilly, H. Zhang, W. Yao, J. Huang. Carbon Quantum Dot/TiO₂ Nanohybrids: Efficient Photocatalysts for Hydrogen Generation via Intimate Contact and Efficient Charge Separation. *ACS Appl. Nano Mater.* **2019**, *2*, 1027. <https://doi.org/10.1021/acsanm.8b02310>
109. A. Samanta, J. C. Breger, K. Susumu, E. Oh, S. A. Walper, N. Bassim, I. L. Medintz. DNA-Nanoparticle Composites Synergistically Enhance Organophosphate Hydrolase Enzymatic Activity. *ACS Appl. Nano Mater.* **2018**, *1*, 3091. <https://pubs.acs.org/doi/abs/10.1021/acsanm.8b00933>
110. E. G. Durmusoglu, Y. Turker, H. Y. Acar. Luminescent PbS and PbS/CdS QDs with Hybrid Coatings as Nanotags for Authentication of Petroleum Products. *ACS Appl. Nano Mater.* **2019**, *2*, 7737. <https://doi.org/10.1021/acsanm.9b01780>
111. F. M. de Melo, D. Grasseschi, B. B. N. S. Brandao, Y. Fu, H. E. Toma. Superparamagnetic Maghemite-Based CdTe quantum dots as Efficient Hybrid Nanoprobes for Water-Bath Magnetic Particle Inspection. *ACS Appl. Nano Mater.* **2018**, *1*, 2858. <https://doi.org/10.1021/acsanm.8b00502>
112. L. Meng, Q. Chen, X. Li, H. Zhang, Y. Hai, Y. Hai, Y. Yang, X. Wang, and M. Luo. Enhanced photocatalytic nitrogen reduction via bismuth nanoparticle-decorating ZnCdS solid solution. *Inorg. Chem.* **2024**, *63*, 5065. <https://doi.org/10.1021/acs.inorgchem.3c04566>
113. L. Sun, J. J. Choi, D. Stachnik, A. C. Bartnik, B. R. Hyun, G. G. Malliaras, T. Hanrath, F. W. Wise. Bright infrared quantum-dot light-emitting diodes through inter-dot spacing control. *Nature Nanotech.* **2012**, *7*, 369. <https://doi.org/10.1038/nnano.2012.63>
114. X. Yang, F. Ren, Y. Wang, T. Ding, H. Sun, D. Ma, X. W. Sun. Iodide capped PbS/CdS core-shell QDs for efficient long-wavelength near-infrared light-emitting diodes. *Sci. Rep.* **2017**, *7*, 14741. <https://doi.org/10.1038/s41598-017-15244-5>
115. X. Gong, Z. Yang, G. Walters, R. Comin, Z. Ning, E. Beauregard, V. Adinolfi, O. Voznyy, E. H. Sargent. Highly efficient quantum dot near-infrared light-emitting diodes. *Nat. Photonics* **2016**, *10*, 253. <https://doi.org/10.1038/nphoton.2016.11>
116. S. Pradhan, F. D. Stasio, Y. Bi, S. Gupta, S. Christodoulou, A. Stavrinadis, G. Konstantatos. High-efficiency colloidal quantum dot infrared light-emitting diodes via engineering at the supra-nanocrystalline level. *Nat. Nanotech.* **2019**, *14*, 72. <https://doi.org/10.1038/s41565-018-0312-y>
117. G. J. Supran, K. W. Song, G. W. Hwang, R. E. Correa, J. Scherer, E. A. Dauler, Y. Shirasaki, M. G. Bawendi, V. Bulović. High-performance shortwave-infrared light-emitting devices using core-shell (PbS-CdS) colloidal quantum dots. *Adv. Mater.* **2015**, *27*, 1437. <https://doi.org/10.1002/adma.201404636>
118. X. Dai, Z. Zhang, Y. Jin, Y. Niu, H. Cao, X. Liang, L. Chen, J. Wang, X. Peng. Solution-processed, high-performance light-emitting diodes based on quantum dots. *Nature* **2014**, *515*, 96. <https://doi.org/10.1038/nature13829>
119. H. -M. Kim, D. Geng, J. Kim, E. Hwang, J. Jang. Metal-Oxide stacked electron transport layer for highly efficient inverted quantum-dot light emitting diodes. *ACS Appl. Mater.* **2016**, *8*, 28727. <https://doi.org/10.1021/acsami.6b10314>
120. B. Mahler, N. Lequeux, B. Dubertret. Ligand-controlled polytypism of thick-shell CdSe/CdS nanocrystals. *J. Am. Chem. Soc.* **2010**, *132*, 953. <https://doi.org/10.1021/ja9034973>
121. B. Chon, S. J. Lim, W. Kim, J. Seo, H. Kang, T. Joo, J. Hwang, S. K. Shin. Shell and ligand-dependent blinking of

- CdSe-based core/shell nanocrystals. *Phys. Chem. Chem. Phys.* **2010**, *12*, 9312. <https://doi.org/10.1039/B924917F>
122. B. N. Pal, Y. Ghosh, S. Brovelli, R. Laocharoensuk, V. I. Klimov, J. A. Hollingsworth, H. Htoon., Giant CdSe/CdS core/shell nanocrystal QDs as efficient electroluminescent materials: strong influence of shell thickness on light-emitting diode performance. *Nano Lett.* **2012**, *12*, 331. <https://doi.org/10.1021/nl203620f>
 123. O. Chen, J. Zhao, V. P. Chauhan, J. Cui, C. Wong, D. K. Harris, H. Wei, H. S. Han, D. Fukumura, R. K. Jain and M. G. Bawendi. Compact high-quality CdSe/CdS core/shell nanocrystals with narrow emission linewidths and suppressed blinking. *Nat. Mater.* **2013**, *12*, 445. <https://doi.org/10.1038/nmat3539>
 124. C. Pu, X. Dai, Y. Shu, M. Zhu, Y. Deng, Y. Jin, X. Peng. Electrochemically-stable ligands bridge the photoluminescence-electroluminescence gap of quantum dots. *Nat. Commun.* **2020**, *11*, 937. <https://doi.org/10.1038/s41467-020-14756-5>
 125. S. Kim, J.-A. Kim, T. Kim, H. Chung, S. Park, S.-M. Choi, H.-M. Kim, D.-Y. Chung, E. Jang. Efficient blue-light-emitting Cd-free colloidal quantum well and its application in electroluminescent devices. *Chem. Mater.* **2020**, *32*, 5200. <https://doi.org/10.1021/acs.chemmater.0c01275>
 126. J. Jiang, S. Zhang, Q. Shan, L. Yang, J. Ren, Y. Wang, S. Jeon, H. Xiang, H. Zeng. High-color-rendition white QLEDs by balancing red, green, and blue centres in eco-friendly ZnCuGaS:In@ZnS quantum dots. *Adv. Mater.* **2024**, *36*, e2304772. <https://doi.org/10.1002/adma.202304772>
 127. S. Zhou, Y. Ma, X. Zhang, W. Lan, X. Yu, B. Xie, K. Wang, X. Luo. White-Light-Emitting Diodes from Directional Heat-Conducting Hexagonal Boron Nitride Quantum Dots. *ACS Appl. Nano Mater.* **2020**, *3*, 814. <https://doi.org/10.1021/acsanm.9b02321>
 128. J. Choi, W. Choi, D. Y. Jeon. Ligand-Exchange-Ready CuInS₂/ZnS QDs via Surface-Ligand Composition Control for Film-Type Display Devices. *ACS Appl. Nano Mater.* **2019**, *2*, 5504. <https://doi.org/10.1021/acsanm.9b01085>
 129. T. Afrin, S. Fatma. Anticipating behavior of advanced materials in healthcare, In: A. Tiwari, A.N. Nordin (Eds.), *Advanced biomaterials and biodevices*, Scrivener Publishing LLC, Beverly, **2014**, pp. 243-287. <https://doi.org/10.1002/9781118774052.ch7>
 130. W. Su, D. Yang, Y. Kong, W. Zhang, J. Wang, Y. Fei, R. Guo, J. Ma, L. Mi. AgInS₂/ZnS QDs for noninvasive cervical cancer screening with intracellular pH sensing using fluorescence lifetime imaging microscopy. *Nano Res.* **2022**, *15*, 5193. <https://doi.org/10.1007/s12274-022-4104-1>
 131. Z. Piao, D. Yang, Z. Cui, H. He, S. Mei, H. Lu, Z. Fu, L. Wang, W. Zhang, R. Guo. Recent advances in metal chalcogenide quantum dots: from material design to biomedical applications. *Adv. Funct. Mater.* **2022**, *32*, 2207662. <https://doi.org/10.1002/adfm.202207662>
 132. X. Wu, H. Liu, J. Liu, K. N. Haley, J. A. Treadway, J. P. Larson, N. Ge, F. Peale, M. P. Bruchez. Immunofluorescent labeling of cancer marker her2 and other cellular targets with semiconductor quantum dots. *Nat. Biotechnol.* **2003**, *21*, 41. <https://doi.org/10.1038/nbt764>
 133. S. Mallick, P. Kumar, A. L. Koner. Freeze-Resistant Cadmium-Free QDs for Live-Cell Imaging. *ACS Appl. Nano Mater.* **2019**, *2*, 661. <https://doi.org/10.1021/acsanm.8b02231>
 134. A. T. Nguyen, D. R. Baucum, Y. Wang, C. D. Heyes. Compact, fast blinking Cd-free QDs for super-resolution fluorescence imaging. *Chem. Biomed. Imaging* **2023**, *1*, 251. <https://doi.org/10.1021/cbmi.3c00018>
 135. Y. Li, P. Zhang, W. Tang, K. J. Mchugh, S. V. Kershaw, M. Jiao, X. Huang, S. Kalytchuk, C. F. Perkinson, S. Yue, Y. Qiao, L. Jing, M. Gao, B. Han. Bright, magnetic NIR-II quantum dot probe for sensitive dual-modality imaging and intensive combination therapy of cancer. *ACS Nano* **2022**, *16*, 8076. <https://doi.org/10.1021/acsnano.2c01153>
 136. H. Xue, J. Zhao, Q. Zhou, D. Pan, Y. Zhang, Y. Zhang, Y. Shen. Boosting the Sensitivity of a Photoelectrochemical Immunoassay by Using SiO₂@polydopamine Core-Shell Nanoparticles as a Highly Efficient Quencher. *ACS Appl. Nano Mater.* **2019**, *2*, 1579. <https://doi.org/10.1021/acsanm.9b00050>
 137. M. Freitas, M. M. P. S. Neves, H. P. A. Nouws, C. Delerue-Matos. Quantum dots as nanolabels for breast cancer biomarker HER2-ECD analysis in human serum. *Talanta* **2020**, *208*, 120430. <https://doi.org/10.1016/j.talanta.2019.120430>
 138. M. Freitas, H. P. A. Nouws, E. Keating, V. C. Fernandes, C. Delerue-Matos. Immunomagnetic bead-based bioassay for the voltammetric analysis of the breast cancer biomarker HER2-ECD and tumor cells using QDs as detection labels. *Mikrochim. Acta* **2020**, *187*, 184. <https://doi.org/10.1007/s00604-020-4156-4>
 139. S. A. Diaz, G. Lasarte-Aragones, R. G. Lowery, Aniket, J. N. Vranish, W. P. Klein, K. Susumu, I. L. Medintz. Quantum dots as Förster Resonance Energy Transfer Acceptors of Lanthanides in Time-Resolved Bioassays. *ACS Appl. Nano Mater.* **2018**, *1*, 3006. <https://doi.org/10.1021/acsanm.8b00613>
 140. D. N. Williams, S. Pramanik, R. P. Brown, B. Zhi, E. McIntire, N. V. Hudson-Smith, C. L. Haynes, Z. Rosenzweig. Adverse interactions of luminescent semiconductor quantum dots with liposomes and *Shewanella oneidensis*. *ACS Appl. Nano Mater.* **2018**, *1*, 4788. <https://doi.org/10.1021/acsanm.8b01000>
 141. G. Lv, W. Guo, W. Zhang, T. Zhang, S. Li, S. Chen, A. S. Eltahan, D. Wang, Y. Wang, J. Zhang, P. C. Wang, J. Chang, X. -J. Liang. Near-infrared emission CuInS/ZnS quantum dots: all-in-one theranostic nanomedicines with intrinsic fluorescence/photocoustic imaging for tumor phototherapy. *ACS Nano* **2016**, *10*, 9637. <https://doi.org/10.1021/acs.nano.6b05419>
 142. V. K. Singh, H. Mishra, R. Ali, S. Umrao, R. Srivastava, S. Abraham, A. Misra, V. N. Singh, H. Mishra, R. S. Tiwari, A. Srivastava. In situ functionalized fluorescent WS₂-QDs as sensitive and selective probe for Fe³⁺ and a detailed study of its fluorescence quenching. *ACS Appl. Nano Mater.* **2019**, *2*, 566. <https://doi.org/10.1021/acsanm.8b02162>
 143. S. R. Ahmed, J. Cirone, A. Chen. Fluorescent Fe₃O₄ quantum dots for H₂O₂ detection. *ACS Appl. Nano Mater.* **2019**, *2*, 2076. <https://doi.org/10.1021/acsanm.9b00071>
 144. C. Wei, X. Wei, Z. Hu, D. Yang, S. Mei, G. Zhang, D. Su, W. Zhang, R. Guo. A fluorescent probe for Cd²⁺ detection based on the aggregation-induced emission enhancement of aqueous Zn-Ag-In-S quantum dots. *Anal. Methods* **2019**, *11*, 2559. <https://doi.org/10.1039/C9AY00716D>
 145. C. C. Hewa-Rahinduwage, X. Geng, K. L. Silva, X. Niu, L. Zhang, S. L. Brock, L. Luo. Reversible electrochemical gelation of metal chalcogenide quantum dots. *J. Am. Chem. Soc.* **2020**, *142*, 12207. <https://doi.org/10.1021/jacs.0c03156>
 146. A. Mirzaei, Z. Kordrostami, M. Shahbaz, J. Y. Kim, H. W. Kim. Resistive-based gas sensors using quantum dots: a review. *Sensors* **2022**, *22*, 4369. <https://doi.org/10.3390/s22124369>
 147. X. Geng, X. Liu, L. Mawella-Vithanage, C. C. Hewa-Rahinduwage, L. Zhang, S. L. Brock, T. Tan, L. Luo. Photoexcited NO₂ enables accelerated response and recovery kinetics in light-activated NO₂ gas sensing. *ACS Sens.* **2021**, *6*, 4389. <https://doi.org/10.1021/acssensors.1c01694>
 148. T. Jiang, X. Liu, J. Sun. UV-enhanced NO₂ sensor using ZnO QDs sensitized SnO₂ porous nanowires. *Nanotechnology* **2022**, *33*, 185501. <https://doi.org/10.1088/1361-6528/ac49c1>

149. Q. Lin, F. Zhang, N. Zhao, L. Zhao, Z. Wang, P. Yang, D. Lu, T. Dong, Z. Jiang. A flexible and wearable nylon fiber sensor modified by reduced graphene oxide and ZnO QDs for wide-range NO₂ gas detection at room temperature. *Materials* **2022**, *15*, 3772. <https://doi.org/10.3390/ma15113772>
150. Y. Liu, H. Wang, K. Chen, T. Yang, S. Yang, W. Chen. Acidic site-assisted ammonia sensing of novel CuSbS₂ quantum dots/reduced graphene oxide composites with an ultralow detection limit at room temperature. *ACS Appl. Mater. Interfaces* **2019**, *11*, 9573. <https://doi.org/10.1021/acsami.8b20830>
151. I. Sharma, K. N. Kumar, J. Choi. Highly sensitive chemiresistive detection of NH₃ by formation of WS₂ nanosheet and SnO₂ quantum dot heterostructures. *Sensors Actuators B Chem.* **2023**, *375*, 132899. <https://doi.org/10.1016/j.snb.2022.132899>
152. K. Rathi, K. Pal. Ruthenium-decorated tungsten disulfide quantum dots for a CO₂ gas sensor. *Nanotechnology* **2020**, *31*, 135502. <https://doi.org/10.1088/1361-6528/ab5cd3>
153. B. Bertrand, S. Hermelin, S. Takada, M. Yamamoto, S. Tarucha, A. Ludwig, A. D. Wieck, C. Bäuerle, T. Meunier. Fast spin information transfer between distant quantum dots using individual electrons, *Nature Nanotech.* **2016**, *11*, 672. <https://doi.org/10.1038/nnano.2016.82>
154. L. Pavesi, L. D. Negro, C. Mazzoleni, G. Franzo, F. Priolo. Optical gain in silicon nanocrystals. *Nature*. **2000**, *408*, 440. <https://doi.org/10.1038/35044012>
155. Y. J. Jeong, D. -J. Yun, S. H. Noh, C. E. Park, J. Jang. Surface modification of CdSe quantum-dot floating gates for advancing light-erasable organic field-effect transistor memories. *ACS Nano*. **2018**, *12*, 7701. <https://doi.org/10.1021/acs.nano.8b01413>
156. Y. Wu, Y. Wei, Y. Huang, F. Cao, D. Yu, X. Li, H. Zeng. Capping CsPbBr₃ with ZnO to improve performance and stability of perovskite memristors. *Nano Res.* **2017**, *10*, 1584. <https://doi.org/10.1007/s12274-016-1288-2>
157. S. R. Bauers, M. B. Tellekamp, D. M. Roberts, B. Hammett, S. Lany, A. J. Ferguson, A. Zakutayev, S. U. Nanoyakkara. Metal chalcogenides for neuromorphic computing: emerging materials and mechanisms. *Nanotechnology* **2021**, *32*, 372001. <https://doi.org/10.1088/1361-6528/abfa51>
158. K. C. Kwon, J. H. Baek, K. Hong, S. Y. Kim, H. W. Jang. Memristive devices based on two-dimensional transition metal chalcogenides for neuromorphic computing. *Nano-micro Lett.* **2022**, *14*, 58. <https://doi.org/10.1007/s40820-021-00784-3>
159. G. Cao, P. Meng, J. Chen, H. Liu, R. Bian, C. Zhu, F. Liu, Z. Liu. 2D material based synaptic devices for neuromorphic computing. *Adv. Funct. Mater.* **2020**, *31*, 2005443. <https://doi.org/10.1002/adfm.202005443>
160. M. Xu, X. Mai, J. Lin, W. Zhang, Y. Li, Y. He, H. Tong, X. Hou, P. Zhou, X. Miao. Recent advances on neuromorphic devices based on chalcogenide phase-change materials. *Adv. Funct. Mater.* **2020**, *30*, 2003419. <https://doi.org/10.1002/adfm.202003419>
161. Z. Lv, Y. Wang, J. Chen, J. Wang, Y. Zhou, S. -T. Han. Semiconductor quantum dots for memories and neuromorphic computing systems. *Chem. Rev.* **2020**, *120*, 3941. <https://doi.org/10.1021/acs.chemrev.9b00730>

REVIEW ARTICLE

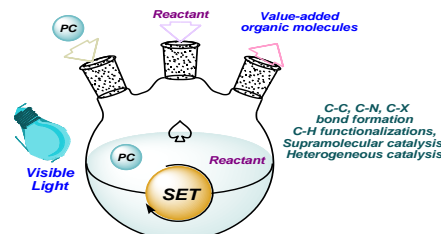
Advances in Green and Sustainable Photo Redox Catalysis for Organic Transformation

Yafia Kousin Mirza, Partha Sarathi Bera, Ajeet Kumar Pandey and Milan Bera* 

Photocatalysis & Synthetic Methodology Lab (PSML), Amity Institute of Click Chemistry Research & Studies (AICCRS), Amity University, Noida 201303, INDIA.

*Correspondence: mbera@amity.edu

Abstract: Advances in visible-light-mediated photo redox catalysis have created an exceptional approach for small-molecule activation and new chemical bond formation in organic synthesis. This is an alternative technique to generate new reactive intermediates and enable distinct synthetic strategies that were previously unthinkable. Of the many trademarks, photochemistry is often classified as “green” technology, promoting organic reactions under mild conditions without the necessity for potent and wasteful solvents, oxidants and reductants. This mini review covers the overview of the primary principles of photoredox catalysis, discussing various metal-based and organophotocatalysts. It further surveys a variety of reactions, including trifluoromethylation, cyanation, C-H functionalizations, supramolecular catalysis, and heterogeneous catalysis in both aqueous and alcoholic mediums.



Keywords: Photoredox catalysis, sustainable approach, single electron transfer.

Contents

Biographical Information	47
1. Introduction	47
1.1 Water as a Hydride Source	48
1.2 Water Mediated Rate Acceleration in the Photocatalytic Synthesis of Isoxazolidines	49
1.3 Deboronative Cyanation	49
1.4 LUMO Lowering Effect by Water	49
1.5 Water Influences Chemo selectivity	50
1.6 C-H Functionalization of Heteroarenes in Water by Photoredox Catalyst	50
1.7 Remote C-H Bromination	51
1.8 Metallocarboranes as Photoredox Catalyst in Water	51
1.9 Photoredox-Micellar Catalysis	52
1.10 Dual Hypervalent Iodine Reagent and Photocatalyst Enabled Decarboxylation	53
1.11 Photoredox Catalyst Mediated Trifluoromethylation in Alcoholic Medium	53
1.12 Merging Nickel with Photoredox Catalysis in Water	53
1.13 Supramolecular Photoredox Catalysis in Water	53
1.14 Dual catalysis for C-H bond activation	54
1.15 Au Catalysis	54
1.16 Cross-coupling with EDA complex	55
1.17 Double C-H Functionalization	55
2. Conclusion & Outlook	55
Author Contribution Declaration	55
Data Availability Declaration	55
Acknowledgements	55
References	56

1. Introduction

Photodynamic therapy (PDT) is a light-promoted approach that in the realm of synthetic chemistry, chemist typically utilizes pre-generated high-energy species, heat activation, or catalytic activation to facilitate the functionalization of molecules in organic synthesis when navigating reaction coordinates. However, there has been a recent upsurge in interest in unconventional chemical activation techniques, such as photochemical and electrochemical methods, aimed at providing novel pathways for retrosynthetic assessment. These emerging approaches have brought about significant changes in contemporary synthetic strategies. Notably, advancements in photochemical techniques have led to improved accessibility to highly reactive intermediates such as radical ions, radicals, and charge transfer complexes.

Yafia Kousin Mirza, born in New Delhi, India, earned her B.Sc. in Chemistry from Jamia Millia Islamia University in 2021. She completed her M.Sc. in Chemistry from Jamia Hamdard in 2023. Then, she joined Amity University, Noida, as a Ph.D. scholar under the supervision of Dr. Milan Bera at the Photocatalysis and Synthetic Methodology lab (PSML). Mirza's research focuses on selective allene functionalizations. Her meticulous approach and dedication to chemical research highlight her commitment to advancing the field and contributing to scholarly exploration.



Partha Sarathi Bera completed his B.Sc. in 2015 and M.Sc. in Organic Chemistry in 2017 from Vidyasagar University, West Bengal. Then, he completed his Ph.D. at NIT Durgapur in 2024. Currently, he is working as a post-doctoral fellow at Dr. Bera's group (PSML), Amity University, Noida. His research focuses on photocatalytic organic transformations via allene functionalizations.



Ajeet Kumar Pandey completed his graduation and post-graduation from S.M. Joshi College, Hadapsar, Pune, India. In 2023, he joined under Dr. Bera's group as Ph.D. scholar at Amity University Noida. His research topic focuses on transition-metal catalyzed C-H functionalization.



Dr. Milan Bera received his Ph.D. from IIT Kharagpur under the supervision of Prof. Sujit Roy. After couple of postdoctoral studies (with Prof. Ryoichi Kuwano, Kyushu University, Japan & Prof. Debabrata Maiti, IIT Mumbai) and industrial research (Sun Pharma, India), he joined as Research Professor in the Department of Chemistry at Chung-Ang University, Seoul, South Korea. In 2023, he moved to India and joined as Ramanujan Faculty Fellow at Amity University, Noida, Uttar Pradesh. His group's research interests are focused on the development of new and sustainable synthetic and catalytic methods for molecular diversification.



Consequently, the photoredox process has opened new avenues for discovering reactions and developing bond disconnection tactics that were previously challenging or unattainable with traditional methods.¹

In the last decade, synthetic photochemistry has experienced a revival, particularly focusing on establishing sustainable methods. Light-absorbing chromophores are commonly employed to facilitate a variety of organic transformations of small molecules that traditionally don't react to light. In this process, called photocatalysis, chromophores typically facilitate either electron transfer (ET) or energy transfer (EnT) process. ET, also known as photoredox catalysis, operates by

transferring single electrons based on the redox properties of both the excited photocatalyst (PC) and the reacting substrate. Photoredox

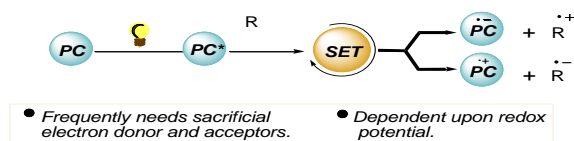


Figure 1. Photo-redox process

reactions often require additional electron donors or acceptors to complete the catalytic cycle. Moreover, ensuring that the redox potentials of both the PC and the organic substrate are appropriately controlled, is crucial for successful photoredox catalysis (Figure 1).²

Photoredox-initiated reactions generally proceeded via utilization of two type of photocatalysts: transition metal-based inorganic photoredox complexes and organic dyes, also known as organic photoredox catalysts (Figure 2). Transition metal-based photoredox reactions typically utilize metal polypyridyl complexes, like Ru(II) polypyridine complexes or cyclometalated Ir(III) complexes. On the other hand, metal-free conditions make use of organic dyes such as eosin, rhodamine, 9-fluorenone, xanthone, methylene blue, rose Bengal, acridiniums, etc., which are proficient of absorbing visible light or near-visible light.³

Photoredox catalysts (PC) can harness visible light, which is a cost-effective, eco-friendly, and readily available source of sustainable energy. When exposed to visible light, PC generates long-lasting photoexcited states (PC*), which readily participate in bimolecular electron-transfer reactions,

either releasing or capturing electrons from molecules. In reductive quenching cycles, PC* accepts an electron from a substrate (Sub) or a reductant (Red), forming the radical anion [PC]^{•-}, followed by its oxidation. Alternatively, in oxidative quenching reactions, PC* transfers an electron to either a substrate (Sub) or an oxidant (Ox) in the reaction mixture, resulting in the formation of the radical cation [PC]^{•+}, which is subsequently reduced. These single electron transfer (SET) events facilitate radical generation and provide new pathways for radical conversion in organic synthesis (Figure 3).^{3,4}

In 1912, Giacomo Ciamician, a prominent figure in organic photochemistry, delivered an inspiring speech at the 8th International Congress of Applied Chemistry. Titled “The Future of Photochemistry,” Ciamician envisioned a future where clean and economical photochemical processes would replace high-energy synthetic methods in a new, environmentally conscious chemical industry.⁵ This sustainable approach adheres to a set of guidelines aimed at reducing or eliminating the use of harmful toxic compounds throughout the chemical production process.

The pinnacle of sustainable chemical reactivity and the objective of green chemistry reflects photosynthesis. Recent progress in photochemical techniques, especially photoredox catalysis, appears to have advanced us toward this aim. Similar to how leaves intake air, these methods generate reactive radicals using coloured catalysts (like organic dyes or transition metal complexes) to absorb light and activate stable organic molecules through single-electron processes (oxidation or reduction).

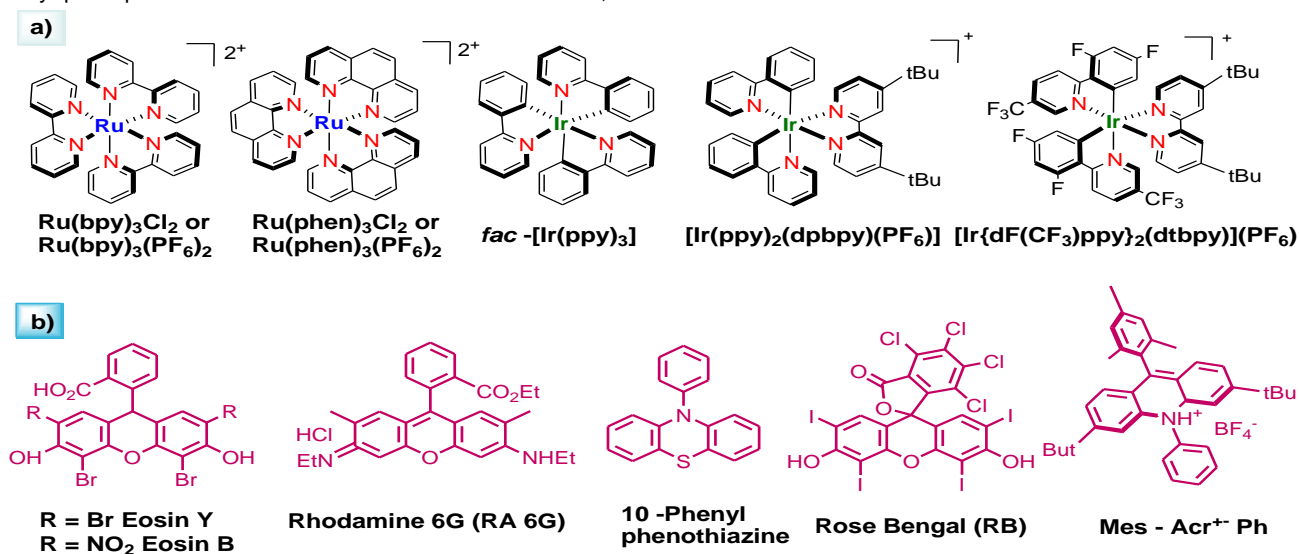


Figure 2. Representative examples of photocatalyst.

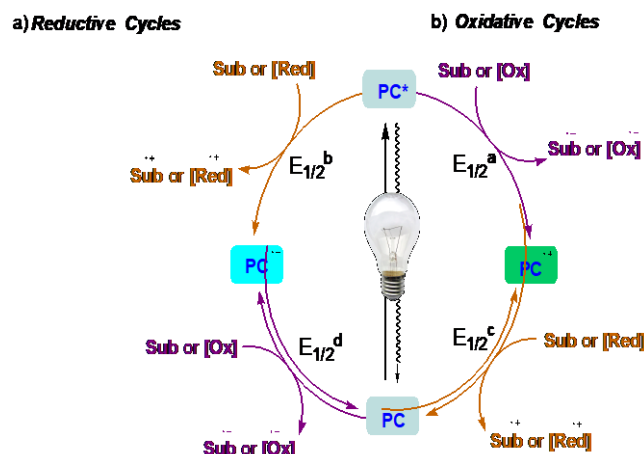


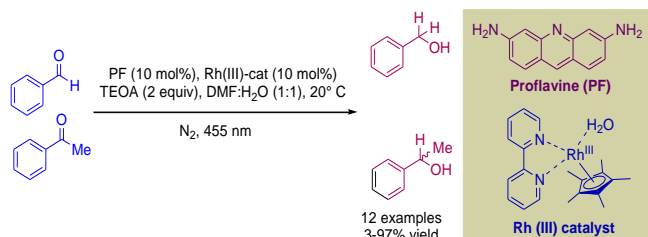
Figure 3. The photoredox quenching cycles.

The aim is to utilize water or alcohol as the reaction medium and harness visible light as the primary energy source, paving the way for innovative sustainable chemistry. This section delves into the latest developments in sustainable organic transformation through photoredox catalysis, outlining both the benefits and constraints associated with these catalysts.

1.1 Water as a Hydride Source

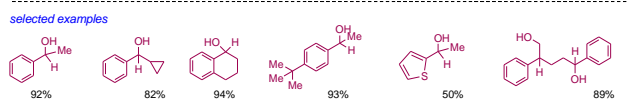
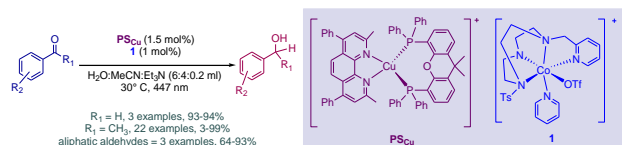
Using proflavine (PF) as a photocatalyst, [Cp*Rh(III)(bpy)H]Cl as a mediator, and triethanolamine (TEOA) as a sacrificial electron donor leads to the selective reduction of aldehydes over ketones (Scheme 1).⁶ In-depth mechanistic studies indicate that the primary reaction pathway entails the photochemical reduction of proflavine triplets, followed by the reduction of the Rh catalyst to produce reactive Rh(III)–H intermediate *in situ*. Water is essential in this process, providing the protons needed to form Rh(III)–H.

dismissed the idea that substances like H_3O^+ and H_2O in the reaction mixture might catalyze the cycloaddition process.¹³



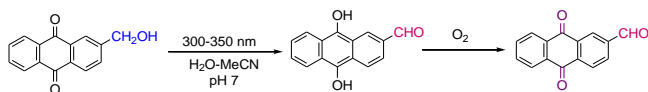
Scheme 1. Photocatalytic generation of alcohols using Rh(III)-H species.

Fillol's group reported a dual cobalt-copper photoredox catalyst that effectively reduces aldehydes and aromatic ketones to corresponding 1° and 2° alcohol in the presence of water as a hydride source and sacrificial electron donor (iPr₂EtN/Et₃N) when exposed to 447 nm light (**Scheme 2**).⁷ Mechanistic investigations demonstrated that the reduction of the organic substrates is facilitated by the formation of a [Co-H] intermediate.



Scheme 2. Dual catalysis for the photoreduction of aldehydes and aromatic ketones.

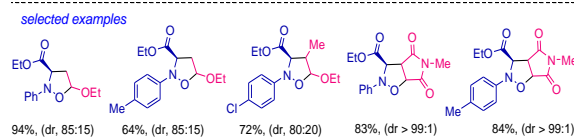
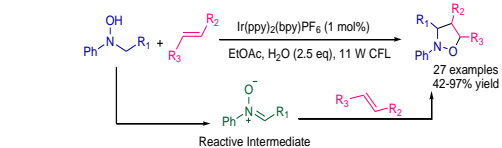
Wan and his team discovered that water is essential for an intramolecular reaction of 2-(hydroxymethyl)anthraquinone under UV light (300 – 350 nm) (**Scheme 3**).^{8,9} This reaction results in an intramolecular redox product, which quickly oxidizes the anthraquinone derivative when it comes into contact with air or oxygen.



Scheme 3. Intramolecular photoredox reaction in aqueous solution.

1.2 Water Mediated Rate Acceleration in the Photocatalytic Synthesis of Isoxazolidines

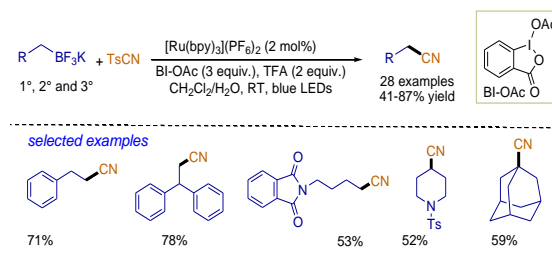
The study described an oxidative [3+2] cycloaddition reaction between *N*-alkyl-substituted hydroxylamines and alkenes. They used a 1 mol% [Ir(ppy)₂(bpy)]PF₆ photoredox catalyst under an 11 W CFL light source in ethyl acetate solvent (**Scheme 4**).¹⁰ Interestingly, they noticed that adding 2.5 equivalents of water to the reaction mixture sped up the reaction rate, giving the desired isoxazolidine products in good amounts. This finding suggests that water is essential to the reaction. To explain why water enhances the reaction rate, the authors proposed that the photoredox catalyst might split water, forming active species like HO•, HO⁻, and H₂O₂, which could participate in the reaction.^{11,12} However, they



Scheme 4. [3 + 2] cycloaddition reaction.

1.3 Deboronative Cyanation

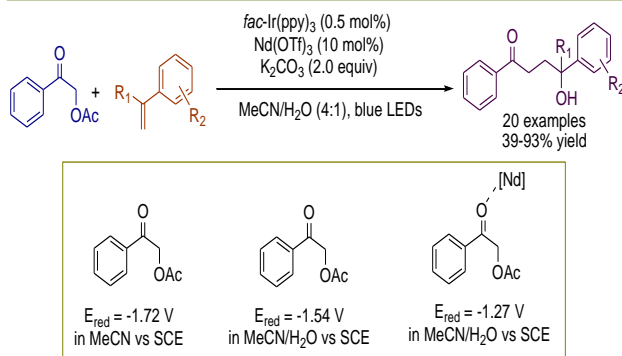
The mechanistic impact of the reaction has been overlooked in many photocatalytic methods that utilize water, either as a co-solvent or additive. It should be noted that radical precursors such as trifluoroborate salts, diazonium salts, and alkyl & aryl bromides are stable under aqueous conditions.¹⁴ Alkyl nitrile was successfully generated through the direct photocatalytic cyanation reaction of alkyltrifluoroborates, utilizing [Ru(bpy)₃](PF₆)₂ as a photocatalyst, hypervalent iodine as an oxidant, and TFA as an additive (**Scheme 5**).¹⁵ The reaction demonstrated tolerance towards various functionalities with a broad substrate scope. The involvement of an alkyl radical intermediate in the reaction was confirmed by trapping the free radical using a radical scavenger, TEMPO.



Scheme 5. Deboronative cyanation reaction of alkyltrifluoroborates.

1.4 LUMO Lowering Effect by Water

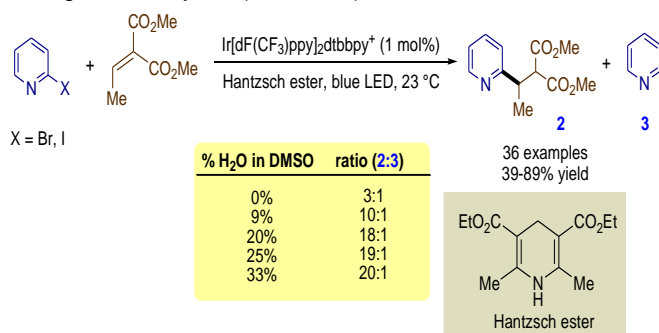
In the photocatalytic cross-coupling reaction between α -acetoxy acetophenones and styrene derivatives, a reduction in the lowest unoccupied molecular orbital (LUMO) energy level of the carbonyl was observed, resulting in the formation of 1,4-substituted products via Markovnikov functionalization (**Scheme 6**).¹⁶ This coupling mechanism was achieved by deactivating the photocatalyst fac-Ir(ppy)₃ through oxidation, in combination with activating the carbonyl group in the presence of water and Nd(OTf)₃ serving as a Lewis acid catalyst. The inclusion of an aqueous medium, along with the water-compatible Lewis acid, amplified the reduction in LUMO energy levels of carbonyls, shifting the E_{red} of α -acetoxy acetophenones from -1.72 V to -1.27 V vs SCE. This enhancement facilitated a more energetically favourable electron transfer process, as evidenced by cyclic voltammetry and Stern–Volmer experiments. Significantly, the lack of the Lewis acid catalyst led to the inability to generate the 1,4-difunctionalized product.



Scheme 6. C–C cross-coupling reaction.

1.5 Water Influences Chemo selectivity

Water can serve not only as a solubilizer for polar substrates but also for its ability to act as a nonsolvent for lipophilic hydrophobic additives. Jui et al. showcased an impressive demonstration of these properties through the radical method for heteroaryl radical conjugate addition. A photocatalyst consisting of 1 mol% $(\text{Ir}[\text{d}(\text{CF}_3)\text{ppy}]_2(\text{dtbpy}))\text{PF}_6$ was utilized, which is proficient in generating redox active 2-pyridyl radicals under blue LED irradiation. In their study, Hantzsch ester was employed to maintain redox neutrality by donating both an H-atom and an electron. The authors illustrated the solubility of the reactants by introducing water as a cosolvent, where the presence of Hantzsch ester enhanced the selectivity for the formation of the radical conjugate addition product over the reduction of nitrogen heterocycles (**Scheme 7**).¹⁷



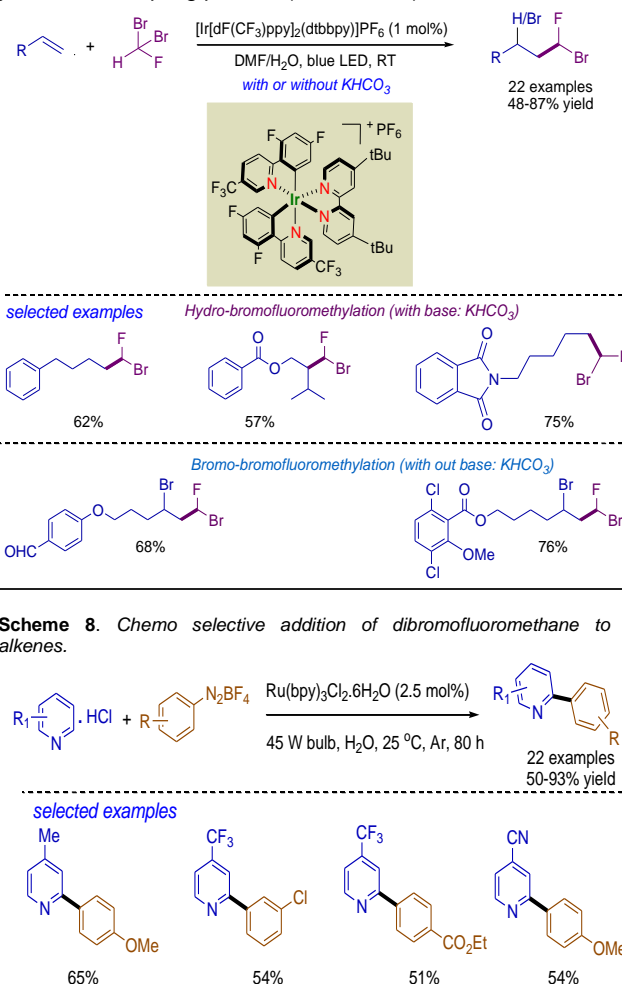
Scheme 7. *Heteroaryl radical conjugate addition.*

Qing recently unveiled an intriguing solvent effect in the chemoselective addition to alkenes. This involved a shifting from THF to a combination of DMF and water as the reaction solvent, facilitating the selective synthesis of dibromofluoromethylated products through radical addition of CHBr_2F to alkenes under photoredox catalysis. Notably, the use of a 1:4 ratios of DMF to water yielded superior results for the desired product compared to alternative solvents (**Scheme 8**).¹⁸

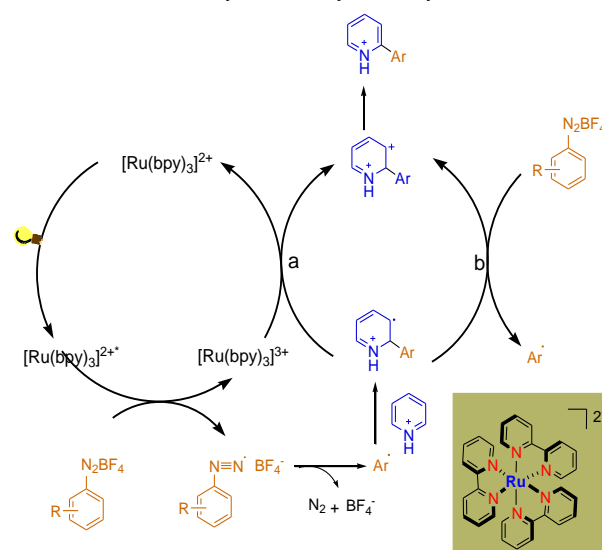
1.6 C-H Functionalisation of Heteroarenes in Water by Photoredox Catalyst

A new technique has been created for directly arylating C–H bonds in electron-deficient *N*-heteroarenes. This method uses aryldiazonium salts as coupling agents within a photocatalytic system. The photocatalyst, [Ru(bpy)₃]Cl₂·6H₂O, was activated using a 45 W LED bulb that emits visible light. This process successfully produced various aryl-heteroaryl structures (**Scheme 9**). Water was chosen as the solvent for its eco-friendly properties and its capacity to effectively dissolve and stabilize both the substrates and the catalyst.¹⁹ The mechanism was explored by introducing the radical quencher TEMPO into the optimized reaction conditions. The TEMPO experiments did not yield the desired product and confirm the presence of radical species in the reaction

medium. In light of these findings, a mechanism was suggested with three pivotal steps: (1) the generation of the excited $[\text{Ru}(\text{bpy})_3]^{II*}$ species by light irradiation of the $[\text{Ru}(\text{bpy})_3]^{III}$ catalyst, (2) the formation of a phenyl radical through single electron transfer (SET) from $[\text{Ru}(\text{bpy})_3]^{II*}$ to the aryldiazonium salt, leading to the oxidation of the catalyst to $[\text{Ru}(\text{bpy})_3]^{III}$, and (3) the combination of the phenyl radical with pyridine hydrochloride resulting in another radical intermediate, which transforms into a carbocation *via* two possible pathways. Deprotonation of the intermediate yielded the coupling product (**Scheme 10**).¹⁹

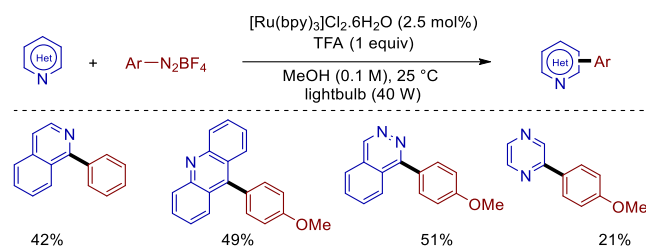


Scheme 9. *Synthesis of aryl-heteroaryl motifs.*



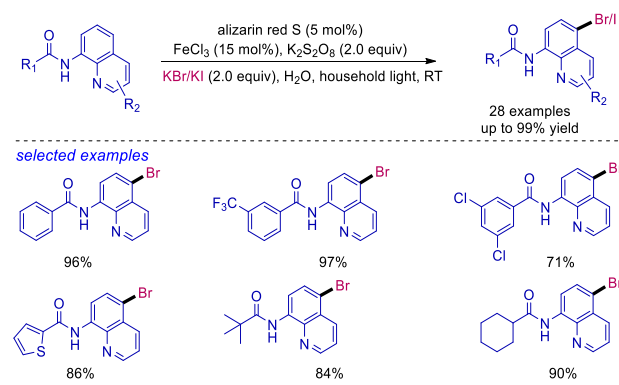
Scheme 10. Plausible mechanistic pathway for arylation of heteroarenes.

Lei *et al.* established a similar method to arylate isoquinolines using $[\text{Ru}(\text{bpy})_3]\text{Cl}_2 \cdot 6\text{H}_2\text{O}$ as a photosensitizer (**Scheme 11**). Unlike the previous study, which employed pyridinium salts as the initial substrates, Lei group employed TFA for *in situ* protonation of the *N*-heterocycles in the reaction medium.²⁰



Scheme 11. Arylation of isoquinolines.

1.7 Remote C-H Bromination

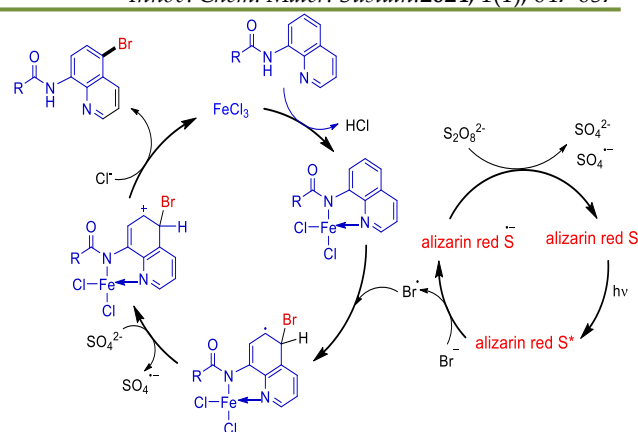


Scheme 12. Synthesis of halogenated 8-aminoquinoline amides.

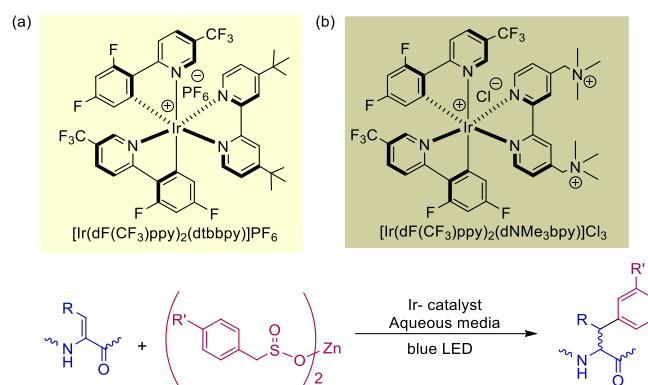
Research into visible-light photocatalysis that works well in water is a fascinating field. Pursuing these goals, scientists have created various photocatalysts that function in aqueous environments. One such catalytic system combines FeCl_3 with Alizarin Red S, a water-soluble organic photocatalyst, to carry out the C5–H halogenation of 8-aminoquinoline. This reaction achieved highly selective C5 halogenation of 8-aminoquinoline amides at room temperature, using $\text{K}_2\text{S}_2\text{O}_8$ as an oxidant and KBr as an additive, under the irradiation of standard household light in the presence of air (**Scheme 12**).²¹

The potential reaction pathway suggested by Wu and his team is illustrated in **Scheme 13**. In this pathway, the excited state of Alizarin Red S* generates a bromine radical (Br^\bullet) and an Alizarin Red S radical anion by reducing the bromide ion. With $\text{K}_2\text{S}_2\text{O}_8$ present, the Alizarin Red S radical anion undergoes oxidation, which completes the photocatalytic cycle and regenerates the ground state Alizarin Red S.

Most Ir- and Ru-polypyridyl complexes used as photoredox catalysts have limited solubility in water, ranging from less than 1 ppm to 1000 ppm, depending on their substituents and counterions. As a result, organic solvents are typically needed to dissolve both the catalyst and the substrates.²² Despite this, using these complexes as catalysts has become appealing because they do not require an excess of oxidants. Roelfes and colleagues tackled the solubility issue by designing and synthesizing a water-soluble photocatalyst, $[\text{Ir}(\text{dF}(\text{CF}_3)\text{ppy})_2(\text{dNMe}_3\text{bpy})]\text{Cl}_3$, through ligand modification.²³ They replaced the *tert*-butyl groups on the ligand with quaternary ammonium groups to enhance water solubility. This newly developed catalyst has shown promise for modifying dehydroalanine (Dha) containing natural products in aqueous environments under physiological conditions and across a wide pH range (**Scheme 14**).

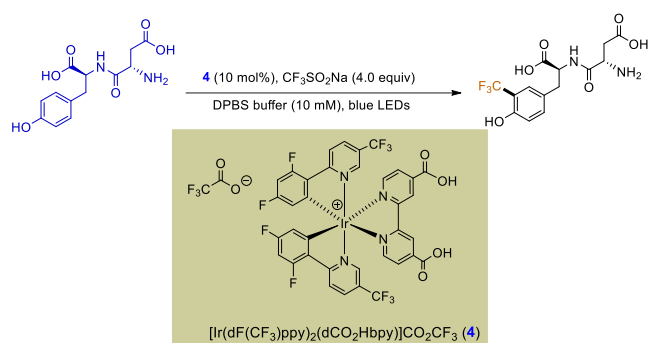


Scheme 13. Probable reaction mechanism.



Scheme 14. Ir-catalysed modification of the Amino acid, (a) commercially available photoredox catalyst and (b) charged Ir(III)-based photoredox catalyst.

Conrad *et al.* Further advanced this field by designing similar heteroleptic Ir-complexes, incorporating carboxylate groups onto the bipyridyl ligands. This modification led to the creation of a new catalyst, $[\text{Ir}(\text{dF}(\text{CF}_3)\text{ppy})_2(\text{dCO}_2\text{Hbpy})]\text{CO}_2\text{CF}_3$ (**4**), with enhanced water solubility. The performance of this photocatalyst was evaluated in the trifluoromethylation of polar molecules and peptides, using phosphate-buffered saline as the solvent. The Langlois reagent ($\text{CF}_3\text{SO}_2\text{Na}$) served as the CF_3^\bullet radical precursor, and a light source was used for photoexcitation (**Scheme 15**).²⁴

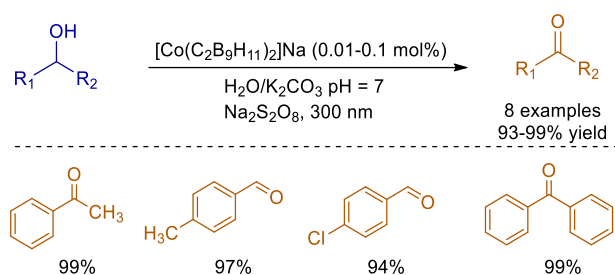


Scheme 15. Trifluoromethylation of biomolecule substrates.

1.8 Metallocarboranes as Photoredox Catalyst in Water

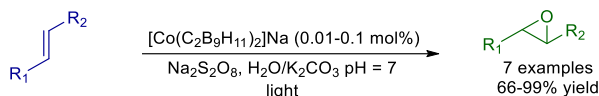
A cobalt metallocarborane, $[3,3'\text{-Co}(1,2\text{-C}_2\text{B}_9\text{H}_{11})_2]\text{Na}$, which exhibits an unusual structure compared to established photoredox catalysts, facilitates hydrogen and dihydrogen bonding. This unique bonding contributes to its self-assembly

properties,²⁵ water solubility,²⁶ and micelle formation.²⁷ The use of cobaltabisdicarbollide, $[3,3'\text{-Co}(1,2\text{-C}_2\text{B}_9\text{H}_{11})_2]^-$, along with its chloro derivatives, as photoredox catalysts in the oxidation of alcohols in water *via* single-electron transfer (SET) processes has been investigated by Teixidor and colleagues (**Scheme 16**).²⁸



Scheme 16. Metallacarborane catalysed oxidation reaction of alcohols.

Researchers also examined the effectiveness of the same photocatalyst in generating epoxides from aromatic and aliphatic alkenes in water.²⁹ They noticed a significant increase in epoxide production with a short reaction time and minimal catalyst usage. The proposed mechanism suggests that when exposed to water and $\text{S}_2\text{O}_8^{2-}$ ions under light, the photoredox $[\text{Co}^{\text{III}}(\text{C}_2\text{B}_9\text{H}_{11})_2]^-$ catalyst oxidizes to form $[\text{Co}^{\text{IV}}(\text{C}_2\text{B}_9\text{H}_{11})_2]$, along with OH^\bullet radicals, H^+ ions, and SO_4^{2-} ions. Subsequently, the alkene undergoes oxidation by $[\text{Co}^{\text{IV}}(\text{C}_2\text{B}_9\text{H}_{11})_2]$, resulting in the creation of the corresponding epoxide through interaction with the hydroxyl radical (OH^\bullet) (**Scheme 17**).



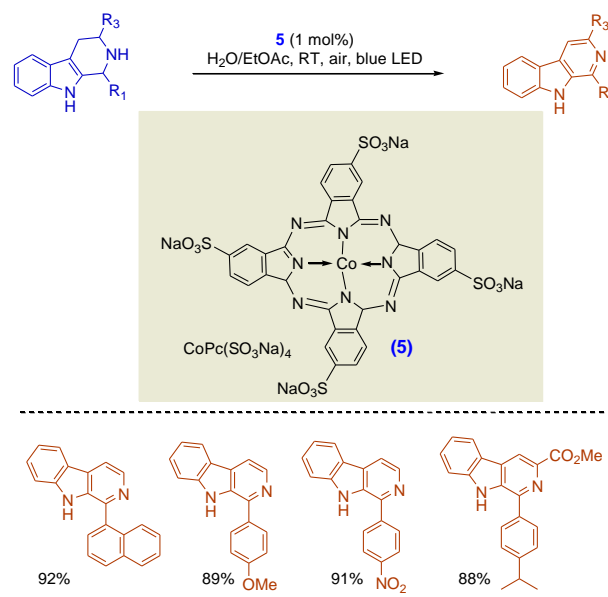
Scheme 17. Alkene epoxidation.

This metallacarborane was attached to silica-coated magnetic nanoparticles, resulting in a catalyst that can be easily separated using an external magnet.³⁰ A collaborative photoredox catalytic system was constructed using ruthenium-cobaltabis(dicarbollide), $[\text{Ru}^{\text{II}}(\text{try})\text{(bpy)}(\text{H}_2\text{O})][3,3'\text{-Co}(1,2\text{-C}_2\text{B}_9\text{H}_{11})_2]$, with the metallacarborane acting as the photoredox catalyst and Ru^{II} serving as the oxidation catalyst, coupled by noncovalent contacts. This technique was utilised for the photooxidation of alcohols using ultraviolet light.³¹ A water-soluble cobalt-based phthalocyanine photoredox catalyst (**5**) enabled the oxidative dehydrogenation of tetrahydro-(iso)quinoline, tetrahydro- β -carbolone, and indoline derivatives in a biphasic media (**Scheme 18**).³² This setup enabled easy product separation and permitted the catalyst to be reused up to five times while maintaining similar levels of reactivity.

1.9 Photoredox-Micellar Catalysis

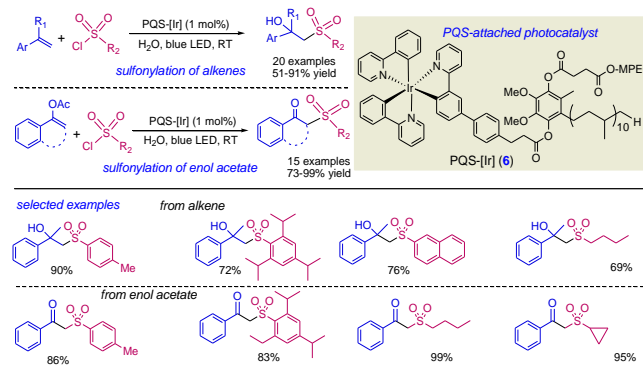
The field of synthetic organic chemistry has recently shown a growing interest in the development of water-soluble photocatalysts. Many substances commonly used in drug manufacturing, as well as certain photocatalysts, are not soluble in water, which hampers efforts to adhere to green chemistry principles. Integrating photoredox catalysis with micellar catalysis may provide a viable solution to this issue. Micelles, formed by adding surfactants to water, create an environment conducive to organic transformations in water. In 2018, Lipshutz and colleagues introduced a PQS-[Ir] photocatalyst.³³

This catalyst is formed through the covalent binding of PQS (polyethyleneglycolubiquinol succinate, the reduced form of the dietary supplement CoQ₁₀) with the photocatalyst $\text{Ir}(\text{ppy})_3$.



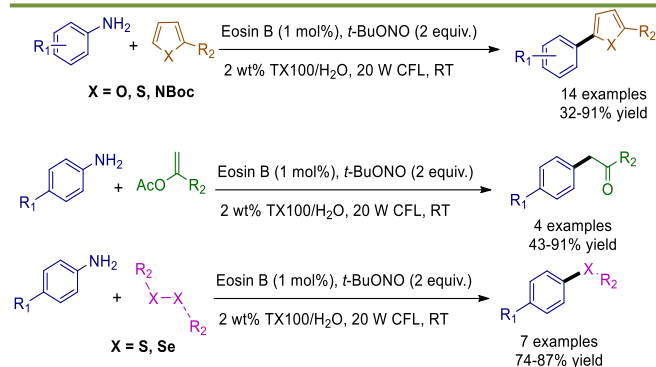
Scheme 18. A photoredox catalyzed oxidative dehydrogenation N-heterocycles.

This process leads to self-aggregation in an aqueous medium, producing nanomicelles. The amphiphilic PQS species includes a hydrophilic group (MPEG), a lipophilic side chain with 50 carbon atoms, and an $-\text{OH}$ group located within the hydrophobic inner core where catalysis occurs. The efficiency of the newly developed PQS-[Ir] photocatalyst was investigated in the sulfonation of alkenes and enol acetates, yielding the desired product with good efficiency (**Scheme 19**). Notably, this catalyst can be reused multiple times without compromising the product yield.



Scheme 19. Sulfonation of alkenes and enol acetates catalyzed by the PQS-[Ir].

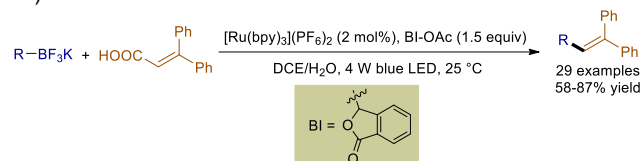
Organic dyes are frequently employed as photoredox catalysts due to their cost-effectiveness compared to precious metal-polypyridyl complexes.³⁴⁻³⁷ Cai and Jiang's research team devised a micellar photocatalytic setup, utilizing an organic photoredox catalyst to arylate *in situ*-nitrosated aniline.³⁸ They employed commercially available Triton X-100 and Eosin B as the surfactant and photocatalyst, respectively, in the reaction conducted under the control of a 20 W CFL. Remarkably, the reaction proceeded smoothly at room temperature without the need for any organic cosolvent. Additionally, the authors investigated the synthesis of unsymmetrical sulfides and selenides from substituted disulfides/diselenides and anilines, as well as the [4+2] benzannulation of 2-aminobiphenyl with alkynes under their developed photocatalytic conditions (**Scheme 20**).



Scheme 20. Arylation in photocatalytic conditions.

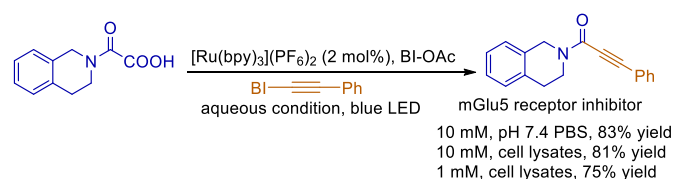
1.10 Dual Hypervalent Iodine Reagent and Photocatalyst Enabled Decarboxylation

Organic carboxylates, readily available and removable, serve as latent activating groups for constructing diverse organic motifs.³⁹ Typically, transition metal catalysts activate these carboxylates through coordination, necessitating strong oxidants or high temperatures to facilitate CO₂ extrusion.^{40,41} Hypervalent iodine reagents (HIR) have garnered significant interest due to their similar activation properties to transition metals, enabling radical addition followed by subsequent decarboxylation under mild conditions. Building on this concept, researchers developed a photoredox system utilizing HIR with dual catalytic properties to promote decarboxylative radical alkenylation and ynonelation reactions.^{42,43} Chen's group demonstrated alkyl-alkene synthesis *via* coupling alkyl trifluoroborate with aryl- or acyl-substituted vinyl carboxylic acids using a hypervalent iodine photocatalyst.⁴² Optimal yields were achieved using blue LED irradiation with BI-OAc as the iodinating reagent in a DCE Medium at 25 °C (Scheme 21).



Scheme 21. Decarboxylative radical alkenylation reaction.

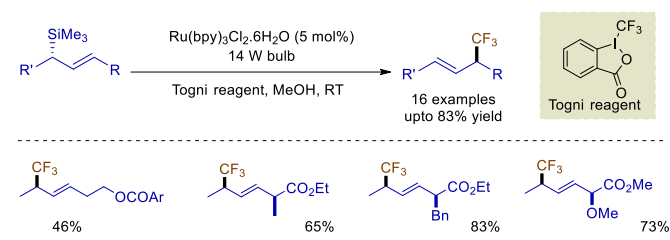
Furthermore, they have demonstrated the biological applications of the hypervalent iodine photoredox system in synthesizing biomolecules, such as the mGlu5 receptor inhibitor, under neutral aqueous conditions (Scheme 22).⁴⁴



Scheme 22. Synthesis of bioactive molecules in neutral aqueous medium.

1.11 Photoredox Catalyst Mediated Trifluoromethylation in Alcoholic Medium

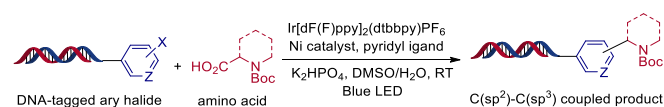
Gouverneur group introduced a trifluoromethylation approach for allylsilanes through photoredox catalysis, resulting in enantioenriched branched allylic-CF₃ products. The Togni reagent served as the CF₃[•] radical source for the trifluoromethylation reaction in the presence of the photocatalyst Ru(bpy)₃Cl₂·6H₂O. This process was conducted in a methanolic or ethanolic medium and exposed to a household 14 W light bulb, as illustrated in Scheme 23.⁴⁵



Scheme 23. Trifluoromethylation of allylsilanes.

1.12 Merging Nickel with Photoredox Catalysis in Water

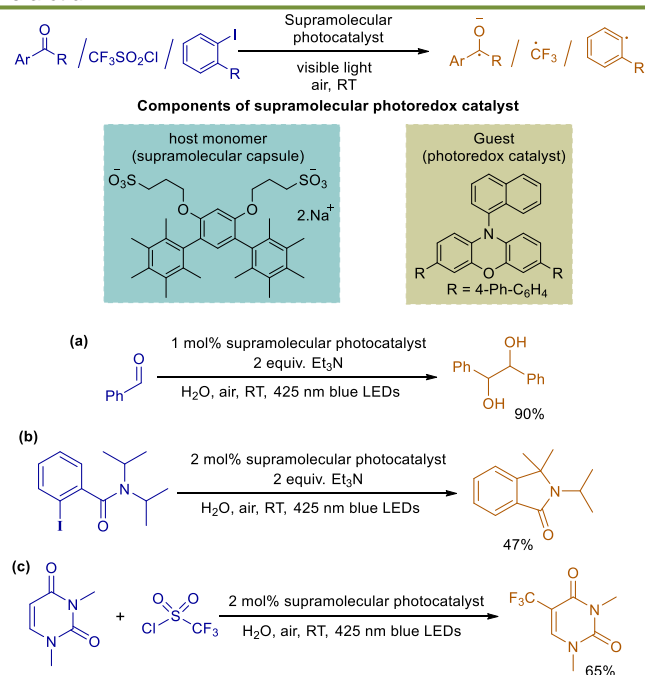
The fusion of transition metals with photoredox catalysts, known as metallaphotoredox catalysis, has surfaced as an intriguing method for the straightforward creation of complex structures pertinent to drug discovery. This approach holds promise as a valuable addition to DNA-encoded chemistry techniques. Recently, a breakthrough was achieved where amino acids underwent successful decarboxylation in aqueous conditions using an iridium-based photocatalyst. This process yielded the necessary C-centered radicals, which were subsequently integrated into various DNA-tagged radical acceptors.⁴⁶ Additionally, the same research group combined photoredox catalysts with nickel in water, facilitating DNA-compatible decarboxylative arylation reactions. Utilizing a novel nickel precatalyst featuring a pyridyl carboxamidate ligand in conjunction with an iridium-based photocatalyst, they achieved the synthesis of structurally diverse DNA-encoded libraries from readily available amino acids and a range of DNA-tagged aryl halides (Scheme 24).⁴⁶



Scheme 24. Decarboxylative arylation in aqueous medium.

1.13 Supramolecular Photoredox Catalysis in Water

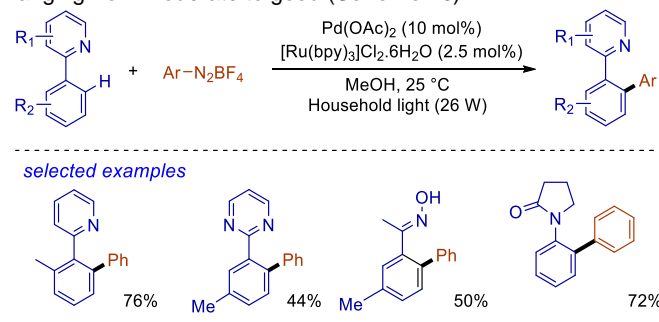
Supramolecular photoredox catalysis offers a metal-free approach in water for various photoredox reactions. Utilizing a nanosized supramolecular capsule containing V-shaped aromatic amphiphiles with pentamethylphenyl groups, it efficiently absorbs an organic photoredox catalyst in aqueous conditions, with the flexibility to modify the host-guest combination. Under visible light exposure, this catalyst effectively reduces organic compounds, generating a range of carbon-centered radicals like aryl, ketyl, and trifluoromethyl radicals in water (Scheme 25).⁴⁷ The ketyl radicals were applied to synthesize a series of pinacol derivatives (Scheme 25a), while the in situ generated aryl radical facilitated intramolecular cyclization through a 1,5-hydrogen atom transfer reaction (Scheme 25b). Additionally, the CF₃[•] radical was utilized in trifluoromethylation of 1,3-dimethyluracil (Scheme 25c).



Scheme 25. Supramolecular photoredox catalyst generates carbon-centered radicals in water

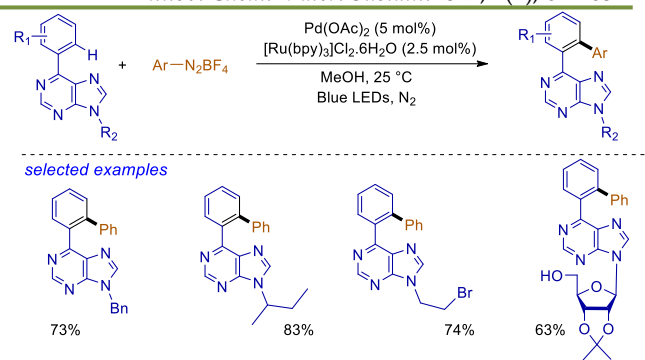
1.14. Dual catalysis for C–H bond activation

Diazonium salts could be utilized as one of the coupling partners for C–H activation reaction. In recent years, under photoredox conditions, it has acquired significant importance, particularly for the C–H bond activation. Sanford group described a visible light supported photoredox catalysis of [Ru(bpy)₃]₂.6H₂O, in combination with Pd(OAc)₂ as transition metal catalyst, which catalyzed the C–H arylation of the phenylpyridine derivatives at 25 °C.⁴⁸ A variety of phenylpyridine derivatives with various functionalities and substituted aryl diazonium salts were successfully employed for this method produced the desired product with yields ranging from moderate to good. (**Scheme 26**).



Scheme 26. Arylation of phenylpyridines

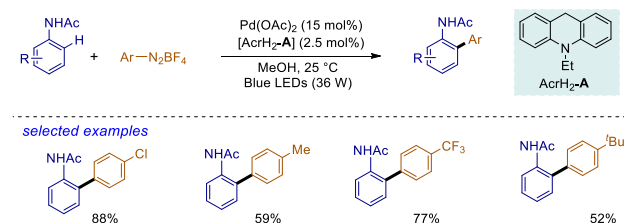
Succeeding this methodology, another work has been reported for *ortho* C–H Arylation of 6-arylpurine nucleosides attached arene system, using [Ru(bpy)₃]₂.6H₂O as photoredox catalyst and Pd(OAc)₂ as metal catalyst. Diazonium salts were used as aryl source under irradiation of visible light (**Scheme 27**).⁴⁹ This arylation approach recommended a wide scope of substrates including functionalized purines which may be very important in medicinal chemistry.



Scheme 27. C–H arylation of purine nucleosides.

Recently, a dual catalytic system was developed that combines Pd(OAc)₂ as a metal catalyst with 9,10-dihydro-10-ethylacridine (AcrH₂-A) serving as an organic photoredox catalyst. This system facilitates the *ortho*-directed arylation of acetanilides and benzamides under mild reaction conditions. (**Scheme 28**).⁵⁰

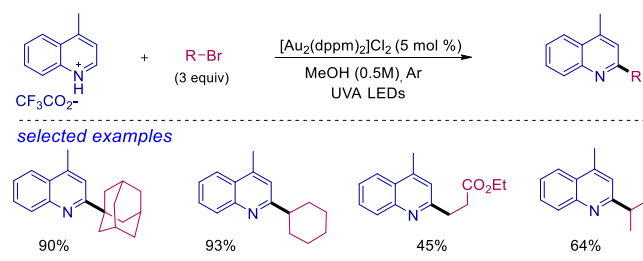
The arylation of *N*-heteroarenes can be accomplished using [Ru(bpy)₃]₂.6H₂O as photosensitizer and aryldiazonium salts as the arylating coupling agent in the presence of household light bulb under inert atmosphere.⁵¹



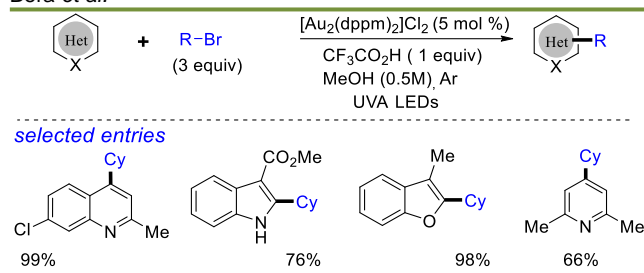
Scheme 28. C–H Arylation of acetanilides.

1.15 Au Catalysis

An unactivated bromoalkanes effectively generates the alkyl radicals under light source and argon environment in the presence of a dimeric gold(I) photoredox catalyst, [Au₂(dppm)₂]₂Cl₂ in MeOH solvent. The generated alkyl radical species subsequently leads to direct C–H alkylation of various heteroarenes. This method is efficient for alkylation of heteroarenes in the absence of directing groups. [52] They first reported the 2-alkylation of lepidine-TFA salt with several bromoalkanes in the presence of MeOH as a green solvent with 5 mol% of [Au₂(dppm)₂]₂Cl₂ catalyst under UVA LEDs (365 nm) (Scheme 29). The applicability of this method was expanded for various heterocyclic coupling partners, such as benzofuran, indole or pyridine for the alkylation with bromoalkanes (**Scheme 30**).⁵²

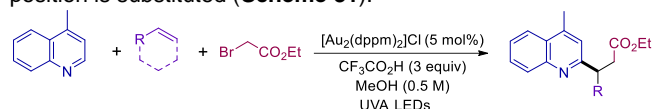


Scheme 29. 2-Alkylation of lepidine-TFA salt



Scheme 30. Alkylation of heterocycles

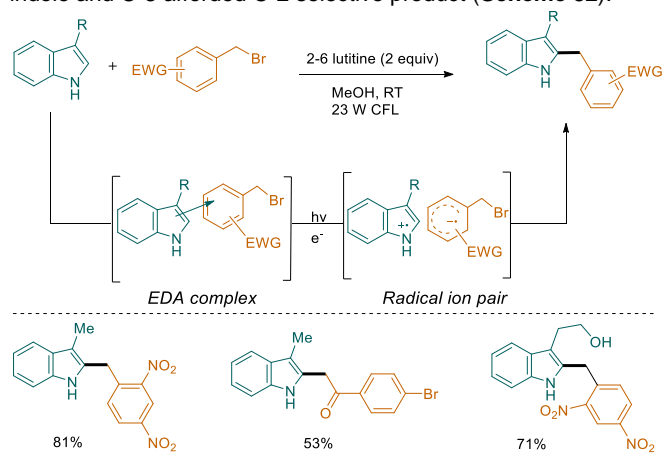
Furthermore, the same greener conditions can be utilized for alkylation of lepidine under multicomponent manner with an alkene and α -bromoester. The alkene is merged with the radical generated by the α -bromoester, ensuing in an alkylation at the C-2 position of heteroarenes unless this position is substituted (Scheme 31).⁵²



Scheme 31. Multicomponent reaction of lepidine

1.16 Cross-coupling with EDA complex

Melchiorre group developed the metal-free unique photoredox technique, engaging an electron donor-acceptor complex (EDA) formed between substituted indoles and electron-accepting benzyl or phenacyl bromides to accelerate the direct alkylation of indoles.⁵³ They isolated and characterized the reactive EDA complex that is generated by the interaction of 3-methylindole and 2, 4-dinitrobenzyl bromide by X-ray single-crystallographic technique. When exposed to visible light, this EDA complex produced a radical ion pair, enabling the formation of a benzyl radical anion. This radical then reacted with the indole, yielding benzylated indole in good yields, all without the need for an additional photosensitizer. The substrate scope depended on the substitution pattern of indole motif. C-2 substituted indole provided the C-3 alkylated indole and C-3 afforded C-2 selective product (Scheme 32).

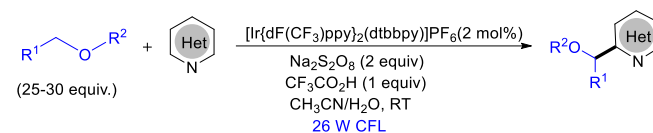


Scheme 32. 2-Benzylation of indoles

1.17 Double C-H Functionalization

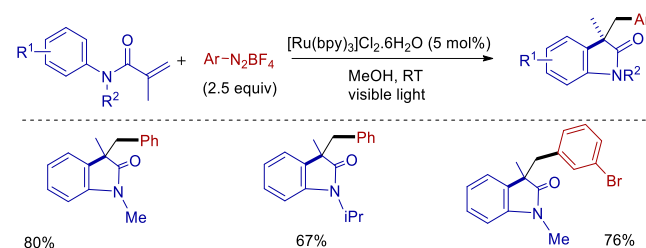
The modification of two distinct carbon-hydrogen bonds could generate a new carbon-carbon bond. In 2015, MacMillan group revealed the formation of α -oxyalkyl radicals from several frequently used ethers through hydrogen atom transfer (HAT). Consequently, these radicals were combined with various heteroarenes engaging *via* Minisci-type approach. The process of HAT on dialkyl ethers, employing [Ir(dF(CF₃)ppy)₂(dtbbpy)]PF₆ as a photoredox catalyst, (NH₄)₂S₂O₈ as the oxidizing agent, and TFA in CH₃CN/H₂O under a 26 W CFL irradiation, facilitates the formation of α -

oxyalkyl radicals, thereby enabling α -heteroarylation of ethers (Scheme 33).⁵⁴



Scheme 33. 2-Alkylation of heteroarenes

Fu and colleagues outlined a durable, environmentally friendly cascade process for the difunctionalization of *N*-arylacrylamides using aryldiazonium salts (Scheme 34). [Ru(bpy)₃]Cl₂ serves as a photoredox catalyst in methanol under visible light exposure, enabling the synthesis of 3,3-disubstituted oxindoles featuring a broad array of functionalities (e.g., F, Br, Cl, OMe, CN, CF₃, and pyridine). Importantly, no supplementary substances such as bases or reductants were necessary for the reaction to proceed.⁵⁵

Scheme 34. Difunctionalization of *N*-arylacrylamides

2. Conclusion & Outlook

In recent times, photoredox catalysis has emerged as a potent tool in organic synthesis, driving rapid advancements in the field over the past few decades. Overall, it enables the execution of numerous coupling reactions under considerably milder conditions, often at room temperature, while accommodating a wide range of functional groups. This mini-review provides an overview of the fundamental principles of photoredox chemistry, discussing various metal-based and organophotocatalysts. It further explores a variety of reactions, including trifluoromethylation, cyanation, C-H functionalizations, supramolecular catalysis, and heterogeneous catalysis in both aqueous and alcoholic mediums.

Looking ahead, the focus will be on designing and developing new photoredox-mediated sustainable approaches for cascades and multicomponent reactions, particularly aiming at generating multiple C-C and C-heteroatom bonds. This area of research holds significant promise for laying the groundwork for constructing complex organic molecular architectures in a more environmentally friendly manner.

Author Contribution Declaration

Yafia and Partha designed the article, conceived the review plan and write-up strategy with the help of lead author Dr. Bera. The manuscript is finalized by Dr. Bera after discussing with all the authors.

Data Availability Declaration

Write here the data availability declaration. There are no new data were created hence data sharing is not applicable here.

Acknowledgements

We gratefully acknowledge the financial support from Science and Engineering Research Board (SERB), India for

research grant (RJF/2022/000092) under Ramanujan Fellowship.

References

- J. Liu, L. Lu, D. Wood, S. Lin. New Redox Strategies in Organic Synthesis by Means of Electrochemistry and Photochemistry. *ACS Cent. Sci.*, **2020**, 6, 1317. <https://doi.org/10.1021/acscentsci.0c00549>
- M. Bera, D. S. Lee, E. J. Cho. Advances in N-centered intermediates by energy transfer. photocatalysis, *Trends Chem.*, **2021**, 3, 877. <https://doi.org/10.1016/j.trechm.2021.06.001>
- C. S. Wang, P. H. Dixneuf, J. F. Soulé. Photoredox Catalysis for Building C–C Bonds from C(sp²)–H Bonds. *Chem. Rev.*, **2018**, 118, 7532. <https://doi.org/10.1021/acs.chemrev.8b00077>
- G. E. M. Crisenza, P. Melchiorre. Chemistry glows green with photoredox catalysis. *Nat. Commun.*, **2020**, 11, 803. <https://doi.org/10.1038/s41467-019-13887-8>
- T. P. Yoon, M. A. Ischay, J. Du. Visible light photocatalysis as a greener approach to photochemical synthesis. *Nat. Chem.*, **2010**, 2, 527. <https://doi.org/10.1038/nchem.687>
- T. Ghosh, T. Slanina, B. König. Visible light photocatalytic reduction of aldehydes by Rh(III)–H: a detailed mechanistic study. *Chem. Sci.*, **2015**, 6, 2027. <https://doi.org/10.1039/C4SC03709J>
- A. Call, C. Casadevall, F. Acuña-Parés, A. Casitas, J. Lloret-Fillol. Dual cobalt–copper light-driven catalytic reduction of aldehydes and aromatic ketones in aqueous media. *Chem. Sci.*, **2017**, 8, 4739. <https://doi.org/10.1039/C7SC01276D>
- Y. Hou, P. Wan. Formal intramolecular photoredox chemistry of anthraquinones in aqueous solution: photodeprotection for alcohols, aldehydes and ketones. *Photochem. Photobiol. Sci.*, **2008**, 7, 588. <https://doi.org/10.1039/B718970B>
- Y. Hou, L. A. Huck, P. Wan. Long-range intramolecular photoredox reaction via coupled charge and proton transfer of triplet excited anthraquinones mediated by water. *Photochem. Photobiol. Sci.*, **2009**, 8, 1408. <https://doi.org/10.1039/B909479B>
- H. Hou, S. Zhu, F. Pan, M. Rueping. Visible-light photoredox-catalyzed synthesis of nitrones: unexpected rate acceleration by water in the synthesis of isoxazolidines. *Org. Lett.*, **2014**, 16, 2872. <https://doi.org/10.1021/o1500893g>
- M. Goetz, M. Schiewek, M. H. O. Musa. Near-UV Photoionization of [Ru (bpy) 3]²⁺: A Catalytic Cycle with an Excited Species as Catalyst. *Angew. Chem. Int. Ed.*, **2002**, 41, 1535. [https://doi.org/10.1002/1521-3773\(20020503\)41:9<1535::AID-ANGE1535>3.0.CO;2-1](https://doi.org/10.1002/1521-3773(20020503)41:9<1535::AID-ANGE1535>3.0.CO;2-1)
- M. Goetz, D. V. Ramin-Marro, M. H. O. Musa, M. Schiewek. Photoionization of [Ru (bpy) 3]²⁺: A catalytic cycle with water as sacrificial donor. *J. Phys. Chem. A*, **2004**, 108, 1090. <https://doi.org/10.1021/jp036790r>
- Z. J. Xu, D. Xu, X. Zheng, F. Wang, B. Tan, Y. Hu, Y. Lv, G. Zhong. Diastereoselective HOTf-catalyzed three-component one-pot 1,3-dipolar cycloaddition of α -diazo ester, nitrosobenzene and electron-deficient alkene. *Chem. Comm.*, **2010**, 46, 2504. <https://doi.org/10.1039/B924575H>
- A. J. J. Lennox, G. C. L. Jones. Organotrifluoroborate Hydrolysis: Boronic Acid Release Mechanism and an Acid–Base Paradox in Cross-Coupling. *J. Am. Chem. Soc.*, **2012**, 134, 7431. <https://doi.org/10.1021/ja300236k>
- J. J. Dai, W. M. Zhang, Y. J. Shu, Y. Y. Sun, J. Xu, Y. S. Feng, H. J. Xu. Deboronative cyanation of potassium alkyltrifluoroborates via photoredox catalysis. *Chem. Comm.*, **2016**, 52, 6793. <https://doi.org/10.1039/C6CC01530A>
- E. Speckmeier, P. J. W. Fuchs, K. Zeitler. A synergistic LUMO lowering strategy using Lewis acid catalysis in water to enable photoredox catalytic, functionalizing C–C cross-coupling of styrenes. *Chem. Sci.*, **2018**, 9, 7096. <https://doi.org/10.1039/C8SC02106F>
- R. A. Aycock, H. Wang, N. T. Jui. A mild catalytic system for radical conjugate addition of nitrogen heterocycles. *Chem. Sci.*, **2017**, 8, 3121. <https://doi.org/10.1039/C7SC00243B>
- F. Chen, X-H Xu, F-L Qing. Photoredox-catalyzed addition of dibromofluoromethane to alkenes: direct synthesis of 1-bromo-1-fluoroalkanes. *Org. Lett.*, **2021**, 23, 2364. <https://doi.org/10.1021/acs.orglett.1c00639>
- D. Xue, Z. H. Jia, C. J. Zhao, Y. Y. Zhang, C. Wang, J. Xiao. Direct Arylation of N-Heteroarenes with Aryldiazonium Salts by Photoredox Catalysis in Water. *Chem. Eur. J.*, **2014**, 20, 2960. <https://doi.org/10.1002/chem.201304120>
- J. Zhang, J. Chen, X. Zhang, X. Lei. Total Syntheses of Menisporphine and Daurioxoisoporphine C Enabled by Photoredox-Catalyzed Direct C–H Arylation of Isoquinoline with Aryldiazonium Salt. *J. Org. Chem.*, **2014**, 79, 10682. <https://doi.org/10.1021/jo5020432>
- H. Qiao, S. Sun, F. Yang, Y. Zhu, J. Kang, Y. Wu, Y. Wu. Merging Photoredox Catalysis with Iron (III) Catalysis: C5–H Bromination and Iodination of 8-Aminoquinoline Amides in Water. *Adv. Synth. Catal.*, **2017**, 359, 1976. <https://doi.org/10.1002/adsc.201601053>
- D. Jespersen, B. Keen, J. I. Day, A. Singh, J. Biles, D. Mullins, J. D. Weaver III. Solubility of Iridium and Ruthenium Organometallic Photoredox Catalysts. *Org. Process Res. Dev.*, **2018**, 23, 1087. <https://doi.org/10.1021/acs.oprd.9b00041>
- R. C. W. van Lier, A. D. de Bruijn, G. Roelfes. A Water-Soluble Iridium Photocatalyst for Chemical Modification of Dehydroalanines in Peptides and Proteins. *Chem. Eur. J.*, **2021**, 27, 1430. <https://doi.org/10.1002/chem.202002599>
- T.-T.H. Nguyen, C. J. O'Brien, M. L.N. Tran, S. H. Olson, N. S. Settineri, S. B. Prusiner, N. A. Paras, J. Conrad. Water-soluble iridium photoredox catalyst for the trifluoromethylation of biomolecule substrates in phosphate buffered saline solvent. *Org. Lett.*, **2021**, 23, 3823. <https://doi.org/10.1021/acs.orglett.1c00871>
- D. Brüssel, P. Bauduin, L. Girard, A. Zaulet, C. Viñas, F. Teixidor, I. Ly, O. Diat. Lyotropic lamellar phase formed from monolayered θ -shaped carborane-cage amphiphiles. *Angew. Chem. Int. Ed.*, **2013**, 52, 12114. <https://doi.org/10.1002/anie.201307357>
- M. Tarres, C. Vinas, P. González-Cardoso, M. M. Hänninen, R. Sillanpää, V. Đorđović, M. Uchman, F. Teixidor, P. Matějček. Aqueous self-assembly and cation selectivity of cobaltabisdicarbollidedianionic dumbbells. *Chem. Eur. J.*, **2014**, 20, 6786. <https://doi.org/10.1002/chem.201402193>
- M. Uchman, V. Đorđović, Z. Tošner, P. Matějček. Classical amphiphilic behavior of nonclassical amphiphiles: a comparison of metallacarborane self-assembly with SDS micellization. *Angew. Chem.*, **2015**, 127, 14319. <https://doi.org/10.1002/ange.201506545>
- I. Guerrero, Z. Kelemen, C. Viñas, I. Romero, F. Teixidor. Metallacarboranes as Photoredox Catalysts in Water, Metallacarboranes as Photoredox Catalysts in Water. *Chem. Eur. J.*, **2020**, 26, 5027. <https://doi.org/10.1002/chem.201905395>
- I. Guerrero, C. Viñas, I. Romero, F. Teixidor. A stand-alone cobalt bis (dicarbollide) photoredox catalyst epoxidates alkenes in water at extremely low catalyst load. *Green Chem.*, **2021**, 23, 10123. <https://doi.org/10.1039/D1GC03119H>
- I. Guerrero, A. Saha, J. A. M. Xavier, Clara Vinas, I. Romero, F. Teixidor. Noncovalently linked metallacarboranes on functionalized magnetic nanoparticles as highly efficient, robust, and reusable photocatalysts in aqueous medium. *ACS Appl. Mater. Interfaces.*, **2020**, 12, 56372. <https://doi.org/10.1021/acsami.0c17847>
- G. Troyano, I. C. Viñas, X. Fontrodona, I. R. García, F. T. Bombardó. Aqueous Persistent Noncovalent Ion-Pair Cooperative Coupling in a Ruthenium Cobaltabis (dicarbollide) System as a Highly Efficient Photoredox Oxidation Catalyst. *Inorg. Chem.*, **2021**, 60, 8898. <https://doi.org/10.1021/acs.inorgchem.1c00751>
- S. Srinath, R. Abinaya, A. Prasanth, M. Mariappan, R. Sridhar, B. Baskar. Reusable, homogeneous water soluble photoredox catalyzed oxidative dehydrogenation of N-heterocycles in a biphasic system: application to the synthesis of biologically active natural products. *Green Chem.*, **2020**, 22, 2575. <https://doi.org/10.1039/D0GC00569J>
- M.-j. Bu, C. Cai, F. Gallou, B. H. Lipshutz. PQS-enabled visible-light iridium photoredox catalysis in water at room temperature. *Green Chem.*, **2018**, 20, 1233. <https://doi.org/10.1039/C7GC03866F>
- N. A. Romero, D. A. Nicewicz. Organic photoredox catalysis. *Chem. Rev.*, **2016**, 17, 10075. <https://doi.org/10.1021/acs.chemrev.6b00057>
- D. P. Hari, B. König. Synthetic applications of eosin Y in photoredox catalysis. *Chem. Comm.*, **2014**, 50, 6688. <https://doi.org/10.1039/C4CC00751D>
- K. A. Margrey, D. A. Nicewicz. A general approach to catalytic alkene anti-Markovnikov hydrofunctionalization reactions via acridinium photoredox catalysis. *Acc. Chem. Res.*, **2016**, 49, 1997. <https://doi.org/10.1021/acs.accounts.6b00304>
- M. Majek, A. J. V. Wangelin. Mechanistic perspectives on organic photoredox catalysis for aromatic substitutions. *Acc. Chem. Res.*, **2016**, 49, 2316. <https://doi.org/10.1021/acs.accounts.6b00293>
- M.-j. Bu, G.-p. Lu., J. Jiang, C. Cai. Merging visible-light photoredox and micellar catalysis: arylation reactions with anilines nitrosated in situ. *Catal. Sci. Technol.*, **2018**, 8, 3728. <https://doi.org/10.1039/C8CY01221K>
- L. J. Gooßen, N. Rodríguez, K. Gooßen. Carboxylic acids as substrates in homogeneous catalysis. *Angew. Chem. Int. Ed.*, **2008**, 47, 3100. <https://doi.org/10.1002/anie.200704782>
- W.-P. Mai, G. Song, G.-C. Sun, L.-R. Yang, J.-W. Yuan, Y.-M. Xiao, P. Mao, L. –B. Qu. Cu/Ag-catalyzed double decarboxylative cross-coupling reaction between cinnamic acids and aliphatic acids in aqueous solution. *RSC Adv.*, **2013**, 3, 19264. <https://doi.org/10.1039/C3RA43144D>
- H. Yang, H. Yan, P. Sun, Y. Zhu, L. Lu, D. Liu, G. Rong, J. Mao. Iron-catalyzed direct alkenylation of sp³ C–H bonds via decarboxylation of cinnamic acids under ligand-free conditions. *Green Chem.*, **2013**, 15, 976. <https://doi.org/10.1039/C3GC37131J>
- H. Huang, K. Jia, Y. Chen. Hypervalent Iodine Reagents Enable Chemoselective Deboronative/Decarboxylative Alkenylation by Photoredox Catalysis. *Angew. Chem.*, **2015**, 127, 1901. <https://doi.org/10.1002/ange.201410176>
- H. Huang, G. Zhang, Y. Chen. Dual Hypervalent Iodine(III) Reagents and Photoredox Catalysis Enable Decarboxylative Ynylation under Mild Conditions. *Angew. Chem.*, **2015**, 127, 7983. <https://doi.org/10.1002/ange.201502369>
- S. Mizuta, K. M. Engle, S. Verhoog, O. G. López, M. O'Duill, M. Médebielle, K. Wheelhouse, G. Rassias, A. L. Thompson, V.

- Gouverneur. Trifluoromethylation of allylsilanes under photoredox catalysis. *Org. Lett.*, **2013**, *15*, 1250. <https://doi.org/10.1021/ol400184t>
45. D. K. Kölmel, R. P. Loach, T. Knauber, M. E. Flanagan. Employing Photoredox Catalysis for DNA-Encoded Chemistry: Decarboxylative Alkylation of α -Amino Acids. *ChemMedChem*, **2018**, *13*, 2159. <https://doi.org/10.1002/cmdc.201800492>
46. D. K. Kölmel, J. Meng, M.-H. Tsai, J. Que, R. P. Loach, T. Knauber, J. Wan, M. E. Flanagan. On-DNA decarboxylative arylation: merging photoredox with nickel catalysis in water. *ACS Comb. Sci.*, **2019**, *21*, 588. <https://doi.org/10.1021/acscombsci.9b00076>
47. N. Noto, Y. Hyodo, M. Yoshizawa, T. Koike, M. Akita. Transition Metal-Free Supramolecular Photoredox Catalysis in Water: A Phenoxazine Photocatalyst Encapsulated in V-Shaped Aromatic Amphiphiles. *ACS Catal.*, **2020**, *10*, 14283. <https://doi.org/10.1021/acscatal.0c04221>
48. D. Kalyani, K. B. McMurtrey, S. R. Neufeldt, M. S. Sanford. Room-temperature C–H arylation: merger of Pd-catalyzed C–H functionalization and visible-light Photocatalysis. *J. Am. Chem. Soc.*, **2011**, *133*, 18566. <https://doi.org/10.1021/ja208068w>
49. L. Liang, M.-S. Xie, H.-X. Wang, H.-Y. Niu, G.-R. Qu, H.-M. Guo. Visible-light-mediated monoselective ortho C–H arylation of 6-aryluracil nucleosides with diazonium salts. *J. Org. Chem.* **2017**, *82*, 5966. <https://doi.org/10.1021/acs.joc.7b00659>
50. J. Jiang, W.-M. Zhang, J.-J. Dai, J. Xu, H.-J. Xu. Visible-light-promoted C–H arylation by merging palladium catalysis with organic photoredox catalysis. *J. Org. Chem.*, **2017**, *82*, 3622. <https://doi.org/10.1021/acs.joc.7b00140>
51. D. Xue, Z.-H. Jia, C.-J. Zhao, Y.-Y. Zhang, C. Wang, J. Xiao. Direct Arylation of N-Heteroarenes with Aryldiazonium Salts by Photoredox Catalysis in Water. *Chem. Eur. J.*, **2014**, *20*, 2960. <https://doi.org/10.1002/chem.201304120>
52. T. McCallum, L. Barriault. Direct alkylation of heteroarenes with unactivated bromoalkanes using photoredox gold catalysis. *Chem. Sci.*, **2016**, *7*, 4754. <https://doi.org/10.1039/C6SC00807K>
53. S. R. Kandukuri, A. Bahamonde, I. Chatterjee, I. D. Jurberg, E. C. Escudero-Adán, P. Melchiorre. X-Ray Characterization of an Electron Donor–Acceptor Complex that Drives the Photochemical Alkylation of Indoles. *Angew. Chem. Int. Ed.*, **2015**, *54*, 1485. <https://doi.org/10.1002/anie.201409529>
54. J. Jin, D. W. C. MacMillan. Direct α -Arylation of Ethers through the Combination of Photoredox-Mediated C–H Functionalization and the Minisci Reaction. *Angew. Chem.*, **2015**, *127*, 1585. <https://doi.org/10.1002/ange.201410432>
55. W. Fu, F. Xu, Y. Fu, M. Zhu, J. Yu, C. Xu, D. Zou. Synthesis of 3, 3-disubstituted oxindoles by visible-light-mediated radical reactions of aryl diazonium salts with N-arylacrylamides. *J. Org. Chem.*, **2013**, *78*, 12202. <https://doi.org/10.1021/jo401894b>

Polypharmacological Constituents and Potential Activities of *Bergenia ciliata*: A Concise Review

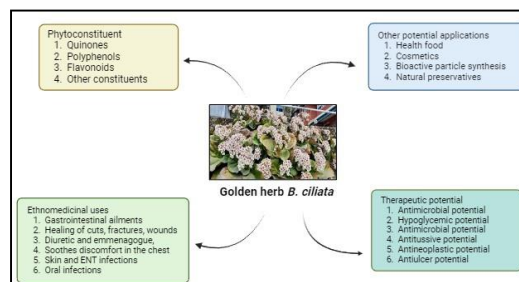
Nirza Moktan^{a,b}, and Anindita Banerjee^{b*} 

^aDepartment of Microbiology, Dhruva Chand Halder College, Dakshin Barasat, West Bengal, India.

^bUG, PG & Research Department of Microbiology, St. Xavier's College (Autonomous), Kolkata, West Bengal, India.

*Correspondence: anindita.banerjee@sxccal.edu

Abstract: *Bergenia ciliata* is an evergreen perennial herb belonging to the family Saxifragaceae and has been employed in traditional medicine since long. When compared to pharmaceutical medication, traditional herbal medicine is seen as the lifeline and the first option. Due to *Bergenia ciliata*'s wide range of biological activity, several traditional uses have been documented. Investigations into the discovery of its phytochemicals, chemistry, pharmacology, and medicinal use of *Bergenia* plants have been conducted in recent years. It is reported to be beneficial in breaking up bladder and kidney stones, it also aids in the removal of blockages and hazardous waste products from alimentary canal and urinary system. Additionally, it relieves pain in the ribs and chest brought on by too much cold humour and is a great emmenagogue and diuretic. It also exhibits hepato & nephro-protective, antidiabetic, antioxidant, and bio prospective qualities. *Bergenia ciliata* when subjected to a polypharmacological composition screening, identified the presence of tannins, steroids, flavonoids, terpenoids, alkaloids, and saponins. *Bergenia ciliata* has a potential use in pharmacology and medicine because of the presence of plethora of polyphenols. The purpose of this article is to compile and evaluate the existing data about the phytochemistry and potential activities of *Bergenia ciliata*.



Keywords: *Bergenia ciliata*, ethnomedicine, phytochemicals, pharmacological potential.

Contents

Biographical Information	58
1. Introduction	58
2. Review Methodology	60
3. Polypharmacological Constituents	60
3.1. Polyphenols	60
3.2. Flavonoids	60
3.3. Other Phytochemicals	60
4. Ethnomedicinal Uses	61
5. Pharmacological and Therapeutic Potential	61
5.1. Antimicrobial Potential	61
5.2. Hypoglycemic Potential	61
5.3. Antioxidant Potential	62
5.4. Antitussive Potential	62
5.5. Antineoplastic Potential	62
5.6. Antiulcer Potential	62
6. Other Potential Applications of <i>Bergenia Ciliata</i>	62
6.1. Health Foods	62
6.2. Cosmetics	62
6.3. Synthesis of Bioactive Nanoparticles	62
6.4. Natural Preservative	62
7. Discussion and Way Forward	63
8. Conclusion	63
Author Contribution Declaration	63
Data Availability Declaration	63
Acknowledgements	63
References	63

1. Introduction

Natural products are a crucial source of many important pharmacological compounds. In many developing countries 80% of population still exclusively depend on traditional or herbal medicine for treating diseases. Many contemporary medications are developed from ancient herbal medicine and are being utilized in modern pharmacotherapy as alternative or complementary medicine.¹ Traditional medicine system in many parts around the world have been using medicinal plants for thousands of years.^{2,3} The empirical information regarding the beneficial impacts of medicinal plants and herbal products have been handed down along different ethnic communities throughout ages.²

Nirza Moktan completed her B.Sc and M.Sc degrees from the University of North Bengal, West Bengal (W.B.), India and she is a PhD scholar in the Department of Microbiology, St. Xavier's College (Autonomous), Kolkata. Her research interests focus on traditional and ethnomedicine, as well as plant secondary metabolites. She is also working as an Assistant Professor in the Department of Microbiology, Dhruva Chand Halder College, Dakshin Barasat, WB, India. She enjoys reading books, painting, and finds solace in mother nature.



Dr. Anindita Banerjee completed her Ph.D. the CSIR-Indian Institute of Chemical Biology, Kolkata (W.B.), India on plant biotechnology and currently working as an Assistant Professor in the Department of Microbiology, UG, PG & Research Department of Microbiology, St. Xavier's College (Autonomous), Kolkata. Her research interests include exploring plant extracts and cell suspension cultures to extract new antibacterial compounds, assessing their antimicrobial properties, and chemically characterizing these compounds for use in combinatorial drug therapy against microbes.



A vital step in the investigation of the bioactive compounds derived from plant sources is the extraction process. Modern extraction techniques, like ultrasound-assisted and supercritical fluid extraction methods, are currently being used in addition to more conventional approaches.⁴ The ethnobotanical and ethnopharmacological research have drawn interest from scientists worldwide. Numerous medicinal plants' phytochemical makeup and possible health advantages have not yet been investigated or needs to be more deeply investigated, and thus has a hopeful future for further drug development and research.

The introduction of sophisticated instruments for the qualitative and quantitative evaluation of phytochemical, such as HPLC (high-performance liquid chromatography) and (LC/MS) (liquid chromatography/mass spectrometry) has greatly enhanced phytochemical research. Phytochemical though of various kinds can be broadly categorized as polyphenols, alkaloids, glycosides, flavonoids, tannins, resins, gums and terpenes.

The synergistic effects of plant secondary metabolites together result in the useful therapeutic properties. The curative properties of medicinal plants present a mostly untapped pool of possible drug sources.⁵ Bioactivity of phytochemical synergistically in a single plant extract is an unmatched

challenge for individual synthetic medications to match. We propose that plant templates could be used to create "hybrid phytochemicals" that replicate this synergistic effect.



Figure 1. *Bergenia ciliata* (a) Flowers (b) Leaves (c) Rhizome and (d) Whole plant

Herbal remedies represent the medical industry's future. Worldwide, traditional medicine and phytomedicines are becoming more and more well-known. In 2012, it was estimated that the yearly value of the global export of plants with potentially therapeutic qualities and traits was around USD 2.2 billion.⁶ Three main types of benefits are frequently associated with medicinal plants: economic gains for those who harvest, process, sell, or distribute them; health benefits for those who use them as medications; and societal benefits like increased tax revenue, employment possibilities, and a more robust labor force.⁷ Herbal nutritional supplements, herbal cosmetics, and herbal health care formulations are being produced with renewed interest in the pharmaceutical sector due to the growing demand for items derived from medicinal plants. Herbal remedies represent the medical industry's future. Worldwide, traditional medicine and phytomedicines are becoming more and more well-known.

Bergenia ciliata (haw.) Sternb is a member of the family Saxifragaceae, which comprises of 30 genera and 580 species.^{8,9,10} Within the family Saxifragaceae, the three genera *Saxifrage*, *Heuchera*, and *Bergenia* hold the greatest economic significance. *Bergenia* refers to a genus of around 10 distinct species of flowering plants.¹¹ Three species of *Bergenia* have been documented from India, by Hooker in the Flora of British India (1888). Similar reports have also been documented by Wehmer in The Wealth of India (1948). *Bergenia ciliata*, *Bergenia ligulata* and *Bergenia stracheyi* are the important species of *Bergenia* found in India.

Bergenia is a hardy perennial plant indigenous to the cold and temperate Himalayan region at an altitude of around 4000 to 12000 feet stretching from Central to East Asia.^{12,13} It remains distributed in Afghanistan, Pakistan, South Tibet, China, Mongolia, India, Nepal, Bhutan.^{14,15,16,17} In India it remains distributed in the Himalayan regions of Eastern states such as West Bengal, Sikkim, Uttarakhand, Meghalaya, Jammu and Kashmir.^{15,17,18} In Bhutan it occurs in districts of Ha, Phuntsoling, Mongar, Deothang. In Nepal it is found to be distributed in districts of Dolakha, Karepalanchwok, Makenwanpur.^{14,19,20} In Pakistan it occurs in northern regions mainly, Chitral, Poonch valley, Swat, Abbottabad, Galliyat.^{13,21,22}

Bergenia thrives well even under unfavorable weather conditions and nutrient deficient soil. It exhibits lithotrophic characteristic, as it grows between the rocks and gives the impression that it is breaking them. As a result, the plant is sometimes referred to as rock foil in English and Paashanbheda (bheda = perforating, paashan = rock stone) in Hindi. These evergreen perennials which are around 50 cm in height gracefully occupies the shaded or dappled areas of the garden that other plants like to avoid. They make useful cover plants. While plants can withstand direct sunlight, they thrive well in location with moisture-retaining soil that is shaded in the afternoon. They have broadly obovate, thick leaves, which are rounded at the base and apex. Soft hairs skirt the delicately denticulated and densely ciliated leaf edges. Leaves are opposing, alternating, and ex-stipulative. Flowers are beautiful pinkish white, purple with obovate petals, lobed acute and denticulated near the apex. The basal whorl does not instantly

support the bunch of blossoms in the plant, rather it lies well above. Flowers bloom in springtime from the months of February to April. Fruiting period is March to July.^{15,17,23} Rhizomes exhibits a woody texture and are coated in leaf bases. The plant can grow all year round. The whole plant and its parts are shown in **Figure 1**. Numerous traditional applications of *Bergenia* have been reported due to its diverse biological activity. It is widely utilized in traditional medicine systems throughout many different locations, particularly in Asian nations like India, Pakistan, Nepal, China, Bhutan. Of the three species of *Bergenia* listed, *Bergenia ciliata* is the one that is most frequently used in traditional medicine and has been shown to have antibacterial, antioxidant, antitussive, antiulcer, hypoglycemic, toxicological, anticancer, and ant-adiabatic properties.²⁴

Many rural populations in the Himalayan area employ *B. ciliata* for treating a variety of illnesses. Over the past few years, efforts have been undertaken to investigate the compound identification, chemistry, pharmacology, and therapeutic use of *Bergenia* plants.^{12,25} It has been demonstrated that *B. ciliata* rhizome extracts possess antimicrobial and antitussive qualities.^{26, 27} Bergenin, an important constituent of *Bergenia* is used to manufacture expectorant and antitussive medications in China. Furthermore, fresh leaf paste is applied to the skin in Tibet to shield from UV radiation. Traditionally in the Himalayan regions, the leaf or leaf juice is used to ease earaches and constipation. *Bergenia* species are used in ayurvedic treatments to dissolve kidney and bladder stones in India.³ However, because people use drugs differently in different countries and areas, the pharmacological consequences vary significantly as well. As a result, contemporary pharmacological research based on the plant's traditional applications is required.

Table 1. 3 Pharmacological constituents *Bergenia ciliata*

Groups	Bioactive compounds	References
Quinones	Hydroquinone, Aloe emodin, Chrysophanein, Aloe emodin 8-O-glucoside, Emodin 1-O-β-D-glucopyranoside, Hydroquinone monomethylether	31,74
Polyphenols	Bergenin, Tannic acid, Gallic acid, Catechin, 3-O-galloylecatechin, 3-O-galloylepicatechin, Arbutin, β-sitosterol, Stigmasterol, Methyl gallate, Paashaanolactone	18, 15, 37
Flavonoids	Kaempferol, (+) Afzelechin, quercetin 3-o-β-D xylopyranoside, quercetin 3-o-α-L-arabinofuranoside, 4',5 - dihydroxy 6,7-dimethoxyflavone, Luteolin -7-O-glucoside A, Acacetin-7-O-α-L-rhamnopyranoside	15, 17
Others	Saponin, Terpenes, Glycoside, Amino acids, Volatile oils, Sterols.	18, 19, 20

It is reported to be beneficial in clearing kidney-stones and bladder stones. Additionally, it aids in the removal of waste materials and obstacles that are still present in the urinary system and alimentary canal. Certain species are used to treat

gastrointestinal ailments in various South East Asian folk medicine.¹⁵ Additionally, plants are used as a demulcent and deobstruent, it also works as an excellent diuretic and emmenagogue and soothes discomfort in the chest and ribs caused by excessive cold humours. There are also reports on the anti-oxidant and the DNA protection abilities of the extracts.²⁸ The antioxidant, antidiabetic, hepato & nephro-protective, and bio prospective properties of *Bergenia ciliata* were investigated. Histological investigations showed that daily treatment of the extract in a dose-dependent manner also resulted in the regeneration of islets of Langerhans α -cells were investigated. Histological investigations showed that daily treatment of the extract in a dose-dependent manner also resulted in the regeneration of islets of Langerhans α -cells.²⁹

2. Review Methodology

Searching pertinent literature on *B. ciliata* was the first step in our information gathering process. To provide succinct and creative information about the geographical distribution, phytochemistry, indigenous medicinal uses, and pharmacological characteristics of the *Bergenia* species, a systematic review of the current literature (abstracts, blogs, full-text articles, PhD theses, and books) was conducted. Google Scholar, Web of Science, Science Direct, Scopus, PubMed as well as CAB abstracts, INMEDPLAN, NATTS, EMBASE, SciFinder, and MEDLINE, were among the several online databases and search engines that were employed for this purpose. Only publications that were published in the English language were considered for this review and thus a total of 75 references were selected for detailed analysis.

3. Polypharmacological Constituents

The natural world contains a vast reservoir of incredibly creative and diverse phytoconstituents. There has been a noticeable growth in demand for herbal medications over the past 20 years, making it necessary to guarantee the efficacy, safety, and quality of these products. Phytochemical evaluation, which comprises chemo profiling, phytochemical screening, and marker compound analysis, is a tool for quality evaluation.^{30,31} Polypharmacological composition characterization of *B. ciliata*, revealed the presence of steroids, tannins, flavonoids, terpenoids, alkaloids and saponins.^{12,31,32} Eleven major groups of phytochemicals found in *B. ciliata* were reported.⁸ The roots, stems, and leaves of *B. ciliata* are rich in various bioactive components which can be broadly divided into three major groups viz., quinones, flavonoids, and polyphenols as shown in Table 1

3.1 Polyphenols

While the entire *Bergenia* plant can be utilized medicinally, the majority of its active components have been found to be polyphenols, among which bergenin is one that has been researched and most widely used.³³ Bergenin and gallic acid were simultaneously determined in many *Bergenia* species. The highest amounts of bergenin were detected in *B. ciliata* and *B. stracheyi*, at 3.28 and 3.28%, respectively while *B. ligulata* had 2.42 %.³⁴ Terpenoids, tannins, flavonoids, saponins, minerals, wax, mucilage and ketone, two -containing compounds, are some prominent constituents found in *B. ciliata*.^{35,36} The most significant components of *B. ciliata* are phenols. *B. ciliata* contains a variety of phenolic compounds, including bergenin, paashaanolactone, tannic acid, gallic acid, catechin. The primary component of the *Bergenia* species is the important phenolic chemical "bergenin," which makes up over 0.9% of the total. Other phenolic compounds are present in smaller amounts.³⁷ Afzelechin, leucocyanidin, gallic acid, tannic acid, paashaanolactone, 7-O- β -D-glucopyranoside and methyl gallate are among the phenolic chemicals that have been included.

Bergenin is the most prevalent and significant phytochemical found in the family Saxifragaceae. Bergenin containing plants are beneficial for arrhythmias. In several animal models, bergenin at different doses proved

beneficial for treating arrhythmias.³⁸ Bergenin shown germicidal effects against *Pseudomonas aeruginosa* and *E. coli*. Due to its ability to inhibit yeast alcohol dehydrogenase, an enzyme essential for fermentation activities, bergenin is also efficient against fungi.³⁹ Bergenin has a significant function in the breakdown of fats, which is why it is a common ingredient in dietary supplements that promote thermogenic fat burning. Although it doesn't directly contribute to lipolysis, it does boost norepinephrine activity.

Gallic acid is another important phenolic compound present in *B. ciliata*. Gallic acid is commonly used as a standard in the Folin-Ciocalteu test to measure the phenol concentration. Gallic acid present in the plant confers it with properties such as antiviral, antifungal, and antioxidant. In ointments, it is used to treat psoriasis. For the purpose of simultaneously determining the bioactive compounds bergenin and gallic acid in three species of *Bergenia*-*B. ligulata*, *B. ciliata*, and *B. stratcheyia*-a straightforward and extremely accurate approach has been developed through the use of highly precise photodiode-array paired with RP-HPLC technique. From this method the highest amount of bergenin were detected in *B. ciliata* and *B. stracheyi*, with 3.28 and 3.28%, respectively, while *B. ligulata* had 2.42%.^{30,33,40} Tannic acid is essentially a polyphenol called tannin that is found in *B. ciliata*. There are several other names for tannic acid, including digallic acid, gallotannin, tanninum, quercotannic acid, Because of the many phenol groups that are present in its structure, tannic acid exhibits modest acidity. Tannic acid has the ability to protect iron objects from corrosion. It is also used as a natural clarifying agent, colour stabiliser and flavour enhancer. Tannic acid can be effectively used to treat burns and injuries. Pharmaceutical companies employ tannic acid as an antihistamine, anti-diarrhoea and anti-tussive.^{27,41,42,43}

Catechin or Flavan-3-ol is a kind of phenol that is linked to epicatechin or (+)-catechin and is found in plants as a secondary metabolite. As a histidine decarboxylase inhibitor, catechin helps to reduce potentially harmful histamine-related local immunological responses by blocking the conversion of histidine to histamine. Both epicatechin and (+)-catechin are inhibitors of monoamine oxidase. With these, Alzheimer's and Parkinson's disease can be managed.^{10,17,44,45}

β -sitosterol is a white, waxy, hydrophobic powder with a distinct scent.⁴⁶ As β -sitosterol has a significant role in lowering blood cholesterol levels, preventing intestinal absorption of cholesterol it is used to treat hypercholesterolemia. Benign prostatic hyperplasia is also treated with β -sitosterol.

Arbutin is found to be present in the rhizome of *B. ciliata* and is also known as hydroquinone β -D-glucopyranoside.⁴⁷ Arbutin inhibits the production of melanin, which is why it is employed as a skin-lightening agent. It is also traditionally utilized for treating urinary tract infection.^{48,49}

3.2. Flavonoids

Numerous biological activities, including antibacterial, antioxidant, anti-inflammatory, and anticancer properties have been widely linked to flavonoids. (+) Afzelechin a flavonoid present in the rhizome of *B. ciliata* exhibits inhibitory action against α -glucosidase.^{18,50}

Quercetin exhibits antioxidant, anti-radical and iron chelating properties. Additionally, quercetin lowers oxidative stress and lipid peroxidation, which helps control diabetes and its consequences.^{12,51,52}

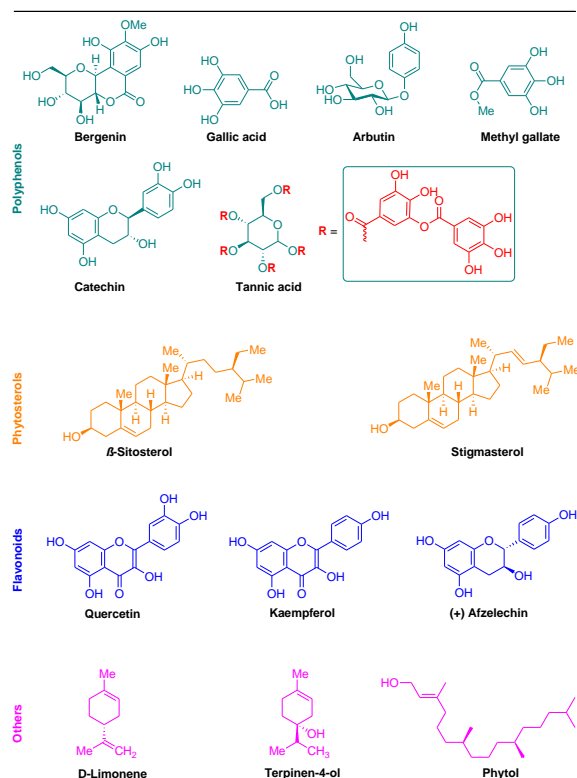
Kaempferol is shown to have antimicrobial, neuroprotective, anti-inflammatory, antioxidant, anti-anxiety, and cognitive-enhancing properties.

3.3. Other phytochemicals

Terpene present in *B. ciliata* is limonene which has antibacterial properties and is also used in chemotherapy. Linalool is a food additive that exhibits bioactivities. β -caryophyllene and α -Terpineol are also present in *B. ciliata*.³⁵ Due to spicy and woody aroma, β -caryophyllene is utilized as a fragrance ingredient while α -Terpineol exhibits antispasmodic, anti-inflammatory, antitumor properties and is a myorelaxant.^{53,54,55}

The fatty acids found in *B. ciliata* are decanoic acid, nonanoic acid.²⁰ While nonanoic acid has herbicidal properties, decanoic acid demonstrates antibacterial and antifungal properties.

Table 2. Structures of important phytochemicals found in *Bergenia ciliata*.



4. Ethnomedicinal Uses

The last ten years have seen a phenomenal resurgence in interest and use of therapeutic plant products. Herbal remedies are more efficient than allopathic remedies in treating a variety of illnesses and have no adverse effects. Compared to the contemporary synthetic medications, their method of therapy is more affordable and accessible.⁵⁶

B. ciliata has historically been used for a variety of medical purposes in traditional medicine systems across the globe, especially in Asian countries like Pakistan, Nepal, and India. Given its wide range of applications in the treatment of ailments such as gastrointestinal issues, lung infections, cardiac conditions, ophthalmic conditions, haemorrhoids, kidney, and gall bladder stones, *B. ciliata* is regarded as a "miracle herb." Studies have indicated that the species is utilized to cure gastrointestinal ailments in some South East Asian traditional medicine.^{15,57} Chronic dysenteries may be effectively treated with boiling the juice of crushed *B. ciliata* rhizome in water. The rhizome of *Bergenia* has long been used in the Himalayan region to heal cuts, fractures, wounds, treat respiratory infections, treat gastrointestinal disorders, diarrhoea.^{20,58} In the state of Sikkim and the regions under the Darjeeling district of West Bengal, traditional healers and residents have been employing the rhizome of *B. ciliata* in the form of juice as an antitussive medication.⁵⁹ Additionally, it was used to cure ophthalmia, haemorrhoids, stomach problems, and heart disease. Adults in Nepal have been using the rhizomes of *B. ciliata* as an anthelmintic. In Nepal, postpartum women take one tea spoonful of the juice from the dried rhizome of *B. ciliata* with honey orally two to three times a day as a carminative and tonic for digestive issues. Asthma has reportedly been treated using boiled *B. ciliata* roots combined with salt. In Manipur, *B. ciliata* leaves and roots were also utilized to cure blood cancer.⁶⁰ The extracts offer great potential for the production of medications that may target tumours and further inhibit the growth and aggressiveness of neoplastic growth.³ The plant also functions as an excellent diuretic and emmenagogue,

soothes discomfort in the chest and ribs caused by severe cold humours, and is demulcent and deobstruent. *Bergenia* is combined with other plants in the Indian Ayurvedic polyherbal preparation "Cystone," which is used to treat urolithiasis. To promote the growth of milk teeth, the root and honey combination is administered. The leaves are crushed in a mortar and the juice is used to treat ear infections in the Indo-Chinese region.

Reportedly, *B. ciliata* plant is maximally used for treating gastrointestinal infections (23%), followed by skin illnesses (17%), respiratory diseases (8%), muscular/skeletal disorders (10%), eye diseases, oral infections, worm infections, gynecological infections (3%), ENT, and cancer.^{8,53} *B. ciliata* reportedly had the highest UV (0.87) and RFC (0.36) values which is an indication of a plant being widely distributed and well known by the indigenous community for their therapeutic potentials. There are reports of the use of *B. ciliata* rhizome for treating toothache and tooth decay.⁵⁵ Decoction, juice, paste, powder, tea, and extract were among the methods of use or preparations. It was seen that powder was the most widely used form, this might be because roots and rhizome are hard.⁶¹

5. Pharmacological and Therapeutic Potential

5.1. Antimicrobial Potential

The primary global cause of the rising incidence of infectious illnesses is bacteria which is a serious public health issue.⁴³ The increasing demands for natural antioxidants and antimicrobial medications has necessitated the need to look for new natural sources. Different extracts of *B. ciliata* plant were utilized to combat human pathogens. Aqueous, ethanol, butanol, ethyl acetate, chloroform and hexane extracts of *B. ciliata* roots and leaves when subjected to antibacterial activity exhibited promising outcomes against both gram positive and gram-negative bacteria.^{26,62,63}

Comparably, it was shown that extracts of *B. ciliata* roots and leaves has antifungal properties and worked well against *Candida albicans*, *Pleurotus ostreatus*, and *Microsporum canis*.¹³ By preventing yeast alcohol dehydrogenase, an enzyme essential for fermentation processes, bergenin has germicidal activity against a variety of fungi and has been shown to be efficient against *E. coli* and *Pseudomonas aeruginosa*.^{64,65}

Methanolic extract from *B. ciliata* suppressed HSV-1, influenza virus, herpes simplex virus. *B. ciliata* methanolic and methanolic aqueous extract showed potent anti-influenza viral activity. The findings suggest that *B. ciliata* could be a powerful source of antiviral drugs.^{27,32}

The antibacterial activity of *B. ciliata* root extract is reported to be much higher than that of the leaf extract.^{10,15} This might be because *B. ciliata*'s roots and rhizome have higher concentrations of active chemicals than its leaves.

5.2. Hypoglycemic Potential

The mode of action of *B. ciliata* as an anti-diabetic plant was first published in literature by some researchers.⁶⁶ They proposed that the plant's ability to reduce glucose levels is due to its suppression of the digestive enzymes α -glucosidase and α -amylase. The ability of *B. ciliata* extracts to reduce blood sugar levels in rats treated with streptozotocin (STZ) was used to assess their hypoglycemic activity. The ethanolic extract of *B. ciliata* leaves was shown to bring about a 70.13% reduction in blood glucose levels, aqueous extract decreased blood glucose levels by 71.34%, ethyl acetate extracts by 45.67 %. However, there has been no discernible drop in glucose levels or hypoglycemic action in the extract treated with hexane and butanol. Similarly, the ethanolic extract of *B. ciliata* rhizomes was shown to bring about a 71.34 % reduction in blood glucose levels, hexane extract decreased blood glucose levels by 70.13 %, ethyl acetate extract by 57.88 %.¹³ These investigations show that the *Bergenia ciliata* has promising antidiabetic property. Two active compounds, (-)-3-O-

galloyl catechin and (-)-3-O-galloyl catechin, which were isolated showed potential anti-diabetic activity.^{4,34,66}

Table 3. Some important phytoconstituents of the golden herb *B. ciliata* and its uses

Sl.No	Compound name	Chemical Formula	Activity	References
1	Bergenin	C ₁₄ H ₁₆ O ₉	Antioxidant, antimicrobial, norepinephrine, lipolysis anarctic effect	38, 39
2	Gallic acid	C ₇ H ₆ O ₅	Antioxidant, Antifungal, Antiviral, Cytotoxicity	33
3	Tannic acid	C ₇₆ H ₅₂ O ₄₆	Anti-corrosive, clarifying agent, colour stabiliser, flavour enhancer, pharmaceutical applications	32
4	Catechin	C ₁₅ H ₁₄ O ₆	histidine decarboxylase inhibitor, monoamine oxidase inhibitor.	10
5	β-sitosterol	C ₂₉ H ₅₀ O	Treating hyper cholesterolemia, Benign prostatic hyperplasia, lowering cholesterol	46
6	Arbutin	C ₁₂ H ₁₆ O ₇	Melanin inhibitor	48
7	(+) Afzelechin	C ₁₅ H ₁₄ O ₅	α-glucosidase inhibitor	18, 50
8	Quercetin	C ₁₅ H ₁₀ O ₇	Antioxidant, anti-radical, iron chelating	12
9	Kaempferol	C ₁₅ H ₁₀ O ₆	Antimicrobial, neuroprotective, anti-inflammatory, antioxidant, anti-anxiety	10
10	β-caryophyllene	C ₁₅ H ₂₄	Fragrance ingredient	53, 54
11	α-Terpineol	C ₁₀ H ₁₈ O	Antispasmodic, anti-inflammatory, antitumor, myorelaxant	20
12	Fatty acids (decanoic acid, nonanoic acid)		Anticonvulsant, fragrance ingredient	20, 35

5.3. Antioxidant Potential

It was shown that *B. ciliata* rhizome extracts, both methanolic and aqueous, have antioxidant properties, such as the ability to reduce, scavenge free radicals, and prevent lipid peroxidation. All of the antioxidant tests showed that the methanolic extract had more potential. The aqueous extract did, however, show much more DNA protection, even though it was not as effective as its methanolic counterpart in terms of antioxidant activity.^{13,26,66}

5.4. Antitussive Potential

The antitussive potential of *B. ciliata* methanolic rhizome extract has been assessed through a cough model in mice induced by sulphur dioxide gas. With codeine phosphate being used as a standard it has been observed that the extract exhibited a substantial dose-dependent anti-tussive effect. Within 90 minutes of the trial, the extract at dosages of 100, 200, and 300 mg/kg body weight significantly inhibited the cough reflex by 28.7, 33.9, and 44.2%, respectively.^{10,15,18}

5.5. Antineoplastic Potential

B. ciliata methanolic and aqueous extracts has been shown to possess strong anti-neoplastic potential and concentration dependent cytotoxicity, with IC₅₀ value for both extracts falling well within the prescribed threshold (except the aqueous

extract with higher IC₅₀).¹⁸ Thus, the extracts efficacy demonstrates that it has great promising potential for the synthesis of medications that target tumours for chemoprevention and chemotherapy, the goal being to limit the development, growth and malignancy of lesions.³

5.6. Antiulcer Potential

In several parts of South East Asia, traditional medicine utilizes *Bergenia ciliata* to cure gastrointestinal problems. Rats with stomach ulcers caused by pylorus ligation, indomethacin, and ethanol/HCl were used in the antiulcer activity experiment of *B. ciliata* to assess its gastroprotective effects. One hour following ulcerogenic therapy, doses of the rhizome's aqueous and methanol extracts, ranging from 15, 30, and 60 mg/kg, were given. It was observed that although the impact was diminished at higher dosages, the aqueous extract significantly reduced the ulcer lesion in all rat compared to the methanol extract. Furthermore, rather than inhibiting the release of stomach acid or reducing pH and acidity, the antiulcer action seems to be mediated by cytoprotective benefits provided by improvement of the mucosal barrier.^{18,67,68}

6. Other Potential Applications of *Bergenia Ciliata*

6.1 Health Food

Bergenia being a rich reserve of a plethora of nutrients, amino acids, phenolic compounds and minerals can be used in a variety of gourmet preparations, cuisines, various kinds of herbal tea, syrups, beverages. Arbutin present in *Bergenia* is also known to prevent the breakdown of insulin.⁶⁹ The food industry uses a variety of essential oils derived from plants as effective flavourings and antibacterial agents. Today's balance leans towards using natural dietary components instead of the already accessible synthetic antioxidants.⁷⁰ Due to the aforementioned points, it is possible that the *Bergenia* species be utilized as a natural preservative, flavouring ingredient in international trade and food manufacturing.

6.2. Cosmetics

A naturally occurring derivative of hydroquinone is arbutin, which is a β-D-glucopyranoside. It is a powerful inhibitor of melanin synthesis and is not linked to the cytotoxicity or mutagenicity of melanocytes. *Bergenia* being rich in arbutin is thus utilized in the field of cosmetics.⁶² Arbutin inhibits tyrosinase activity and lowers melanin (pigment) in the skin, that might lead to skin whitening.^{28,42} Evidently, *Bergenia* might also be used in the pharmaceutical or cosmetic industries as a possible skin-whitening or brightening agent, anti-wrinkle agent and under eye cream.³⁷

6.3. Synthesis of Bioactive Nanoparticles

Furthermore, as *B. ciliata* is rich in a large number of phenolic compounds it has a great potential to be utilized for creating metallic nanoparticles. Nanoparticles have become significant in recent years, as the matter at this scale presents a more compact arrangement of atoms and molecules, acquiring or enhancing properties that are entirely distinct from those of their macroscopic counterparts in the areas of mechanical, electrical, magnetic, optical, catalytic and antibacterial.⁷¹

6.4. Natural Preservative

Consumers today expect the food preservative used to be ecologically friendly and biobased. The bacteriostatic and antioxidant qualities of *Bergenia* extracts have been shown to extend the shelf life of the produced items while at the same time maintaining its physico-chemical and organoleptic properties. The assessment of the economically significant attributes of biologically active substances from this plant

source could be a promising preservative with excellent consumer qualities.^{72,73,74,7}

7. Discussion and Way Forward

There is a continued prevalence of plant-based medicine and the critical role that local traditional knowledge plays in meeting basic healthcare needs. When compared to pharmaceutical medication, traditional herbal medicine is seen as the lifeline, the first option, and cultural recognition. Social life in rural communities has always included medicinal plants and their traditional formulations, which have shown to be quite beneficial in treating a variety of health-related conditions. The integration of traditional knowledge into high-level decision-making processes and the expanded use and modification of ethnomedicinal plant applications are crucial. Pharmaceutical medicines treat a wide range of illnesses, but their uses are limited by their greater costs and adverse effects.

Clinical trials should be carried out in the future to evaluate *B. ciliata*'s effectiveness against a variety of illnesses as well as the appropriate use and advancement in medication. Future clinical applications of *B. ciliata* in contemporary medicine will be strongly supported by the findings of these studies. There is an urgent need for experimental research and proof in the future even in the face of scientific data about pharmacological and medical purposes.

Due to disorganized methods of passing on information to the next generation, the fast changes in urbanization and its impact on cultural contexts in recent decades have resulted in the loss of traditional knowledge in a number of regions, including the Himalayas. If appropriate documentation is not maintained, this situation may result in the extinction of a significant amount of ethnomedicinal knowledge about the area. Compiling this data and creating a database of therapeutic plants are therefore crucial for future studies and the possible development of novel herbal remedies. Medicinal plants are vulnerable to both specific threats such as over-collection and general threats including habitat destruction and climate change. Thus, government authorities and agencies should develop more effective conservation and management plans for the medicinal plants.

8. Conclusion

The main goal of this review was to compile the most polarized work about the ethnobotany, ethnopharmacology, and phytochemistry of *Bergenia ciliata*. This review aims to shed light on the various diseases that the golden herb *Bergenia ciliata* may effectively treat, as well as the chemicals that hold its significant medicinal properties. This would strengthen the link between modern knowledge and the folktales that have been passed down through the years, serving as inspiration for future research that may uncover new, unique substances and drugs derived from the three species. It comes to light that many people throughout the Himalayan area of the world have been long employing this miraculous plant for treating various disorders and diseases. Nearly every component of the plant is utilized to treat various illnesses, with the rhizome being the most utilized. The species possesses antifungal, antiviral, antibacterial, antioxidant, antitussive, anti-inflammatory, anti-neoplastic, and anti-ulcer properties as proven by various biological and pharmacological research. The primary phytochemicals identified in this species are phenols, flavonoids, fatty acids, and terpenoids, among others. In addition, the plant has fewer adverse effects on living organisms than contemporary medications.

Further clinical research on this plant is required for the future discovery of drugs because some pharmaceutical activities have also been observed *in vitro* and *in vivo*, and deficiencies in clinical trials of some activities have also been noted. The current medicinal potential of *B. ciliata* may be expanded with more phytochemical research. We further recommend that thorough ethno-pharmaceutical and toxicological research be done in light of the current assessment. These investigations

will yield important information about many illnesses and aid in the development of novel medications. In addition, this paper would fill in logical gaps in current understanding and facilitate international research collaboration on projects including the identification of new chemicals and pharmaceuticals derived from *Bergenia ciliata*.

Author Contribution Declaration

Nirza: engaged in data curation, writing, conceptualization, and production of the initial draft. **Anindita:** involved in supervision, editing and reviewing.

Data Availability Declaration

There are no new data was created.

Acknowledgements

We are thankful to the Principal, Head of Department (HOD) and administration of St. Xavier's College, Kolkata for providing the necessary laboratory and internet facilities for executing the studies.

References

1. A. Hussain, M. Kanth, P. K. Shrivastava, M. Sharma, J. Tripath, M. A. Khan. Phytochemical analysis of the rhizomes of *Bergenia ciliata* (Haw) Sternb. *J. Drug Deliv Therap.*, **2019**, 9, 412.
2. C. P. Bahu, R. T. Seshadri. Advances in research in "Indian Medicine", "Pashanbedi" drugs for urinary calculus, Udupa K.N.(Eds)., **1970**, 77.
3. L. Singh, A. Kumar, A. Paul. *Bergenia ciliata*: The medicinal herb of cold desert. *Int. J. Chem. Sci.*, **2018**, 6, 3609.
4. M. S. Bagul, M. Ravishankara, H. Padh, M. Rajani. Phytochemical evaluation and free radical scavenging properties of rhizome of *Bergenia ciliata* (Haw.) Sternb. forma ligulata Yeo. *J. Nat. Remedies.*, **2003**, 3, 83. <https://doi.org/10.18311/jnr/2003/369>
5. A. J. Grierson, D. G. Long. Flora of Bhutan: including a record of plants from Sikkim. Edinburgh: Royal Botanic Garden Edinburgh. **1983**.
6. G. Y. Zuo, Z. Q. Li, L. R. Chen, L. R. X. J. Xu. in vitro anti-Hcv activities of *Saxifraga melanocentra* and its related polyphenolic compounds. *Antiviral Chem. Chemoth.*, **2005**, 16, 393. <https://doi.org/10.1177/095632020501600606>.
7. B. Joshi, S. Lekhak, A. Sharma. Antibacterial property of different medicinal plants: *Ocimum sanctum*, *Cinnamomum zeylanicum*, *Xanthoxylum armatum* and *Origanum majorana*. Kathmandu Univ. *J Sci Eng Technol.*, **2009**, 5, 143. <https://doi.org/10.3126/kuset.v5i1.2854>
8. K. Krasniewska, M. Gniewosz, A. Synowiec, J. L. Przybyl, K. Baczek. the application of pullulan coating enriched with extracts from *Bergenia crassifolia* to control the growth of food microorganisms and improve the quality of peppers and apples. *FBP.*, **2014**, <https://doi.org/10.1016/j.fbp.2014.06.001>
9. D. P. Singh, S. K. Srivastava, R. Govindarajan, A. K. S. Rawat. High performance liquid chromatographic determination of bergenin in different *Bergenia* species. *Acta Chromatogr.*, **2007**, 19, 246.
10. N. Khan, A. M. Abbasi, G. Dastagir, A. Nazir, G. M. Shah, M.M. Shah, M.H. Shah. Ethnobotanical and antimicrobial study of some selected medicinal plants used in Khyber Pakhtunkhwa (KPK) as a potential source to cure infectious diseases. *BMC Complement. Altern. Med.*, **2014**, 14, 122. <https://doi.org/10.1186/1472-6882-14-122>

11. R. Zhang, K. Eggleston, V. Rotimi, R. J. Zeckhauser. Antibiotic resistance as a global threat: evidence from China, Kuwait and the United States, *Glob. Health.*, **2006**, 2, 6. <https://doi.org/10.1186/1744-8603-2-6>
12. C. Das, B. Kumari, M. P. Singh, S. Singh. A Literary Review and Therapeutic Action of Pashanbheda (*Bergenia ligulata* Wall.) described by Shamita in Ashmari Roga. *J. Ayurveda Integ. Med. Sci.*, **2022**, 7, 105-114. <https://jaims.in/jaaims/article/view/1861>.
13. K. Ruby, R. Chauhan, S. Sharma, J. Dwivedi. Polypharmacological activities of *Bergenia* species, *Int. J. Pharm. Pharm. Sci.*, **2012**, 1, 100.
14. K. Mishra, L. Ganju, M. Sairam, P. Banerjee, R. Sawhney. A review of high throughput technology for the screening of natural products, *Biomed. Pharmacother.*, **2008**, 62, 94. <https://doi.org/10.1016/j.biopha.2007.06.012>.
15. P. Chase, O. Singh. Ethnomedicinal plants used by angami tribe of Nagaland, India. *Indian J. Trop. Biodivers.*, **2013**, 21, 29.
16. P. M. Shrestha, S. S. Dhillon. Medicinal plant diversity and use in the highlands of Dolakha district Nepal, *J. Ethnopharmacol.*, **2003**, 86, 81. [https://doi.org/10.1016/s0378-8741\(03\)00051-5](https://doi.org/10.1016/s0378-8741(03)00051-5)
17. S. Karki, S. Chowdhury, S. Nath, K. C. Dora, P. Murmu. Phytochemistry and ethnomedicinal use of *Bergenia* species-a miraculous herb. *Indian J. Anim Health.*, **2021**, 60, 143
18. J. L. Yuan, J. L. Suo. Research progress in medicinal plant genus *Bergenia* Moench. *J. Baoji Univ. Arts Sci. Nat. Sci.*, **2011**, 31, 46.
19. N. Singh, V. Juya, A. K. Gupta, M. Gahlot. Evaluation of ethanolic extract of root of *Bergenia ligulata* for hepatoprotective, diuretic and antipyretic activities. *J. Pharm. Res.*, **2009**, 2, 958.
20. P. Shrestha, S. Adhikari, B. Lamichhane, B. G. Shrestha. Phytochemical screening of the medicinal plants of Nepal. *IOSR J. Environ. Sci. Toxicol. Food Technol.*, **2015**, 11–17
21. M. Yuldashev, È. K. Batirov, V. Malikov. Anthraquinones of *Bergenia hissarica*. *Chem. Nat. Compd.*, **1993**, 29, 543. <https://doi.org/10.1007/BF00630591>
22. R. A. Moreau, B. D. Whitaker, K. B. Hicks. Phytosterols, phytosteranols, and their conjugates in foods: structural diversity, quantitative analysis, and health-promoting uses. *Prog. Lipid Res.*, **2002**, 41, 457. DOI: [https://doi.org/10.1016/s0163-7827\(02\)00006-1](https://doi.org/10.1016/s0163-7827(02)00006-1)
23. A. Yaginuma, K. Murata, H. Matsuda. Beta-glucan and *Bergenia ligulata* as cosmetics ingredient. *Fragrance J.* **2003**, 31, 114. DOI: <https://doi.org/10.22270/jddt.v9i3.2687>
24. R. Árok, K. Végh, Á. Alberti, Á. Kéry. Phytochemical comparison and analysis of *Bergenia crassifolia* L. (fritsch.) and *Bergenia cordifolia* Sternb. *Eur. Chem. Bull.* **2012**, 1, 31.
25. B. Patwardhan, A. Vaidya, M. Chorghade, S. Joshi. Reverse pharmacology and systems approach for drug discovery and development. *Curr. Bioact. Compd.*, **2008**, 4, 201. DOI: <https://doi.org/10.2174/157340708786847870>.
26. K. Satyavani, S. Gurudeeban, V. Manigandan, E. Rajamanickam, T. Ramanathan. Chemical compositions of medicinal mangrove species *Acanthus ilicifolius*, *Excoecaria agallocha*, *Rhizophora apiculata* and *Rhizophora mucronata*. *Curr. Res. Chem.*, **2015**, 7, 1. <https://doi.org/10.3923/crc.2015.1.8>
27. L. K. Han, H. Ninomiya, M. Taniguchi, K. Baba, Y. Kimura, H. Okuda. Norepinephrine Augmenting Lipolytic Effectors from *Astilbe t hunbergii* Rhizomes, *J. Nat. Prod.* **1998**, 61, 1006. <https://doi.org/10.1021/np980107o>
28. N. Moktan, A. Banerjee. Polyphenol oxidases: challenges and future prospects. *De Gruyter.*, **2024**, 293. <https://doi.org/10.1515/9783111033525-011>
29. S. Chowdharya, H. Kumar, K. Verma. Quantitative Assessment of Current Status and Biomass of *Bergenia ciliata* and *Bergenia stracheyi* from Kumaun Himalaya, *International Journal of Applied Biology and P.*, **2010**, 360.
30. M. Roselli, G. Lentini, S. Habtemariam. Phytochemical, antioxidant and anti- α -glucosidase activity evaluations of *Bergenia cordifolia*, *Phytother. Res.*, **2012**, 26, 908.
31. A. Kumar, M. Mitra, B. Adhikari, G. S. Rawat. Depleting indigenous knowledge of medicinal plants in cold-arid region of Nanda Devi Biosphere Reserve, Western Himalaya. *Med. Aromat. Plants.*, **2015**, 4, 2167. <https://doi.org/10.4172/2167-0412.1000195>
32. M. Ahmad, M. A. Butt, G. Zhang, S. Sultana, A. Tariq, M. Zafar. *Bergenia ciliata*: A comprehensive review of its traditional uses, phytochemistry, pharmacology and safety. *Biomedicine & Pharmacotherapy.*, **2018**, 97, 708. <https://doi.org/10.1016/j.biopha.2017.10.141>
33. M. R. Bhandari, N. Jong-Anurakkun, G. Hong, J. Kawabata. α -Glucosidase and α -amylase inhibitory activities of Nepalese medicinal herb Pakhanbhed (*Bergenia ciliata*, Haw.), *Food Chem.*, **2008**, 106, 247. <https://doi.org/10.1016/j.foodchem.2007.05.077>
34. B. K. Sapkota, K. Khadayat, K. Sharma, B. K. Raut, D. Aryal, B. B. Thapa, N. Parajuli. Phytochemical Analysis and Antioxidant and Antidiabetic Activities of Extracts from *Bergenia ciliata*, *Mimosa pudica*, and *Phyllanthus emblica*. *Adv. Pharmacol. Pharma. Sci.*, **2022**, 5, 4929824. <https://doi.org/10.1155/2022/4929824>
35. P. C. Santos-Gomes, M. Fernandes-Ferreira. Organ-and season-dependent variation in the essential oil composition of *Salvia officinalis* L. cultivated at two different sites, *J. Agric. Food Chem.*, **2001**, 49, 2908. <https://doi.org/10.1021/jf001102b>
36. S. Roychoudhury, D. Das, S. Das, N. K. Jha, M. Pal, A. Kolesarova, K. K. Kesari, J. C. Kalita, P. Slama. Clinical Potential of Himalayan Herb *Bergenia ligulata*: Evidence Based Study. *Molecules*, **2022**, 27, 7039. <https://doi.org/10.3390/molecules27207039>
37. R. Venkatadri, G. Guha, A. K. Rangasamy. Anti-neoplastic activity of *Bergenia ciliata* rhizome. *J. Pharm. Res.*, **2011**, 4, 44
38. I. Azhar, K. Usmanghani, M. A. Gill, A. Ahmad, A. Ahmad. Antifungal activity evaluation of *Bergenia ciliata*. *Pak J Pharm Sci.*, **2002**, 19, 1.
39. K. Dhalwal, V. M. Shinde, Y. S. Biradar, K. R. Mahadik. Simultaneous quantification of bergenin, catechin, and gallic acid from *Bergenia ciliata* and *Bergenia ligulata* by using thin-layer chromatography. *J. Food Compos. Anal.*, **2008**, 21, 496. <https://doi.org/10.4172/2153-2435.1000104>
40. M. Rajbhandari, U. Wegner, T. Schoepke, U. Lindequist, R. Mentel. Inhibitory effect of *Bergenia ligulata* on influenza virus A. *Int. J. Pharm. Sci.* **2003**, 58, 268.
41. N. N. Azwanida. A review on the extraction methods uses in medicinal plants, principle, strength and limitation. *Med. Aromat. Plants.*, **2015**, 4, 196. <https://dx.doi.org/10.4172/2167-0412.1000196>
42. P. Carmen, L. Vlase, M. Tamas. Natural resources containing arbutin. Determination of arbutin in the leaves of *Bergenia crassifolia* (L.) Fritsch. Acclimated in Romania. *Notulae Botanicae Horti Agrobotanici Cluj-Napoca.*, **2009**, 37, 129. <https://doi.org/10.15835/nbha3713108>
43. R. Chauhan, K. Ruby, J. Dwivedi. *Bergenia ciliata* mine of medicinal properties: A Review. *Int. J. Pharm. Sci. Rev. Res.*, **2012**, 15, 20.
44. S. A. Gilani, R. A. Qureshi, S. J. Gilani. Indigenous uses of some important ethnomedicinal herbs of Ayubia

- National Park, Abbottabad, Pakistan, *Ethnobot. Leaflet*, **2006**, 1, 32.
45. S. S. Shah, A. Dawood, K. Ibrahim, I. Muhammad, A. J. Sohail. *Bergenia ciliata* as antibacterial agent. *GSC Bio. Pharma. Sci.*, **2020**, 12, 37
 46. R. Gyawali. Phytochemical screening and anti-microbial properties of medicinal plants of Dhungharka community, Kavrepalanchowk, Nepal. *Int. J. Pharm. Biol. Arch.*, **2011**, 2
 47. R. Gyawali, K. S. Kim. Bioactive volatile compounds of three medicinal plants from Nepal. *Kathmandu University J. Sci. Eng. Technol.*, **2011**, 8, 51. <https://doi.org/10.3126/kuset.v8i1.6043>
 48. M. Khan, M. A. Khan, G. Mujtaba, M. Hussain. Ethnobotanical study about medicinal plants of Poonch valley Azad Kashmir. *J. Anim. Plant Sci.*, **2012**, 22, 493. <https://api.semanticscholar.org/CorpusID:27813371>
 49. N. Kushwana, A. Singh. *Bergenia ciliata*-Phytochemistry and Pharmacology: A review. *J. Biomed Mat & amp.*, **2024**, 2, 891. <https://doi.org/10.1007/s44174-024-00156-6>
 50. M. Hasan, P. Gatto, P. Jha. Traditional uses of wild medicinal plants and their management practices in Nepal—a study in Makawanpur district. *Int. J. Med. Aromat. Plants.*, **2013**, 3, 102.
 51. V. V. Byahatti, K. V. Pai, M. G. Dsouza. Effect of phenolic compounds from *Bergenia ciliata* (Haw.) Sternb. leaves on experimental kidney stones. *Ancient Sci. Life.*, **2010**, 30, 14.
 52. V. Chahar, B. Sharma, G. Shukla, A. Srivastava. A. Bhatnagar. Study of Antimicrobial Activity of Silver Nanoparticles Synthesized Using Green and Chemical Approach. *Colloids Surf. A Physicochem. Eng. Asp.*, **2018**, 554, 149.
 53. E. Ali, N. Arshad, N. I. Bukhari, M. N. Tahir, S. Zafar, A. Hussain, S. Praveen, S. Qamar, N. Shehzadi, K. Hussain. Linking traditional anti-cancer use of rhizomes of *Bergenia ciliata* (Haw.) Sternb. to its anti-Helicobacter pylori constituents. *Nat. Prod. Res.*, **2020**, 34, 541. <https://doi.org/10.1080/14786419.2018.1488711>.
 54. N. P. Manandhar. Medicinal folklore about the plants used as anthelmintic agents in Nepal. *Fitoterapia.*, **1995**, 66, 149.
 55. R. Verma, A. Tapwal, D. Kumar, S. Puri. Assessment of Antimicrobial Potential and Phytochemical Profiling of Ethnomedicine Plant *Bergenia ciliata* (Haw.) Sternb. In Western Himalaya. *J. Micro. Biotech. Food Sci.*, **2019**, 9, 15. <https://doi.org/10.15414/jmbfs.2019.9.1.15-20>.
 56. Y. Subba, S. Hazra, C. H. Rahaman. Medicinal plants of Teesta Valley, Darjeeling district, West Bengal, India: A quantitative ethnomedicinal study. *J. App. Pharma. Sci.*, **2023**, 13, 93. <https://doi.org/10.7324/JAPS.2023.130109>
 57. P. Pokhrel, R. R. Parajuli, A. K. Tiwari, J. Banerjee. A short glimpse on promising pharmacological effects of *Bergenia ciliata*. *JOAPR.*, **2014**, 2, 1.
 58. V. Kumar, D. Tyagi. Review on phytochemical, ethnomedical and biological studies of medically useful genus *Bergenia*. *Int J Curr Microbiol App Sci.*, **2015**, 2, 328.
 59. M. Stuffness, J. M. Pezzuto. Assay related to cancer drug discovery. In Hostettmann K. (ed). *Methods in plant biochemistry. Assays for Bioactivity*, 6. Academic press-London. **1990**, 71-133.
 60. M. Y. Khan, V. Kumar. Phytopharmacological and Chemical Profile of *Bergenia ciliata*. *Intern.J. Phytopharmacy.*, **2016**, 6, 90.
 61. R. Hafidh, A. Abdulmir, F. Jahanshiri, F. Abas, F. Abu Bakar, Z. Sekawi. Asia is the mine of natural antiviral products for public health. *Open Complement Med. J.*, **2009**, 1, 58.
 62. H. Khan. Medicinal plants in light of history: Recognized therapeutic modality. *J. Evid. Based Integr. Med.*, **2014**, 19, 216. <https://doi.org/10.1177/2156587214533346>.
 63. S. V. Tsyrenzhieva, I. V. Khamaganova. The use of black leaves of *Bergenia* in food production. *Food Processing: Techniques and Technology.*, **2017**, 2, 81-86. <https://naukaru.ru/en/nauka/article/27170/view>
 64. C. Smith-Hall, H. O. Larsen, M. Pouliot. People, plants and health: a conceptual framework for assessing changes in medicinal plant consumption. *J Ethnobiol Ethnomed.*, **2012**, 8, 43. <https://doi.org/10.1186/1746-4269-8-43>.
 65. M. G. Castejón, A. R. Casado. Dietary phytochemicals and their potential effects on obesity: a review. *Pharmacol. Res.*, **2011**, 64, 438. <https://doi.org/10.1016/j.phrs.2011.07.004>
 66. M. Rajbhandari, R. Mentel, P. K. Jha, R. P. Chaudhary, S. Bhattarai, M. B. Gewali, N. Karmacharya, M. Hipper, U. Lindequist. Antiviral activity of some plants used in Nepalese traditional medicine. *Evidence-Based Comple. Altern. Med.*, **2007**, 6, 517. <https://doi.org/10.1093/ecam/nem156>
 67. M. Islam, I. Azhar, K. Usmanhani, M. Aslam, A. Ahmad. Bioactivity evaluation of *Bergenia ciliata*. *Pak. J. Pharm.Sci.*, **2002**, 15, 15. <https://doi.org/10.1002/ptr.3655>
 68. X. Yang, Z. Wang, Wang, R. Li. Analysis of nutritive components and mineral element of *Bergenia pacumbis* in Tibet. *J. Chang. Veg.*, **2009**, 22, 57.
 69. S. Rehman, Z. Iqbal, R. Qureshi, T. S. AlOmar, N. Almasoud, M. Younas, A. Rauf, M. Irfan. Ethno Dentistry of Medicinal Plants Used in North Waziristan, Pakistan. *International Dental Journal.*, **2024**, 74, 310. <https://doi.org/10.1016/j.identi.2023.10.001>
 70. K. Ahn. The worldwide trend of using botanical drugs and strategies for developing global drugs. *BMB Reports.*, **2017**, 50, 111. <https://doi.org/10.5483/BMBRep.2017.50.3.221>
 71. S. Gurav, N. Gurav. A comprehensive review: *Bergenia ligulata* wall-a controversial clinical candidate. *Int. J. Pharm. Sci. Rev. Res.*, **2014**, 5, 1630. [https://doi.org/10.13040/IJPSR.09758232.5\(5\).1630-42](https://doi.org/10.13040/IJPSR.09758232.5(5).1630-42)
 72. H. Kour, R. Rana, P. K. Verma, N. K. Pankaj, S. P. Singh. Phytochemical ingredients and pharmacological properties of *Bergenia ciliata*. *Journal Of Veterinary Pharmacology and Toxicology.*, **2019**, 18, 1
 73. R. M. Kunwar, L. Mahat, R. P. Acharya, R. W. Bussmann. Medicinal plants, traditional medicine, markets and management in far-west Nepal. *J. Ethnobiol. Ethnomed.*, **2013**, 9, 24. <https://doi.org/10.1186/1746-4269-9-24>
 74. V. Manandhar, G. Guha, R. A. Kumar. Anti-neoplastic activities of *Bergenia ciliata* rhizome. *J. Pharm. Res.*, **2011**, 4, 443.
 75. G. Uddin, A. Rauf, M. Arfan, M. Ali, M. Qaisar, M. Saadiq, M. Atif. Preliminary phytochemical screening and antioxidant activity of *Bergenia ciliata*. *Middle-East J. Sci. Res.*, **2012**, 11, 1140.

The Significance of Air Pollution in the Process of Stone Deterioration

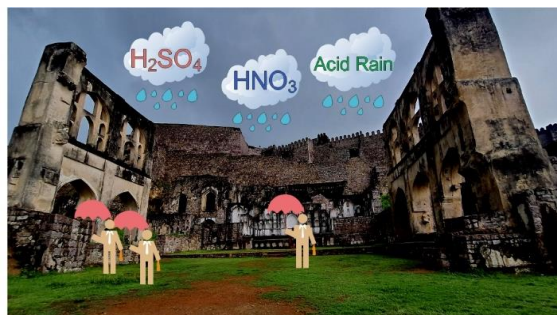
Abhishek Singh^a, Tanvir Arfin^{a,b*} , Nikhila Mathew^a and Abha Tirpude^a

^aAir Resource, Environmental Resource Planning and Management, CSIR-National Environmental Engineering Research Institute (NEERI), Nehru Marg, Nagpur-440020, India

^bAcademy of Scientific and Innovative Research (AcSIR), Ghaziabad-21002, India.

*Correspondence: tanvirarfin@gmail.com

Abstract: Stone materials used in monuments, structures, and sculptures are highly vulnerable to the effects of air pollution. Sulphur and nitrogen oxides are among the most harmful pollutants, especially for carbonate stones. When these oxides come into contact with atmospheric moisture, they form acids that gradually corrode the stone's surface, weakening its structural integrity. These acids may also react with solid particles in the air, such as heavy metals and salts, to create black crusts that blemish the stone's original appearance. These crusts not only compromise the structural stability of the stone but also pose a significant threat to the preservation of important monuments and buildings. Our research shows that stone structures exposed to air pollution for extended periods can provide valuable insight into historical pollution levels through their weathering crusts. These findings offer important insights for improving long-term geochemical records and restoring past air quality conditions. Additionally, this methodology can enhance the study and preservation of stone weathering while enabling more accurate reconstructions of historical pollutant levels.



Keywords: Stone, surface, air pollution, calcium carbonate, monument.

Contents

Biographical Information	66
1. Introduction	66
2. Historical Episode	67
3. Cultural Heritage	69
4. Damage to monuments	69
4.1. Weathering	70
4.2. Pollution	70
4.3. Stone Damage	70
4.4. Aesthetic Damage: Blackening	71
4.5. Rate of Blackening	71
4.6. Perception of Blackening	71
4.7. Setting aesthetic Thresholds	71
4.8. Blackening Patterns	71
5. Discussion and way forward	72
6. Conclusion	72
Author Contribution Declaration	73
Data Availability Declaration	73
Acknowledgements	73
References	73

1. Introduction

Materials science encompasses a wide range of substances and their applications.¹⁻³ Throughout history, epochs have been named to reflect human progress intertwined with the evolution and utilization of materials.⁴⁻⁶ While materials may lack inherent functionality in isolation, their absence renders human endeavors futile.⁷⁻⁹ Nature has harnessed atomic hierarchies similar to those employed in human-made structures over time.¹⁰⁻¹²

In contemporary society, sustainable development is a pivotal concept.¹³⁻¹⁵ Its significance lies in its potential to ensure equitable utilization of resources and foster harmonious interaction between humanity and the ecosystem.¹⁶⁻¹⁸ Therefore, the discovery and innovation of exceptional materials are paramount in our era of progress.¹⁹⁻²¹ These materials find application across various branches and

subfields of analytical chemistry, facilitating identifying and analyzing substances with complex patterns. The quality

Abhishek Singh is an accomplished professional in the field of mechanical engineering with a focus on air quality management. With a background in engineering, he has dedicated their career to developing innovative solutions for air emission control. Their expertise spans the fabrication of air emission control units, including designing and implementing systems to reduce pollutants and mitigate environmental impact.



Tanvir Arfin, with BSc and MSc in physical chemistry from Aligarh Muslim University, holds a PhD in electrochemistry from the same institution. Beginning as a lecturer at NIT Raipur, he pursued postdocs at North-West University and the University of Johannesburg. As a senior scientist at CSIR-NEERI, his expertise garnered research projects from prestigious organizations. With over 130 research articles, a patent, and contributions to esteemed publications, Arfin actively participates in conferences, specializing in composites and porous materials for water and air quality management.



Nikhila Mathew, holding an M.Sc. in Analytical Chemistry since 2020, presently serves as a Project Associate at NEERI, Nagpur. With a robust background in chemical analysis, laboratory techniques, and instrumentation, she specializes in the study of air pollution. Mathew's proficiency extends to data analysis and crafting comprehensive reports, which play a pivotal role in advancing her field. Through her diligent research and practical applications, she strives to deepen insights and offer solutions within the realm of analytical chemistry.



Abha Tirpude earned her M.Sc. in Chemistry in 2020 and is currently a Project Associate at NEERI, Nagpur. Her professional expertise encompasses chemical analysis, laboratory work, and instrumentation with a focus on air pollution. Tirpude is skilled in data analysis and report writing, contributing significantly to her field through meticulous research and practical applications. Her work aims to enhance understanding and solutions in environmental chemistry.



of material required for such analyses, known as the "minimum volume," plays a critical role.²²⁻²⁴

<https://doi.org/10.63654/icms.2024.01066>

Received: 12 May 2024; Revised: 09 July 2024; Accepted: 07 September 2024; Published (online): 28 October 2024

Published by Insuf Publications (OPC) Pvt. Ltd. This is an open access article under the CC BY-NC-ND license

The system provides convenience, simplicity, and outstanding life-sustaining components, meeting universally accepted standards.²⁵⁻²⁷ Numerous industrialized nations' economic advancement and sustained growth owe much to such materials.²⁸⁻³⁰ An analysis delves into utilizing natural resources and active substances.³¹⁻³³ This involves employing various approaches, tools, and strategies as integral developmental components.³⁴⁻³⁶ This juncture is pivotal in advancing current scientific understanding and holds promise for future applications across various fields.³⁷⁻³⁹

Throughout history, the material of preference has often been a defining factor in various periods.⁴⁰⁻⁴² From the Stone Age to the Steel Age, epochs have been demarcated by significant material shifts, albeit somewhat arbitrarily.

As an enduring and environmentally friendly natural substance, stone is cherished in human culture.⁴³⁻⁴⁵ Its usage as a construction material dates back to antiquity, manifesting in structures such as stone walls, barrows, and rune stones during the Stone Age. Even today, the construction industry continues to rely on this versatile material.

Environmental pollution is the depletion of energy or matter from the earth's renewable resources, such as air, water, or land.⁴⁶ This depletion harms the environment and its ecological well-being, affecting people's lives in terms of quantity and quality.⁴⁷ Activities like mining, farming, and manufacturing can contribute to this damage. Urbanization adds to the environmental challenges, making smart cities a potential solution.⁴⁸ Improving the accuracy of air quality data is essential for epidemiological investigations, as air pollution levels can vary significantly across different regions and over time.

There has been an alarming increase in the release of air pollutants into the atmosphere, including persistent organic pollutants (POPs).⁴⁹ POPs are harmful because they resist various biochemical and photolytic breakdown processes persisting in the atmosphere, soils, and sediments. Due to their high toxicity and long-lasting nature, POPs accumulate in the adipose tissues of humans and wildlife, resulting in observable changes related to growth, development, and reproduction.⁵⁰ POPs pose a significant threat because of their poisonous, bioaccumulative, and persistent nature and their ability to travel long distances from various sources.⁵¹

The degradation of stone materials is closely linked to air pollution, with urban areas experiencing high levels of human-caused emissions exacerbating this issue.⁵² Studying the effects of atmospheric pollution on outdoor cultural heritage is of significant interest. Additionally, preserving world heritage is a crucial focus of various UNESCO initiatives.⁵³

Extensive research efforts have been focused on the deterioration of stone materials for decades, especially concerning preserving cultural heritage.⁵⁴ It is essential to understand the mechanisms behind this phenomenon to develop effective and long-lasting conservation strategies. Air pollution, particularly in urban areas, where sulphation processes are predominant, is a significant factor in stone decay.⁵⁵

It is generally agreed that the primary mechanisms of deterioration related to pollution involve the formation of gypsum ($\text{CaSO}_4 \cdot 2\text{H}_2\text{O}$) and carbonate dissolution.⁵⁶ However, there is still much debate surrounding the weathering of limestone crusts, which occurs when calcium carbonate (CaCO_3) transforms into calcium sulfate (CaSO_4) due to air pollutants and anthropogenic sulfur deposition.⁵⁶ This accumulation of calcite and gypsum crystals on the stone's surface gradually erodes it. Despite efforts to reduce SO_2 concentrations in recent decades, weathering crust degradation remains a persistent issue. These crusts periodically fracture, revealing the extent of the damage and exposing a pristine surface underneath. The corrosion of stone materials caused by acid rain as shown in Figure 1, resulting from pollution of rainwater with carbon oxides (CO_x), nitrogen (N), sulfur (S), and leads to the deterioration of rock-

making minerals.⁵⁷ Pollution has become a complex issue, with rising levels of particulate matter intensifying the acidic effects through dust deposition.⁵⁸



Figure 1. Adverse impact of acid rain

Weathering crusts are made up of afresh designed minerals such as gypsum. These minerals incorporate atmospheric particles, including sleek aluminosilicate particles, porous carbonaceous particles (soot), and metal particles primarily composed of iron.⁵⁹ The sources of these atmospheric particles are diverse and may include combustion of fuel from power plants and residential heating, combustion of coal, and the emissions from petrol oil.⁶⁰ Additionally, sources such as vehicle exhaust⁶¹ and biomass combustion⁶² have been identified.

Stone decay can occur due to a combination of chemical, physical, and biological factors that frequently work together. Water acts a crucial role in both weathering and co-agent functions. It acts as a solvent by dissolving specific components such as gypsum, which are soluble in water. Water can cause stone degradation by carrying salts or pollutants onto the surface or penetrating its porous structure. Additionally, water creates favorable conditions for microbial nutrients, mainly when interacting with composites from the substrate of stone (e.g., carbonates) or atmospheric NO_x contaminants, thereby facilitating biological decay. In general, degradation methods are predisposed by various factors such as environmental conditions, materials, strategy, construction methods, and preservation practices. Among these, environmental factors notably play a significant role in the decay procedures of stone.⁶³ Aspects like building orientation and architectural intricacies also play a role in determining how moisture source and drying affect deprivation.⁶⁴

Acknowledging that environmental factors can lead to changes in all types of stone materials is crucial. However, human activities, such as the emission of pollutants, can speed up this process. This review will concentrate on the importance of air pollution on in the degradation of stone, especially the darkening of buildings in heavily polluted urban areas.

2. Historical Episode

The Cologne Cathedral is an important cultural monument in northern Europe, but it is facing significant stone degradation. Different types of building stones within the cathedral are experiencing various weathering circumstance. The Drachenfels trachyte, utilized in the medieval construction phase, exhibits evident structural deterioration and an extensive formation of gypsum crusts. Various researchers have explored the environmental and geological factors contributing to the degradation of the building stones in Cologne Cathedral.^{65,66} In the 1970s, a research program was conducted to investigate the effects of air pollutants, specifically, the impact of flue gas on the deprivation of ordinary building stones and possible methods for protective conservation will be explored.⁶⁷ Further studies focused on various deterioration processes affecting natural building stones within Cologne Cathedral.^{67,68} Some researchers found negative interactions between different types of stones used in the construction, which were primarily deteriorating the sandstone and consequently affecting the neo-Gothic architectural construction.^{69,70}

The building stones have suffered significant deterioration, which is particularly noticeable in the situation of the Drachenfels trachyte.⁷¹ The stones are covered with black framboidal crusts, laminar, and thin, laminar that contain particles from contamination deposits. Additionally, weathering crusts have formed on silicate stones, which subscribe to the mortification of the historical building substantial. It is noteworthy that crust creation on the Drachenfels trachyte powerfully associates with stone disintegration. Gypsum is found not only in the crusts but also in extensive layers of deteriorating stone material. These crusts have a tendency to detach, exacerbating the structural deterioration.

The Drachenfels trachyte exhibits characteristic decay features like contour scaling, flaking, and exfoliation, resulting in gritty decomposition and deterioration. Weathering crusts develop on Stenzelberg late and Obernkirchener sandstone in narrow layers, usually around 2–3 mm thick, which are susceptible to get detachment from the surface of stone. Schlaitdorfer sandstone displays dense black crusts, frequently lead by extensive contour rise measuring some centimeters wide and notable granular erosion. For Krensheimer Muschelkalk, these crusts provide temporary stabilization to the stone surface.⁷² Exposed surfaces subjected to rain may display solution phenomena like microkarst formations. Surfaces exposed to rain may exhibit solution situation such as microkarst.⁷¹

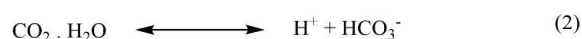
Thin slices of crust samples were collected from buildings in various cities across Northern Italy. These samples were then examined using both optical and electron microscopy techniques. The investigation revealed some key findings⁷³ that can be summarized as follows:

- ❖ Elevated concentrations of black carbonaceous particles from fuel oil consistently appeared within the calcite gypsum mixture.
- ❖ Coal-derived carbonaceous particles were not commonly detected in the samples.
- ❖ There is a direct correlation between the thickness of the crust and the quantity of black particles from oil-fired sources found within it.
- ❖ Black particles are predominantly associated with gypsum and are frequently observed to be embedded within it.
- ❖ On occasion, the orientation of gypsum crystals suggests growth around the surfaces of the black particles.

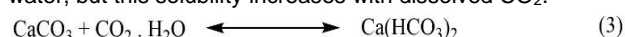
The theory suggests that soot particles from oil combustion have a significant impact on stone sulphation in urban environments. This aligns with several experimental findings conducted at the Lawrence Laboratory in Berkeley. The experiments showed that carbonaceous particles catalyze the oxidation of SO₂ to sulfate when present in liquid water.⁷⁴ Furthermore, it has been observed that the catalytic oxidation of SO₂ on carbonaceous particles suspended in water remains largely unaffected by the pH levels encountered in urban atmospheres.⁷⁵ Under laboratory-simulated environmental conditions, a direct correlation has been established between the reaction rate and the concentration of suspended carbonaceous particles. However, no significant correlation was found with the concentration of dissolved SO₂.⁷⁵ This implies that under similar conditions, the rate of sulphation is approximately proportional to the concentration of black carbonaceous particles deposited on wet stone, yet shows little dependence on airborne SO₂ levels. It is important to note that trace metal catalysis may influence the sulphation rate. However, crust samples from Venice, where damage is most pronounced, contain these metals at much lower concentrations than samples from other cities.⁷³ The absence of motor vehicle traffic in Venice explains this discrepancy.

Air pollution has been a major concern since the beginning of the Industrial Revolution. It has significantly affected human well-being, habitat, and the integrity of stone. The root

cause of this problem is human activity, especially the burning of wood and fossil fuels, which liberate various solid and gaseous chemicals within the atmosphere. The main culprits behind the certain oxides in stone materials' degradation undergo reactions with water, resulting in acidic conditions. These oxides include carbon dioxide (CO₂), sulfur oxides (SO_x), and nitrogen oxides (NO_x).⁷⁶ These acids interact with stone surfaces, particularly carbonate-based materials like marble and limestone, causing them to deteriorate. CO₂ reacts with water through the following reactions:

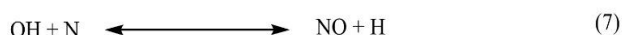


An increase in atmospheric CO₂ leads to higher levels of CO₂ in water, which increases its acidity. CaCO₃, which is commonly found in stone materials, has low solubility in water, but this solubility increases with dissolved CO₂.



Henry's law explains that the levels of CO₂ in the environment and the temperature of the water play a significant role in the solubility of CO₂ in water. Lower temperatures increase the rate of dissolution, leading to an increase in carbonate dissolution in urban areas with high CO₂ levels and during the winter season when temperatures are lower. Equation (3) shows that the state of equilibrium can be changed towards the reactants by water evaporation or a temperature rise resulting in the regeneration of calcium carbonate. CaCO₃ can dissolve and precipitate in the same location or other areas, leading to significant changes in the microstructure of the stone in the dispersed regions, making it more prone to further degradation.

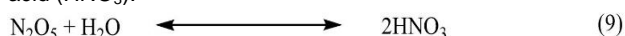
The atmospheric CO₂ level is expected to rise to about 700 ppm in 100 years based on the Keeling curve, compared to the current level of around 420 ppm.⁷⁷ This increase has a relatively small impact compared to the 2500 ppm level of CO₂ found in indoor settings. Dissolving CO₂ can pose a threat to fragile and expensive surfaces of wall paintings that contain calcium carbonate in the setting layers or pigments.⁷⁸



At temperatures above 2200 K (~1900 °C), the initial reaction (Equation (4)) occurs, followed by responses (Equations (5)-(7)). Therefore, nitric oxide (NO) generation requires high temperatures and an excess of oxygen in a particular area, such as in interior combustion machine. Additionally, NO can undergo conversion to NO₂ via a reaction with ozone.



NO₂ can react with oxygen to produce dinitrogen pentoxide (N₂O₅), which can then dissolve in water (H₂O) to form nitric acid (HNO₃).



The acid described can undergo a chemical reaction with CaCO₃.



HNO₃ can corrode the stone substrate, which can result in the creation of Ca(NO₃)₂. This substance has a greater solubility in comparison to carbonates. This reaction cannot be reversed. Unlike Equation (3), and the process does not involve any carbonate re-precipitation at the end.

SO₂ is a major threat to the preservation of stone materials. It is predominantly produced by human pursuits, particularly the burning of fossil fuels like dense parts of mineral oil and

coal. When SO_2 undergoes oxidation from S(IV) to S(VI), it can take various pathways involving NO_2 , O_3 , metals, and particulate matter ($\text{PM}_{1, 2.5}$, and PM_{10}).⁷⁹ This chemical process leads to the formation of sulfur trioxide (SO_3), which subsequently interacts with H_2O to generate sulfuric acid (H_2SO_4). As a result, H_2SO_4 interacts with CaCO_3 , leading in the formation of CaSO_4 .



CaSO_4 , which is often found in the hydrated arrangement of $\text{CaSO}_4 \cdot 2\text{H}_2\text{O}$, has a solubility that is similar to calcium carbonate. When CaSO_4 precipitates, it forms a crust. While NO_x and SO_2 emissions have decreased in recent years, they still remain high in countries like China and other emerging nations.⁸⁰ Therefore, the technique described in Equation (11) remains crucial in such settings.

Particulate matter (PM) is a type of air pollution that consists of small particles and liquid droplets. These particles can include acids, metals, dust, soil particles, and organic compounds. PM comes from both natural sources such as volcanoes, sea spray, and dust storms, and artificial sources such as industrial and mechanical operations and automobile emissions.⁸¹

The contaminants listed in Equation (3), (10), and (11) can be deposited onto a stone's surface through either wet or dry processes. Dry deposition happens when gases and particle matter settle on a surface without water. In contrast, wet deposition occurs when atmospheric gases and particulate matter combine with water and are removed through precipitation, such as fog or rain. It appears at a slower pace but maintains a greater level of consistency, while wet deposition is quicker and more effective. Water functions both as a solvent and occasionally as a reactant during the process and facilitates the reactions involving the substrate mentioned in Equations (3), (10), and (11).⁸²

CaSO_4 can be effectively eliminated from stone surfaces through washing since it exhibits higher solubility than CaCO_3 . Nevertheless, these deposits tend to accumulate and amalgamate with particulate matter, frequently developing dark crusts in sheltered areas. The colour of deterioration byproducts can range from grey to white and is influenced by the concentration of PM present. The ICOMOS Glossary defines a "black crust" as a generally cohesive collection of elements on the surface. It may consist of exogenic deposits and elements originating after the stone. These crusts usually appear dark in colour but can also exhibit bright hues. Crusts can either have a consistent thickness, mimicking the stone surface, or an uneven thickness that may obscure the features of the stone surface.⁸³

3. Cultural Heritage

Cultural heritage plays a crucial role in human civilization, reflecting important social development processes. It is tangible evidence that is necessary for the sustainable progress of society. Protecting our cultural heritage is fundamental to nurturing social and artistic advancement. Atmospheric pollutants pose a significant risk to heritage materials, particularly stone, resulting in substantial losses beyond economic implications. The impact of air pollution on immovable heritage as shown in Figure 2.

Air pollution, which includes gaseous and fine particulate matter pollutants, is a major threat to the sustainable preservation of cultural heritage. Acidic and oxidizing gases in air pollutants cause severe corrosive effects on heritage materials such as stone, wood, metals, and paints, through acidification and oxidation reactions.

Acidic and oxidizing substances present significant dangers to the preservation of ancient buildings and monuments. Acidic substances such as acid rain and industrial emissions chemically react with stone materials like limestone and marble, causing erosion, pitting, and decreased structural strength. They gradually degrade the surface and erode intricate features by reacting with the calcium carbonate in

the stone. Similarly, oxidizing chemicals like ozone and chlorine hasten the decomposition of organic substances and contribute to the erosion of metals, compromising the strength of structural components and decorative features. Furthermore, these treatments induce surface deterioration, altering the original aesthetic of the monuments. To counter these detrimental effects and ensure the cultural and historical importance of these monuments for future generations, it is imperative to implement effective conservation techniques, such as monitoring, protective coatings, and new treatments.

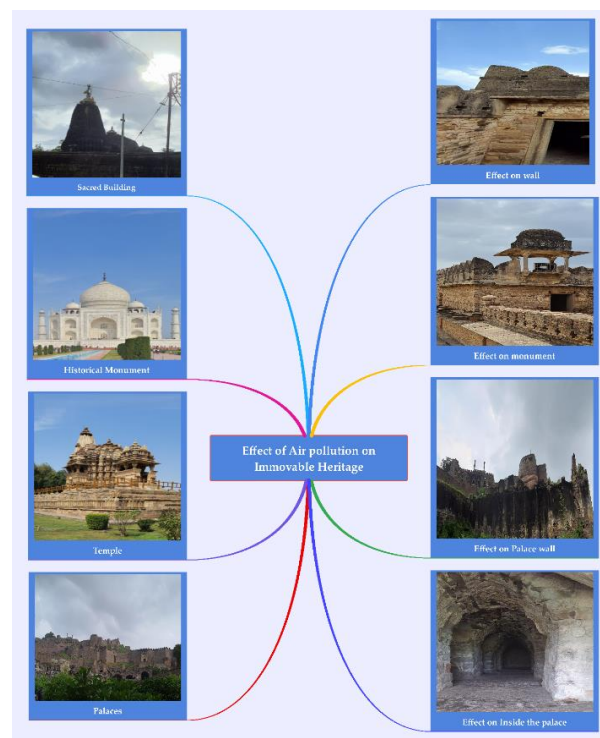


Figure 2. Effect of air pollution on immovable heritage

4. Damage to monuments

Did you know that monuments can suffer from various types of deterioration? To help understand this better, we have categorized these types into eight groups, which are shown in Figure 3. By being aware of the different types of deterioration, we can take proactive measures to preserve and protect these important cultural and historical landmarks for future generations.

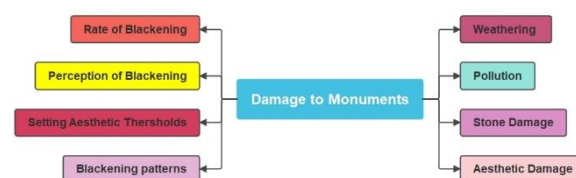


Figure 3. Different forms of damage to monuments

4.1. Weathering

Stone structures are subject to a gradual decline over time, commonly known as 'weathering'. Initially, the term 'weathering' referred to the positive effects of weather and drying, but it is now associated with climate-induced damage. Architects and geologists have long recognized how weathering can erode and break down structures. Three

hundred years ago, architects believed buildings deteriorated due to 'time, smoke, and weather'.⁸⁴

In areas with mild climate, the most noticeable sign of climate degradation is often frosting damage. When moisture in stone freezes, it leads to a change in volume and causes the outer layers to shatter. Additionally, the presence of salts in the stone and alternating wetting and drying cycles can contribute to similar types of damage. Salts are usually found near the ground but can also be deposited on structures by salty rains, a phenomenon more prevalent in coastal areas experiencing strong winds. Speaking of strong winds, they can directly damage buildings by dislodging tiles and demolishing vulnerable sections of a structure. Although lightning strikes are infrequent, they can cause damage, especially to projecting sections of buildings like steeples.⁸⁵ Repetitive exposures to sunlight and subsequent cooling can also create temperature differences that result in the deterioration of stone surfaces. Marbles and granites are more vulnerable to heat compared to porous stones. Calcite in marbles exhibits anisotropic expansion, expanding across one crystallographic axis and contracting along the other two, whereas the primary minerals in granite have varying thermal expansion coefficients.⁸⁶

Preserving historical monuments and buildings is crucial, and the air pollution-induced degradation of stone structures is a complex challenge that demands our attention. Airborne pollutants, such as SO₂ and NO₂, chemically react with atmospheric moisture to form acids like SO₂ and NO₂. These corrosive acids gradually erode the minerals in stone, particularly calcium carbonate in limestone and marble, leading to the deterioration of these precious structures. It is imperative that we address this issue to safeguard our cultural heritage for future generations.

4.2. Pollution

Complaints about buildings getting dirty have been documented since the time of the Romans. However, in the 17th century, the widespread practice of coal in London led to a significantly more serious issue. Architects like Wren and Hawksmoor were troubled by the thick black layers of sulfate that accumulated on structures exhibited to coal smoke.

It is challenging to accurately measure the degradation of building materials over centuries. However, some people believe that the pace of deterioration increased significantly during the 20th century. But before coming to a conclusion, it is crucial to consider that once a building's capabilities are removed, the impact is permanent and cumulative over time. This can make it hard to comprehend the extent of the damage, as we tend to see the effects gradually. It would be more helpful to know the rate of defilement at a specific point in time. While long-term monitoring may be challenging, associating the pace of degradation of monuments in rural and urban regions can demonstrate the significant impact of urban air pollution on building materials.⁸⁷

The relationship between air pollution and its harmful effects on the environment can be quite complex. While cities have seen a decline in corrosive primary pollutants like SO₂ and smoking since the early 20th century, this does not align with the fast and escalating deterioration of structures and monuments that are considered characteristic of this century. It seems that advances in the deterioration rate of the environment have only sometimes accompanied enhancements in urban air quality. There could be several explanations for this. While the overall number of corrosive pollutants in the city air may have dropped, some elements like ozone, nitrogen oxides, and components that make up photochemical smog could not be reduced. These pollutants may accelerate the deterioration of building materials or serve as catalysts to exacerbate the impact of conventional pollutants.⁸⁸ Additionally, building materials have a kind of 'memory', and the current degradation results from contaminants that were deposited in the past.⁸⁷

In recent times, the high levels of sulphate deposition have decreased considerably. As of now, the deposits mainly comprise of diesel soot and nitrogen compounds. In the future, the crusts on buildings may show more organic chemistry, which can lead to a change in the color of building surfaces due to the oxidation of the deposited organic material. If we can reduce soot levels in metropolitan areas, it may result in natural cleaning of ancient structures by rain and wind.⁸⁹

4.3. Stone Damage

Numerous studies have investigated the effects of atmospheric contamination, specifically SO₂, on stone as it is widely used in historic buildings. The primary consequences of airborne pollutants on the stone are chemical breakdown, which causes damage to the substance, soiling, blackening, leading to visual nuisance.⁹⁰

Recently, the primary process of deterioration in metropolitan areas was the dry accumulation of SO₂. This was primarily emitted from the ignition of fossil fuels, followed by its conversion into sulphate due to oxidation. Two critical prerequisites are essential for the occurrence of the oxidation process. Firstly, moisture is required on the surface or within the pores close to it. Secondly, an oxidation process is necessary to transform SO₂ into H₂SO₄ or an in-between sulphite (SO₂-) salt into a sulfate, namely CaSO₄ dihydrate. In urban atmospheres, NO_x and other gases can also stick to stone surfaces through deposition. When there is moisture, NO_x can increase the oxidation of SO₂.⁸⁸

A stone's permeability and specific surface area can significantly affect the movement of moisture and the accumulation of pollutants on its surface. The accumulation of air particles can also be influenced by surface roughness. If the pollution results in soluble salts, they can penetrate the stone and cause degradation. Salts present on building surfaces can increase humidity levels within the stone, which can lead to the accumulation of more contaminants.

Stones that contain carbonate are highly vulnerable to the negative effects of contamination. When subjected to elevated concentration of SO₂ contamination, carbonate stones that have not been sufficiently washed by rain can produce a tough outer layer of gypsum, which becomes darkened due to the inclusion of soot particles.⁹¹ The expansion of gypsum within the stone can cause stresses that result in physical damage to the structure in various ways, as gypsum possesses a larger molar volume compared to CaCO₃. Carbonate stones that are frequently and intensely exposed to rainfall can also undergo a dissolving process on their surfaces. The breakdown occurs more rapidly when the stone has been previously exposed to air contaminated with sulfur dioxide (SO₂).⁹¹

Dolomite-containing carbonate stones (CaMg(CO₃)₂) undergo a reaction with SO₂ to yield CaSO₄ and MgSO₄. As a result of this reaction, CaSO₄ forms a coating of soot and gypsum, while magnesium sulphate, which is highly soluble, can cause more extensive damage due to the crystallization process of this particular salt penetrating deeper. Calcareous sandstones are prone to erosion in heavily polluted areas due to the corrosive effects of atmospheric sulfuric acids. The dissolution of calcite in small quantities can release numerous sand grains, aggravating the damage caused by the crystallization of this particular kind of salt.⁸⁶ Sandstones composed primarily of quartz exhibit high resistance to sulfuric acids but are prone to accumulating significant dirt.⁸⁶

Acidic gases can have a significant impact on certain categories of roofing slates. If the slate comprises calcite, when SO₂ dissolves in rainwater, it reacts to generate an acidic solution, which can be retained by capillary action within the crevices of the slate and corrode the calcite. This interaction can also cause the formation of gypsum crystals, which can add to the harm. In situations where the slate

includes unstable pyrite (iron sulphide) and calcite, rainwater may combine with the pyrite to produce sulfuric acid. This acidic solution can corrode the calcite and potentially cause the slate to collapse.⁸⁶

Granite is a popular material for building sites because of its durability and resistance to acidic pollutants. However, recent research suggests that it can still be damaged by air pollution.⁹² There are two types of damage that granite surfaces can experience: gypsum crusts from airborne contaminants and weathering layers of clay-calcitic elements inherent to the granite's composition. In regions with high humidity and temperate climates, air pollution containing SO₂ can have a twofold effect on the deterioration of granite.⁹³ It can cause sulphate precipitation and convert feldspars into kaolin. Moreover, the process of plagioclase weathering can provide the necessary Ca²⁺ ions for forming gypsum crystals.

4.4. Aesthetic Damage: Blackening

In the past few decades, there has been a significant reduction in the levels of acidic pollutants, resulting in fewer chemical reactions and surface degradation of stones. However, this has resulted in an increase in the prominence of the problem of darkening or soiling of building materials, which has led to greater attention being paid to aesthetic factors.

Buildings can darken due to the accumulation of particle debris caused by fine carbonaceous particles that cover their exposed surfaces.⁹⁴ This is an aesthetic problem that has been a concern for centuries, dating back to ancient times. For instance, the defacement of sacred structures in Ancient Rome was a significant concern for the poet Horace. In the 17th century, John Evelyn also expressed significant concerns about the unsightliness caused by the accumulation of soot on buildings in London.⁸⁴ The carbonaceous deposits on building surfaces have high optical absorptivity, making them highly efficient in darkening surfaces.⁹⁵

It is noteworthy that even in the latter part of the 20th century, blackening remained a problem.⁹⁶ While coal usage decreased in many cities, diesel soot became the primary contributor of elemental carbon. Even to this day, there is ongoing concern about this issue. However, some regions have experienced a decline in soot in the air, resulting in cleaner surfaces. Rain also plays a significant role in washing away pollutants, which has led to cleaner buildings in some cases.⁸⁹ Nevertheless, biological activity can significantly worsen the blackening of stone surfaces, especially when combined with increased organic pollution.⁹⁷

4.5. Rate of Blackening

The rate at which monuments become darkened by air pollution is determined by several critical factors. Urban areas with heavy industrial activity and high traffic often experience accelerated darkening due to elevated levels of pollutants such as soot and sulfur dioxide. The choice of materials for monuments is also crucial; porous stones like limestone and marble are more susceptible to damage than sturdy materials like granite. Environmental elements, such as humidity, temperature fluctuations, and precipitation patterns, also impact the rate at which pollutants settle and react on the surfaces of monuments. Implementing efficient maintenance practices, such as applying protective coatings and regular cleaning, can slow down the darkening process. To maintain the visual and structural integrity of monuments in the face of ongoing environmental challenges, it is essential to implement proactive conservation measures and enforce strict air quality laws.

According to a study, when analyzing lengthy data records to understand the blackening process, the bounded exponential fit model is a more precise model than others.⁹⁸ Rather than using a reflectance meter to detect color

variations, a colorimeter is often used as it provides more comprehensive information.

Materials can turn yellow due to various processes like sulphation,⁹⁰ deposition or oxidation of organic compounds, or iron.⁹⁹ If the atmosphere remains contaminated with organic pollutants, the yellowing process may become more pronounced, especially for materials that are prone to damage.

4.6. Perception of Blackening

The human eye can distinguish between clean and dirty areas on a white surface when 0.2% of the surface is covered by dark particulate matter.^{100,101} In a study by Lanting,⁹⁵ it was found that complaints are likely to arise when the coverage reaches 2%, and they become more severe at 5%. A more recent study by Bellan *et al.*¹⁰² discovered that observers can only identify that a sample is getting dirty when black carbon particles cover the surface to a level of 2.4%. However, when it comes to buildings, the problems become more complex, especially within a specific setting.

Several individuals had concerns about the cleanliness of the buildings. They formed their opinion based on specific old structures that displayed stark contrasts between clean and dark (sometimes green) areas. At times, entire facades were covered in thick soot. Visitors were more inclined to notice changes in brightness rather than color or saturation, which do not vary significantly with respect to the stone used.

4.7. Setting Aesthetic Thresholds

It is crucial to understand what level of blackening is acceptable for managing air pollution and maintaining the aesthetic appeal of structures. To determine the permissible concentrations of elemental carbon (EC) in the atmosphere, it is possible to calculate the derivative of the sigmoid curve related to perceived lightness, which helps analyze the various segments of the curve and possible thresholds. However, the acceptable levels chosen should take into account the specific political and cultural considerations of the area.

This argument suggests that the color of buildings changes gradually over time, often following an exponential pattern. The study mainly focuses on light-colored stone, which is considered more vulnerable to aesthetic changes. Pollution exposure tends to stabilize the color of buildings at a relatively consistent level after several years. It is hypothesized that dark-colored stones may be more tolerant of higher levels of soot accumulation.

4.8. Blackening Patterns

Blackening patterns are a type of discoloration that do not necessarily cover the entire exterior of a building uniformly. These patterns have been widely considered offensive for a significant period of time. However, there is a need for more studies regarding public perception of blackening patterns. Grossi and Brimblecombe⁹⁸ conducted a study to determine the level of acceptance of different blackening patterns, utilizing two desktop efforts that employed a strategy identical to studies in art psychology.

When making decisions, it is important to take into account the effect of perceived lightness versus opinions about unsightly patterns. Although it may be challenging to determine, unattractive patterns can have a significant impact on visitors' experience. To preserve the visual authenticity of historic buildings, it is essential to closely monitor patterns of dirt buildup. This is particularly critical when utilizing selective cleaning methods for stone surfaces.

The impact of air pollutants can obscure the beauty and historical significance of old buildings. This darkening diminishes the cultural and aesthetic value. Conservation efforts are essential to apply cleaning techniques and protective measures, ensuring the preservation of these monuments' authentic appearance.

5. Discussion and Way forward

The occurrence of blackening is a significant issue for stone materials in heavily polluted urban areas. Scientists from various fields such as chemistry, physics, geology, and conservation have extensively studied this phenomenon. Their research ranges from examining the macroscopic to microscopic levels, investigating the structure and composition of affected objects, their interactions with pollutants, and the influence of environmental factors. This report emphasizes the importance of a multidisciplinary approach in understanding the complexity of this subject.

The data collected have significant scientific value and practical applications. Various analytical methods have been used to determine the composition of these blackened crusts. The findings are also valuable for stone conservators, helping them develop effective strategies to protect original substrates and prevent further pollution accumulation. The paper discusses a range of cleaning and conservation techniques, from traditional methods to advanced approaches such as laser cleaning.

Moreover, the research sheds light on the formation process of these crusts, which has social significance. Stakeholders involved in heritage management are encouraged to advocate policies that promote the preservation of cultural assets while addressing environmental concerns such as reducing greenhouse gas emissions.

The research findings also highlight the link between blackening and airborne pollution, positioning these phenomena as indicators of past pollution levels. However, definitive methods for acquiring precise information still need to be discovered. Unresolved questions persist, such as the oxidation of sulfur dioxide and its catalytic processes on stone surfaces, potentially involving additional pollutants like O_3 , NO_x , metals, or soot. While bacterial involvement has been suggested, the mechanisms remain poorly understood.

There is a critical inquiry into the future implications of predicted pollution patterns on blackening occurrence and broader stone preservation. Decreased emissions of sulfur oxides (SO_x), nitrogen oxides (NO_x), and particulate matter may reduce blackening concerns over time. However, anticipated climate changes, including rising temperatures, elevated atmospheric carbon dioxide levels, and increased frequency of extreme weather events, introduce uncertainties regarding the preservation of cultural assets. It is conceivable that a new equilibrium will emerge between materials and the environment, shifting the focus from "air pollution - conservation of built heritage" to "climate change - conservation of built heritage."

5. Conclusion

Research into the degradation of stone materials, particularly in urban settings, is crucial for preserving cultural heritage.¹⁰³ Air pollution, which is especially prevalent in cities, significantly contributes to stone deterioration.¹⁰⁴ The primary mechanisms driving this degradation are gypsum formation and carbonate dissolution.¹⁰⁵ Weathering crust degradation is also a major issue, which occasionally results in the fracturing of crusts, revealing the extent of damage. Acid rain, which results from the contamination of rainwater by sulphur, nitrogen, and carbon oxides, accelerates the breakdown of rock-forming minerals.

Weathering crusts predominantly comprise newly formed minerals, such as gypsum, that encapsulate airborne particles. These particles encompass three main types:

predominantly iron-based metal particles, smooth aluminosilicate particles, and porous carbonaceous particles (soot). Environmental factors, including moisture supply, drying, architectural design, construction practices, and maintenance, significantly influence degradation processes.

The Cologne Cathedral, a prominent cultural icon in northern Europe, is currently facing substantial stone degradation. Specifically, the Drachenfels trachyte exhibits visible structural deterioration and the proliferation of extensive gypsum crusts. Signs of deterioration include contour scaling, flaking, and exfoliation, leading to the dissolution and collapse of its granular structure, with rain-exposed surfaces displaying solution phenomena like microcars formation.

Analysis of crust samples from structures in Northern Italy revealed high concentrations of black carbonaceous particles from fuel oil within calcite and gypsum mixtures. These particles, primarily associated with gypsum, are often enclosed within it. It is theorized that soot particles from oil combustion significantly influence the stone sulphation process in urban environments.

Experiments conducted at the Lawrence Laboratory in Berkeley demonstrated that carbonaceous particles act as catalysts for oxidizing sulphur dioxide (SO_2) to sulphate in the presence of liquid water. A direct correlation between the rate of reaction and the suspended carbonaceous particle quantity was observed under laboratory conditions, with no significant relationship identified with dissolved SO_2 concentrations. Trace metal catalysis may affect sulphation rates, although crust samples collected from Venice showed significantly lower metal quantities than from other cities.

Since the onset of the Industrial Revolution, the issue of air pollution has become increasingly prominent, posing significant threats to human well-being, ecosystems, and the integrity of various stone materials. Certain oxides undergoing chemical reactions with water are primary contributors to stone degradation, resulting in acidic conditions affecting stone surfaces, particularly carbonate-based materials like marble and limestone.

Particulate matter (PM), comprising liquid droplets and tiny particles containing soil particles, metals, acids, dust and organic substances, poses another threat. Originating from both natural and artificial sources, including industrial operations and vehicular emissions, PM can be deposited on stone surfaces via dry or wet processes.

Cultural heritage is paramount in human civilization, yet it faces severe risks from air pollution, leading to substantial losses beyond economic implications. Monument damage can be classified into various categories, including weathering and pollution, with urban air pollution notably impacting architectural materials.

Understanding the rate of building material deterioration over centuries is challenging but vital. Analyzing monument deterioration rates in urban and rural settings highlights the significant influence of urban air pollution on architectural materials.

The relationship between air pollution and its adverse environmental consequences is complex. Despite decreases in harmful primary pollutants since the early 20th century, ongoing building and monument degradation persist due to ozone, nitrogen oxides, and photochemical smog.

SO_2 , a prominent air pollutant, has been extensively studied for its effects on stone and commonly affects historical structures. Airborne contaminants have three primary effects on stone: chemical degradation, soiling or darkening, and aesthetic concerns, primarily reliant on dry deposition of SO_2 and subsequent conversion into sulphate by oxidation.

Stones containing carbonate are particularly vulnerable to pollution, developing resilient gypsum outer layers in high SO_2 concentrations. Calcareous sandstones are susceptible to erosion due to atmospheric sulfuric acid corrosion. Despite granite's longevity and resistance to acidic pollutants, it can develop gypsum crusts and layers of clay-calcitic materials.

Recent declines in acidic pollutants have led to increased concerns regarding the darkening or soiling of building materials, necessitating greater aesthetic focus. Particulate matter buildup, especially carbonaceous particles, contributes to surface darkening over time.

Author Contribution Declaration

Abhishek Singh: Graphic Design, **Tanvir Arfin:** Writing-original draft, review, editing, proofreading and supervision, **Nikhila Mathew:** Literature survey, conceptualization and writing, **Abha Tirpude:** Literature survey, conceptualization and writing. All authors have read and agreed to the published version of the manuscript.

Data Availability Declaration

No new data was used for the research described in the article.

Acknowledgements

The authors are grateful to director, CSIR-NEERI, for providing the necessary facilities for this work. The manuscript is checked for plagiarism using licensed version of iThenticate software and recorded in the Knowledge Resource Centre, CSIR-NEERI, Nagpur for anti-plagiarism (KRC No.: CSIR-NEERI/KRC/2024/MAY/AR/1).



References

1. S. A. Mandavgane, S. Rayulu, A. A. Chilkalwar, S. M. Anjankar, A. A. Moinuddin, T. Arfin, A. A. Mandavgane. Kinetics and thermodynamics studies of photocatalytic hydrogen generation by Au/Pt/TiO₂. *Rasayan. J. Chem.* **2023**, *16*, 2239. <http://dx.doi.org/10.31788/RJC.2023.1648617>
2. P. K. Obulapuram, T. Arfin, F. Mohammad, K. Kumari, S. K Khiste, H. A. Al-Lohedan, M. Chavali. Surface enhanced biocompatibility and adsorption capacity of a zirconium phosphate-coated polyaniline composite. *ACS Omega* **2021**, *6*, 33614. <https://doi.org/10.1021/acsomega.1c04490>
3. P. K. Obulapuram, T. Arfin, F. Mohammad, S. K Khiste, M. Chavali, A. N Albalawi, H. A. Al-Lohedan. Adsorption, equilibrium isotherm, and thermodynamic studies towards the removal of reactive orange 16 dye using Cu(1)-polyaniline composite. *Polymers* **2021**, *13*, 3490. <https://doi.org/10.3390/polym13203490>
4. T. Arfin, D. A. Bhaisare, S. S. Waghmare. Development of a PANI/Fe (NO₃)₂ nanomaterial for reactive orange 16 (RO16) dye removal. *Anal. Methods* **2021**, *13*, 5309. <http://dx.doi.org/10.1039/D1AY01402A>
5. T. Arfin, K. Sonawane, A. Tarannum. Review on detection of phenol in water. *Adv. Mater. Lett.* **2019**, *10*, 753. <http://dx.doi.org/10.5185/amlett.2019.0036>
6. F. Mohammad, T. Arfin, H. A. Al-Lohedan. Biocompatible polyactic acid-reinforced nickel-arsenate composite: studies of electrochemical conductivity, mechanical stability, and cell viability. *Mater. Sci. Eng. C* **2019**, *102*, 142. <https://doi.org/10.1016/j.msec.2019.04.046>
7. F. Mohammad, T. Arfin, H. A. Al-Lohedan. Enhanced biosorption and electrochemical performance of sugarcane bagasse derived a polyactic acid-graphene oxide-CeO₂ composite. *Mater. Chem. Phys.* **2019**, *229*, 117. <http://dx.doi.org/10.1016/j.matchemphys.2019.02.085>
8. T. Arfin, A. Tarannum. Rapid determination of lead ions using polyaniline—zirconium (IV) iodate-based ion selective electrode. *J. Environ. Chem. Eng.* **2019**, *7*, 102811. <https://doi.org/10.1016/j.jece.2018.102811>
9. F. Mohammad, T. Arfin, H. A. Al-Lohedan. Synthesis, characterization and applications of ethyl cellulose-based polymeric calcium (II) hydrogen phosphate composite. *J. Electron. Mater.* **2018**, *47*, 2954. <http://dx.doi.org/10.1007/s11664-018-6118-8>
10. T. Arfin, S.N. Rangari. Graphene oxide-ZnO nanocomposite modified electrode for the detection of phenol. *Anal. Methods* **2018**, *10*, 347. <https://doi.org/10.1039/C7AY02650A>
11. F. Mohammad, T. Arfin, H.A. Al-Lohedan. Sustained drug release and electrochemical performance of ethyl cellulose-magnesium hydrogen phosphate composite. *Mater. Sci. Eng. C* **2017**, *71*, 735. <https://doi.org/10.1016/j.msec.2016.10.062>
12. F. Mohammad, T. Arfin, H. A. Al-Lohedan. Enhanced biological activity and biosorption performance of trimethyl chitosan-loaded cerium oxide particles. *J. Ind. Eng. Chem.* **2017**, *45*, 33. <http://dx.doi.org/10.1016/j.jiec.2016.08.029>
13. N. Malik, A. U. Khan, S. Naqvi, T. Arfin. Ultrasonic investigation of α-amino acids with aqueous solution of urea at different temperatures: A physicochemical study. *J. Appl. Sol. Chem. Model.* **2016**, *5*, 168. <http://dx.doi.org/10.6000/1929-5030.2016.05.04.2>
14. N. Malik, A. U. Khan, S. Naqvi, T. Arfin. Ultrasonic studies of different saccharides in α-amino acids at various temperatures and concentrations. *J. Mol. Liq.* **2016**, *221*, 12. <http://dx.doi.org/10.1016/j.molliq.2016.05.061>
15. T. Arfin, F. Mohammad. Electrochemical, Antimicrobial and Anticancer Effect of Ethyl Cellulose-Nickel (II) Hydrogen Phosphate. *Innov. Corros. Mater. Sci.* **2016**, *6*, 10. <http://dx.doi.org/10.2174/2352094906999160307182012>
16. R. Bushra, T. Arfin, M. Oves, W. Raza, F. Mohammad, M. A. Khan, A. Ahmad, A. Azam. Development of PANI/MWCNTs decorated with cobalt oxide Nanoparticles towards Multiple Application sites of Electrochemical, Photocatalytic and Biotechnology. *New J. Chem.* **2016**, *40*, 9448. <http://dx.doi.org/10.1039/C6NJ02054B>
17. T. Arfin, R. Bushra, F. Mohammad. Electrochemical sensor for the sensitive detection of o-nitrophenol using graphene oxide-poly(ethyleneimine) dendrimer-modified glassy carbon electrode. *Graphene Technol.* **2016**, *1*, 1. <https://dx.doi.org/10.1007/s41127-016-0002-1>
18. S. S. Waghmare, D. Lataye, T. Arfin, N. Manwar, S. Rayalu, N. Labhsetwar. Adsorption behavior of eggshell modified polyalthia longifolia leaf-based alumina as a novel adsorbent for fluoride removal from drinking water. *International Journal of Advance Research and Innovative Ideas in Education* **2015**, *1*, 904.
19. T. Arfin, Md. O. Aquatar, S. S. Waghmare. Mitigation strategies to greenhouse gas emission control: a database for emission factors. *Int. J. Sci. Res. Dev.* **2015**, *3*, 908.
20. R. V. Kalbandhe, S. S. Deshmukh, S. S. Waghmare, T. Arfin. Fabrication and performance analysis of downdraft biomass gasifier using sugarcane industry waste. *Int. J. Sci. Res. Dev.* **2015**, *3*, 903.
21. S. S. Waghmare, T. Arfin, S. Rayalu, D. H. Lataye, S. Dubey, S. Tiwari. Adsorption behavior of modified zeolite as novel adsorbents for fluoride removal from drinking water: surface phenomena, kinetics and thermodynamics studies. *International Journal of Science, Engineering and Technology Research* **2015**, *4*, 4114.
22. S. S. Waghmare, D. H. Lataye, T. Arfin, S. Rayalu. Defluoridation by nano-materials, building materials and other miscellaneous materials: A systematic review. *Int. J. Innov. Res. Sci. Eng. Technol.* **2015**, *4*, 11998. <http://dx.doi.org/10.15680/IJRSET.2015.0412046>
23. T. Arfin, F. Mohammad. Electrical conductivity, mechanical stability, antibacterial and anticancer activities of ethyl cellulose-tin (II) hydrogen phosphate. *Adv. Mater. Lett.* **2015**, *6*, 1058. <http://dx.doi.org/10.5185/amlett.2015.5896>
24. S. S. Waghmare, T. Arfin. Fluoride removal by clays, geomaterials, minerals, low-cost materials and zeolites by adsorption: A Review. *International Journal of Science, Engineering and Technology Research* **2015**, *4*, 3663.
25. S. S. Waghmare, T. Arfin. Defluoridation by adsorption with chitin-chitosan-alginate-polymers-cellulose-resins-algae and fungi-A Review. *Int. Res. J. Eng. Technol.* **2015**, *2*, 1179.
26. S. S. Waghmare, T. Arfin. Fluoride removal by industrial, agricultural and biomass wastes as adsorbents: Review. *International Journal of Advance Research and innovative Ideas in Education* **2015**, *1*, 628.
27. S. S. Waghmare, T. Arfin. Fluoride removal from water by carbonaceous materials: Review. *Int. J. Mod. Trends Eng. Res.* **2015**, *2*, 355.
28. R. K. Morchhale, S. S. Waghmare, T. Arfin. Assessing Quality in Machine Foundation Using UPV Measurements. *Int. J. Innov. Res. Sci. Eng. Technol.* **2015**, *4*, 8081. <http://dx.doi.org/10.15680/IJRSET.2015.0409012>
29. S. S. Waghmare, T. Arfin. Fluoride removal from water by aluminium-based adsorption: A Review. *J. Biol Chem. Chron.* **2015**, *1*, 1.
30. S. S. Waghmare, T. Arfin. Fluoride induced water pollution issue and its health efficacy in India- A review. *Int. J. Eng. Res. Gen. Sci.* **2015**, *3*, 345.
31. S. S. Waghmare, T. Arfin. Fluoride removal from water by various techniques: Review. *Int. J. Innov. Sci. Eng. Technol.* **2015**, *2*, 560.

32. S. S. Waghmare, T. Arfin. Fluoride removal from water by calcium materials: A state-of-the-art Review. *Int. J. Innov. Res. Sci. Eng. Technol.* **2015**, 4, 8090.
33. S. S. Waghmare, T. Arfin. Fluoride removal from water by mixed metal oxide adsorbent materials: A state-of-the-art review. *Int. J. Eng. Sci. Res. Technol.* **2015**, 4, 519.
34. L. K. Thakur, Y.M. Sonkhaskar, S. S. Waghmare, N. S. Duryodhan, T. Arfin. Fabrication and Performance Analysis of a biomass cook Stove. *Int. J. Sci. Res. Dev.* **2015**, 3, 440.
35. S. S. Waghmare, T. Arfin, N. Manwar, D. H. Lataye, N. Labhsetwar, S. Rayalu. Preparation and characterization of Polyalthia longifolia based adsorbent for removing fluoride from drinking water. *Asian J. Adv. Basic Sci.* **2015**, 4, 12.
36. D. C. Onwudiwe, T. Arfin, Christien A. Strydom. Surfactant mediated synthesis of ZnO nanospheres at elevated temperature, and their dielectric properties. *Superlattices Microstruct.* **2015**, 81, 215. <http://dx.doi.org/10.1016/j.spmi.2015.02.003>
37. F. Mohammad, T. Arfin. Thermodynamics and electrochemical characterization of core-shell type gold-coated superparamagnetic iron oxide nanoparticles. *Adv. Mater. Lett.* **2014**, 5, 315. <http://dx.doi.org/10.5185/amlett.2014.amwc.1030>
38. D. C. Onwudiwe, T. Arfin, C. A. Strydom. Fe(II) and Fe(III) complexes of N-ethyl-N-phenyl dithiocarbamate: Electrical conductivity studies and thermal properties. *Electrochim. Acta* **2014**, 127, 283. <http://dx.doi.org/10.1016/j.electacta.2014.02.034>
39. D. C. Onwudiwe, T. Arfin, Christien A. Strydom. Synthesis, characterization, and dielectric properties of N-butyl aniline capped CdS nanoparticles. *Electrochim. Acta* **2014**, 116, 217. <http://dx.doi.org/10.1016/j.electacta.2013.11.046>
40. T. Arfin, F. Mohammad. Electrochemical, dielectric behavior and in vitro antimicrobial activity of polystyrene-calcium phosphate. *Adv. Ind. Eng. Manag.* **2014**, 3, 25. <http://dx.doi.org/10.7508/AIEM-V3-N3-25-38>
41. T. Arfin, C. Kumar. Synthesis, characterization, conductivity and antibacterial activity of ethyl cellulose manganese (II) hydrogen phosphate. *Anal. Bioanal. Electrochem.* **2014**, 6, 403.
42. T. Arfin, S. Fatma. Synthesis, influence of electrolyte solutions on impedance properties and in-vitro antibacterial studies of organic-inorganic composite membrane. *Adv. Ind. Eng. Manag.* **2014**, 3, 19. <http://dx.doi.org/10.7508/AIEM-V3-N2-19-32>
43. T. Arfin, S. Fatima. Conductometric Studies with Polystyrene Calcium Phosphate Membrane. *Asian J. Adv. Basic Sci.* **2013**, 2, 1.
44. T. Arfin, F. Mohammad, DC electrical conductivity of nano-composite polystyrene-titanium-arsenate membrane. *J. Ind. Eng. Chem.* **2013**, 19, 2046. <http://dx.doi.org/10.1016/j.jiec.2013.03.019>
45. F. Mohammad, T. Arfin. Cytotoxic effects of polystyrene-titanium-arsenate composite in cultured H9c2 cardiomyoblasts. *Bull. Environ. Contam. Toxicol.* **2013**, 91, 689. <http://dx.doi.org/10.1007/s00128-013-1131-3>
46. S. Ahmad, R. Singh, T. Arfin, K. Neeti. Fluoride contamination, consequences and removal techniques in water: a review. *Environ. Sci. Adv.* **2022**, 1, 620. <https://doi.org/10.1039/D1VA00039J>
47. N. Mathew, A. Somanathan, A. Tirpude, T. Arfin. The impact of short-lived climate pollutants on the human health. *Environ. Pollut. Manag.* **2024**, 1, 1. <http://dx.doi.org/10.1016/j.epm.2024.04.001>
48. T. Arfin, A.M. Pillai, N. Mathew, A. Tirpude, R. Bang, P. Mondal. An overview of atmospheric aerosol and their effects on human health. *Environ. Sci. Pollut. Res.* **2023**, 30, 125347. <https://doi.org/10.1007/s11356-023-29652-w>
49. T. Arfin, P. Kate, A. Singh, K. Kumari. *Persistent Organic Pollutants*, CRC Press, **2021**, *Alternatives to POPs for a healthy life*, p. 201-226.
50. K. Kumari, T. Arfin. *Pollutants of Global Concern. Emerging Contaminants and Associated Technologies*, Springer, **2024**, Hexabromobiphenyl (HBB), p.195-204. https://doi.org/10.1007/978-3-031-50996-4_14
51. T. Arfin, N. Mathew, A. Tirpude, A. M. Pillai, P. Mondal. *Bioremediation Technologies: For Wastewater and Sustainable Circular bioeconomy*, Walter de Gruyter GmbH, **2023**, *Emerging Contaminants in air Pollution and their Sources, Consequences, and future*, p. 235-274. <https://doi.org/10.1515/9783111016825-014>
52. M. Pillai, T. Arfin. *Electrocatalytic Materials for Renewable Energy*, John Wiley, **2024**, *Environmental Electrocatalysis for Air Pollution Applications*, p. 303-331. <https://doi.org/10.1002/9781119901310.ch11>
53. A. Somanathan, N. Mathew, A. M. Pillai, T. Arfin. *Handbook of Nanofillers*, Springer Nature, **2024**, *Policy, Regulations, and safety of Nanofillers in Environment*, p. 1-40. https://doi.org/10.1007/978-981-99-3516-1_155-1
54. M. F. La Russa, S. A. Ruffolo. Mortars and plasters—How to characterize mortar and plaster degradation. *Archaeol. Anthropol. Sci.* **2021**, 13, 165. <https://doi.org/10.1007/s12520-021-01405-1>
55. E. Charola, J. Pühringer, M. Steiger. Gypsum: a review of its role in the deterioration of building materials. *Environ. Geol.* **2007**, 52, 339. <https://doi.org/10.1007/s00254-006-0566-9>
56. C. Sabbioni, *The effects of air pollution on the built environment*, Imperial College Press, **2003**, *Mechanism of air pollution damage to stone*. p.63-106.
57. G. M. Martinez, E. N. Martinez. Characterization of stone from the metropolitan cathedral and from the façade of the National Museum at Tepotzotlan, Mexico. *Studies in conservation* **1991**, 36, 99. <https://doi.org/10.1179/sic.1991.36.2.99>
58. P. Brimblecombe. *The effects of air pollution on the built environment*. Vol.2, Imperial College Press, 2003, p. 1-428.
59. R. M. Esbert, F. Diaz-Pache, F. J. Alonso, J. Ordaz, G. C. Wood. *Proceedings of the 8th international congress on deterioration and conservation of stone*, Möller, **1996**, *Solid particles of atmospheric pollution found on the Hontoria Limestone of Burgos Cathedral (Spain)*1, p. 393–399. <https://doi.org/10.1007/s12665-012-2161-6>
60. C. Sabbioni. Contribution of atmospheric deposition to the formation of damage layers. *Sci. Total Environ.* **1995**, 167, 49. [https://doi.org/10.1016/0048-9697\(95\)04568-L](https://doi.org/10.1016/0048-9697(95)04568-L)
61. Rodríguez-Navarro, E. Sebastian. Role of particulate matter from vehicle exhaust on porous building stones (limestone) sulfation. *Sci Total Environ.* **1996**, 187, 79. [https://doi.org/10.1016/0048-9697\(96\)05124-8](https://doi.org/10.1016/0048-9697(96)05124-8)
62. P. Ausset, F. Bannery, R. A. Lefèvre. *7th International congress on deterioration and conservation of stone*, Lab. Nat. engenharia Civil, **1992**, Black-crust and air microparticles contents at Saint-Trophime, Arles, p. 325–334. <https://doi.org/10.1007/s12665-012-2161-6>
63. R. P. J. Hees, L. Binda, I. Papayianni, E. Toumbakari. Characterisation and damage analysis of old mortars. *Mater. Struct.* **2004**, 37, 644. <https://doi.org/10.1007/BF02483293>
64. P. Maurenbrecher. Water-Shedding Details Improve Masonry Performance; Construction Technology Update 23; Institute for Research in Construction, National research Council: Ottawa, ON, Canada, **1998**.
65. B. Graue, S. Siegesmund, P. Oyhantcabal, R. Naumann, T. Licha, K. Simon. The effect of air pollution on stone decay: the decay of the drachenfels trachyte in industrial, urban, and rural environments—a case study of the Cologne, Altenberg and Xanten cathedrals. *Environ. Earth Sci.* **2013**, 69, 1095. <https://doi.org/10.1007/s12665-012-2161-6>
66. G. Knetsch. Geologie am Kölner Dom. *Geol Rundsch.* **1952**, 40, 57. <https://doi.org/10.1007/BF01803211>
67. P. W. Mirwald, K. Kraus, A. Wolff. *Durability of building materials 3/4*, Elsevier, **1988**, *Stone deterioration on the Cathedral of Cologne*. p. 549-570.
68. Y. Efes, H. P. Lühr. Natursteine am Bauwerk des Kölner Doms und ihre Verwitterung. *Kölner Domblatt* **1976**, 41, 167.
69. von Plehwe-Leisen, H. Leisen, E. Wendler. Der Drachenfels-Trachyt—ein wichtiges Denkmalgestein des Mittelalters—Untersuchungen zur Konservierung. *Z.d.Ges. Geowis* **2007**, 158, 985.
70. A. Wolff. Dombaubericht von oktober 1991 bis September 1992: 10.1 Londerfer Basaltlava und Schlaettdorfer Sandstein. *Kolner Domblatt* **1992**, 57, 89.
71. Graue, S. Siegesmund, B. Middendorf. Quality assessment of replacement stones for the Cologne Cathedral: mineralogical and petrophysical requirements. *Environ. Earth Sci.* **2011**, 63, 1799. <https://doi.org/10.1007/s12665-011-1077-7>
72. S. Siegesmund, A. Török, A. Hüpers, C. Müller, W. Klemm. Mineralogical, geochemical and microfabric evidences of gypsum crusts: a case study from Budapest. *Environ. Geol.* **2007**, 52, 358. <https://doi.org/10.1007/s00254-006-0588-3>
73. M. D. Monte, C. Sabbioni, O. Vittori. Airborne carbon particles and marble deterioration. *Atmos. Environ.* **1981**, 15, 645. [https://doi.org/10.1016/0004-6981\(81\)90269-9](https://doi.org/10.1016/0004-6981(81)90269-9)
74. T. S. Novakov, S. G. Chang, A. B. Harker. Sulfates as pollution particulates: Catalytic formation on carbon (soot) particles. *Science* **1974**, 186, 259. <https://doi.org/10.1126/science.186.4160.259>
75. S. G. Chang, R. Brodzinsky, R. Toossi, S. S. Markowitz, T. Novakov. Catalytic oxidation of SO₂ on carbon in aqueous suspensions. Conference on Carbonaceous Particles in the Atmosphere, **1978**, p. 122.

76. V. Fassina, M. Favaro, F. Crivellari, A. Naccari. The stone decay of monuments in relation to atmospheric environment. *Ann. Di Chim.* **2001**, 91, 767.
77. The Early Keeling Curve Scripps CO₂ Program. Available online: scrippsco2.ucsd.edu (accessed on 15 May 2024)
78. Y. B. Zeldovich. The Oxidation of Nitrogen in Combustion Explosions. *Acta Physicochim. USSR*, **1946**, 21, 577. <https://doi.org/10.3390/pr10010130>
79. J. Wang, J. Li, J. Ye, J. Zhao, Y. Wu, J. Hu, D. Liu, D. Nie, F. Shen, X. Huang. Fast sulfate formation from oxidation of SO₂ by NO₂ and HONO observed in Beijing haze. *Nat. Commun.* **2020**, 11, 2844. <https://doi.org/10.1038/s41467-020-16683-x>
80. P. Wang. China's air pollution policies: Progress and challenges. *Curr. Opin. Environ. Sci. Health* **2021**, 19, 100227. <https://doi.org/10.1016/j.coesh.2020.100227>
81. Particulate Matter|Air & Radiation|US EPA. US Environmental Protection Agency. Available online: <http://www.epa.gov/pm/> (accessed on 14 May 2024).
82. G. Amoroso, V. Fassina. Stone Decay and Conservation. Atmospheric Pollution, Cleaning, Consolidation and Protection, New York, **1983**, p. 474.
83. V. Vergès-Belmin. Illustrated Glossary on Stone Deterioration Patterns; ICOMOS: Paris, **2008**.
84. P. Brimblecombe. Air pollution and architecture, past, present and future. *J. Archit. Conserv.* **2000**, 6, 30. <https://doi.org/100/13556207.2000.10785268L>
85. P. Brimblecombe. The NOAHs ARK project: The impact of future climate change on cultural heritage. The European Geosciences Union Newsletter, **2005**, 12, 31. <http://www.the-eggs.org/articles.php?id=70>
86. B. Honeyborne. Weathering and decay of masonry. In Conservation of building and decorative stone, **2007**, p.153-178.
87. C. M. Grossi, P. Brimblecombe. Effect of long-term changes in air pollution and climate on the decay and blackening of European stone buildings. Geological Society, London, Special Publications, **2007**, 271, 117. <https://doi.org/10.1144/GSL.SP.2007.271.01.13>
88. L. G. Johansson, O. Lindqvist, R. E. Mangio. Corrosion of calcareous stones in humid air containing SO₂ and NO₂. *Durability of building Materials*, **1988**, 5, 439.
89. C. Davidson, W. Tang, S. Finger, V. Etyemezian, F. Struegel, S. Sherwood. Soiling patterns on a tall limestone building: changes over 60 years. *Environ. Sci. Technol.* **2000**, 34, 560. <https://doi.org/10.1021/es990520y>
90. C. M. Grossi, P. Brimblecombe. The effect of atmospheric pollution on building materials. *J. Phys.* **2002**, 12, 197. <https://doi.org/10.1051/jp4:20020460>
91. S. Trudgill. Environment, agriculture and conservation--Crumbling Heritage? Studies of stone weathering in polluted atmospheres by RU Cooke and GB Gibbs. *J. George Sys.* **1994**, 160-346.
92. V. V. Tran, D. Park, Y. C. Lee. Indoor air pollution, related human diseases, and recent trends in the control and improvement of indoor air quality. *Int. J. Environ. Res. Public Health.* **2020**, 17, 2927. <https://doi.org/10.3390/ijerph17082927>
93. N. Schiavon. Proceedings of the 9th international congress on deterioration and conservation of stone. **2000**. Science Granitic building stone decay in an urban environment: A Case of Authigenic kaolinite formation by heterogenous sulphur dioxide attack. P. 411-421. <https://doi.org/10.1016/B978-044450517-0/50124-0>
94. H. Haynie. Theoretical model of soiling of surfaces by airborne particles. *Aerosols. Lewis Publ, Chelsea (MI)*, **1986**, 951-959.
95. R. W. Lanting. Black smoke and soiling. aerosols, Lewis Publishers, **1986**, 923-932.
96. P. T. Newby, T. A. Mansfield, R. S. Hamilton. Sources and economic implications of building soiling in urban areas. *Sci. Total Environ.* **1991**, 100, 347. [https://doi.org/10.1016/0048-9697\(91\)90385-R](https://doi.org/10.1016/0048-9697(91)90385-R)
97. H. A. Viles, A.A. Gorbushina. Soiling and microbial colonization on urban roadside limestone: a three year study in Oxford, England, **2003**, 38, p. 1217-1224. [https://doi.org/10.1016/S0360-1323\(03\)00078-7](https://doi.org/10.1016/S0360-1323(03)00078-7)
98. C. M. Grossi, P. Brimblecombe. Air Pollution and cultural Heritage. **2004**. The rate of darkening of material surfaces. Rotterdam, p.193-198.
99. S. Simon, R. Snethlage. *8th International Congress on Deterioration and Conservation of Stone. 1996*. Marble weathering in Europe - Results of the Eurocare-Euromarble exposure programme 1992-1994. Berlin, p. 159-166.
100. W. F. Carey. Atmospheric deposits in Britain-a study of dinginess. *International Journal of Air Pollution*, **1959**, 2, 1.
101. R. P. Hancock, N. A. Esmen, F. P. Furber. Visual response to dustiness. *J. Air Pollut. Control. Assoc.* **1976**, 26, 54. <https://doi.org/10.1080/00022470.1976.10470221>
102. L. M. Bellan, L. G. Salmon, R. Cass. A study on the human ability to detect soot deposition onto works of art. *Environ. Sci. Technol.* **2000**, 34, 1946. <https://doi.org/10.1021/es990769f>
103. A. Somanathan, N. Mathew, T. Arfin. *Waste-derived nanoparticles: synthesis, Applications, and sustainability*, Elsevier, **2024**, *Environmental impacts and developments in waste-derived nanoparticles for air pollution control*, p. 281-318. <https://doi.org/10.1016/B978-0-443-22337-2.00018-X>
104. T. Arfin, N. Mathew, P. Mondal, *Biobased packaging materials: sustainable alternative to conventional packaging materials*, Springer Nature, **2024**, *Life cycle analysis of biobased materials*, p. 279-311. https://doi.org/10.1007/978-981-99-6050-7_11
105. A. Somanathan, N. Mathew, A. M. Pillai, P. Mondal, T. Arfin, *Bioplastics for sustainability: manufacture, technologies, and environment*, Elsevier, **2024**, *Bioplastics for clean environment*, p. 313-354. <https://doi.org/10.1016/B978-0-323-95199-9.00009-3>

Composites of Chitosan for Biomedical Applications

Ayanjeet Chowdhury¹, Samyak Dhale¹, RBK Dinesh Kumar¹, Andrew Biju John¹, Jaya Lakkakula^{1,2*}  and Nilesh S. Wagh^{1,3*} 

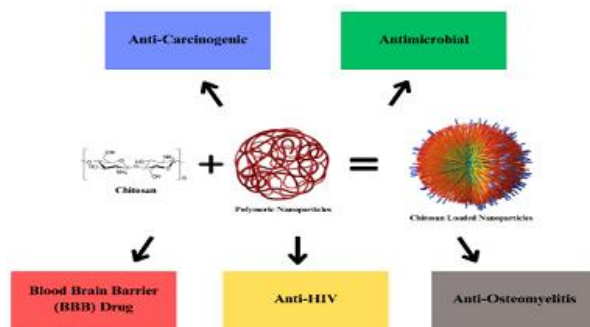
¹Amity Institute of Biotechnology, Amity University Maharashtra, Mumbai, 410206, India

²Centre for Computational Biology and Translational Research, Amity University Maharashtra, Mumbai, 410206, India

³Centre for Drug Discovery and Development, Amity University Maharashtra, Mumbai, 410206, India

*Correspondence: spencerjaya@gmail.com; waghnail@gmail.com

Abstract: Chitosan (CS) is a cationic polysaccharide that consists of jumble distributed units of N-acetyl-D-glucosamine (acetylated unit) and β -(1 \rightarrow 4)-linked D-glucosamine (deacetylated unit). CS has gained significant importance in the field of biomedicine due to its non-toxicity, biodegradability, and biocompatibility properties. It has numerous potential applications, including in the development of bandages that can reduce bleeding and serve as antibacterial agents, as well as DDSs that can transport medication across the skin and BBB. CS can be used alone or in amalgamation with antibiotics and extracts to create antimicrobial wound dressings that are effective in treating infections. Overall, CS and its derivatives hold great promise for biomedical implicatives, particularly in wound healing and DD. Due to its qualities, CS-based NPs are being studied as possible DDS against diseases like Leishmaniasis, Bacterial Diseases, and Cancer. Throughout the chapter we will have an overview of these properties of CS, their possible applications in the biomedical field and their possible role against these diseases.



Keywords: chitosan, drug delivery system (DDS), blood brain barrier, cancer, antimicrobial

Contents

Biographical Information	76
1. Introduction	76
2. Properties of Chitosan Nanoparticles	77
2.1 Anti-Carcinogenic	77
2.2 Antimicrobial	80
2.3 Blood-Brain Barrier (BBB) Drug Carrier	82
2.4 Anti-HIV	84
2.5 Anti-Osteomyelitis	86
3. Conclusion	88
Author Contribution Declaration	89
Data Availability Declaration	89
Acknowledgements	89
References	89

1. Introduction

Chitosan, a biopolymer derived from chitin, has gained significant interest in biomedicine due to its unique properties. Composed of β -(1 \rightarrow 4)-linked D-glucosamine and N-acetyl-D-glucosamine, it is biocompatible, biodegradable, and non-toxic, making it an excellent candidate for various biomedical uses. This review focuses on chitosan composites and their diverse biomedical applications, highlighting their biochemical and biomedical significance.¹

Chitosan has strong antimicrobial properties because of its polycationic nature,² which permits it to interact with negatively charged microbial membranes, leading to cell death. Its antimicrobial activity extends to bacteria, fungi, and viruses, making it valuable in wound dressings, antimicrobial coatings, and drug delivery systems.³

In antiviral research, chitosan has shown promising results against HIV by inhibiting viral replication and preventing the virus from binding to host cells. This makes chitosan a potential tool for developing new therapies to control viral load and prevent HIV progression.⁴

Chitosan also exhibits anti-osteomyelitis properties, addressing the challenge of delivering therapeutic agents to infected bone sites. Chitosan-based composites can deliver antibiotics directly to affected areas, promoting localized treatment and enhancing bone healing.⁵

Ayanjeet Chowdhury born and raised in Chennai, India. He completed his B.Tech. degree in Biotechnology from Amity University Maharashtra, Mumbai. He is currently pursuing his final year M. Tech. in biotechnology from the same university. His areas of interest in biotechnology for future sustainability.



Samyak Dhale was born and raised in Mumbai, India. He completed his B.Tech. degree in Biotechnology from Amity University Maharashtra, Mumbai and is currently pursuing PG Diploma in Archaeology in same institute. Samyak is building a career in Archeogenomics.



RBK Dinesh Kumar was born in Mumbai. He earned his B. Tech. degree in Biotechnology from Amity University Maharashtra, Mumbai. He was associated with Chaitanya Doshi, CEO of Kore AMMR (Additive Manufacturing and Medical Reconstruction) Pvt. Ltd for his B. Tech Project focused on developing microfluidic devices for cancer research and drug testing. Presently, Dinesh is employed as a Research Engineer at Kore AMMR Pvt. Ltd.



Andrew Biju John was born and brought up in Mumbai. He received his B.Tech. degree in Biotechnology degree from Amity University Maharashtra, Mumbai. He did his B.Tech project with Dr. Sudhir Singh BARC, Mumbai on Validation and expression analysis of selected curcumin biosynthesis. Currently he is working as a Research Trainee at ACTREC.



Dr. Jaya Lakkakula completed her Ph.D. at the University of Johannesburg, South Africa, and is a recipient of the UJ-Commonwealth Bursary award. She is currently serving as an Assistant Professor at Amity University Maharashtra, Mumbai. Her expertise lies in the green synthesis of nanoparticles, drug delivery, and the development of smart nanosensors, with a particular focus on cancer therapy.



Dr. Nilesh S. Wagh earned his Ph.D. in Biotechnology from Swami Ramanand Teerth Marathwada University in Nanded, Maharashtra, India. He is currently an Assistant Professor at Amity University Maharashtra, Mumbai. His research focuses on plant phytochemicals and their molecular interactions, with contributions to medicine, agriculture, and functional foods through numerous articles and book chapters.



Another key property of chitosan is its anticarcinogenic potential.⁶ It has been shown to inhibit cancer cell growth through mechanisms such as apoptosis induction, cell proliferation inhibition, and metabolic disruption. These attributes make chitosan a potential adjuvant in cancer therapies, either alone or with standard treatments.⁷

Chitosan is also a promising material for drug delivery across the blood-brain barrier (BBB).⁸ The BBB restricts the passage of most therapeutic agents, making treatment of neurological disorders difficult. Chitosan-based nanoparticles can cross the BBB, enabling effective drug delivery for diseases like Alzheimer's, Parkinson's, and brain tumors.⁹

The versatility of chitosan extends to forming composites with other materials, enhancing its properties and expanding its applications.¹⁰ These composites can be designed to improve mechanical strength, control degradation, and boost biological activity. Combining chitosan with polymers, ceramics, and metals has led to innovations in tissue engineering, wound healing, and regenerative medicine.¹¹

This review provides an in-depth overview of chitosan composites in biomedical applications, discussing their synthesis, characterization, and interaction with biological systems. It also explores the potential of chitosan composites to advance medical science, based on recent research and development.

2. Properties of Chitosan Nanoparticles

Chitosan nanoparticles have garnered considerable interest in biomedical research and applications due to their exceptional physicochemical properties and biocompatibility. These nanoparticles, typically ranging in size from 1 to 1000 nanometers, are produced through various methods such as ionic gelation, emulsion crosslinking, and self-assembly techniques.¹² The synthesis of chitosan nanoparticles involves the interplay of chitosan's amino groups and crosslinking agents or polyanions, resulting in a stable and uniform nanoscale structure. One of the critical attributes of chitosan nanoparticles is their size and surface charge, which significantly influence their interaction with biological systems. The small size of these nanoparticles allows for enhanced cellular uptake, improved tissue penetration, and increased surface area for functionalization with therapeutic agents or targeting ligands. Furthermore, the positive surface charge of chitosan nanoparticles, due to the protonation of amino groups in acidic environments, facilitates their interaction with negatively charged cell membranes, enhancing cellular internalization and bioavailability.

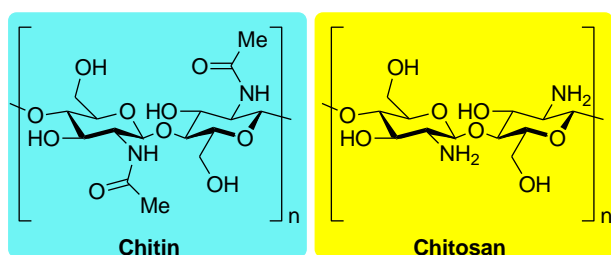


Figure 1: The chemical structure of Chitin and Chitosan

In addition to their size and charge, chitosan nanoparticles exhibit excellent biodegradability and biocompatibility, making them suitable for a wide range of biomedical applications (**Figure 1**).¹³ The degradation of chitosan nanoparticles occurs through enzymatic hydrolysis by lysozymes and other enzymes present in the human body, leading to the formation of non-toxic, bioresorbable byproducts such as glucosamine and N-acetylglucosamine. This biodegradability ensures that chitosan nanoparticles do not accumulate in tissues, reducing the risk of long-term toxicity and adverse effects. Moreover, chitosan is well-tolerated by the human body, exhibiting minimal immunogenicity and cytotoxicity. This inherent biocompatibility, coupled with its ability to be chemically modified, allows for the creation of tailor-made chitosan nanoparticles with specific properties and functionalities.

These modifications can enhance the solubility, stability, and targeting capabilities of chitosan nanoparticles, further broadening their application in drug delivery, gene therapy, and tissue engineering.¹⁴

One of the most notable properties of chitosan nanoparticles is their mucoadhesive nature, which arises from the interaction between the cationic chitosan and the negatively charged mucin found in mucus layers.¹⁵ This mucoadhesive property prolongs the residence time of chitosan nanoparticles at mucosal surfaces, enhancing the absorption and bioavailability of encapsulated drugs or therapeutic agents. This feature is particularly advantageous in the delivery of drugs via mucosal routes such as oral, nasal, ocular, and vaginal administration. Additionally, chitosan nanoparticles possess inherent antimicrobial activity, attributed to their ability to disrupt microbial cell membranes and inhibit the growth of bacteria, fungi, and viruses. This antimicrobial property not only makes chitosan nanoparticles effective in preventing infections but also enhances their potential as carriers for antimicrobial agents, providing a synergistic effect.¹⁶ Furthermore, chitosan nanoparticles have been extensively studied for their ability to facilitate the transport of drugs across biological barriers, including the blood-brain barrier (BBB), gastrointestinal tract, and pulmonary epithelium. This property is crucial for the development of targeted and efficient drug delivery systems, enabling the treatment of various diseases and conditions that are otherwise challenging to address with conventional drug formulations.

2.1 Anti – Carcinogenic

Chitosan nanoparticles have attracted considerable attention in cancer research due to their potent anti-carcinogenic properties, which hold promise for developing more effective and targeted cancer therapies. These nanoparticles exhibit a multifaceted mechanism of action against cancer cells, including the induction of apoptosis, inhibition of cell proliferation, and disruption of tumor cell metabolism.¹⁷ Apoptosis, or programmed cell death, is a crucial process that is often dysregulated in cancer cells, allowing them to proliferate uncontrollably. Chitosan nanoparticles can trigger apoptosis by activating caspase enzymes and promoting the discharge of cytochrome c from mitochondria, which are key steps in the apoptotic pathway. Additionally, chitosan nanoparticles can interfere with the cell cycle of cancer cells, arresting their progression in critical phases such as the G2/M phase, thereby inhibiting cell division and growth. This cell cycle arrest is often mediated through the modulation of cyclin-dependent kinases (CDKs) and other regulatory proteins that are essential for cell cycle progression.¹⁸

Moreover, chitosan nanoparticles can disrupt the metabolic processes of cancer cells, which are typically characterized by high rates of glycolysis and altered energy metabolism, known as the Warburg effect. By interfering with these metabolic pathways, chitosan nanoparticles can reduce the energy supply to cancer cells, impairing their growth and survival. Metabolic disruption is often achieved through the inhibition of key enzymes involved in glycolysis and oxidative phosphorylation, resulting in reduced ATP production and elevated levels of reactive oxygen species (ROS) within the cancer cells. The upraised ROS levels can persuade oxidative stress, further damaging cellular components and promoting cell death. This multifaceted approach not only targets cancer cells directly but also creates an unfavorable environment for their survival and proliferation.¹⁹

The surface properties of chitosan nanoparticles also play a crucial role in their anti-carcinogenic efficacy. Functionalization of chitosan nanoparticles with specific ligands, such as folic acid, peptides, or antibodies, can enhance their targeting capabilities, allowing for selective delivery to cancer cells while sparing healthy tissues. This targeted delivery is particularly important in minimizing the side effects associated with conventional chemotherapy, which often affects both cancerous and non-cancerous cells. The enhanced permeability and retention (EPR) effect is a phenomenon in which nanoparticles selectively accumulate in tumor tissues due to their sieve-like vasculature and poor

lymphatic drainage, further aids in the selective targeting of chitosan nanoparticles. Once localized in the tumor microenvironment, the nanoparticles can release their therapeutic payload in a controlled manner, maximizing the anti-cancer effects while reducing systemic toxicity.²⁰ Furthermore, chitosan nanoparticles can serve as carriers for delivering a range of anti-cancer agents, including chemotherapeutic drugs, siRNA, and genes, enhancing their therapeutic efficacy. The encapsulation of chemotherapeutic drugs within chitosan nanoparticles can improve their solubility, stability, and bioavailability, while also protecting them from premature degradation. This encapsulation also allows for a controlled and sustained drug release, maintaining therapeutic concentrations at the tumor site for extended periods. In gene therapy, chitosan nanoparticles can facilitate the delivery of genetic material into cancer cells, promoting the expression of tumor-suppressor genes or silencing oncogenes. The non-viral nature of chitosan nanoparticles makes them a safer alternative to viral vectors, reducing the risk of immunogenicity and insertional mutagenesis.

For example, Jaiswal *et al.* (2019) synthesized a methyl methacrylate (MMA) modified chitosan (CS) conjugate (CSMMA) through a Michael addition reaction, aiming to create a novel biopolymer for gene and drug delivery.²¹ The resulting conjugate exhibited a highly porous framework, confirmed by FT-IR, ¹H NMR, X-ray diffraction spectrometry, and SEM analysis. The CSMMA demonstrated significant potential as a gene delivery agent, showing good transfection efficacy in various mammalian cancer cell lines (A549, HeLa, and HepG2). Curcumin-loaded CSMMA nanoparticles were prepared and characterized for drug delivery applications. These nanoparticles achieved maximal entrapment efficiency of up to 68% and exhibited pH-sensitive drug release, with more rapid release at pH 5.0 compared to physiological pH. This study underscores the potential of CSMMA nanoparticles in targeted drug delivery systems, improving the bioavailability and therapeutic effectiveness of encapsulated drugs (Figure 2).²¹

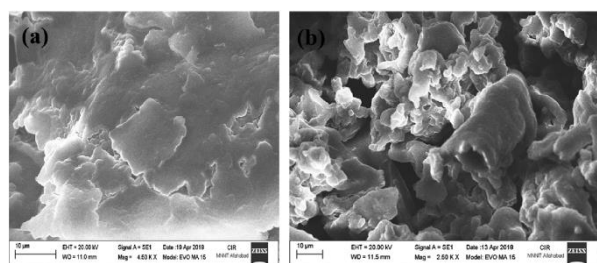


Figure 2: SEM image of (a) chitosan (b) chitosan conjugated with methyl methacrylate [Represented with permission from Ref [5].

Another study conducted by Subramanian *et al.* (2006), explored the use of chitosan nanoparticles for the delivery of phytochemicals in chemotherapy, emphasizing their potential in enhancing the bioavailability and therapeutic efficacy of poorly soluble compounds.²² The study demonstrated that chitosan nanoparticles could effectively encapsulate and release various phytochemicals, such as curcumin, resulting in improved anti-cancer activity. The nanoparticles exhibited controlled release properties, maintaining a sustained release of the encapsulated drugs over an extended period. This approach not only improved the solubility and stability of the phytochemicals but also allowed for targeted delivery to cancer cells, thereby enhancing the therapeutic outcomes and reducing side effects associated with conventional chemotherapy. This research highlights the versatility of chitosan nanoparticles in developing efficient drug delivery systems for cancer treatment.²²

Furthermore, Vivek *et al.* (2013) investigated the use of pH-responsive chitosan nanoparticles as carriers for tamoxifen in breast cancer therapy.²³ The study found that these nanoparticles could significantly improve the delivery and efficacy of tamoxifen, a commonly used anti-cancer drug. The chitosan nanoparticles were synthesized through ionic

gelation, providing a stable and biocompatible platform for drug delivery. In vitro studies demonstrated enhanced cellular uptake and cytotoxicity against breast cancer cells, attributed to the pH-sensitive release mechanism of the nanoparticles. This pH-responsive behavior ensured that the drug was preferentially released in the acidic microenvironment of the tumor, maximizing its therapeutic effect while minimizing systemic toxicity. This research underscores the potential of chitosan nanoparticles in enhancing the targeted delivery and efficacy of anti-cancer drugs.²³

Kim and co-workers (2014) evaluated polyethylenimine-grafted polyamidoamine (PAMAM) dendrimers for gene delivery, focusing on their efficiency and cytotoxicity. The study synthesized a novel gene delivery system by conjugating PAMAM dendrimers with low molecular weight polyethylenimine (PEI) through a Michael addition reaction. The resulting nanoparticles showed high gene transfection efficiency and low cytotoxicity in vitro. The researchers attributed these properties to the enhanced buffering capacity and reduced aggregation of the nanoparticles. The study highlighted the potential of these modified PAMAM dendrimers in delivering genetic material effectively and safely, paving the way for their application in gene therapy and other biomedical fields.^{24–26}

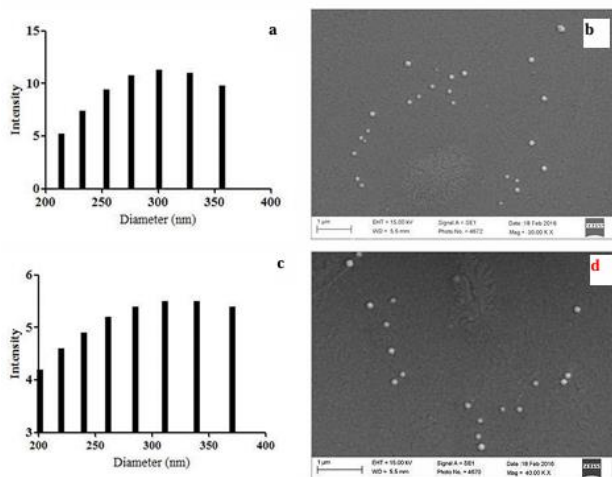
Park *et al.* (2006) investigated the use of glycol chitosan nanoparticles for the delivery of doxorubicin, a widely used chemotherapeutic agent.²⁷ The nanoparticles were synthesized through self-assembly and characterized for their size, surface charge, and drug loading capacity. In vivo studies demonstrated that these nanoparticles could efficiently accumulate in tumor tissues, enhancing the therapeutic efficacy of doxorubicin while reducing its systemic toxicity. The glycol chitosan nanoparticles provided a stable and biocompatible platform for drug delivery, with the potential to improve the therapeutic outcomes of chemotherapy. This research highlights the advantages of using chitosan-based nanoparticles for targeted drug delivery in cancer treatment, offering a promising strategy for enhancing the efficacy and safety of chemotherapeutic agents.²⁷

In the investigation by Hattori and co-workers (2002), the focus was on the evaluation of the anticarcinogenic properties of chitosan and its derivatives. The study utilized real-time zymography and reverse zymography techniques to detect the activities of matrix metalloproteinases (MMPs) and their inhibitors. Chitosan, a biopolymer derived from chitin, was modified to enhance its therapeutic efficacy. The results demonstrated that chitosan derivatives could effectively inhibit MMPs, which are enzymes involved in the degradation of the extracellular matrix and are often associated with cancer metastasis. By inhibiting MMP activity, chitosan derivatives could potentially prevent the invasion and spread of cancer cells. This study provided significant insights into the molecular mechanisms through which chitosan exerts its anticarcinogenic effects, highlighting its potential as a therapeutic agent in cancer treatment.²⁸

In a subsequent study, Zhang and Zhao (2015) explored the preparation, characterization, and evaluation of β -chitosan nanoparticles loaded with tea polyphenol-Zn complexes. These nanoparticles were designed to enhance the delivery and efficacy of bioactive compounds in cancer therapy. The research demonstrated that the β -chitosan nanoparticles significantly improved the stability and bioavailability of the tea polyphenol-Zn complex. Moreover, the in vitro cytotoxicity assays revealed that these nanoparticles exhibited potent anticarcinogenic activity against various cancer cell lines. The study concluded that β -chitosan nanoparticles could serve as an effective delivery system for natural polyphenols, providing a promising approach for cancer prevention and treatment.²⁹

Deshpande's team (2017) investigated the use of zinc-complexed chitosan/TPP nanoparticles as a micronutrient nanocarrier suited for foliar application.³⁰ The study aimed to assess the anticarcinogenic potential of these nanoparticles when used to deliver zinc, an essential micronutrient with known anticancer properties. The findings indicated that the chitosan/TPP nanoparticles effectively delivered zinc to target sites, enhancing its bioavailability and anticarcinogenic activity. The in vitro studies showed that zinc-complexed

Rodrigues *et al.* (2012) focused on the biocompatibility of chitosan carriers with applications in drug delivery, particularly in the context of cancer therapy. The study evaluated the interaction of chitosan-based nanoparticles with biological systems, including their cytotoxicity, cellular uptake, and anticarcinogenic effects. The results showed that chitosan nanoparticles exhibited minimal cytotoxicity while effectively delivering anticancer drugs to target cells. The nanoparticles facilitated sustained drug release, enhancing the therapeutic outcomes in cancer treatment. This research highlighted the potential of chitosan carriers in improving the efficacy and safety of cancer therapeutics, emphasizing their role in advanced drug delivery systems (**Figure 3**).³¹



Again, Wang and co-workers (2004) examined the preparation, characterization, and antimicrobial activity of chitosan-Zn complexes. While the primary focus was on antimicrobial properties, the study also explored the potential anticarcinogenic effects of these complexes. The research demonstrated that chitosan-Zn complexes exhibited significant inhibitory effects on the growth of cancer cells, suggesting their potential use in cancer therapy. The study provided a comprehensive analysis of the physicochemical properties of chitosan-Zn complexes and their biological activities, offering valuable insights into their application as multifunctional therapeutic agents in both antimicrobial and anticancer treatments.³²

Tharanathan and co-workers (2004) provided a comprehensive overview of the modifications of chitosan and

Chen (2015) explored the use of hierarchical targeted hepatocyte mitochondrial multifunctional chitosan nanoparticles for anticancer drug delivery.³⁶ Their study focused on enhancing the delivery and efficacy of anticancer drugs specifically to hepatocellular carcinoma cells. The multifunctional chitosan nanoparticles were designed to target hepatocytes selectively and deliver drugs directly to the mitochondria, improving therapeutic outcomes. The nanoparticles exhibited a high drug-loading capacity, stability, and targeted delivery, leading to increased drug accumulation in cancer cells and reduced systemic toxicity. This innovative approach underscores the potential of chitosan nanoparticles in improving the precision and effectiveness of cancer treatments, particularly for hepatocellular carcinoma, by ensuring that therapeutic agents are delivered specifically to cancer cells while minimizing adverse effects on healthy tissues.³⁶

Collectively, these studies highlight the diverse and significant potential of chitosan nanoparticles in cancer treatment. While Chang (2017) pointed out the risk of chitosan promoting cancer progression through Wnt signaling,³³ Harish Prashanth and Tharanathan (2007) and Yang (2015) emphasized its selective cytotoxicity and effective gene delivery capabilities. Chen *et al.*³⁵ (2015) and Gao *et al.*³⁷ (2010) further demonstrated the precision targeting and low toxicity of chitosan-based systems. These findings suggest that while chitosan holds promise for cancer therapy, its application must be carefully tailored to harness its benefits while mitigating potential risks. The diverse approaches and outcomes in these studies reflect the complex interplay between chitosan's biochemical properties and its interactions

with cancer cells, underscoring the need for continued research and optimization.

In comparing these studies, it becomes evident that the functional modifications of chitosan are crucial in determining its therapeutic efficacy. The ability to modify chitosan to enhance its selectivity and reduce toxicity, as shown by Harish Prashanth and Tharanathan (2004), is a critical factor in its application in cancer therapy.³⁴ The targeted delivery systems developed by Chen (2015) and Yang (2015) highlight the potential of chitosan to improve the precision of cancer treatments. However, the study by Chang (2017) serves as a cautionary reminder of the complexities involved in using chitosan, particularly its potential to enhance tumor progression if not properly controlled.

Overall, these studies collectively underscore the need for a nuanced approach in developing chitosan-based cancer therapies. The promising results in targeted delivery and gene transfection indicate that chitosan nanoparticles can significantly enhance the efficacy of cancer treatments. However, the potential risks, such as those identified by Chang (2017), must be carefully managed through precise engineering and thorough understanding of chitosan's interactions with cancer cells. The continuous advancements in chitosan research are opening new possibilities for more effective and safer cancer therapies, highlighting the importance of interdisciplinary collaboration in this field.

In conclusion, the exploration of chitosan nanoparticles in cancer therapy reveals a promising yet complex potential. The benefits of targeted delivery, selective cytotoxicity, and low toxicity offer significant advancements in cancer treatment. However, the potential risks necessitate a careful and well-informed approach to harness the full therapeutic potential of chitosan. Future research should focus on optimizing chitosan modifications and understanding its interactions with biological systems to develop safe and effective cancer therapies. The integration of these findings into clinical practices holds the promise of improving patient outcomes and advancing the fight against cancer.

Overall, the anti-carcinogenic properties of chitosan nanoparticles, combined with their ability to deliver a range of therapeutic agents, present a powerful tool in the fight against cancer. Their multifaceted mechanisms of action, targeting capabilities, and potential for controlled drug release position them at the forefront of next-generation cancer therapeutics, offering hope for more effective and less toxic treatment options.

2.2 Antimicrobial

Chitosan nanoparticles have been extensively studied for their antimicrobial properties, making them a valuable tool in combating a wide range of pathogens, including bacteria, fungi, and viruses.³⁸ The antimicrobial activity of chitosan is mainly due to its polycationic nature, which permits it to interact with the negatively charged membranes of microbial cells. This interaction leads to the disruption of the integrity of the cell membrane, causing leakage of intracellular contents and ultimately resulting in cell death. Additionally, chitosan nanoparticles can penetrate microbial cells, binding to DNA and inhibiting RNA and protein synthesis, further enhancing their antimicrobial efficacy. The size and surface charge of chitosan nanoparticles can be finely tuned to optimize their interaction with different types of microorganisms, enhancing their effectiveness. Research has shown that smaller nanoparticles with higher surface charge densities exhibit stronger antimicrobial activities due to their increased surface area and higher interaction potential with microbial cells.³⁹ Moreover, chitosan nanoparticles can be functionalized with various antimicrobial agents, such as silver nanoparticles, antibiotics, and essential oils, to create synergistic effects and enhance their spectrum of activity.

The versatility of chitosan nanoparticles extends to their ability to form coatings and films on medical devices, implants, and wound dressings, providing long-lasting antimicrobial protection and preventing biofilm formation. This is particularly important in clinical settings where device-associated infections are a significant concern. Furthermore, chitosan nanoparticles exhibit inherent biocompatibility and biodegradability, creating them safe for use in various

biomedical applications. Their non-toxic nature ensures that they do not cause adverse effects when applied to human tissues, making them suitable for usage in wound healing, tissue engineering, and drug delivery systems. The sustained release of encapsulated antimicrobial agents from chitosan nanoparticles provides prolonged protection against infections, reducing the need for frequent application and minimizing the risk of resistance development. Recent studies have highlighted the potential of chitosan nanoparticles in addressing the global challenge of antibiotic resistance.

By enhancing the efficacy of existing antibiotics and reducing the required dosage, chitosan nanoparticles can help mitigate the spread of resistant strains and extend the useful life of current antimicrobial agents. The ability of chitosan nanoparticles to target and disrupt biofilms, which are often resistant to conventional antibiotics, further underscores their potential in managing chronic and recalcitrant infections. Moreover, the incorporation of chitosan nanoparticles into food packaging materials has shown promise in extending the shelf life of fragile goods by obstructing microbial growth and preventing spoilage. This application not only improves food safety but also reduces food waste, contributing to sustainable practices. The broad-spectrum antimicrobial activity, combined with the customizable properties of chitosan nanoparticles, positions them as a versatile and powerful tool in the fight against infectious diseases. As research continues to uncover new functionalizations and applications, chitosan nanoparticles are poised to play a pivotal role in advancing antimicrobial strategies in both medical and non-medical fields. The ongoing development of chitosan-based antimicrobial systems promises to deliver innovative solutions for infection control, enhancing public health and safety on a global scale.

The chitosan and its derivatives antimicrobial properties have been widely studied, demonstrating significant potential in various biomedical applications. Chitosan's ability to inhibit a broad spectrum of microorganisms, including bacteria, fungi, and viruses, is attributed to its unique chemical structure and physicochemical properties. This biopolymer's effectiveness as an antimicrobial agent is influenced by numerous factors, such as its molecular weight, degree of deacetylation, and the presence of functional groups that can interact with microbial cell membranes. The studies discussed in this section highlight the diverse mechanisms through which chitosan exerts its antimicrobial effects and its potential applications in clinical settings.

Mohamed and Al-Mehbad (2013) synthesized novel chitosan hydrogels cross-linked with terephthaloyl thiourea, which exhibited significant antibacterial and antifungal activities.⁴⁰ The study found that these hydrogels had a broad spectrum of antimicrobial action against both Gram-positive and Gram-negative bacteria, as well as several fungal species. The cross-linking with terephthaloyl thiourea enhanced the mechanical strength and stability of the chitosan hydrogels, making them suitable for use in various biomedical applications, including wound dressings and drug delivery systems. The antimicrobial mechanism was primarily attributed to the ability of chitosan to disrupt microbial cell membranes, causing the leakage of cellular contents and ultimately resulting in cell death. The study also highlighted the biocompatibility of hydrogels, which is crucial for their safe application in medical treatments.

Mohseni (2019) conducted a comparative analysis of wound dressings incorporating silver sulfadiazine and silver nanoparticles. They evaluated the *in vitro* and *in vivo* antimicrobial efficacy of these dressings against common wound pathogens. The incorporation of silver nanoparticles into chitosan-based dressings significantly enhanced their antimicrobial properties. Silver nanoparticles are known for their potent antimicrobial activity, and when combined with chitosan, they provide a synergistic effect that enhances the overall antimicrobial performance. The study demonstrated that these dressings effectively reduced bacterial load and promoted faster wound healing in animal models. The authors proposed that the combination of chitosan and silver nanoparticles could serve as a highly effective antimicrobial

wound dressing, offering both infection control and improved healing (Figure 4).⁴¹

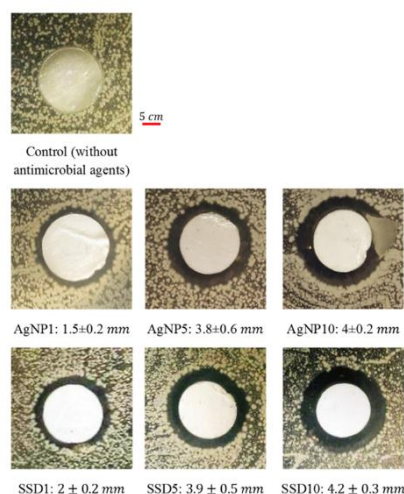


Figure 4: Antimicrobial characterization of wound dressings against *Staphylococcus aureus* using the inhibition zone measurement technique ($n=5$). [Reprinted with permission from 36].

Moura (2011) developed in situ forming chitosan hydrogels via ionic and covalent co-crosslinking, aiming to create a versatile and effective antimicrobial material. These hydrogels demonstrated excellent antimicrobial activity against wide range of bacterial strains, including both Gram-positive and Gram-negative bacteria. The dual cross-linking approach not only improved the mechanical properties and stability of the hydrogels but also enriched their antimicrobial efficacy. The ionic and covalent bonds in the hydrogels provided a robust structure that could be applied in various biomedical fields, including tissue engineering and drug delivery. The study concluded that these hydrogels are promising candidates for applications requiring strong antimicrobial action combined with biocompatibility and biodegradability.⁴²

Munoz-Bonilla (2019) reviewed the development of bio-based polymers with antimicrobial properties, focusing on sustainable materials like chitosan. They discussed various strategies for enhancing the antimicrobial properties of chitosan, including chemical modifications and the incorporation of metallic nanoparticles. The review highlighted the versatility of chitosan as an antimicrobial agent and its potential in developing environmentally friendly and effective antimicrobial materials. The authors emphasized that chitosan's biocompatibility and biodegradability make it an attractive option for medical applications, particularly in areas where conventional antimicrobial agents may pose environmental and health risks.⁴³

Nandi (2009) explored local antibiotic delivery systems for treating osteomyelitis, with a particular focus on chitosan-based carriers. Their research demonstrated that chitosan could be effectively used to deliver antibiotics directly to the infection site, thereby enhancing the local concentration of the drug and reducing systemic side effects. The study found that chitosan-based delivery systems provided sustained release of antibiotics, maintaining therapeutic levels over extended periods. This approach not only improved the efficacy of the treatment but also minimized the development of antibiotic resistance by ensuring consistent drug exposure. The authors concluded that chitosan-based antibiotic delivery systems hold great promise for the treatment of chronic bone infections like osteomyelitis.⁴⁴

Keaton Smith (2010) explored the potential of chitosan films loaded with antibiotics as a treatment for infections associated with bone fracture fixation devices. The study primarily focused on methicillin-resistant *Staphylococcus aureus* (MRSA), a significant concern in musculoskeletal wound treatment. Chitosan films with varying degrees of deacetylation (DDA) were evaluated for their antibiotic

uptake, elution, and activity. The study found that 80% DDA chitosan films were most effective for absorbing and releasing antibiotics, maintaining mechanical integrity and adhesive strength when applied to fracture fixation devices. The films effectively eluted antibiotics, which were active against *S. aureus*, demonstrating the potential of chitosan films as a complementary clinical treatment to reduce or prevent infections in musculoskeletal injuries.⁴⁵

Monteiro (2015) investigated the antibacterial activity of gentamicin-loaded liposomes immobilized on electrospun chitosan nanofiber meshes (NFM). The study highlighted the importance of chitosan as a support structure for binding liposomes, which provided a sustained release of gentamicin. Disk diffusion and broth dilution assays demonstrated the effectiveness of gentamicin release from the liposomes immobilized on the chitosan NFM in inhibiting the growth of *S. aureus*, *E. coli*, and *P. aeruginosa*. These results suggest that the developed nanostructured delivery system could be used in local applications to eradicate pathogens involved in infections, showing promising performance for wound dressing applications.⁴⁶

Peng (2011) reported on the development of a polycationic antimicrobial hydrogel derived from dimethyldecylammonium chitosan grafted with poly(ethylene glycol) methacrylate. This hydrogel demonstrated excellent antimicrobial efficiency against *P. aeruginosa*, *E. coli*, *S. aureus*, and *Fusarium solani*. The suggested mechanism of antimicrobial activity involved the attraction and disruption of microbial membranes by the hydrogel's nanopores, leading to microbe death. The hydrogel was also found to be biocompatible with rabbit conjunctiva and showed no toxicity to epithelial cells or the underlying stroma. This study highlighted the potential of chitosan-based hydrogels for use in preventing infections associated with medical implants and devices.⁴⁷

A study by Shao (2016) explored the antimicrobial properties of chitosan/silver sulfadiazine (CS/AgSD) composite sponges designed for wound dressing applications. The composite sponges exhibited a broad spectrum of antibacterial activity without significant cytotoxicity, as confirmed by MTT viability assay and fluorescence staining technique on HEK293 cell lines. The findings demonstrated the potential application of CS/AgSD composite sponges in antimicrobial wound dressing materials, emphasizing the importance of natural polymers like chitosan in biomedical applications due to their biocompatibility, biodegradability, and antimicrobial properties.⁴⁸

Again, a study by Zhang (2019) evaluated the antimicrobial efficacy of chitosan-based composite films incorporating different types of nanoparticles. The films showed significant antibacterial activity against various pathogens, with enhanced mechanical properties and thermal stability. The incorporation of nanoparticles such as silver, copper, and titanium dioxide into the chitosan matrix enhanced the antimicrobial activity and mechanical strength of the films, making them suitable for use as antimicrobial wound dressings and other biomedical applications. The study highlighted the versatility of chitosan in forming composites with nanoparticles to enhance its inherent antimicrobial properties.⁴⁹

The study conducted by Lal (2016) examined the antibacterial performance of Schiff base chitosan against various microbial strains including *Aspergillus niger*, *Bacillus subtilis*, *Staphylococcus aureus*, and *Escherichia coli*. The results demonstrated a notable inhibitory effect of Schiff base chitosan on fungi and gram-positive bacteria, whereas its outcome on gram-negative bacteria was less pronounced. The study highlighted that the antibacterial properties of chitosan derivatives are influenced by factors such as environmental pH and molecular weight (MW) of chitosan. Specifically, the agar diffusion experiment revealed that the antibacterial activity against gram-negative bacteria increased with an increase in MW up to a threshold, beyond which the activity decreased. This was particularly evident when the MW reached 30,000, showing a decline in antibacterial efficacy. The evaluation of antifungal efficacy through food toxicology testing indicated that the antibacterial efficiency of Schiff base chitosan could exceed 70%, demonstrating its potential as an effective antimicrobial agent.⁵⁰

In a study by Piegat (2021), the antibacterial activity of N-O acylated chitosan derivatives (CH-LA) was evaluated against *Escherichia coli*, *Helicobacter pylori*, and *Staphylococcus aureus* using various methods including microdilution, agar immersion, and disk diffusion. The results indicated that the environmental pH and concentration of CH-LA significantly influenced the antibacterial activity. The acylated chitosan derivatives showed improved antibacterial activity against the tested bacteria, with the highest concentration and acidic environment (pH = 5) yielding survival rates of 22%, 23%, and 8% for *Escherichia coli*, *Helicobacter pylori*, and *Staphylococcus aureus*, respectively. This confirmed that gram-positive bacteria, like *Staphylococcus aureus*, are more sensitive to CH-LA than gram-negative bacteria such as *Helicobacter pylori* and *Escherichia coli*. These findings underscore the potential of N-O acylated chitosan derivatives as effective antimicrobial agents, particularly against gram-positive bacteria.⁵¹

Considering these papers together, a comprehensive overview reveals a diverse range of methodologies and outcomes regarding the antimicrobial properties of chitosan and its derivatives. The studies collectively demonstrate that chitosan's antimicrobial activity is affected by its molecular weight, degree of deacetylation, and the presence of functional groups. Additionally, environmental factors such as pH and the type of microorganism significantly impact chitosan's efficacy. The use of chitosan in combination with other antimicrobial agents or modifications, such as quaternization or acylation, generally enhances its antimicrobial properties, making it a versatile and effective biopolymer for various applications.

A notable trend across the studies is the higher efficacy of chitosan derivatives against gram-positive bacteria compared to gram-negative bacteria. This is endorsed to the differences in the cell wall structures of these bacteria, with gram-positive bacteria having a thicker peptidoglycan layer that is more susceptible to disruption by chitosan. The studies also highlight the potential of chitosan derivatives in various applications, including food preservation, medical treatments, and environmental protection. The antimicrobial activity of chitosan-coated films, hydrogels, and nanoparticles has been shown to be effective in controlling microbial growth, thereby prolonging the shelf life of food products and enhancing the efficacy of medical treatments.

In conclusion, the collective findings from these studies underscore the significant prospective of chitosan and its derivatives as antimicrobial agents. The variations in antimicrobial activity based on molecular weight, degree of deacetylation, and functional modifications highlight the importance of optimizing these parameters for specific applications. The ability of chitosan to interact synergistically with other antimicrobial agents further enhances its efficacy, making it a promising candidate for a extensive range of applications in food safety, medical treatments, and environmental protection. Future research should focus on addressing the challenges related to the stability and practical applications of chitosan in various industries to fully realize its potential.

2.3. Blood Brain Barrier (BBB) Drug Carrier

The Blood-Brain Barrier (BBB) is a selectively permeable barrier that safeguards the brain from potentially harmful substances in the bloodstream while permitting the passage of essential nutrients.⁵² This barrier, formed by endothelial cells, tight junctions, and astrocyte end-feet, presents a noteworthy challenge for transporting therapeutic agents to the brain to treat central nervous system (CNS) disorders. Traditional drug delivery methods frequently fail to reach sufficient drug concentration in the brain because of the restrictive properties of the BBB.⁵³ Chitosan nanoparticles have emerged as a promising solution for overcoming this obstacle, owing to their unique physicochemical properties and ability to be functionalized for targeted delivery. Chitosan, a biopolymer derived from chitin, exhibits biocompatibility, biodegradability, and low toxicity, making it suitable for various biomedical applications. Its polycationic nature allows

for the interaction with the negatively charged components of the BBB, enhancing its permeability and facilitating drug transport. The versatility of chitosan nanoparticles lies in their ability to be modified with ligands, peptides, or antibodies that can target specific receptors on the BBB, thereby improving the selectivity and efficiency of drug delivery to the brain.⁵⁴

One of the primary benefits of using chitosan nanoparticles for BBB drug delivery is their competency to encapsulate a extensive range of therapeutic agents, such as small molecules, peptides, proteins, and nucleic acids. This encapsulation protects the therapeutic agents from degradation and premature clearance, ensuring that a higher concentration reaches the brain.⁵⁵ Additionally, the surface modification of chitosan nanoparticles with targeting ligands including transferrin, lactoferrin, and antibodies against specific BBB receptors can significantly enhance their uptake by brain endothelial cells through receptor-mediated transcytosis. This targeted tactic not only improves the efficiency of drug delivery but also minimizes potential side effects by reducing systemic exposure. Furthermore, chitosan nanoparticles can be engineered to exhibit controlled and sustained release of the encapsulated drugs, maintaining therapeutic levels in the brain over extended periods and reducing the frequency of administration.

Recent studies have demonstrated the efficacy of chitosan nanoparticles in delivering a variety of therapeutic agents across the BBB for the treatment of neurological disorders including Alzheimer's disease, Parkinson's disease, brain tumors, and stroke. For instance, chitosan nanoparticles loaded with anti-Alzheimer's drugs have shown improved drug bioavailability and therapeutic efficacy in animal models, resulting in enhanced cognitive function and reduced amyloid-beta plaques in the brain. Similarly, chitosan-based delivery systems have been successful in transporting chemotherapeutic agents to brain tumors, increasing drug accumulation at the tumor site and inhibiting tumor growth. The ability of chitosan nanoparticles to cross the BBB and deliver drugs effectively opens new avenues for treating CNS disorders that are currently difficult to manage with conventional therapies.⁵⁵

The safety profile of chitosan nanoparticles further supports their potential as BBB drug carriers. Studies have shown that chitosan and its derivatives exhibit low cytotoxicity and immunogenicity, making them well-tolerated in both in vitro and in vivo models. The biodegradability of chitosan ensures that the nanoparticles are gradually decomposed into non-toxic byproducts, minimizing the risk of long-term buildup and harmful effects. Additionally, the ease of production and scalability of chitosan nanoparticles make them a cost-effective option for large-scale drug delivery applications.

In the study by Wohlfart (2012), the transport of drugs across the BBB using nanoparticles was investigated, highlighting the effectiveness of chitosan nanoparticles in enhancing drug delivery to the brain. The authors demonstrated that the mucoadhesive properties of chitosan significantly improve the retention time of the nanoparticles at the nasal mucosa, facilitating the transport of encapsulated drugs to the brain via the olfactory and trigeminal nerve pathways. This non-invasive delivery route bypasses the BBB, which is a major obstacle in CNS drug delivery. Additionally, the study found that the positive charge of chitosan nanoparticles enhances their interaction with the negatively charged cell membranes, endorsing cellular uptake and enhancing the drug concentration in the brain.

These findings underscore the potential of chitosan nanoparticles in delivering therapeutics for treating neurological diseases such as gliomas, Alzheimer's disease, and Parkinson's disease.⁵⁶

A study by Freiherr (2013) focused on the nasal delivery of insulin using chitosan nanoparticles for the treatment of Alzheimer's disease. The authors explored the potential of intranasal administration of insulin-loaded chitosan nanoparticles to improve cognitive function in Alzheimer's patients. The results exposed that the nanoparticles significantly increased the bioavailability of insulin in the brain, leading to improved cognitive performance in animal models. The study also highlighted the ability of chitosan

nanoparticles to protect insulin from degradation in the nasal cavity and enhance its transport across the nasal epithelium into the brain. These findings suggest that chitosan nanoparticles could be a viable strategy for delivering therapeutic proteins to the brain, providing a non-invasive and effective treatment option for neurodegenerative diseases.⁵⁷ Chen (2017) investigated the use of vitamin E succinate-grafted chitosan oligosaccharide nanoparticles for delivering paclitaxel to brain tumors. The study demonstrated that the nanoparticles effectively delivered paclitaxel to glioma cells, resulting in significant inhibition of tumor growth. The authors attributed the enhanced delivery and therapeutic efficacy to the mucoadhesive properties of chitosan, which increased the retention time of the nanoparticles at the tumor site, and the antioxidative properties of vitamin E, which provided additional protection to the encapsulated drug. The findings of this study underscore the prospective of chitosan-based nanoparticles in enhancing the delivery and efficacy of chemotherapeutic agents for treating brain tumors.⁵⁸ In another study, Md (2013) developed bromocriptine-loaded chitosan nanoparticles for the purpose of treating Parkinson's disease via the nose-to-brain delivery route. The pharmacokinetic and pharmacodynamic evaluations indicated that the nanoparticles provided a sustained release of bromocriptine, leading to prolonged therapeutic effects and improved bioavailability in the brain. The study also demonstrated that the nanoparticles significantly reduced the frequency and severity of Parkinsonian symptoms in animal models. These results highlight the potential of chitosan nanoparticles in delivering dopamine agonists directly to the brain, offering a promising approach for managing Parkinson's disease.⁵⁹ Zhao (2017) explored the use of a nano-in-nano polymer-dendrimer system based on chitosan for the controlled delivery of multiple drugs to the brain and the system was designed to encapsulate; co-deliver chemotherapeutic agents and gene therapy vectors to brain tumors. The study demonstrated that the chitosan-based nanosystem effectively delivered therapeutic payloads to glioma cells, resulting in enhanced apoptosis and reduced tumor growth. The authors emphasized the importance of the chitosan matrix in providing stability, controlled release, and targeted delivery of the encapsulated agents, which collectively improved therapeutic outcomes. This study highlights the versatility and efficacy of chitosan nanoparticles in complex drug delivery systems for treating brain tumors (Refer Figure 5).⁶⁰

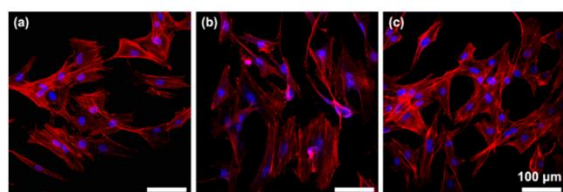


Figure 5: CLSM images of osteoblasts adhered to (a) native Ti, (b) TNT and LBL substrates after 2 days culture with staining of actin (red) and nucleus (blue)[Reprinted with permission from 57].

Meng (2016) investigated the use of Pluronic F127 and D-alpha-Tocopheryl Polyethylene Glycol Succinate (TPGS) based mixed micelles for targeted drug delivery across the BBB. Their study focused on the encapsulation of a hydrophobic drug, docetaxel, within these mixed micelles and evaluated their stability, drug release profile, and cellular uptake. The results demonstrated that the mixed micelles had a high drug loading capacity and could sustain drug release over an extended period. Additionally, in vitro studies using brain endothelial cells showed that these micelles significantly enhanced the cellular uptake of docetaxel compared to free drug solutions. The authors also reported that the micelles could reduce the cytotoxicity of docetaxel to non-target cells, suggesting a more targeted delivery mechanism. There are in vivo experiments further confirmed that the micelles could effectively deliver docetaxel to the brain, resulting in improved therapeutic outcomes in a glioma mouse model.⁶¹

The study by Rip (2014) explored the pharmacokinetics and brain delivery capabilities of glutathione PEGylated liposomes. The research aimed to improve the delivery of antioxidant enzymes to the brain to treat neurodegenerative diseases. The PEGylation of liposomes with glutathione allowed for the enhanced crossing of the BBB, leveraging the natural transport mechanisms of glutathione. Their findings showed that these modified liposomes had increased stability in the bloodstream and prolonged circulation times. In vivo studies in rats demonstrated that the glutathione PEGylated liposomes could efficiently deliver encapsulated enzymes to the brain, significantly reducing oxidative stress markers. This study provided strong evidence for the potential of PEGylated liposomes as a viable strategy for delivering therapeutic proteins and enzymes to the brain, offering a promising approach for treating diseases characterized by oxidative damage.⁶²

In the research conducted by Salvalaio (2016), the focus was on developing targeted polymeric nanoparticles for delivering high molecular weight molecules to the brain in lysosomal storage disorders. The study utilized nanoparticles made from poly(lactic-co-glycolic acid) (PLGA) and polycaprolactone (PCL) that were functionalized with specific ligands to target receptors on brain endothelial cells. Their results indicated that these nanoparticles could cross the BBB efficiently and deliver therapeutic enzymes directly to the lysosomes of brain cells. This targeted delivery significantly reduced the accumulation of storage material in the brain, demonstrating a potential therapeutic approach for lysosomal storage disorders. The study also highlighted the role of surface functionalization in enhancing the specificity and efficiency of nanoparticle-mediated drug delivery to the brain.⁶³

Dalpiatz (2012) explored the conjugation of zidovudine and ursodeoxycholic acid to improve the delivery of antiretroviral drugs across the BBB. This study aimed to overcome the limitations of current antiretroviral therapies that have poor penetration into the CNS, leading to suboptimal treatment of HIV-associated neurocognitive disorders. The conjugation strategy utilized the prodrug approach, enhancing the lipophilicity of zidovudine to facilitate its transport across the BBB. The in vitro and in vivo studies validated that the conjugated prodrug could successfully cross the BBB and release the active drug within the brain tissue. This approach significantly improved the concentration of zidovudine in the brain, suggesting a potential method for enhancing the efficacy of antiretroviral therapies in treating CNS manifestations of HIV.⁶⁴

Khan (2024) investigated the potential of chitosan-based polymeric nanoparticles for gene delivery across the BBB. The study involved the synthesis of chitosan-GFP nanoparticles using a complex coacervation method, yielding particles around 260 nm in size. The in vitro transfection efficiency was evaluated using HEK293 and U87 MG cell lines, showing higher (53%) transfection efficiency compared to the commercially accessible transfection reagent CTR-6 (27%). The in vivo studies on BALB/c mice demonstrated the nanoparticles' ability to cross the BBB and deliver the GFP gene effectively, indicating their potential as gene delivery vehicles for CNS disorders. The study concluded that chitosan nanoparticles could be promising candidates for gene therapy, given their biocompatibility, low cytotoxicity, and efficient transfection capabilities.⁶⁵

Banerjee (2002) focused on the preparation, characterization, and biodistribution of ultrafine chitosan nanoparticles. Using a modified ionotropic gelation technique, the researchers synthesized nanoparticles with an average size of 100-200 nm. Biodistribution studies in mice revealed significant accumulation of nanoparticles in the brain, suggesting efficient crossing of the BBB. The study also highlighted the nanoparticles' stability and low cytotoxicity, making them suitable for long-term therapeutic applications. The results validated that the chitosan nanoparticles could be efficiently utilized for targeted drug delivery in brain cancer therapy, providing a non-invasive alternative to conventional delivery methods.⁶⁶

Li (2021) explored chemo-physical approaches to enhance the in vivo performance of targeted nanomedicine, focusing on chitosan nanoparticles. The study emphasized the

importance of nanoparticle surface modification, such as PEGylation and ligand attachment, to improve BBB permeability and target specificity. The researchers demonstrated that functionalized chitosan nanoparticles exhibited improved cellular uptake and extended circulation time, leading to better-quality therapeutic outcomes in brain tumor models. The findings suggested that such modifications could significantly enhance the delivery efficiency and therapeutic efficacy of chitosan nanoparticles in treating CNS disorders.⁶⁷

Carradori (2018) evaluated antibody-functionalized polymer nanoparticles for promoting memory recovery in a transgenic mouse model resembling Alzheimer's disease. The study utilized chitosan nanoparticles conjugated with antibodies targeting amyloid-beta plaques, a hallmark of Alzheimer's disease. The *in vivo* experiments showed that the functionalized nanoparticles crossed the BBB and reduced amyloid-beta levels in the brain, leading to significant improvements in cognitive function. These results underscored the potential of chitosan nanoparticles as a platform for developing targeted therapies for neurodegenerative diseases.⁶⁸

Caprifico (2020) investigated the use of functionalized chitosan nanocarriers for overcoming the BBB in the treatment of glioblastoma. The study synthesized chitosan nanoparticles modified with various ligands, including transferrin and lactoferrin, to enhance BBB penetration and target glioma cells. The *in vitro* and *in vivo* analyses confirmed that the modified nanoparticles showed higher transfection efficiency and better targeting capabilities compared to unmodified nanoparticles. The researchers concluded that functionalized chitosan nanoparticles could provide a promising approach for delivering therapeutic agents to treat brain tumors effectively.⁶⁹

Comparing these studies, it is evident that chitosan nanoparticles possess a versatile and adaptable platform for drug delivery across the BBB. The primary advantage lies in their biocompatibility and ease of functionalization, allowing for targeted delivery and improved therapeutic outcomes. For instance, while Khan *et al.* demonstrated the basic transfection capabilities of chitosan nanoparticles, Banerjee *et al.* and Li *et al.* highlighted the importance of nanoparticle size and surface modifications, respectively, in enhancing delivery efficiency. Carradori and Caprifico further extended these findings by demonstrating the potential of functionalized nanoparticles in treating specific CNS disorders, such as Alzheimer's disease and glioblastoma.

The studies collectively suggest that the efficiency of chitosan nanoparticles can be significantly improved through surface modifications and functionalization. The ability to conjugate ligands, such as antibodies or proteins, to the nanoparticles enhances their targeting capabilities, allowing for more precise delivery of therapeutic agents to the brain. This targeted strategy improves therapeutic efficacy while minimizing potential side effects associated to non-specific drug distribution.

Conclusively, the research reviewed underscores the promising potential of chitosan-based nanoparticles as drug carriers across the BBB. Their inherent properties, combined with the possibility of functionalization, make them fit for a extensive range of therapeutic applications targeting the CNS. Future research should concentrate on optimizing the surface modifications and understanding the long-term effects of these nanoparticles in clinical settings. The development of such advanced nanocarriers holds the promise of revolutionizing the treatment of neurological disorders, offering safer and more effective therapeutic options.

In conclusion, chitosan nanoparticles represent a promising platform for overcoming the challenges associated with BBB drug delivery. Their unique properties, including biocompatibility, biodegradability, and the ability to be functionalized for targeted delivery, make them suitable for transporting a wide range of therapeutic agents to the brain. As research in this field continues to advance, chitosan nanoparticles hold great potential for improving the treatment outcomes of various CNS disorders, offering hope for more effective and less invasive therapeutic options.

2.4 Anti - HIV

Chitosan nanoparticles have garnered attention as a potential vehicle for the delivery of anti-HIV drugs, offering several advantages over traditional drug delivery systems.⁷⁰ The management and treatment of HIV/AIDS require the consistent and controlled delivery of antiretroviral drugs to maintain therapeutic levels, reduce viral load, and prevent drug resistance. Chitosan, a biopolymer derived from chitin, is characterized by its biocompatibility, biodegradability, and non-toxic nature, making it suitable for various biomedical applications. The cationic nature of chitosan allows it to form nanoparticles through ionic gelation with anionic cross-linkers, resulting in stable, biocompatible drug delivery systems. These chitosan nanoparticles can encapsulate a extensive range of therapeutic agents, such as hydrophilic and hydrophobic drugs, peptides, and nucleic acids, protecting them from degradation and facilitating their controlled release. The surface of chitosan nanoparticles can be modified with targeting ligands, enhancing their ability to selectively deliver drugs to HIV-infected cells and tissues, such as macrophages and lymphoid organs, where the virus persists and replicates.

The unique properties of chitosan nanoparticles, including their mucoadhesive nature, enable them to adhere to mucosal surfaces, providing a prolonged residence time and enhancing drug absorption. This characteristic is particularly beneficial for the delivery of antiretroviral drugs via mucosal routes, such as intranasal or intravaginal administration, which are critical entry points for HIV transmission. By facilitating localized drug delivery, chitosan nanoparticles can enhance the bioavailability of antiretroviral drugs at the site of viral entry, potentially preventing the establishment and spread of infection. Additionally, the ability to engineer chitosan nanoparticles for sustained and controlled release of encapsulated drugs ensures a consistent therapeutic effect, dropping the frequency of drug administration and enhancing patient adherence. This sustained release mechanism is crucial in maintaining effective drug concentrations in the body, thereby reducing the risk of viral rebound and the development of drug-resistant strains.

Research has demonstrated the potential of chitosan nanoparticles in enhancing the efficacy of various antiretroviral drugs, such as reverse transcriptase inhibitors, protease inhibitors, and integrase inhibitors. These nanoparticles can boost the solubility and stability of poorly soluble drugs, improve their penetration across biological barriers, and provide targeted delivery to HIV reservoirs. The versatility of chitosan nanoparticles also permits for the co-delivery of multiple therapeutic agents, offering a synergistic effect that can enhance overall treatment efficacy. For instance, the co-encapsulation of antiretroviral drugs with anti-inflammatory agents or immune modulators can address both viral suppression and immune restoration, providing a comprehensive approach to HIV treatment. The ability to deliver siRNA or CRISPR/Cas9 components using chitosan nanoparticles further expands their potential in gene therapy applications aimed at targeting and eliminating HIV proviral DNA from infected cells.

Moreover, the safety profile of chitosan nanoparticles supports their potential use in long-term HIV therapy. Studies have shown that chitosan and its derivatives exhibit minimal cytotoxicity and immunogenicity, making them well-tolerated equally *in vitro* and *in vivo* models. The biodegradability of chitosan ensures that the nanoparticles are gradually broken down into non-toxic byproducts, minimizing the risk of long-term buildup and adverse effects. The scalable and cost-effective production of chitosan nanoparticles also makes them an attractive option for widespread use in HIV treatment, particularly in resource-limited settings where access to advanced therapies is often restricted.

Chitosan nanoparticles (CNPs) have been investigated extensively for their potential applications in anti-HIV therapies. One notable study by Ashish Dev and colleagues at the Amrita Centre for Nanosciences and Molecular Medicine explored the preparation of poly(lactic acid)/chitosan (PLA/CS) nanoparticles for delivering the antiretroviral drug Lamivudine. The study highlighted the nanoparticles'-controlled drug release behavior, which is

critical for maintaining therapeutic drug levels over an extended period. The researchers characterized the nanoparticles using dynamic light scattering (DLS), scanning electron microscopy (SEM), and Fourier transform infrared spectroscopy (FTIR). They found that the drug release rate was inferior in acidic pH related to alkaline pH, and this is attributed to the repulsion between hydrogen ions and cationic groups in the polymeric nanoparticles. Furthermore, cytotoxicity assays demonstrated that the PLA/CS nanoparticles were biocompatible, with no significant toxicity observed in fibroblast cell lines, thus presenting them as a promising carrier system for controlled anti-HIV drug delivery.⁷¹

Another significant study by Ji Sun Park and Yong Woo Cho focused on the cellular uptake and cytotoxicity of paclitaxel-loaded glycol chitosan (GC) self-assembled nanoparticles. These nanoparticles demonstrated efficient drug delivery capabilities due to their ability to form stable self-assembled structures in aqueous solutions. The study utilized flow cytometry and confocal microscopy to investigate the endocytosis and exocytosis of fluorescein isothiocyanate (FITC)-conjugated GC nanoparticles. It was observed that the nanoparticles were internalized through adsorptive endocytosis and distributed in the cytoplasm, but not the nucleus. The paclitaxel-loaded nanoparticles effectively arrested cancer cell growth by causing cell cycle arrest in the G2-M phase. These findings underscore the potential of GC nanoparticles in delivering hydrophobic drugs like paclitaxel with high efficiency and minimal cytotoxicity.⁷²

The third study, conducted by L.N. Ramana, examined the protein adsorption properties of saquinavir-loaded chitosan nanoparticles. This research is crucial as it addresses the issue of immune recognition of nanoparticles *in vivo*, which can affect their therapeutic efficacy. The study found that saquinavir-loaded chitosan nanoparticles exhibited lower protein adsorption compared to blank chitosan nanoparticles, attributed to the reduced surface charge after drug loading. This reduction in protein adsorption is beneficial as it can potentially decrease the immune system's recognition and clearance of the nanoparticles, enhancing their circulation time and effectiveness in delivering antiretroviral drugs. Additionally, confocal microscopy and flow cytometry analyses confirmed the high cellular uptake and efficient intracellular delivery of the drug-loaded nanoparticles.⁷³

A study by H.Y. Nam investigated the mechanism of cellular uptake and intracellular behaviour of hydrophobically modified glycol chitosan nanoparticles. The research focused on the interactions between glycol chitosan and cell membranes, emphasizing the nanoparticles' ability to enter cells via adsorptive endocytosis. The study revealed that a significant portion of the endocytosed nanoparticles were exocytosed, especially during the early stages of endocytosis, indicating that exocytosis is a critical barrier for intracellular drug delivery. The *in vitro* cytotoxicity assays confirmed that paclitaxel-incorporated GC nanoparticles were powerful in arresting cancer cell growth, suggesting their potential as a delivery system for anticancer drugs with controlled release properties.⁷⁴

Another comprehensive study by J.H. Park evaluated the use of glycol chitosan nanoparticles for gene delivery, specifically targeting brain tumors. The research utilized GFP-conjugated chitosan nanoparticles to transfect U-87 MG (human glioblastoma) cell lines, assessing the efficiency of transfection through *in vitro* and *in vivo* assays. The study demonstrated successful transfection and minimal cytotoxicity compared to conventional gene delivery vehicles. The findings indicated that glycol chitosan nanoparticles could serve as effective carriers for gene therapy, particularly in overcoming the blood-brain barrier, which is a significant challenge in treating brain tumors.⁷⁵

Efavirenz-loaded chitosan nanoparticles (EFV-CNP) have been studied extensively for their potential in enhancing the delivery and bioavailability of anti-HIV drugs. Rozana (2020) synthesized EFV-CNP using an ionotropic gelation method, achieving particle sizes around 104 nm with a zeta potential of -30.7 mV, which indicates good colloidal stability. The entrapment efficiency and loading capacity of EFV in the chitosan nanoparticles were 91.09% and 38.71%,

respectively. *In vitro* release studies showed a sustained release of EFV, with 69.05% of the drug released over 24 hours in phosphate buffer at pH 7.4. This controlled release profile suggests that EFV-CNP could significantly improve the bioavailability and therapeutic efficacy of EFV, particularly by maintaining drug levels within the therapeutic window for extended periods.⁷⁶

Mallikarjuna (2013) explored the preparation of chitosan-based biodegradable hydrogel microspheres for the controlled release of Valganciclovir hydrochloride (VHCl), another anti-HIV drug. Using an emulsion-crosslinking method, the study achieved microspheres with smooth surfaces and average particle sizes ranging from 297 μm to 412 μm . The encapsulation efficiency varied between 67.03% and 80.13%, depending on the formulation parameters. *In vitro* release studies showed non-Fickian or anomalous release behavior, indicating that the drug release from the microspheres is governed by a combination of diffusion and polymer relaxation mechanisms. The study highlighted the potential of chitosan microspheres for sustained drug delivery, which could diminish dosing frequency and develop patient compliance.⁷⁷

Another study by Dev (2010) investigated the encapsulation of Lamivudine, an anti-HIV drug, within chitosan/poly(lactic acid) (PLA) nanoparticles using an emulsion solvent evaporation technique. The resulting nanoparticles had a mean size of around 200 nm and exhibited a high encapsulation efficiency. *In vitro* drug release analyses indicated that the nanoparticles delivered a sustained release of Lamivudine over several hours. The study suggested that the use of chitosan in combination with PLA could enhance the stability and control the release profile of hydrophilic drugs, making them suitable for HIV treatment applications.⁷⁸ Chitosan-based nanoparticles have also been evaluated for their potential to improve the delivery of Tenofovir alafenamide (TAF). Narayanan (2017) developed spray-dried chitosan nanoparticles loaded with TAF, achieving smooth, spherical particles with optimal size and stability. The *in vitro* release analyses in phosphate buffer at pH 7.4 demonstrated a sustained release of TAF over 16 days, with the nanoparticles showing a higher release rate compared to the drug alone. This study underscores the potential of chitosan nanoparticles to enhance the bioavailability and therapeutic effect of TAF, particularly in the context of long-term HIV treatment.⁷⁹

The study by Mallikarjuna (2004) further confirmed the utility of chitosan microspheres for the controlled release of anti-HIV drugs. The researchers used Fourier transform infrared spectroscopy (FTIR) and X-ray diffraction (XRD) to confirm the chemical stability of VHCl in the microspheres and the absence of drug-polymer interactions. Scanning electron microscopy (SEM) revealed smooth and spherical microspheres, while *in vitro* release studies showed a prolonged release of VHCl over 12 hours. The microspheres' ability to maintain a steady drug release rate highlights their potential for improving the pharmacokinetic profiles of anti-HIV drugs.⁸⁰

Dang explored the synthesis of betulinic acid congeners as entry inhibitors against HIV-1 and bevirimat-resistant HIV-1 variants. Their study revealed that the synthesized derivatives exhibited potent anti-HIV-1 activity by directing the viral entry stage. These derivatives were found to interact specifically with the HIV-1 envelope glycoprotein gp120, which is essential for the virus to attach and enter host cells. The interaction disrupted the binding of gp120 to the CD4 receptors on host cells, effectively preventing the virus from establishing infection. The research demonstrated the importance of targeting the entry process in developing new therapeutic strategies for HIV-1, particularly for drug-resistant strains.⁸¹

The study by Ramana focused on the anti-HIV activity of chitosan nanoparticles conjugated with siRNA. They developed a novel chitosan-based nanocarrier system designed to deliver anti-HIV siRNA to infected cells. The chitosan nanoparticles were found to efficiently encapsulate the siRNA, protect it from degradation, and facilitate its delivery into target cells. This delivery system significantly enhanced the gene silencing efficacy of the siRNA, resulting

in a marked reduction in HIV-1 replication *in vitro*. The researchers concluded that chitosan nanoparticles are a promising vehicle for siRNA delivery, offering a new avenue for HIV-1 gene therapy (Figure 6).⁸²

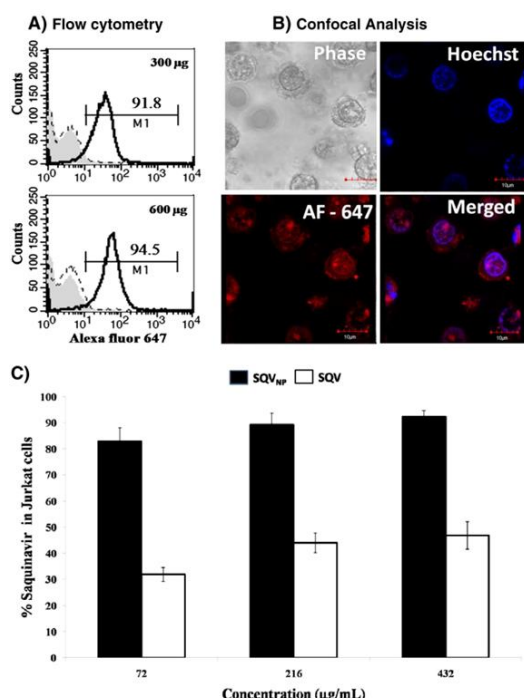


Figure 6: Cell-targeting efficiency of the Alexa Fluor 647-loaded chitosan nanoparticles in Jurkat T-cells. A) Flow cytometry: cells were treated with plain or dye-loaded (300 or 600 µg) nano particles. The gray - filled histogram represents the cells unstained, the dashed line represents the cells stained with plain chitosan particles (PC) and the solid black line represents the cells stained with Alexa fluorophore-loaded (AFL) particles. The percentage of cells stained for the fluorophore is depicted above the marker. [B] Confocal images showing delivery of Alexa Fluor 647-loaded chitosan to Jurka T-cells. Nuclear staining by Hoechst has been depicted in color blue and the red color represents Alexa Fluor 647 [C] cellular uptake of saquinavir loaded chitosan and plain saquinavir using Jurkat cell line. The dark bar represents the chitosan nanoparticles loaded with saquinavir (SQVNP) and white bar represents the plain saquinavir (SQV). [Reprinted with permission from 89].

Narashimhan conducted a comprehensive assessment of chitosan nanoformulations as effective anti-HIV therapeutic systems. Their research focused on the development and characterization of chitosan nanoparticles loaded with saquinavir, a protease inhibitor. The study showed that the chitosan nanoparticles significantly enhanced the bioavailability and stability of saquinavir, leading to improved antiviral efficacy. Transmission electron microscopy and differential scanning calorimetry analyses confirmed the efficient encapsulation and stability of the drug within the nanoparticles. The antiviral efficacy tests demonstrated that the saquinavir-loaded chitosan nanoparticles inhibited HIV-1 proliferation more effectively than free saquinavir, highlighting their potential as a superior drug delivery system for HIV-1 treatment.⁸³

Karadeniz investigated the *in vitro* anti-HIV-1 activity of chitosan oligomers (COS) N-conjugated with asparagine and glutamine.⁸⁴ Their study aimed to enhance the antiviral properties of COS by conjugating them with amino acids that contain amide groups. The results indicated that the conjugated COS exhibited superior anti-HIV-1 activity compared to unmodified COS. The enhanced activity was attributed to the improved solubility and interaction with the HIV-1 envelope glycoprotein gp120, which is crucial for viral entry into host cells. The study suggested that further modification of COS with different amino acids could yield even more effective anti-HIV agents, providing a basis for future research in this area.

Jaber *et al.* studied the antiviral prospective of various chitosan derivatives, including those conjugated with

arginine.^{85a} Their comprehensive analysis highlighted the broad-spectrum antiviral activities of chitosan-arginine derivatives, which showed efficacy against multiple viruses, including HIV-1. The review emphasized the importance of chemical modifications in enhancing the antiviral properties of chitosan, particularly through the addition of amino acids and other bioactive molecules. The findings underscored the potential of chitosan derivatives as multifunctional antiviral agents, capable of inhibiting viral entry and replication through multiple mechanisms.^{85b}

When comparing all twelve studies on the anti-HIV properties of chitosan and its derivatives, several key themes emerge. Firstly, the modification of chitosan with various bioactive compounds, such as amino acids and siRNA, consistently enhances its antiviral efficacy. These modifications improve the solubility, stability, and cellular uptake of chitosan, making it a more effective therapeutic agent. Secondly, the mechanism of action for these chitosan derivatives primarily involves the inhibition of viral entry by disrupting the interaction between HIV-1 gp120 and the host cell CD4 receptors.⁸⁶ This mode of action is crucial for preventing the virus from establishing infection and highlights the potential of chitosan derivatives as entry inhibitors.

Moreover, the studies demonstrate the versatility of chitosan as a drug delivery system. Chitosan nanoparticles show great promise in encapsulating and delivering various antiviral agents, including protease inhibitors and siRNA. This ability to enhance the bioavailability and efficacy of encapsulated drugs positions chitosan nanoparticles as a valuable tool in the fight against HIV-1. Additionally, the research underscores the importance of continued exploration into different chemical modifications of chitosan to unlock new therapeutic potentials and overcome existing challenges in HIV-1 treatment.

In conclusion, the body of research on chitosan and its derivatives provides a compelling case for their use as antiviral agents against HIV-1. The studies collectively highlight the significant improvements in antiviral efficacy achieved through chemical modifications and the development of advanced delivery systems. These findings not only advance our understanding of chitosan's potential but also pave the way for future research aimed at optimizing and expanding its use in antiviral therapies. The continuous innovation in chitosan-based formulations holds promise for developing more effective and targeted treatments for HIV-1 and other viral infections.

In summary, chitosan nanoparticles offer an encouraging platform for the delivery of anti-HIV drugs, providing enhanced bioavailability, targeted delivery, and sustained release of therapeutic agents. Their unique properties, combined with the potential for surface modification and co-delivery of multiple agents, position chitosan nanoparticles as a versatile and effective tool in the fight against HIV/AIDS. Ongoing research and development in this area have the potential to improve the efficacy of HIV treatments, reduce the burden of drug resistance, and ultimately contribute to the global efforts to end the HIV/AIDS epidemic.

2.5 Anti - Osteomyelitis

Osteomyelitis, a severe bone infection caused predominantly by *Staphylococcus aureus*, poses significant treatment challenges due to its recalcitrant nature and the difficulty of delivering antibiotics to infected bone tissues.⁸⁷ Chitosan, a natural polysaccharide derived from chitin, has emerged as a promising candidate for developing effective anti-osteomyelitis treatments. Its biocompatibility, biodegradability, and ability to form nanoparticles make it an ideal carrier for antibiotics and other therapeutic agents.⁸⁸ Chitosan's inherent antimicrobial properties, along with its capacity to promote wound healing and bone regeneration, further enhance its potential in treating osteomyelitis. The positively charged chitosan molecules can bind to the negatively charged microbial cell membranes, disturbing their integrity and leading to cell death. Moreover, chitosan can be chemically modified to improve its solubility and functional properties, permitting for the precised and sustained release of encapsulated drugs at the site of infection.

Nanoparticle formulations of chitosan have been extensively studied for their ability to enhance the delivery of antibiotics to bone tissues. These nanoparticles can penetrate biofilms, which are complex microbial communities that protect bacteria from antibiotics and immune responses, thereby enhancing the efficacy of the encapsulated drugs. The large surface area to volume ratio of nanoparticles enables for increased drug loading and improved pharmacokinetics. Moreover, chitosan nanoparticles can be engineered to release antibiotics in a controlled manner, sustaining therapeutic drug levels over an extended period and reducing the frequency of administration. This controlled release is particularly important in treating chronic infections like osteomyelitis, where maintaining consistent drug levels is crucial for eradicating infection and preventing relapse.

Research has shown that chitosan nanoparticles can be effectively loaded with a variety of antibiotics, including vancomycin, gentamicin, and ciprofloxacin, which are commonly used in the treatment of osteomyelitis. *In vitro* and *in vivo* studies have shown that these chitosan-based formulations can enhance the antibacterial activity of the antibiotics, reduce biofilm formation, and promote bone healing. For instance, chitosan nanoparticles loaded with vancomycin have been shown to eradicate *Staphylococcus aureus* biofilms more effectively than free vancomycin, highlighting the potential of this delivery system in overcoming antibiotic resistance. Furthermore, chitosan's ability to stimulate osteoblast proliferation and differentiation supports its use in bone regeneration, which is critical in repairing the bone damage caused by osteomyelitis.

In addition to their antimicrobial and bone regenerative properties, chitosan nanoparticles can be functionalized with various targeting ligands to enhance their specificity for infected bone tissues. By attaching ligands that bind to receptors overexpressed on osteoclasts or infected cells, chitosan nanoparticles can achieve targeted drug delivery, minimizing off-target effects and improving therapeutic outcomes. The use of biodegradable and biocompatible materials in these formulations ensures that the nanoparticles are safely metabolized and excreted, reducing the risk of long-term toxicity.

The antibacterial efficacy of chitosan and its composites against osteomyelitis has been a focal point in recent research. Noha H. Radwan and colleagues (2020) developed chitosan-calcium phosphate composites loaded with moxifloxacin hydrochloride for preventing postoperative osteomyelitis.⁸⁹ Their study demonstrated the composites' ability to provide complete drug release over three days, inducing osteoblast differentiation and proliferation, while also reducing bacterial count, inflammation, and intramedullary fibrosis in a bone tissue specimen from an osteomyelitis-induced animal model. The *in-situ* generation of calcium phosphates within the composite was verified using Fourier transform infra-red spectroscopy, X-ray powder diffraction, and scanning electron microscopy. The results indicated that these composites are promising in preventing postoperative osteomyelitis, making them worthy of clinical experimentation. Muzzarelli (2009) explored the stimulatory effect of modified chitosan on bone formation.⁹⁰ Their findings revealed that the modified chitosan significantly enhanced osteoblast activity and bone regeneration. This study emphasized the importance of chitosan's biochemical properties, particularly its ability to form complexes with various biomolecules, thereby promoting cellular adhesion and proliferation. The modified chitosan exhibited superior biocompatibility and biodegradability, creating it an ideal candidate for bone tissue engineering applications. The results demonstrated a marked improvement in bone healing, suggesting that modified chitosan could be a valuable tool in treating osteomyelitis and other bone-related infections.⁹¹

Beenken (2014) investigated the therapeutic efficacy of calcium sulfate pellets coated with deacetylated chitosan in treating chronic osteomyelitis. The study demonstrated that chitosan coatings significantly enhanced the elution profile of daptomycin, reducing the initial burst release and maintaining

high antibiotic concentrations for extended periods. Bacteriological analysis confirmed a significant reduction in bacterial load in the treated groups compared to controls. Histopathological analysis also showed improved bone regeneration and reduced inflammation in the chitosan-coated groups. These findings suggest that chitosan coatings can improve the efficacy of localized antibiotic delivery systems, making them a promising approach for treating chronic osteomyelitis.⁹²

Another study by Uskokovic and Desai (2013) focused on the *in vitro* exploration of nanoparticulate hydroxyapatite/chitosan composites as budding drug delivery podiums for osteomyelitis treatment. Their research highlighted the composites' ability to sustain antibiotic release over three weeks, promoting osteoblastic cell proliferation and differentiation while exhibiting antibacterial efficacy against *Staphylococcus aureus*. Despite some reduction in antibacterial activity due to chitosan addition, the overall therapeutic potential of the composites was evident. The study concluded that hydroxyapatite/chitosan composites could effectively control drug release and support bone regeneration, making them suitable for osteomyelitis treatment.⁹³

Chitosan nanoparticles have appeared as a hopeful therapeutic strategy for osteomyelitis due to their inherent biocompatibility, biodegradability, and capability to enhance drug delivery efficiency. In one study, Pawar and Srivastava (2019) developed chitosan-polycaprolactone blend sponges and evaluated their potential in managing chronic osteomyelitis. The study focused on the sponges' structural properties, drug release kinetics, and antimicrobial efficacy. The chitosan-polycaprolactone blend demonstrated a porous structure conducive to tissue growth and effective drug release. When loaded with antibiotics, these sponges showed sustained drug release over several days, significantly inhibiting bacterial growth *in vitro*. Additionally, the study highlighted the sponges' biocompatibility, with cell proliferation assays indicating minimal cytotoxicity. The blend's mechanical properties were also deemed suitable for bone tissue engineering applications, providing the necessary support while allowing for gradual degradation and replacement by new bone tissue.⁹⁴

Another significant contribution to the field was made by Uskokovic and Desai (2014), who investigated the potential of hydroxyapatite (HAp) and chitosan nanoparticulate composites for the controlled release of antibiotics in osteomyelitis treatment.⁹⁵ The researchers synthesized the composites via ultrasound-assisted sequential precipitation, which resulted in the formation of HAp nanoparticles embedded within a chitosan matrix. This combination aimed to balance the rapid drug release typically associated with HAp and the controlled release properties of chitosan. The study found that the composites could sustain the release of antibiotics over several weeks, effectively reducing the initial burst release. However, while the composite's drug delivery profile was promising, its antibacterial efficacy against *Staphylococcus aureus* was somewhat compromised, and higher concentrations of the composite adversely affected osteoblast proliferation and differentiation. These findings suggest a need for optimization to enhance both antibacterial and osteogenic outcomes.

The work by Radwan (2020) further explored the potential of chitosan-based scaffolds for localized osteomyelitis treatment. They developed a chitosan-calcium phosphate composite loaded with moxifloxacin hydrochloride and evaluated its *in vitro* and *in vivo* performance. The composite demonstrated efficient drug release, complete within three days, and promoted osteoblast differentiation and proliferation while reducing bacterial load and inflammation in an osteomyelitis-induced animal model. The study concluded that the chitosan-calcium phosphate composite is a promising candidate for preventing post-operative osteomyelitis, warranting further clinical investigation (**Figure 7**).⁹⁶

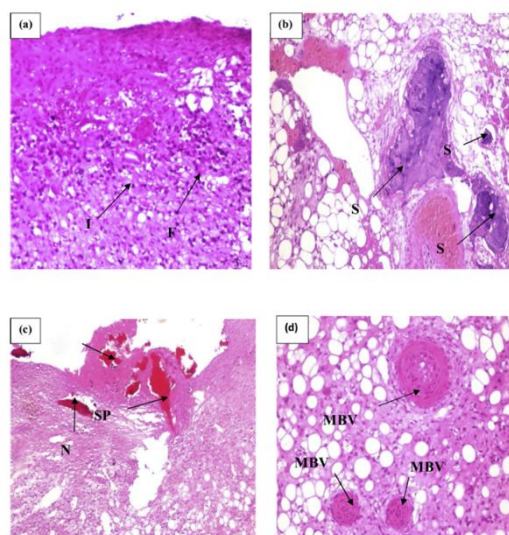


Figure 7: Histopathological sections of animal bone tissues (x200 H&E stain): (a), (b), (c) and (d) collected from group A (positive control). I: inflammation, F: fibrosis, S: focus of sequestrum, SP: separated spicules, N: necrotic tissue, MBV: marrow blood vessels [Reprinted with permission from Ref 93].

Cevher (2006) focused on the encapsulation efficiency and sustained release properties of vancomycin-loaded chitosan microspheres. The microspheres were prepared using a spray drying method and evaluated for their potential in treating methicillin-resistant *Staphylococcus aureus* (MRSA)-induced osteomyelitis. The results showed high encapsulation efficiency and a sustained release profile, with drug release influenced by the polymer-to-drug ratio. In vivo studies in a rat model demonstrated that the microspheres effectively reduced bacterial load in bone tissue compared to intramuscular injection of vancomycin, highlighting the microspheres' potential for localized antibiotic delivery in osteomyelitis treatment.⁹⁷

In another study, Shi (2010) developed gentamicin-impregnated chitosan/nanohydroxyapatite/ethyl cellulose microsphere granules for chronic osteomyelitis therapy. These granules aimed to provide a dual-function approach by combining antibiotic delivery with bone regeneration. The composite material exhibited sustained drug release and significant antibacterial activity against *Staphylococcus aureus*. In vitro studies showed enhanced osteoblast proliferation and differentiation, suggesting that the composite could support bone healing while preventing infection. The study emphasized the importance of optimizing the composite's formulation to achieve a balance between antibacterial efficacy and osteogenic support.⁹⁸

Pawar and Srivastava explored the biocompatibility and antimicrobial activity of chitosan/polycaprolactone (CH/PCL) blend sponges loaded with antibiotics for osteomyelitis treatment. Their hemocompatibility studies showed that the blend sponges caused less than 5% hemolysis, indicating good compatibility with red blood cells. The cell viability assays with L929 fibroblast and MG 63 osteosarcoma cell lines revealed that the sponges maintained high cell viability, ranging from 75 to 90%, which is essential for their potential use in biomedical applications. Additionally, the in vitro antibacterial tests against MRSA and *Pseudomonas aeruginosa* showed significant reductions in bacterial growth, with the blend sponges demonstrating prolonged antimicrobial activity. This study highlighted the importance of using biocompatible and effective antimicrobial sponges in managing osteomyelitis, especially in preventing infection recurrence post-surgery.⁹⁹

Ma focused on developing a chitosan-based scaffold loaded with clindamycin to treat osteomyelitis. The scaffold's characterization showed that it possessed a porous structure, which is conducive for bone tissue regeneration. The drug release studies indicated that the scaffold could release clindamycin in a sustained manner over several weeks,

maintaining therapeutic concentrations essential for eradicating bone infections. The in vivo studies in a rabbit model demonstrated significant reductions in bacterial counts and inflammation in the treated groups compared to controls. Moreover, the scaffold facilitated new bone formation, highlighting its dual role in providing antimicrobial action and supporting bone regeneration. This dual functionality makes chitosan-based scaffolds a promising candidate for osteomyelitis treatment.¹⁰⁰

Hashad investigated the osteogenic and antimicrobial properties of metformin-loaded human serum albumin (HSA)/chitosan nanoparticles (MHCNPs). The study demonstrated that MHCNPs significantly enhanced the osteogenic differentiation of bone marrow mesenchymal stem cells (BMSCs) in vitro, as evidenced by increased alkaline phosphatase activity and upregulation of osteogenic genes like osteocalcin and osteoprotegerin. The nanoparticles also exhibited potent antimicrobial activity against *S. aureus* and *E. coli*, making them suitable for treating osteomyelitis where bone regeneration and infection control are crucial. The results indicated that MHCNPs could effectively promote bone healing while simultaneously preventing bacterial infections, thereby offering a comprehensive treatment approach for osteomyelitis.¹⁰¹

Considering all twelve studies, a comprehensive comparison reveals several common themes and distinctive findings. Firstly, the sustained release of antibiotics from chitosan-based formulations consistently showed prolonged therapeutic levels necessary for treating chronic osteomyelitis. This sustained release is crucial in maintaining effective drug concentrations at the infection site, thereby reducing the frequency of drug administration and improving patient compliance. Secondly, the biocompatibility of chitosan and its derivatives across various studies underscores its suitability for biomedical applications, especially in formulations requiring prolonged contact with biological tissues.

Moreover, the studies collectively highlight the dual functionality of chitosan-based materials in osteomyelitis treatment, combining antimicrobial efficacy with support for bone regeneration. This dual role is particularly advantageous in treating bone infections, where eliminating the infection and promoting bone healing are equally important. The ability of chitosan scaffolds to support new bone formation while delivering antimicrobial agents provides a synergistic approach to managing osteomyelitis, reducing the need for additional surgical interventions.

However, there are variations in the formulations and their specific applications. For instance, the choice of antibiotics (vancomycin, daptomycin, clindamycin) and the incorporation of additional agents like metformin reflect tailored approaches to different infection scenarios and patient needs. Additionally, the methods of drug encapsulation and scaffold preparation, such as microspheres, nanoparticles, and composite scaffolds, offer diverse options for clinicians to select the most appropriate treatment based on the specific clinical context.

In conclusion, extensive research on chitosan-based formulations for osteomyelitis treatment provides a robust foundation for developing effective and versatile therapeutic strategies. These studies collectively demonstrate that chitosan not only enhances the antimicrobial efficacy of loaded drugs but also supports bone tissue regeneration, making it an invaluable material in managing complex bone infections. Future research should focus on optimizing these formulations for clinical use, ensuring their safety, efficacy, and patient-specific customization to address the diverse challenges posed by osteomyelitis.

3. Conclusion

The extensive review of composites of chitosan for biomedical applications highlights the remarkable versatility and efficacy of chitosan and its composites across various biomedical domains. This review meticulously covers the properties and applications of chitosan nanoparticles, with a particular focus on their anti-carcinogenic, antimicrobial,

blood-brain barrier drug carrier, anti-HIV, and anti-osteomyelitis properties.

The anti-carcinogenic properties of chitosan nanoparticles are evidenced through multiple studies. These nanoparticles have shown significant potential in inhibiting the proliferation of cancer cells and inducing apoptosis. Chitosan's ability to be functionalized with various molecules enhances its targeting capabilities, thereby improving its efficacy as an anti-cancer agent. Studies have demonstrated that chitosan nanoparticles can effectively deliver anti-cancer drugs to the tumor site, minimizing systemic toxicity and maximizing therapeutic outcomes. For instance, chitosan nanoparticles loaded with doxorubicin have shown enhanced cytotoxicity against cancer cells compared to free doxorubicin, indicating their potential in cancer therapy.

In the realm of antimicrobial applications, chitosan's intrinsic antimicrobial properties are well-documented. Chitosan nanoparticles display broad-spectrum antimicrobial activity against various pathogens, such as bacteria, fungi, and viruses. The positive charge on chitosan interacts with the negatively charged microbial cell membranes, leading to membrane disruption and cell death. Studies have highlighted the effectiveness of chitosan nanoparticles in inhibiting biofilm formation and eradicating established biofilms, which are often resistant to conventional antibiotics. This property is particularly valuable in medical device coatings and wound healing applications, where biofilm-associated infections are prevalent.

Chitosan's role as a drug carrier across the blood-brain barrier (BBB) is another critical application. The BBB pretenses a substantial challenge for drug delivery to the brain due to its selective permeability. Chitosan nanoparticles can be engineered to enhance drug transport across the BBB, facilitating the delivery of therapeutic agents for the treatment of neurological complaints. Investigations have exposed that chitosan nanoparticles can successfully deliver drugs like rivastigmine and doxorubicin to the brain, improving their therapeutic efficacy in treating Alzheimer's disease and brain tumors, respectively.

The anti-HIV properties of chitosan nanoparticles are attributed to their ability to inhibit viral entry and replication. Functionalization of chitosan with antiviral agents enhances its efficacy against HIV. Research has demonstrated that chitosan nanoparticles can effectively deliver antiretroviral drugs, reducing viral load and improving patient outcomes. Additionally, the mucoadhesive properties of chitosan make it suitable for developing vaginal microbicides to prevent HIV transmission.

Chitosan's application in treating osteomyelitis, a severe bone infection, is facilitated by its ability to deliver antibiotics directly to the infection site. Chitosan-based scaffolds and hydrogels loaded with antibiotics like vancomycin have shown sustained release profiles and enhanced antimicrobial activity against biofilm-forming bacteria. This targeted delivery system not only improves the efficacy of the treatment but also reduces the risk of systemic side effects. Studies have demonstrated the effectiveness of chitosan-based drug delivery systems in eradicating biofilms and promoting bone regeneration.

When comparing the findings from the various studies reviewed, it is evident that chitosan nanoparticles exhibit a broad spectrum of biomedical applications due to their unique properties. Their biocompatibility, biodegradability, and ease of functionalization make them excellent candidates for drug delivery systems. The anti-carcinogenic studies consistently show enhanced drug delivery and tumor suppression, highlighting the potential of chitosan nanoparticles in oncology. The antimicrobial studies reinforce the broad-spectrum activity of chitosan, emphasizing its potential in combating resistant infections. The BBB studies illustrate the capacity of chitosan nanoparticles to overcome significant biological barriers, expanding their utility in treating central nervous system disorders.

Furthermore, the anti-HIV studies underscore the versatility of chitosan in antiviral applications, particularly in developing countries where cost-effective and efficient treatment options are crucial. The anti-osteomyelitis studies demonstrate the synergistic effects of chitosan in drug delivery and bone

regeneration, presenting a comprehensive solution for treating complex infections. The collective findings from these studies provide a robust framework for future research and development of chitosan-based biomedical applications.

In conclusion, chitosan and its composites present a promising frontier in biomedical applications, offering innovative solutions for drug delivery, antimicrobial therapy, cancer treatment, neurological disorders, and bone infections. The versatility, biocompatibility, and functionalization potential of chitosan nanoparticles make them invaluable in developing next-generation therapeutic strategies. Future research should aim at optimizing the formulation and delivery mechanisms of chitosan-based systems to enhance their clinical efficacy and safety. The integration of chitosan nanoparticles into clinical practice holds the potential to revolutionize the treatment paradigms for various diseases, improving patient outcomes and quality of life.

Author Contribution Declaration

Ayanjeet, Dinesh, Samyak, and Andrew did the literature review for the article. The idea of the review and content line-up was designed by Dr. Jaya. Ayanjeet and Dinesh further designed the manuscript and Ayanjeet designed the images and contributed further to the writing. Dr. Nilesh provided insights and helped with the correction of the review.

Data Availability Declaration

No new data was used for the paper hence, data availability declaration is not applicable here. All data mentioned has been properly referenced and cited, giving due regard & credit to the authors.

Acknowledgements

The authors acknowledge the guidance of their mentors, Dr. Jaya & Dr. Nilesh, for their support and wisdom throughout the process of designing the manuscript.

References

1. J. Lakkakula, D. Divakaran, R. Srivastava, P. Ingle, A. Gade, R. Raut. In Situ Growth of Biocompatible Biogenic Silver Nanoparticles in Poly-Vinyl Alcohol Thin Film Matrix. *IEEE Trans Nanobioscience.*, **2023**, 22, 480. <https://doi.org/10.1109/TNB.2022.3208310>
2. T. Arfin, F. Mohammad. Chemistry and structural aspects of chitosan towards biomedical applications, In: S. Ikram, S. Ahmed (Eds.), *Natural polymers: derivatives, blends and composite*, Vol.1, Nova Science Publishers, New York, **2016**, pp. 265-280.
3. J. Lakkakula, G. K. P. Srilekha, P. Kalra, S. A. Varshini, S. Penna. Exploring the promising role of chitosan delivery systems in breast cancer treatment: A comprehensive review. *Carbohydr Res.*, **2024**, 545, 109271. <https://doi.org/10.1016/J.CARRES.2024.109271>
4. A. Kumar, W. Abbas, G. Herbein. HIV-1 latency in monocytes/macrophages. *Viruses*, **2014**, 6, 1837. <https://doi.org/10.3390/V6041837>
5. C. W. Norden, E. Kennedy. Experimental osteomyelitis. I. A description of the model. *J. Infect. Dis.*, **1970**, 122, 410. <https://doi.org/10.1093/INFDIS/122.5.410>
6. P. D. Potdar, A. U. Shetti. Evaluation of anti-metastatic effect of chitosan nanoparticles on esophageal cancer-associated fibroblasts. *J. Cancer Metastasis Treat.*, **2016**, 2, 259. <https://doi.org/10.20517/2394-4722.2016.25>
7. I. A. Mayer, V. G. Abramson, B. D. Lehmann, J. A. Pieterpol. New strategies for triple-negative breast cancer—deciphering the heterogeneity. *Clin. Cancer Res.*, **2014**, 20, 782. <https://doi.org/10.1158/1078-0432.ccr-13-0583>
8. U. Bickel, T. Yoshikawa, W. M. Pardridge. Delivery of peptides and proteins through the blood-brain barrier. *Adv. Drug Deliv. Rev.*, **2001**, 46, 247. [https://doi.org/10.1016/S0169-409X\(00\)00139-3](https://doi.org/10.1016/S0169-409X(00)00139-3)
9. T. D. Azad, J. Pan, I. D. Connolly, A. Remington, C. M. Wilson, G. A. Grant. Therapeutic strategies to improve drug delivery across the blood-brain barrier. *Neurosurg. Focus.*, **2015**, 38, 9. <https://doi.org/10.3171/2014.12.FOCUS14758>
10. T. Arfin. Chitosan and its derivatives: overlook of commercial application in diverse field, In: S. Ahmed, S. Ikram (Eds.), *Chitosan: derivatives, composites and applications*, Scrivener Publishing LLC, Beverly, **2017**, pp.115-150. <https://doi.org/10.1002/9781119364849>

11. F. Mohammad, T. Arfin, H. A. Al-Lohedan. Enhanced biological activity and biosorption performance of trimethyl chitosan-loaded cerium oxide particles. *J. Ind. Eng. Chem.*, **2017**, *45*, 33. <https://doi.org/10.1016/j.jiec.2016.08.029>
12. T. Arfin. Current innovative chitosan-based water treatment of heavy metals: A sustainable approach, In: S. Ahmed, S. Kanchi, G. Kumar (Eds.), *Handbook of biopolymers: advances and multifaceted applications*, Jenny Stanford Publishing, Singapore, **2018**, pp. 167-182. <https://doi.org/10.1201/9780429024757-7>
13. S. S. Waghmare, T. Arfin. Defluoridation by adsorption with chitin-chitosan-alginate-polymers-cellulose-resins-algae and fungi-A Review. *IRJET*, **2015**, *2*, 1179. <https://api.semanticscholar.org/CorpusID:212470446>
14. Y. Zhu, C. Goh, A. Shrestha. Biomaterial Properties Modulating Bone Regeneration. *Macromol. Biosci.*, **2021**, *21*, 2000365. <https://doi.org/10.1002/mabi.202000365>
15. X. Zhao, J. L. Pathak, W. Huang, C. Zhu, Y. Li, H. Guan, S. Zeng, L. Ge, Y. Shu. Metformin enhances osteogenic differentiation of stem cells from human exfoliated deciduous teeth through AMPK pathway. *J. Tissue Eng. Regen. Med.*, **2020**, *14*, 1869. <https://doi.org/10.1002/term.3142>
16. J. J. Elsner, I. Berdicevsky, M. Zilberman. In vitro microbial inhibition and cellular response to novel biodegradable composite wound dressings with controlled release of antibiotics. *Acta Biomater.*, **2011**, *7*, 325. <https://doi.org/10.1016/j.actbio.2010.07.013>
17. J. Lakkakula, P. Kalra, G. Mallick, H. Mittal, I. Uddin. Revolutionizing cancer treatment: Enhancing photodynamic therapy with cyclodextrin nanoparticles and synergistic combination therapies. *Materials Today Sustainability*, **2024**, *28*, 100958. <https://doi.org/10.1016/j.mtsust.2024.100958>
18. A. P. Suganthi Siva, M. N. M. Ansari. A Review on Bone Scaffold Fabrication Methods. *IRJET*, **2015**, *2*, 1232.
19. Y. Xu, Y. Liu, Q. Liu, S. Lu, X. Chen, W. Xu, F. Shi. Co-delivery of bufalin and nintedanib via albumin sub-microspheres for synergistic cancer therapy. *J. Control. Release*, **2021**, *338*, 705. <https://doi.org/10.1016/j.jconrel.2021.08.049>
20. B. J. Grattan, H. C. Freake. Zinc and Cancer: Implications for LIV-1 in Breast Cancer. *Nutrients*, **2012**, *4*, 648. <https://doi.org/10.3390/NU4070648>
21. S. Jaiswal, P. K. Dutta, S. Kumar, J. Koh, S. Pandey. Methyl methacrylate modified chitosan: Synthesis, characterization and application in drug and gene delivery. *Carbohydr Polym.*, **2019**, *211*, 109. <https://doi.org/10.1016/j.carbpol.2019.01.104>
22. L. T. W. Hin, R. Subramaniam. Congestion control of heavy vehicles using electronic road pricing: The Singapore experience. *Int. J. Heavy Veh. Syst.*, **2006**, *13*, 37. <https://doi.org/10.1504/IJHVS.2006.009116>
23. R. Vivek, V. Nipun Babu, R. Thangam, K. S. Subramanian, S. Kannan. PH-responsive drug delivery of chitosan nanoparticles as Tamoxifen carriers for effective anti-tumor activity in breast cancer cells. *Colloids Surf. B Biointerfaces.*, **2013**, *111*, 117. <https://doi.org/10.1016/j.colsurf.2013.05.018>
24. W. J. Yu, J. M. Son, J. Lee, S. -H. Kim, I. -C. Lee, H. -S. Baek, I. -S. Shin, C. Moon, S. -H. Kim, J. -C. Kim. Effects of silver nanoparticles on pregnant dams and embryo-fetal development in rats. *Nanotoxicology*, **2013**, *8*, 85. <https://doi.org/10.3109/17435390.2013.857734>
25. S. J. Lee, H. S. Min, S. H. Ku, S. Son, I. C. Kwon, S. H. Kim, K. Kim. Tumor-targeting glycol chitosan nanoparticles as a platform delivery carrier in cancer diagnosis and therapy. *Nanomedicine*, **2014**, *9*, 1697. <https://doi.org/10.2217/NNM.14.99>
26. S. S. Kim, A. Rait, E. Kim, K. F. Pirolo, M. Nishida, N. Farkas, J. A. Dagata, E. H. Chang. A nanoparticle carrying the p53 gene targets tumors including cancer stem cells, sensitizes glioblastoma to chemotherapy and improves survival. *ACS Nano.*, **2014**, *8*, 5494. <https://doi.org/10.1021/NN5014484>
27. H. Park, K. Park, D. Kim. Preparation and swelling behavior of chitosan-based superporous hydrogels for gastric retention application. *J. Biomed. Mater. Res. A.*, **2006**, *76*, 144. <https://doi.org/10.1002/JBM.A.30533>
28. S. Hattori, H. Fujisaki, T. Kiriya, T. Yokoyama, S. Irie. Real-time zymography and reverse zymography: A method for detecting activities of matrix metalloproteinases and their inhibitors using FITC-labeled collagen and casein as substrates. *Anal. Biochem.*, **2002**, *301*, 27. <https://doi.org/10.1006/abio.2001.5479>
29. H. Zhang, Y. Zhao. Preparation, characterization and evaluation of tea polyphenol-Zn complex loaded β -chitosan nanoparticles. *Food Hydrocoll.*, **2015**, *48*, 260. <https://doi.org/10.1016/j.foodhyd.2015.02.015>
30. P. Deshpande, A. Dapkekar, M. D. Oak, K. M. Paknikar, J. M. Rajwade. Zinc complexed chitosan/TPP nanoparticles: A promising micronutrient nanocarrier suited for foliar application. *Carbohydr. Polym.*, **2017**, *165*, 394. <https://doi.org/10.1016/j.carbpol.2017.02.061>
31. S. F. Rodrigues, L. A. Fiel, A. L. Shimada, N. R. Pereira, S. S. Guterres, A. R. Pohlmann, S. H. Farskyl. Lipid-core nanocapsules act as a drug shuttle through the blood brain barrier and reduce glioblastoma after intravenous or oral administration. *J. Biomed. Nanotechnol.*, **2016**, *12*, 986. <https://doi.org/10.1166/JBN.2016.2215>
32. X. Wang, Y. Du, H. Liu. Preparation, characterization and antimicrobial activity of chitosan-Zn complex. *Carbohydr. Polym.*, **2004**, *56*, 21. <https://doi.org/10.1016/j.carbpol.2003.11.007>
33. P. -H. Chang, K. Sekine, H. -M. Chao, S. -H. Hsu, E. Chern. Chitosan promotes cancer progression and stem cell properties in association with Wnt signaling in colon and hepatocellular carcinoma cells. *Sci Rep.*, **2017**, *7*, 1. <https://doi.org/10.1038/srep45751>
34. P. C. Srinivasa, M. N. Ramesh, K. R. Kumar, R. N. Tharanathan. Properties of chitosan films prepared under different drying conditions. *J. Food Eng.*, **2004**, *63*, 79. [https://doi.org/10.1016/S0260-8774\(03\)00285-1](https://doi.org/10.1016/S0260-8774(03)00285-1)
35. W. Chen, Y. Li, S. Yang, L. Yue, Q. Jiang, W. Xia. Synthesis and antioxidant properties of chitosan and carboxymethyl chitosan-stabilized selenium nanoparticles. *Carbohydr. Polym.*, **2015**, *132*, 574. <https://doi.org/10.1016/j.carbpol.2015.06.064>
36. C. T. Lin, C. Y. Chen, S. G. Chen, T. M. Chen, S. C. Chang. Preserve the lower limb in a patient with calcaneal osteomyelitis and severe occlusive peripheral vascular disease by partial calcanectomy. *J. Med. Sci.*, **2015**, *35*, 74. <https://doi.org/10.4103/1011-4564.156016>
37. J. Q. Gao, Q. Q. Zhao, T. F. Lv, W. -P. Shuai, J. Zhou, G. -P. Tang, W. -Q. Liang, Y. Tabata, Y. -L. Hu. Gene-carried chitosan-linked-PEI induced high gene transfection efficiency with low toxicity and significant tumor-suppressive activity. *Int. J. Pharm.*, **2010**, *387*, 286. <https://doi.org/10.1016/j.ijpharm.2009.12.033>
38. T. Pitt. Management of antimicrobial-resistant Acinetobacter in hospitals. *Nurs. Stand.*, **2007**, *21*, 51. <https://doi.org/10.7748/NS2007.05.21.35.51.C4556>
39. X. Sun, Z. Wang, H. Kadouh, K. Zhou. The antimicrobial, mechanical, physical and structural properties of chitosan-gallic acid films. *LWT.*, **2014**, *57*, 83. <https://doi.org/10.1016/j.lwt.2013.11.037>
40. N. A. Mohamed, N. Y. Al-mehbad. Novel terephthaloyl thiourea cross-linked chitosan hydrogels as antibacterial and antifungal agents. *Int. J. Biol. Macromol.*, **2013**, *57*, 111. <https://doi.org/10.1016/j.ijbiomac.2013.03.007>
41. M. Mohseni, A. Shamloo, Z. Aghababaei, H. Afjoul, S. Abdi, H. Moravvej, M. Vossoughi. A comparative study of wound dressings loaded with silver sulfadiazine and silver nanoparticles: In vitro and in vivo evaluation. *Int. J. Pharm.*, **2019**, *564*, 350. <https://doi.org/10.1016/j.ijpharm.2019.04.068>
42. C. M. de Moura, J. M. de Moura, N. M. Soares, L. A. de Almeida Pinto. Evaluation of molar weight and deacetylation degree of chitosan during chitin deacetylation reaction: Used to produce biofilm. *CEP:PI.*, **2011**, *50*, 351. <https://doi.org/10.1016/J.CEP.2011.03.003>
43. A. Muñoz-Bonilla, C. Echeverria, Á. Sonseca, M. P. Arrieta, M. Fernández-García. Bio-based polymers with antimicrobial properties towards sustainable development. *Materials*, **2019**, *12*, 641. <https://doi.org/10.3390/MA12040641>
44. S. K. Nandi, P. Mukherjee, S. Roy, B. Kundu, D. K. De, D. Basu. Local antibiotic delivery systems for the treatment of osteomyelitis - A review. *Mater. Sci. Eng. C.*, **2009**, *29*, 2478. <https://doi.org/10.1016/j.msec.2009.07.014>
45. J. K. Smith, J. D. Bumgardner, H. S. Courtney, M. S. Smeltzer, W. O. Haggard. Antibiotic-loaded chitosan film for infection prevention: A preliminary in vitro characterization. *J. Biomed. Mater. Res. B Appl Biomater.*, **2010**, *94*, 203. <https://doi.org/10.1002/JBM.B.31642>
46. N. Monteiro, M. Martins, A. Martins, Nuno A Fonseca, J. N. Moreira, R. L. Reis, N. M. Neves. Antibacterial activity of chitosan nanofiber meshes with liposomes immobilized releasing gentamicin. *Acta Biomater.*, **2015**, *18*, 196. <https://doi.org/10.1016/J.ACTBIO.2015.02.018>
47. C. H. Wang, C. W. Chang, C. A. Peng. Gold nanorod stabilized by thiolated chitosan as photothermal absorber for cancer cell treatment. *J. Nanopar. Res.*, **2011**, *13*, 2749. <https://doi.org/10.1007/s11051-010-0162-5>
48. W. Shao, H. Liu, J. Wu, S. Wang, X. Liu, M. Huang, P. Xu. Preparation, antibacterial activity and pH-responsive release behavior of silver sulfadiazine loaded bacterial cellulose for wound dressing applications. *J. Taiwan Inst. Chem. Eng.*, **2016**, *63*, 404. <https://doi.org/10.1016/j.jtice.2016.02.019>

49. Y. Cheng, F. Yang, K. Zhang, Y. Zhang, Y. Cao, C. Liu, H. Lu, H. Dong, X. Zhang. Non-Fenton-Type Hydroxyl Radical Generation and Photothermal Effect by Mitochondria-Targeted WSSe/MnO₂ Nanocomposite Loaded with Isoniazid for Synergistic Anticancer Treatment. *Adv. Funct. Mater.*, **2019**, *29*, 1903850. <https://doi.org/10.1002/ADFM.201903850>
50. R. M. Wang, N. P. He, P. F. Song, Y. F. He, L. Ding, Z. Q. Lei. Preparation of nano-chitosan Schiff-base copper complexes and their anticancer activity. *Polym. Adv. Technol.*, **2009**, *20*, 959. <https://doi.org/10.1002/pat.1348>
51. A. Piegat, A. Żywicka, A. Niemczyk, A. Goszczyńska. Antibacterial Activity of N,O-Acylated Chitosan Derivative. *Polymers*, **2021**, *13*, 107. <https://doi.org/10.3390/POLYM13010107>
52. W. M. Pardridge. Drug transport across the blood-brain barrier. *J. Cereb. Blood Flow Metab.*, **2012**, *32*, 1959. <https://doi.org/10.1038/JCBFM.2012.126>
53. L. Wen, Y. Tan, S. Dai, Y. Zhu, T. Meng, X. Yang, Y. Liu, X. Liu, H. Yuan, F. Hu. Vegf-mediated tight junctions pathological fenestration enhances doxorubicin-loaded glycolipid-like nanoparticles traversing bbb for glioblastoma-targeting therapy. *Drug Deliv.*, **2017**, *24*, 1843. <https://doi.org/10.1080/10701754.2017.1386731>
54. N. J. Abbott, A. A. K. Patabendige, D. E. M. Dolman, S. R. Yusof, D. J. Begley. Structure and function of the blood-brain barrier. *Neurobiol. Dis.*, **2010**, *37*, 13. <https://doi.org/10.1016/J.NBD.2009.07.030>
55. R. Daneman, A. Prat. The blood–brain barrier. *Cold Spring Harb. Perspect. Biol.*, **2015**, *7*, a020412. <https://doi.org/10.1101/cshperspect.a020412>
56. S. Wohlfart, S. Gelperina, J. Kreuter. Transport of drugs across the blood-brain barrier by nanoparticles. *J. Controlled Release*, **2012**, *161*, 264. <https://doi.org/10.1016/j.jconrel.2011.08.017>
57. J. Freiherr, M. Hallschmid, W. H. Frey, Y. F. Brünner, C. D. Chapman, C. Hölscher, S. Craft, F. G. De Felice, C. Benedict. Intranasal insulin as a treatment for alzheimer's disease: A review of basic research and clinical evidence. *CNS Drugs*, **2013**, *27*, 505. <https://doi.org/10.1007/S40263-013-0076-8>
58. Y. Chen, S. Feng, W. Liu, Z. Yuan, P. Yin, F. Gao. Vitamin E succinate-grafted-chitosan oligosaccharide/RGD-conjugated TPGS mixed micelles loaded with paclitaxel for U87MG tumor therapy. *Mol Pharm.*, **2017**, *2017*, 1190. <https://doi.org/10.1021/ACS.MOLPHARMACEUT.6B01068>
59. M. D. Shadab, R. A. Khan, G. Mustafa, K. Chuttani, S. Baboota, J. K. Sahni, J. Ali. Bromocriptine loaded chitosan nanoparticles intended for direct nose to brain delivery: Pharmacodynamic, Pharmacokinetic and Scintigraphy study in mice model. *Eur. J. Pharm. Sci.*, **2013**, *48*, 393. <https://doi.org/10.1016/J.EJPS.2012.12.007>
60. Z. Zhao, S. Lou, Y. Hu, J. Zhu, C. Zhang. A Nano-in-Nano Polymer-Dendrimer Nanoparticle-Based Nanosystem for Controlled Multidrug Delivery. *Mol. Pharm.*, **2017**, *14*, 2697. <https://doi.org/10.1021/ACS.MOLPHARMACEUT.7B00219>
61. L. Gao, X. Wang, J. Ma, D. Hao, P. Wei, L. Zhou, G. Liu. Evaluation of TPGS-modified thermo-sensitive Pluronic PF127 hydrogel as a potential carrier to reverse the resistance of P-gp-overexpressing SMMC-7721 cell lines. *Colloids Surf B Biointerfaces*, **2016**, *140*, 307. <https://doi.org/10.1016/j.colsurfb.2015.12.057>
62. J. Rip, L. Chen, R. Hartman, A. van den Heuvel, A. Reijerkerk, J. van Kregten, B. van der Boom, C. Appeldoorn, M. de Boer, D. Maussang, E. C. M. de Lange, P. J. Gaillard. Glutathione PEGylated liposomes: Pharmacokinetics and delivery of cargo across the blood-brain barrier in rats. *J. Drug Target.*, **2014**, *22*, 460. <https://doi.org/10.3109/1061186X.2014.888070>
63. M. Salvalaio, L. Rigon, D. Belletti, F. D'Avanzo, F. Pederzoli, B. Ruozi, O. Marin, M. A. Vandelli, F. Forni, M. Scarpa, R. Tomanin, G. Tosi. Targeted polymeric nanoparticles for brain delivery of high molecular weight molecules in lysosomal storage disorders. *PLoS One*, **2016**, *11*, e0156452. <https://doi.org/10.1371/JOURNAL.PONE.0156452>
64. A. Dalpiaz, G. Paganetto, B. Pavan, M. Fogagnolo, A. Medici, S. Beggiato, D. Perrone. Zidovudine and ursodeoxycholic acid conjugation: Design of a new prodrug potentially able to bypass the active efflux transport systems of the central nervous system. *Mol Pharm.*, **2012**, *9*, 957. <https://doi.org/10.1021/MP200565G>
65. I. N. Khan, S. Navaid, W. Waqar, D. Hussein, N. Ullah, M. U. A. Khan, Z. Hussain, A. Javed. Chitosan-Based Polymeric Nanoparticles as an Efficient Gene Delivery System to Cross Blood Brain Barrier: In Vitro and In Vivo Evaluations. *Pharmaceuticals*, **2024**, *17*, 169. <https://doi.org/10.3390/PH17020169>
66. T. Banerjee, S. Mitra, A. K. Singh, R. K. Sharma, A. Maitra. Preparation, characterization and biodistribution of ultrafine chitosan nanoparticles. *Int. J. Pharm.*, **2002**, *243*, 93. [https://doi.org/10.1016/S0378-5173\(02\)00267-3](https://doi.org/10.1016/S0378-5173(02)00267-3)
67. J. Li, K. Kataoka. Chemo-physical Strategies to Advance the in Vivo Functionality of Targeted Nanomedicine: The Next Generation. *J. Am. Chem. Soc.*, **2021**, *143*, 538. <https://doi.org/10.1021/JACS.0C09029>
68. D. Carradori, C. Balducci, F. Re, D. Brambilla, B. L. Droumaguet, O. Flores, A. Gaudin, S. Mura, G. Forloni, L. O. -Gutierrez, F. Wandosell, M. Masserini, P. Couvreur, J. Nicolas, K. Andrieux. Antibody-functionalized polymer nanoparticle leading to memory recovery in Alzheimer's disease-like transgenic mouse model. *Nanomedicine*, **2018**, *14*, 609. <https://doi.org/10.1016/J.NANO.2017.12.006>
69. A. E. Caprificio, P. J. S. Foot, E. Polycarpou, G. Calabrese. Overcoming the blood-brain barrier: Functionalised chitosan nanocarriers. *Pharmaceutics*, **2020**, *12*, 1013. <https://doi.org/10.3390/PHARMACEUTICS1211013>
70. S. Debaisieux, F. Rayne, H. Yezid, B. Beaumelle. The Ins and Outs of HIV-1 Tat. *Traffic*, **2012**, *13*, 355. <https://doi.org/10.1111/J.1600-0854.2011.01286.X>
71. A. Dev, N. S. Binulal, A. Anitha, S. V. Nair, T. Furuike, H. Tamura, R. Jayakumar. Preparation of poly(lactic acid)/chitosan nanoparticles for anti-HIV drug delivery applications. *Carbohydr. Polym.*, **2010**, *80*, 833. <https://doi.org/10.1016/J.CARBPOL.2009.12.040>
72. J. S. Park, Y. W. Cho. In vitro cellular uptake and cytotoxicity of paclitaxel-loaded glycol chitosan self-assembled nanoparticles. *Macromol. Res.*, **2007**, *15*, 513. <https://doi.org/10.1007/BF03218824>
73. L. N. Ramana, S. Sharma, S. Sethuraman, U. Ranga, U. M. Krishnan. Investigation on the stability of saquinavir loaded liposomes: Implication on stealth, release characteristics and cytotoxicity. *Int. J. Pharm.*, **2012**, *431*, 120. <https://doi.org/10.1016/j.ijpharm.2012.04.054>
74. H. Y. Nam, S. M. Kwon, H. Chung, S. -Y. Lee, S. -H. Kwon, H. Jeon, Y. Kim, J. H. Park, J. Kim, S. Her, Y. -K. Oh, I. C. Kwon, K. Kim, S. Y. Jeong. Cellular uptake mechanism and intracellular fate of hydrophobically modified glycol chitosan nanoparticles. *J. Control. Release*, **2009**, *135*, 259. <https://doi.org/10.1016/j.jconrel.2009.01.018>
75. S. D. Gioia, A. Trapani, D. Mandracchia, E. D. Giglio, S. Cometa, V. Mangini, F. Arnesano, G. Belgiovine, S. Castellani, L. Pace, M. A. Lavecchia, G. Trapani, M. Conese, G. Puglisi, T. Cassano. Intranasal delivery of dopamine to the striatum using glycol chitosan/sulfobutylether- β -cyclodextrin based nanoparticles. *Eur. J. Pharm. Biopharm.*, **2015**, *94*, 180. <https://doi.org/10.1016/j.ejpb.2015.05.019>
76. R. Rozana, Y. Yulizar, A. Saefumillah, D. O. B. Apriandanu. Synthesis, characterization and in vitro release study of efavirenz-loaded chitosan nanoparticle. *AIP Conf. Proc.*, **2020**, *2242*, 040004. <https://doi.org/10.1063/5.0007923>
77. K. Chaturvedi, K. Ganguly, M. N. Nadagouda, T. M. Aminabhavi. Polymeric hydrogels for oral insulin delivery. *J. Control. Release*, **2013**, *165*, 129. <https://doi.org/10.1016/j.jconrel.2012.11.005>
78. B. Singh, B. Garg, S. C. Chaturvedi, S. Arora, R. Mandsaurwale, R. Kapil, B. Singh. Formulation development of gastroretentive tablets of lamivudine using the floating-bioadhesive potential of optimized polymer blends. *J. Pharm. Pharmacol.*, **2012**, *64*, 654. <https://doi.org/10.1111/J.2042-7158.2011.01442.X>
79. D. A. Cobb, N. Smith, S. Deodhar, A. N. Bade, N. Gautam, B. L. D. Shetty, J. McMillan, Y. Alnouti, S. M. Cohen, H. E. Gendelman, B. Edagwa. Transformation of tenofovir into stable ProTide nanocrystals with long-acting pharmacokinetic profiles. *Nat. Commun.*, **2021**, *12*, 5458. <https://doi.org/10.1038/S41467-021-25690-5>
80. S. A. Agnihotri, N. N. Mallikarjuna, T. M. Aminabhavi. Recent advances on chitosan-based micro- and nanoparticles in drug delivery. *J. Control. Release*, **2004**, *100*, 5. <https://doi.org/10.1016/j.jconrel.2004.08.010>
81. S. Sharma, A. Tyagi, S. Dang. Nose to Brain Delivery of Transferrin conjugated PLGA nanoparticles for clonidine. *Int. J. Biol. Macromol.*, **2023**, *252*, 126471. <https://doi.org/10.1016/j.ijbiomac.2023.126471>
82. L. N. Ramana, S. Sharma, S. Sethuraman, U. Ranga, U. M. Krishnan. Evaluation of chitosan nanoformulations as potent anti-HIV therapeutic systems. *Biochim. Biophys. Acta.*, **2014**, *1840*, 476. <https://doi.org/10.1016/J.BBAGEN.2013.10.002>
83. D. Soundararajan, L. N. Ramana, P. Shankaran, U. M. Krishnan. Nanoparticle-based strategies to target HIV-infected cells. *Colloids Surf B Biointerfaces.*, **2022**, *213*, 112405. <https://doi.org/10.1016/j.colsurfb.2022.112405>
84. F. Karadeniz, S. K. Kim. Chapter three - antidiabetic activities of chitosan and its derivatives: a mini review. *Adv. Food Nutr. Res.*, **2014**, *73*, 33. <https://doi.org/10.1016/B978-0-12-800268-1.00003-2>
85. (a) N. Jaber, M. Al-Remawi, F. Al-Akayleh, N. Al-Muhtaseb, I. S. I. Al-Adham, P. J. Collier. A review of the antiviral activity of Chitosan

- including patented applications and its potential use against COVID-19. *J. Appl. Microbiol.* **2022**, 132, 41. <https://doi.org/10.1111/jam.15202>
86. (b) N. Hsan, S. Kumar, J. Koh, and P. K. Dutta. Chitosan modified multi-walled carbon nanotubes and arginine aerogel for enhanced carbon capture. *Int. J. Biol. Macromol.*, **2023**, 252, 126523. <https://doi.org/10.1016/j.ijbiomac.2023.126523>
 87. P. Heydari, M. Kharaziha, J. Varshosaz, A. Z. Kharazi, S. H. Javanmard. Co-release of nitric oxide and L-arginine from poly (β -amino ester)-based adhesive reprogram macrophages for accelerated wound healing and angiogenesis in vitro and in vivo. *Biomater. Adv.*, **2024**, 158, 213762. <https://doi.org/10.1016/j.bioadv.2024.213762>
 88. Y. Zhang, X. Shen, P. Ma, Z. Peng, K. Cai. Composite coatings of Mg-MOF74 and Sr-substituted hydroxyapatite on titanium substrates for local antibacterial, anti-osteosarcoma and pro-osteogenesis applications. *Mater. Lett.*, **2019**, 241, 18. <https://doi.org/10.1016/j.matlet.2019.01.033>
 89. C. Makarov, V. Cohen, A. Raz-Pasteur, I. Gotman. In vitro elution of vancomycin from biodegradable osteoconductive calcium phosphate-polycaprolactone composite beads for treatment of osteomyelitis. *Eur. J. Pharm. Sci.*, **2014**, 62, 49. <https://doi.org/10.1016/j.ejps.2014.05.008>
 90. N. H. Radwan, M. Nasr, R. A. H. Ishak, N. F. Abdeltawab, G. A. S. Awad. Chitosan-calcium phosphate composite scaffolds for control of post-operative osteomyelitis: Fabrication, characterization, and in vitro-in vivo evaluation. *Carbohydr. Polym.* **2020**, 244, 116482. <https://doi.org/10.1016/j.carbpol.2020.116482>
 91. R. A. A. Muzzarelli. Chitosan composites with inorganics, morphogenetic proteins and stem cells, for bone regeneration. *Carbohydr. Polym.*, **2011**, 83, 1433. <https://doi.org/10.1016/j.carbpol.2010.10.044>
 92. R. A. A. Muzzarelli. Genipin-crosslinked chitosan hydrogels as biomedical and pharmaceutical aids. *Carbohydr. Polym.*, **2009**, 77, 1. <https://doi.org/10.1016/j.carbpol.2009.01.016>
 93. K. E. Beenken, J. K. Smith, R. A. Skinner, S. G. McLaren, W. Bellamy, M. J. Gruenwald, H. J. Spencer, J. A. Jennings, W. O. Haggard, M. S. Smeltzer. Chitosan coating to enhance the therapeutic efficacy of calcium sulfate-based antibiotic therapy in the treatment of chronic osteomyelitis. *J. Biomater. Appl.*, **2014**, 29, 514. <https://doi.org/10.1177/0885328214535452>
 94. V. Uskoković, C. Hoover, M. Vukomanović, D. P. Uskoković, T. A. Desai. Osteogenic and antimicrobial nanoparticulate calcium phosphate and poly-(d,l-lactide-co-glycolide) powders for the treatment of osteomyelitis. *Mater. Sci. Eng. C.*, **2013**, 33, 3362. <https://doi.org/10.1016/j.msec.2013.04.023>
 95. V. Pawar, R. Srivastava. Chitosan-polycaprolactone blend sponges for management of chronic osteomyelitis: A preliminary characterization and in vitro evaluation. *Int. J. Pharm.*, **2019**, 568, 118553. <https://doi.org/10.1016/j.ijpharm.2019.118553>
 96. V. Uskoković, T. A. Desai. In vitro analysis of nanoparticulate hydroxyapatite/chitosan composites as potential drug delivery platforms for the sustained release of antibiotics in the treatment of osteomyelitis. *J. Pharm. Sci.*, **2014**, 103, 567. <https://doi.org/10.1002/jps.23824>
 97. N. H. Radwan, M. Nasr, R. A. H. Ishak, N. F. Abdeltawab, G. A. S. Awad. Chitosan-calcium phosphate composite scaffolds for control of post-operative osteomyelitis: Fabrication, characterization, and in vitro-in vivo evaluation. *Carbohydr. Polym.*, **2020**, 244, 116482. <https://doi.org/10.1016/j.carbpol.2020.116482>
 98. E. Cevher, Z. Orhan, L. Mülazimoğlu, D. Sensoy, M. Alper, A. Yildiz, Y. Ozsoy. Characterization of biodegradable chitosan microspheres containing vancomycin and treatment of experimental osteomyelitis caused by methicillin-resistant *Staphylococcus aureus* with prepared microspheres. *Int. J. Pharm.*, **2006**, 317, 127. <https://doi.org/10.1016/j.ijpharm.2006.03.014>
 99. P. Shi, Y. Zuo, X. Li, Q. Zou, H. Liu, L. Zhang, Y. Li, Y. S. Morsi. Gentamicin-impregnated chitosan/nanohydroxyapatite/ethyl cellulose microspheres granules for chronic osteomyelitis therapy. *J. Biomed. Mater. Res. A.*, **2010**, 93A, 1020. <https://doi.org/10.1002/JBM.A.32598>
 100. V. Pawar, R. Srivastava. Layered assembly of chitosan nanoparticles and alginate gel for management of post-surgical pain and infection. *16th International Conference on Nanotechnology - IEEE NANO.*, **2016**, 241. <https://doi.org/10.1109/NANO.2016.7751388>
 101. D. Słota, J. Jampilek, A. Sobczak-Kupiec. Targeted Clindamycin Delivery Systems: Promising Options for Preventing and Treating Bacterial Infections Using Biomaterials. *Int. J. Mol. Sci.*, **2024**, 25, 4386. <https://doi.org/10.3390/ijms25084386>
 102. R. A. Hashad, R. A. H. Ishak, A. S. Geneidi, S. Mansour. Surface functionalization of methotrexate-loaded chitosan nanoparticles with hyaluronic acid/human serum albumin: Comparative characterization and in vitro cytotoxicity. *Int. J. Pharm.*, **2017**, 522, 128. <https://doi.org/10.1016/j.ijpharm.2017.03.008>

RESEARCH ARTICLE

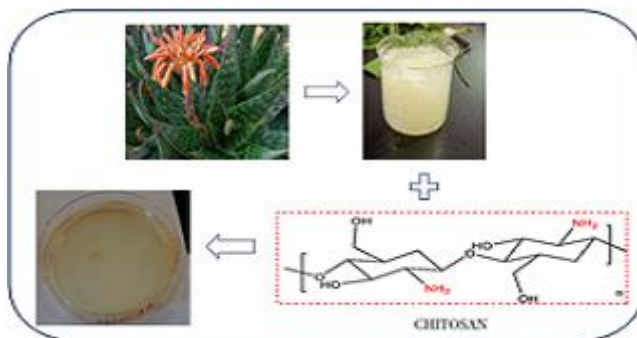
Preparation and Characterization of Aloe Maculata/Chitosan Composite Gel for Wound Healing Application

Hilda Ngomane, Lungiselwa Ndzabandzaba, and Vuyiswa Jane Mkhabela* 

Department of Pharmacy, Faculty of Health Sciences, Eswatini Medical Christian University, Lomkiri Portion 69 of Farm 73, Zone 4 Mbabane, Eswatini

*Correspondence: vuyiswa.mkhabela@emcu.ac.sz; vjmkhabela@gmail.com

Abstract: Aloe has been traditionally applied for its therapeutic and medical properties over thousands of years. The medicinal properties of aloe include being used as an anti-inflammatory, antimicrobial, antibacterial, analgesics, anti-allergic as well as antioxidant. In Eswatini, Aloe maculata has been traditionally used for treating various ailments, suggesting potential antimicrobial properties. In this study, the species of aloe was screened for phytochemicals and a composite hydrogel was prepared with varying concentrations of aloe (10%, 20% and 30% w/v) and the natural polymer chitosan. The composite gel's solubility, water absorption capacity, and antibacterial activity was studied for a potential application in wound healing. The incorporation of different amounts of Aloe maculata gel solution into chitosan was observed to increase the water absorption capacity, solubility, and antibacterial activity. The composite gel with a 20% concentration of aloe seemed to possess better overall properties beneficial for an application in wound healing.



Keywords: Aloe maculata, phytochemicals, chitosan, antibacterial, wound healing

Introduction

With the persistent evolution of global health sector, the care for wounds is still a great concern since no genuine home or a clinical concentration is of existence.¹ According to Queen and Harding (2023:1), the cost of managing wounds in different healthcare systems around the world is high, and estimated to be the following, (in international billions of dollars); United States (126.846), China (26.9452), United Kingdom (10.1114), South Korea (4.7033), Australia (5.140), Egypt (0.5720), Ethiopia (0.1151), South Africa (1.1630), Lesotho, (0.0099), Mozambique (0.0475) and Eswatini (0.0110).²

Most Africans remain destitute because their healthcare services are paid out of pocket. In most African countries, the dressing of wound daily demands a financial requirement beyond the capability of the African families.³ Wounds are an ignored liability and wound management is an overwhelming decision. The treatment options are very diverse; hence, the choice of treatment option is rather a daunting decision than a relief, requiring proper guidance.⁴

Composite gels, also known as hybrid gels or multifunctional gels, are well described as a form of gel material that combines multiple components to achieve enhanced properties and functionalities.⁵ These gels are formed by incorporating different types of materials into a gel matrix, resulting in a synergistic combination of their individual properties. Composite gels incorporate a gel matrix (composed of polymeric network), which maintain the structural integrity and defines the overall properties of the material, enhancing the biological functionality. It also contains components such as nanoparticles, polymers, fibers, or biological molecules, into the gel matrix. These components can be either uniformly dispersed or localized within specific regions of the gel.

Traditionally, Swazis (Eswatini citizens) have utilized various indigenous plants for medicinal purposes, including Aloe maculata. Studies suggest that A. maculata found in Eswatini

possesses a diverse phytochemical profile, potentially contributing to its observed traditional uses.⁶ However, limited scientific research has been performed for its specific antimicrobial potential within the Swazi context. While data specific to Mbabane is scarce, studies within Eswatini suggest diverse environmental factors might influence plant secondary metabolite profiles.

Chitosan, a widely studied natural polymer, is crucial in environmental and biomedical fields due to its cationic properties.⁷ Despite some drawbacks, enhancing its functionality through appropriate modifications is essential for improving its efficiency. Understanding the chemistry behind altering chitosan's surface traits is vital. The polymer is applied in wound healing due to its antibacterial, anti-inflammatory and antifungal property which reduces infection and promotes fast healing. Chitosan promotes cell adhesion, proliferation and differentiation hence used in tissue engineering.⁸ These characteristics make it an ideal candidate for scaffolding materials in regenerative medicine.

The objective of this study was to prepare a composite gel composed of chitosan and Aloe maculata, anticipated to possess physicochemical characteristics and antibacterial properties that are ideal for an application in wound healing.

Material and Methods

Chemicals and Media: The chemicals and all reagents used in this study were purchased from Merck (Pty) Ltd., Johannesburg, South Africa. The Eswatini Medical Christian University, Medical Laboratory Sciences department provided distilled water for the experiments. The bacterial strains used for the study were Staphylococcus aureus (Gram-positive) and Escherichia coli (Gram-negative).⁹

Plant Sampling and Extraction of Phytochemicals: The Aloe maculata plant was identified and authenticated to ensure accurate species identification at the Malkerns Research Station in Eswatini. Fresh leaves of aloe were collected and thoroughly washed with running tap water to remove any soil or dirt. The thick outer layer of the leaves was removed with a scalpel, and the inner leaf pulp (gel) was

cut into small cubes, then centrifuged at 5,000 RPM for 15 minutes. The supernatant was discarded, and the resulting clear gel was collected and half of it homogenized with 100 ml of 70% ethanol, agitated for 5 minutes, and stored in a refrigerator for further analysis.⁹ The *A. maculata* gel extracted from leaves of the plant is shown in Figure 1. Phytochemical screening tests were conducted as shown in Table 1.



Figure 1. The extraction of gel pulp from fresh leaves of *A. maculata*

Preparation of Aloe Maculata/Chitosan Composite: An acetic acid solution was prepared and used to dissolve chitosan. When chitosan was completely dissolved, composite gels were prepared with concentrations of 0%, 10%, 20%, and 30% (w/v) *Aloe maculata* extract. The different composite gel mixtures were dried on petri dishes to form discs.¹⁰

Characterization of Composite Gel: The prepared composite gel was characterized for its water absorption capacity (% fluid absorptivity), solubility (% gel fraction), and antimicrobial activity.

Water absorption capacity (% fluid absorptivity): The composite gels with different aloe extract concentrations were measured by swelling the gels in distilled water at room temperature.¹¹ Each sample from the aloe loaded composite gels was cut into small cubes of 4 cm², weighed and the mass recorded as M1. The samples were then placed in water and immersed for periods of 5, 10, 20, 30, 40, 50, 60 and 90 minutes. After each period the samples were dried weighed again. This weight recorded as M2. The water absorption capacity was calculated from the following equation:

$$W (\%) = ((M2 - M1)) / M1 \times 100$$

Solubility (% gel fraction): For the solubility test, four samples were prepared with each composite gel concentration (0%, 10%, 20%, and 30%). Each sample was weighed (M1) and submerged in a beaker containing water. After immersing for 24 hours, each composite gel was removed from the beaker and dried to a constant weight at 60 degrees Celsius in a Dry oven DHG-9030A. The dried samples were then weighed (M2).¹⁰ The percent gel fraction was calculated using the following equation;

$$\text{Solubility (\% gel fraction)} = ((M1 - M2) / M1) \times 100$$

Evaluation of antibacterial activity: To evaluate antimicrobial activity, all instruments used were sterilized before use. Two strains of bacteria namely, *E. coli* (Gram negative) and *S. aureus* (Gram positive) were selected for the antibacterial activity study. The bacterial strains were cultured on Mueller Hinton (MH) agar medium. 2 ml of solution containing bacteria (concentrated according to McFarland standard), was inoculated onto petri dishes containing MH agar. Small sized discs of the prepared *A. maculata*/chitosan composite gels were placed into agar wells made on the agar plates. The agar plates were then incubated for 24 hours at 37 degrees Celsius. After 24 hours, the zones of inhibition on the agar plates were measured.¹²

Table 1. Phytochemical analysis of *Aloe maculata* gel extract.

Name of Phytochemical	Test Procedure	Results
Alkaloids	Wagner's test: 3 ml of the extract was mixed with 2 drops of Wagner's reagent in a test tube.	-
Flavonoids	Alkaline Reagent Test: To 1 ml of the plant extract, 2 ml of sodium hydroxide and 2 drops of diluted hydrochloric acid were added.	++
Terpenoids	2ml chloroform was added to 5ml aloe extract and 3ml concentrated acid was carefully added. Reaction mixture was boiled for 5 minutes.	+
Saponins	Foam Test: 2 ml of the extract was mixed with 2 ml distilled water and shaken vigorously.	+
Tannins	10% Sodium hydroxide test: 4 ml of 10% sodium hydroxide was mixed with 8 drops of extract and shaken well.	+
Anthraquinones	Bornträger's Test: 10 ml of benzene was mixed with the plant sample and soaked for ten minutes, followed by filtration. 10 ml of 10% ammonia was then mixed in.	+
Phenolic compounds	Ferric chloride test: : 3 drops of 5% ferric chloride solution were mixed with the aloe extract.	++
Protein	2% copper sulfate solution, 1 ml of 95% ethanol, and potassium hydroxide were mixed with 2 ml of plant.	+
Glycosides	Bornträger's Test: 5ml of the sample extract was boiled with 45% ethanol, cooled, and filtered. This was then mixed with chloroform and shaken vigorously. After shaking, ammonium solution was added.	+

Results and Discussion

The *Aloe maculata*/chitosan composite gel showed barrier properties and antibacterial activity which are ideal for wound healing. Phytochemical screening of the *Aloe maculata* leaves revealed the presence of flavonoids, terpenoids, saponins, tannins, anthraquinones, phenolic compounds and proteins. Commonly present in medicinal plants, these secondary metabolites are known to have a number of pharmacological characteristics, such as immune-modulating, antibacterial, anti-inflammatory, and antioxidant effects.

Phytochemical Screening of Aloe Maculata

The tests employed for phytochemical analysis and the results obtained from the aloe gel are shown in Table 1. Positive results for flavonoids, terpenoids, saponins, tannins, anthraquinones, phenolic compounds and proteins, were obtained. The positive results of these chemicals constituents in the aloe plant extract suggests it may have therapeutic potential that could be further explored. A study done by Sonam and Tiwari (2016) revealed the presence of these phytochemicals.^{13,14}

Negative results were obtained for glycosides. The absence of detectable levels of alkaloids in the extract does not necessarily mean they are completely absent. It could be that the concentrations were below the detection limit of the screening methods used. Alternatively, these phytochemicals may not be the major active constituents in this particular aloe plant sample.

Characterization of *Aloe Maculata*/Chitosan Composite Gel

During the preparation of the composite gel, when chitosan was dissolved in acetic acid, it solidified to form a gel like substance as shown in Figure 2. The addition of the aloe gel solution to the chitosan resulted in small white spots on the gel which increased as the concentration of the aloe increased. After drying, it was simple to gather the composite gels because they didn't break, tear, or lose weight. The drying process of the gels was affected by the water content of the aloe which affected the viscosity of the composite gel. The more the *A. maculata* concentration the less viscous the composite gel was.

The physical characteristics of the composite gel were of an essential aspect due to the anticipated application of the gel to be used in a moist environment. A composite gel in wound healing acts as an absorbent of water and carrier of drugs to protect the applied area from moisture and microorganisms.¹⁵

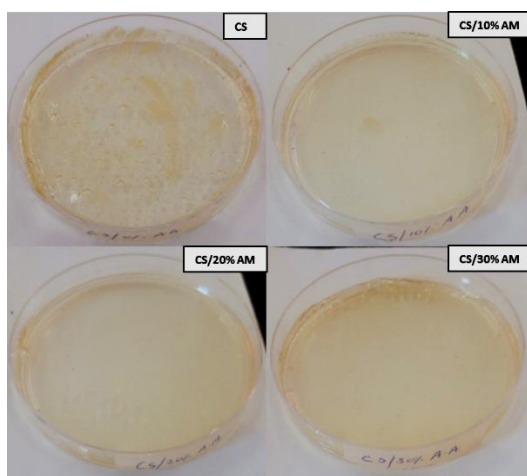


Figure 2: Composite gels of chitosan with different concentrations of *A. maculata*.

The water absorption capacity (% fluid absorptivity) was performed in order to assess the potential of the composite gel to absorb wound exudates, which is an important consideration for gauze and dressing materials in wound care.¹⁶ The results are shown in Figure 3. The sample with chitosan only (0% AM), proved to possess the least ability to absorb water, since at 5 minutes of exposure to water, the water absorption capacity was calculated to be 100 whilst the samples containing *Aloe maculata* (AM) proved to absorb water up to several thousands. This showed a remarkable capacity to absorb water which shows great potential to relieve a wound from exudate, prevent pooling and promote a cleaner wound bed.

On prolonged exposure to water, the CS sample absorptivity increased up to a few thousand after 90 minutes. This observation did not surpass the sample containing 10% AM which significantly increased up to 13800 capacity of absorbing water, when it only began at 4650. This evidently shows that, with 10% AM added to chitosan has a potential in inhibiting infections in wounds as large amounts of fluid would be expelled from them. These results suggest the potential use of AM in the composite gels for the management of exudative wounds.

Studies conducted by Trang et al. and Devi M et al,¹⁰ showed different results on the water absorption capacity of their composite gels prepared from *Aloe vera* and chitosan. Their samples with no aloe vera resulted in higher water absorption capacity compared to those samples with the aloe in it. The results obtained in this study are different from other researchers results because of the different method used

when preparing the samples and that they used *Aloe vera* as their incorporated ingredient. When preparing the samples Trang et. al. included glycerol and Devi et. al. included polyethylene oxide. Trang chose that method, because he was doing a preservation study of fresh fruits which required the addition of glycerol due to its humectant properties and Devi M was doing a comparative study of different plants in wound healing.

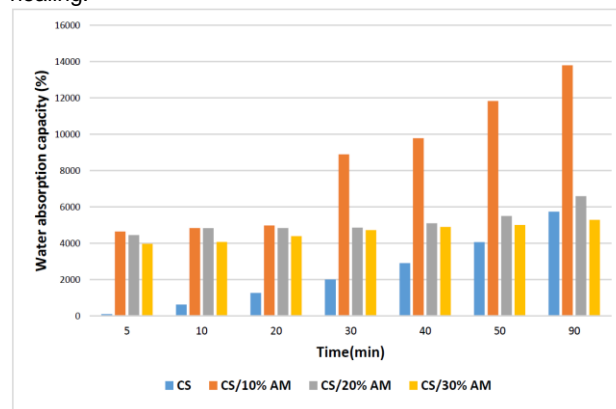


Figure 3: Water absorption capacity of the different composite gels

The solubility of the samples was carried out through the immersion of the different composite gels in 100 ml of distilled water for 24 hours. The samples were weighed before and after drying the samples to a constant weight. According to the collected data on Table 2, the mass of the samples was seen to decrease from mass 1 to mass 2. The decrease in mass indicated that the samples were soluble in the water. Generally, the quality of the composite gel increases with its solubility.¹⁰ Generally, the higher the solubility of the composite gel the higher the quality of the composite gel. This is a good characteristic for application in medical situations, as good water solubility tends to release the loaded drug quickly.¹⁷ The % solubility of the composite gels is presented on Figure 4 below.

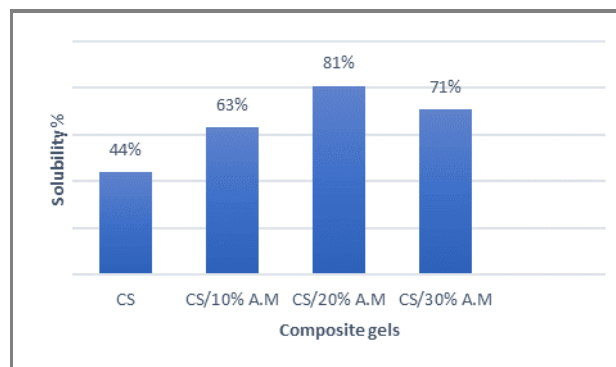


Figure 4: Percent solubility of the different composite gels.

Table 2: The mass of composite gel samples before and after 24 hours of immersion in water.

Name of composite	Mass 1 (g)	Mass 2 (g)
Chitosan	0.710±0.68	0.400±0.88
CS/10% AM	0.290±0.97	0.106±0.90
CS/20% AM	0.440±0.77	0.083±0.89
CS/30% AM	0.350±1.01	0.096±0.99

Antibacterial activity of the prepared composite gels was investigated by conducting Microbial Susceptibility Testing

(MST) on *E. coli* and *S. aureus*.¹⁸ The zone of inhibition of each sample on MH agar plates with the two different bacterial strains was measured. The results presented in Table 3 showed that antibacterial activity increased when AM was added to chitosan compared to the sample without AM. This is apparent on the inhibition zones of *S. aureus* as CS proved to inhibit 2mm diameter zone and on the CS/10 % AM sample the inhibition zone increased to 6mm and kept on increasing up to 11 mm as the AM concentration was increased. Results for *E. coli* inhibition zones show that for the chitosan only sample, an 8 mm diameter zone resulted and as the aloe concentrations were increased so did the inhibition zones. A standard antibiotic, G-penicillin was used as a positive control.

Table 3. The zone of inhibition in diameter of the different composite gels on *E. coli* and *S. aureus*.

Name of sample	<i>E.coli</i> (mm)	<i>S. aureus</i> (mm)
A. maculata	11±0.38	9±0.42
Chitosan	8±0.45	2±0.50
CS/10% AM	4±0.28	6±0.31
CS/20% AM	14±0.11	10±0.22
CS/30% AM	16±1.01	11±0.97
Control	17±0.01	18±0.03

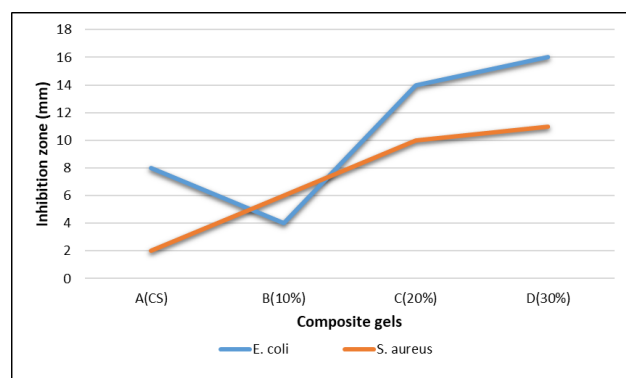


Figure 5: Microbial susceptibility test of the different composite gels on *E. coli* and *S. aureus* after 24 hours.

Generally, the antibacterial activity of the composite gels was higher as the *A. maculata* content was increased and a higher susceptibility was observed for *E. coli* as compared to *S. aureus*. Figure 5 shows a summary of the microbial susceptibility tests on the two bacterial strains. Similar observations were observed in studies by Trang *et al.*, Iqbal *et al.*, and Monzon-Ortega *et al.* who studied the antibacterial activity of chitosan/aloe vera biofilms.^{10,15,19} In this study, *E. coli* was found to be more susceptible to *A. maculata* compared to *S. aureus* which reached up to 16 mm diameter. The antibacterial activity of aloe species is likely attributed to the phytochemicals identified in the screening, such as flavonoids, terpenoids, tannins, and anthraquinones, which are known to have antibacterial properties. Gram-negative bacteria have lipids in their cell walls, while Gram-positive bacteria have a lot of peptides.²⁰ The negatively charged microbial cell membranes can interact with the positively charged chitosan molecules, rupturing their integrity and releasing intracellular components of the bacteria.²¹ This method significantly inhibits the development and proliferation of bacteria and demonstrates substantial bactericidal and bacteriostatic capabilities. This could be the cause of the composite gel's superior inhibitory action against *E. coli* as opposed to *S. aureus*.

Conclusion

Several phytochemicals with pharmacological and antibacterial qualities were found in the whole leaf extract of *A. maculata*. The composite gels from chitosan supplemented with *A. maculata* with varying contents showed the ability to be effective in biological processes. The study emphasized the construction of a composite gel that has a potential to significantly speed the wound healing process and inhibit bacterial growth. The incorporation of chitosan polymer was to ensure the adhesive potential and enhance the mechanical properties of the composite which are required for the intended application in wound healing. Further studies are required to determine the beneficial effects of the composite gel on the healing of wounds. This will be achieved through fibroblast cell culture studies and the use of animal models. Also further characterization to determine mechanical strength and surface morphology of the composite gel would provide a conclusion of the synergy between the aloe and chitosan in the gel matrix.

Author Contribution Declaration

All authors conceived the research plan and experimental strategy. L. Ndzabandzaba performed the phytochemical screening of the aloe extract, analysed and prepared part of the manuscript. H. Ngomane prepared and characterized the composite gel, and prepared draft manuscript. V. J. Mkhabela confirmed the manuscript preparation and assisted in daily laboratory supervision, designed the research, analyzed the results, and wrote manuscript. The authors have no financial conflicts of interest to disclose.

Data Availability Declaration

The data generated and analyzed is included in this article.

Acknowledgements

This work was carried out with the aid of a grant from UNESCO Organization for Women in Science for the Developing World (OWSD) and the International Development Research Centre, Canada. (Award Agreement Number: 4500501109). The views expressed herein do not necessarily represent those of UNESCO-TWAS, OWSD, IDRC or its Board of Governors.

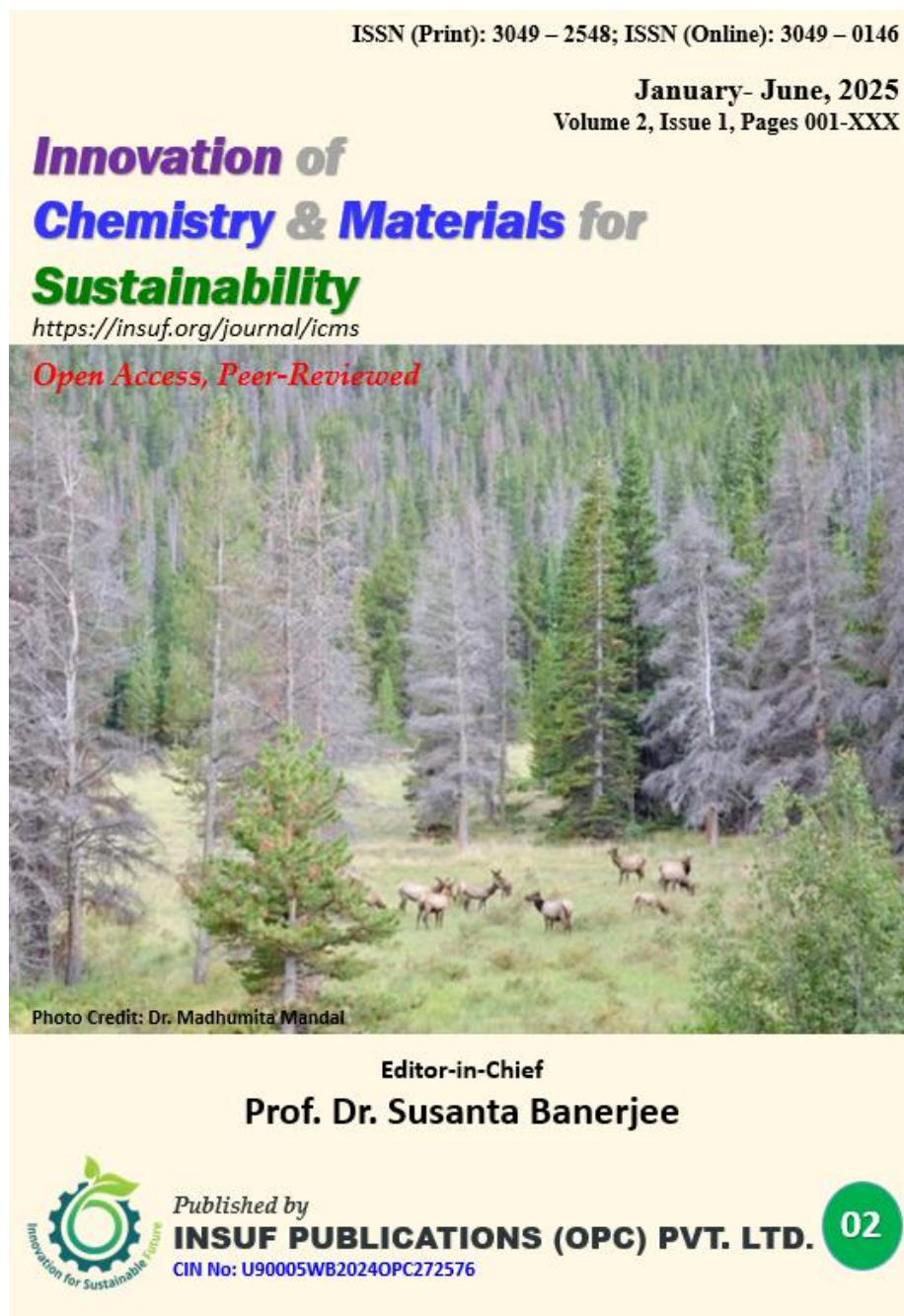
We acknowledge Sibusisiwe Lukhele and Makewell Dlamini, our Pharmacy laboratory technicians who spent long hours and assisted on the availability of apparatus and chemicals in the Pharmacy laboratories. And acknowledge assistance from Sizolwethu Gamedze, Brett Ngubeni and Fezile Ceko, Medical Laboratory Science students who assisted with the antimicrobial activity studies.

References

- Q. Guo, Z. Shi, H. Xu, X. Ma, J. Yin, M. Tian. Fabrication of Super Extensible and Highly Tough Graphene Composite Hydrogels by Thermal Treatment Strategy for the Mixture of Tannin and Graphene Oxide. *Macromol. Chem. Phys.*, **2017**, *218*, 1600549. <https://doi.org/10.1002/macp.201600549>
- D. Queen, K. Harding. Whats the cost of wounds faced by different healthcare systems around the world? *Int. Wound J.* **2023**, *20*, 3935. <https://doi.org/10.1111/iwj.14491>
- K. D. Ogundejì, P. R. Risenga, G. Thupayagale-Tshwenegae. Economic burden of inpatient wound dressing in Nigeria: implication for catastrophic household expenditure. (2022) PREPRINT (Version 1) available at Research Square. <https://doi.org/10.21203/rs.3.rs-1202484/v1>
- C. C. Dobler, N. Harb, C. A. Maguire, C. L. Armour, C. Coleman, M. H. Murad. Treatment burden should be

- included in clinical practice guidelines. *BMJ* **2018**, 363, k4065. <https://doi.org/10.1136/bmj.k4065>
5. C. Bergonzi, G. Gomez d'Ayaba, L. Elviri, P. Laurienzo, A. Bandiera, O. Catanzono. Alginate/Human Elastin like Polypeptide Composite Films with Antioxidant Properties for Potential Wound Healing Application. *Int. J. Biol. Macromol.* **2020**, 164, 586. <https://doi.org/10.1016/j.ijbiomac.2020.07.084>
6. V. V. Dlamini, T. Viljoen. Investigating knowledge on indigenous green leafy vegetable amongst rural women in Eswatini. *J. Consum. Sci. (Special Edition)* **2020**, 5, 52.
7. V. K. Thakur, M. K. Thakur. Recent Advances In Graft Copolymerization and Applications of Chitosan: A Review. *ACS Sustainable Chem. Eng.*, **2014**, 2, 2637. <https://doi.org/10.1021/sc500634p>
8. F. Asghari Sana, M. Çapkin Yurtsever, G. Kaynak Bayrak, E. Ö. Tunçay, A. S. Kiremitçi, M. Gümüşderelioğlu. Spreading, proliferation and differentiation of human dental pulp stem cells on chitosan scaffolds immobilized with RGD or fibronectin. *Cytotechnology*. **2017** 69, 617. <https://doi.org/10.1007/s10616-017-0072-9>
9. B. S. Dandashire, S. M. Shema. Phytochemical Screening and Antimicrobial Activity of Aqueous Stem Extract of Aloe vera on Some Common Pathogenic Bacteria. *J. Microbiol. Res.* **2019**, 4, 49. <https://doi.org/10.47430/ujmr.1942.009>
10. T. Y. D Trang, H. T. Dzung, T. T. Huong, L. Q. Dien, D. T. Hanh, H. T. N. Phuong, Preparation and Characterization of Chitosan/ Aloe vera gel film for fresh fruit preservation. *E3S Web of Conferences* **2023**, 443, 02003 <https://doi.org/10.1051/e3sconf/202344302003>
11. D. M. Escobar-Sierra, Y. P. Perea-Mesa. Manufacturing and Evaluation of Chitosan, PVA and Aloe vera Hydrogels for Skin Application. *DYNA* **2017**, 84, 134. <https://doi.org/10.15446/dyna.v84n203.62742>
12. J. E. Arikibe, R. Lata, D. Rohindra. Bacterial Cellulose/Chitosan Hydrogel Synthesized *in situ* for Biomedical Application. *J. Appl. Biosci.* **2021**, 162, 16676. <https://doi.org/10.35759/JABs.162.1>
13. S. K. Sonam, A. Tiwari. Antibacterial efficacy of aloe species on pathogenic bacteria, *Int. J. Sci. Technol. Manag.* **2015**, 4, 143. www.ijstm.com ISSN 2394-1537
14. M. Ahmed, F. Hussain. Chemical Composition and Biochemical Activity of Aloe vera (Aloe barbadensis Miller) Leaves. *Int. J. Chem. Biochem. Sci.*, **2013**, 3, 29.
15. D. D. Iqbal, A. Munir, M. Abbas, A. Nazir, S. Z. Alshawwa, M. Iqbal, N. Ahmad. Polymeric Membranes of Chitosan/Aloe vera Gel Fabrication with Enhanced Swelling and Antimicrobial Properties for Biomedical Applications, *Dose Response* **2023**, 21, 15593258231169387. <https://doi.org/10.1177/15593258231169387>
16. C. L. Quave. Wound Healing with Botanicals: A Review and Future Perspectives, *Curr. Derm. Rep.* **2018**, 7, 287. <https://doi.org/10.100/s136671-018-0247-4>
17. B. B. Salehi, S. Albayrak, H. Antolak, D. Kregiel, E. Pawlikowska, M. Sharifi-Rad, Y. Upreti, P. V. T. Fokou, Z. Yousef, Z. A. Zakaria, E. M. Varoni, F. SSharopov, I. Martins, M. Iriti, J. Sharifi-Rad. Aloe Genus Plants: From Farm To Food Applications And Phytopharmacotherapy. *Int. J. Mol. Sci.*, **2018**, 19, 2843. <https://doi.org/10.3390/ijms19092843>
18. J. P. Mends, T. Reddy, R. Deepika, M. P. Devi, T. P. Sastry, Preparation and Characterization of Wound Healing Composite of Chitosan, Aloe vera and Calendula officinalis. A Comparative study. *Am. J. Phytomedicine Clin. Ther.*, **2016**, 4, 61. www.ajpct.org
19. K. Monzon-Ortega, M. Salvador-Figueroa, D. Galvez-Lopez, R. Rosas-Quijano, I. Ovando-Medina, A. Vazquez-Ovando, Characterization of Aloe vera -Chitosan Composite Films and their use for Reducing the Disease Caused by Fungi in papaya Maradol. *J. Food Sci. Technol.*, **2018**, 55, 4749. <https://doi.org/10.1007/s13197-018-3397-2>
20. P. Y. Hao, H. Y. Zhou, L. J. Ren, H. J. Zheng, J. N. Tong, Y. W. Chen, H. J. Park, Preparation and antibacterial properties of curcumin-loaded cyclodextrin-grafted chitosan hydrogel. *J. Sol-Gel Sci. Technol.*, **2023**, 106, <https://doi.org/10.1007/s10971-023-06097-8>
21. J. Li, S. Zhuang. Antibacterial activity of chitosan and its derivatives and their interaction mechanism with bacteria: Current state and perspectives. *Eur. Polym. J.*, **2020**, 138, 109984. <https://doi.org/10.1016/j.eurpolymj.2020.109984>
22. A. K. Nakamura-García, E. C. Santos-Garfias, D. I. Alonso-Martínez, T. I. Garambullo-Peña, J. F. Covián-Nares, M. Gómez-Barroso, R. Montoya-Pérez, Healing of Wounds Treated with Chitosan Hydrogels with Extracts from Aloe vera and Calendula officinalis. *Rev. Mex. de Ing. Biomed.*, **2022**, 43, 19. <https://dx.doi.org/10.17488/RMIB.43.1.2>

Cover Page of January-June 2025 issue



About the Cover page

A peaceful scene of a herd of elk grazing among tall coniferous trees in Yellowstone, located in the northwest corner of Wyoming, USA. Elk, living in herds for protection, graze on grass and enjoy the seasons in this stunning area. The forest offers shelter from predators and a variety of plants for foraging. This tranquil image captures the harmony between wildlife and the environment in Yellowstone's ecosystem.

About the Editor-in-Chief

Prof. Dr. Susanta Banerjee has been associated with the Indian Institute of Technology Kharagpur, India, for over 18 years. He previously served as the head of the Materials Science Centre (May 2014 to May 2017) and is currently the Institute Chair Professor and Chairperson of Central Research Facility. Before joining IIT Kharagpur he served 14 years as Scientist at DRDO and GE India Technology Centre, Bangalore. He is the recipient of the prestigious AvH fellowship from Germany and a fellow of the WAST. Prof. Banerjee has supervised over 30 doctoral and 45 master's theses in polymer and materials science and engineering. He has completed many exciting projects at DRDO, GEITC, and IIT-Kharagpur, driven by his passion for advocating future sustainability.

Innovate Today, Sustain Tomorrow



Articles are open access and can be found at:

<https://insuf.org/journal/icms>

Published by

INSUF PUBLICATIONS (OPC) PVT. LTD.

CIN No: U90005WB2024OPC272576

Director: Ms. Gargi Agarwala Mahato

Address: BD51, Gitanjali Apartment, FL 5B, Rabindra Pally, Prafulla Kanan,
Kolkata-700101, West Bengal, INDIA

Email: gargiagarwala@gmail.com; me-icms@insuf.org submission-icms@insuf.org

Contact Nos.: +919933060646; +918902278875. Website: <https://insuf.org/>

